

The background is a complex, abstract composition of glowing golden-yellow lines and circles on a dark, almost black, field. The lines are thin and vary in length and orientation, some forming straight paths while others curve into spirals or loops. The circles are also thin and appear as if they are part of a larger, interconnected network. The overall effect is one of dynamic energy and intricate structure, reminiscent of a particle detector or a complex biological network.

PRRT & ONCOLOGY

Hendrik Bergsma

Peptide Receptor Radionuclide Therapy & Oncology

Hendrik Bergsma

ISBN 978-94-6299-661-8

Cover Art impression of 'Bubble Chamber Film' (Black & White), 1976 from Fermilab. Reproduced by Ton Everaers, 2017.

Lay-out Nikki Vermeulen - Ridderprint BV

Printing Ridderprint BV - www.ridderprint.nl

© 2017 H. Bergsma, Rotterdam, The Netherlands.

All rights reserved. No part of this thesis may be reproduced, stored in a retrieval system, or transmitted in any form or by any means, without prior written permission of the author, or when appropriate, of the publishers of the publications included in this thesis.

Peptide Receptor Radionuclide Therapy & Oncology

Proefschrift

ter verkrijging van de graad van doctor aan de
Erasmus Universiteit Rotterdam
op gezag van de
rector magnificus
Prof.dr. H.A.P. Pols
volgens besluit van het College voor Promoties.

De openbare verdediging zal plaatsvinden op dinsdag 26 september 2017
om 15:30 uur

door
Hendrik Bergsma
geboren te Meppel (Nederland)

PROMOTIECOMMISSIE

Promotoren: Prof.dr.ir. M. de Jong
Prof.dr. D.J. Kwekkeboom†
Prof.dr. W.W. de Herder

Overige leden: Prof.dr. L.J. Hofland
Prof.dr. A.G. Vulto
Prof.dr. M.L. Lam

Copromotor: Dr. M. Konijnenberg

In Memoriam of
Prof. dr. Dik Kwekkeboom
1958 - 2017

CONTENT

	Thesis outline	
Chapter 1	General introduction	11
1.1	Peptide receptor radionuclide therapy (PRRT) & neuroendocrine tumors (NETs)	13
1.2	Dosimetry in PRRT	31
1.3	Peptide receptor radionuclide therapy for GEP-NETs. <i>Best Practice & Research Clinical Gastroenterology. 2012 Dec; 26(6): 867-81</i>	59
Chapter 2	Toxicity after PRRT	83
2.1	Nephrotoxicity after PRRT with ¹⁷⁷ Lu-DOTA-Octreotate. <i>European Journal of Nuclear Medicine and Molecular Imaging. 2016 Sep; 43(10): 1802-11</i>	85
2.2	Subacute haematotoxicity after PRRT with (¹⁷⁷)Lu-DOTA-octreotate: prognostic factors, incidence and course <i>European Journal of Nuclear Medicine and Molecular Imaging. 2016 Mar; 43(3): 453-63</i>	111
2.3	Therapy-related hematological malignancies after PRRT with ¹⁷⁷ Lu-DOTA-Octreotate: Incidence, course & predicting factors <i>Accepted for publication in Journal of Nuclear Medicine</i>	135
2.4	Spleen volume decrease after PRRT: Clinical and dosimetrical correlation <i>Submitted</i>	171
Chapter 3	Nuclear imaging of prostate & breast cancer	185
3.1	Introduction	187
3.2	Preclinical and first clinical experience with the gastrin-releasing peptide receptor-antagonist [⁶⁸ Ga]SB3 and PET/CT <i>European Journal of Nuclear Medicine and Molecular Imaging. 2016 May;43(5):964-73</i>	195

Chapter 4	Summary, discussion and future	219
4.1	Summary (Dutch and English)	221
4.2	Discussion and future perspectives	233
	List of abbreviations	247
	List of symbols	251
	Curriculum Vitae	253
	Portfolio	254
	Acknowledgements (Dankwoord)	256
	List of Publications	260

THESIS OUTLINE

The aims of the studies presented in this thesis are to:

1. Evaluate (long-term) toxicity after treatment with ^{177}Lu -DOTATATE regarding:
 - a. Renal function
 - b. Subacute effects on the bonemarrow: prognostic factors, incidence and course
 - c. Hematological malignancies: incidence, course & predicting factors
 - d. Spleen volume decrease after PRRT: clinical and dosimetric correlation
2. Evaluate a novel gastrin-releasing peptide receptor (GRPR) antagonist in patients with prostate or breast cancer

The first chapter is a general introduction. **Chapter 1.1** is an opening text about neuroendocrine tumors and the different treatment modalities, including peptide radionuclide receptor therapy (PRRT). **Chapter 1.2** gives a theoretical outline of dosimetry used in PRRT. Furthermore practical dosimetric aspects of the critical organs will be discussed. **Chapter 1.3** describes the current literature on peptide radionuclide receptor therapy.

The second chapter covers (long-term) toxicity after PRRT with ^{177}Lu -DOTATATE. In **Chapter 2.1** the renal function over time, the incidence of nephrotoxicity and associated risk factors are investigated in patients treated with ^{177}Lu -DOTATATE. Also, the radiation dose to the kidneys is evaluated and compared to the accepted dose limits in external beam radiotherapy and PRRT with ^{90}Y radiolabelled somatostatin analogues. **Chapter 2.2** describes the incidence, duration and risk factors of (sub)acute hematological toxicity in patients treated with PRRT. Absorbed bonemarrow dose estimates are evaluated and compared with the approved dose limit of 2 Gy. In **Chapter 2.3** the incidence and clinical course of long-term hematological toxicity is analyzed in patients with (suspected) hematological malignancies after PRRT. In **Chapter 2.4** the clinical implications of spleen volume loss and decreased lymphocyte count are studied.

The third chapter deals with targeted nuclear imaging of prostate and breast cancer. **Chapter 3.1** gives an introduction to prostate/breast cancer and the possible targets for nuclear imaging. **Chapter 3.2** characterizes a novel gastrin-releasing peptide receptor (GRPR) antagonist, ^{68}Ga -SB3, in patients with prostate or breast cancer.

Chapter 4.1 provides an English and Dutch summary of the presented data in this thesis whereas **Chapter 4.2** concludes with a general discussion and future remarks.



1

GENERAL INTRODUCTION

1.1

PEPTIDE RECEPTOR RADIONUCLIDE THERAPY (PRRT) & NEUROENDOCRINE TUMORS (NETs)

Neuroendocrine tumors (NETs) are a varied group of neoplasms that arise from neuroendocrine cells throughout the body. They most commonly occur in the intestines, but they are also frequently found in the pancreas and lungs. The term “carcinoid”, introduced by Siegfried Oberndorfer in 1907, is still wrongly used in the clinic and literature (1). The World Health Organization (WHO) replaced the term carcinoid by NET including the degree of differentiation and proliferation (2-5). For the bronchopulmonary NETs, the terminology remains “typical” and “atypical carcinoid” (6). NETs can have special secretory granules and often produce biogenic amines and polypeptide hormones causing tumor-related symptoms (7). The peptide somatostatin inhibits the secretion of hormones by binding to the complementary somatostatin receptor (sst), which are expressed on most NETs (8). Five subtypes of the sst are known, sst₁ - sst₅ (9). Somatostatin analogs, like octreotide and lanreotide, can reduce symptoms (10), but can also be labeled with a radionuclide, like [¹¹¹Indium-DTPA⁰]octreotide (OctreoScan®), for visualization and therapy (11,12).

EPIDEMIOLOGY OF NETS

NETs are relatively rare tumors with an incidence of 2-5 cases per 100,000 persons (13-15). In the Netherlands (between 1989-1996), the incidence of NETs was 1.8 and 1.9 cases per 100,000 persons for men and women, respectively (16). The highest incidence of NETs occurs in the 6th and 7th decade of life (15,16). A strong increase in incidence of NETs has been reported. This increase may reflect the improvement in diagnostic modalities, but also increased awareness of NETs by clinicians can explain this rise in incidence. Survival for all NETs has improved over time, especially for distantly metastasized gastrointestinal NETs and pancreatic NETs in particular, reflecting improvement in therapies (17).

DIAGNOSIS

Clinical Aspects

The clinical presentation of NETs varies according to the anatomic site of origin, tumor size, function and extent of metastatic disease (18). Functioning NETs give hormone-related symptoms, whereas non-functioning NETs are often clinically silent and found by coincidence (19). The hormone-related symptoms (carcinoid syndrome) consist of secretory diarrhea, flushing, wheezing and right sided valvular heart disease, which is caused by serotonin production. Serotonin production can cause small bowel ischemia, due to mesenteric fibrosis. Specific occasional hormone production of insulin, gastrin or VIP can cause hypoglycemia, peptic ulcer disease, and Verner-Morrison syndrome, respectively, in patients with NETs.

Non-specific tumor related symptoms are (localized) pain, loss of weight and/or anorexia.

Biomarkers

Important diagnostics for NETs are biochemical testing, imaging procedures and pathological findings. Frequent laboratory tests used in monitoring therapy and follow-up include Chromogranine A (CgA), urinary 5-Hydroxyindoleacetic acid (5-HIAA) and Neuron-specific enolase (NSE), particularly in patients with functioning NETs. Also liver function tests are routinely performed in patients with liver metastasis.

An important serum marker is CgA, which is found in the secretory granules of neuroendocrine cells. Depending on the extent of disease, serum CgA is elevated in > 60% of the patients with functioning or non-functioning NETs (20). The sensitivity and specificity of CgA for the detection of NETs is between 53-85% and 84-98% respectively (21). CgA levels can also be elevated due to use of medication (proton pump inhibitor), chronic kidney failure or gastritis, therefore medical history and use of medication should be asked. CgA can as well be used as a prognostic factor. Patients with a high serum CgA (> 5,000 µg/l) have a shorter median overall survival (OS) than patients with a low serum CgA (< 5,000 µg/l), 33 versus 57 months (22).

Measurement of the 5-HIAA is relevant in patients with the carcinoid syndrome. 5-HIAA is a breakdown metabolite of serotonin, making it an indirect marker for serotonin production by the tumor. Levels of 24-hour urinary 5-HIAA are correlated with extend of carcinoid heart disease (23). The sensitivity of urinary 5-HIAA in patients with carcinoid syndrome is 90%. However, certain medications and types of food can effect levels of 5-HIAA in the urine and should be abstained during the 24-hour urine collection (24).

NSE levels can be used as a biomarker for both functioning and non-functioning NETs. Serum NSE is a cell-specific isoenzyme and is present in the cytoplasm of neurons and neuroendocrine cells. The marker is elevated in 30-50% of the patients with gastroenteropancreatic NETs (25-27).

Since current biomarkers have clinical limitations, two major types of novel biomarkers have been considered: multigene signatures and circulating tumor cells. Multigene signatures provide characterization of NETs on a molecular level and can provide up-to-date information about tumor activity and treatment response (28). Measurement of circulating tumor cells (CTCs) can be used to accurately identify and acquire genomic information of the NET. Limited data on the use of CTCs is available, but one study demonstrated promising results linking CTC to tumor burden in metastasized NET patients (29).

Imaging

Medical imaging generally can be divided into two categories, anatomical and functional.

Anatomical imaging of NETs can be performed with conventional (film) radiography, ultrasonography, angiography, computed tomography (CT) and magnetic resonance imaging (MRI) (30-33). Primary, (multi-phasic) CT and MRI are performed giving information about tumor localization, size and degree of invasion with surrounding tissue. A major limitation of these two latter imaging modalities is that only a part of the body is scanned, also small (< 10mm) non-pathological lymph nodes cannot be considered 100% tumor-free.

Functional imaging can visualize the distribution of a specific target throughout the body. In case of NETs, somatostatin receptor scintigraphy (SRS) can provide information about the presence of sst's on the tumor. Octreoscan® ([¹¹¹In-DTPA⁰]octreotide) was one of the first successful radiotracers for imaging the somatostatin receptor (mainly sst₂ and sst₅). The overall sensitivity of OctreoScan® in NET patients is 60-90% (34). SRS can be improved by the co-use of CT, combining functional- with anatomical information (35). SRS is more effective for screening the total body for primary lesions and metastasis. Furthermore, Octreoscan® is used to evaluate radioactivity uptake in the tumor for potential peptide receptor radionuclide therapy (PRRT) (36).

Recently, PET imaging with gallium-68-somatostatin analogs has improved somatostatin receptor imaging (37). It has been demonstrated that a ⁶⁸Ga-DOTATATE or ⁶⁸Ga-DOTATOC PET-scan can increase the spatial resolution and lesion detectability compared to Octreoscan® (37,38). Also ⁶⁸Ga-DOTATATE has a major advantage for patients since imaging can be completed in less than 2 hours versus 2 days for OctreoScan® and ⁶⁸Ga-DOTATATE involves lower radiation exposure (39). Another gallium-68-somatostatin analog, ⁶⁸Ga-DOTATOC, has also improved imaging of neuroendocrine tumors (40). [¹⁸F]-fluorodeoxyglucose (FDG)-PET can be used for imaging of poorly differentiated neuroendocrine carcinomas (NECs) or when the Octreoscan® is negative or equivocal (41). Recent studies have demonstrated that intermediate-moderate grade NETs with FDG positive lesions can progress more aggressively (42). Therefore a combination of FDG-PET and ⁶⁸Ga-DOTATATE is increasingly being used prior and during therapy in patients with well- and moderately differentiated NETs (43,44).

Pathology, Staging and Grading

The final diagnosis of NET is mainly based on the pathology report. Therefore, a biopsy of the primary tumor and/or metastasis is fundamental in the workup. Various types of staining are available like hematoxylin and eosin (HE), also immunostaining with

CgA, synaptophysin and sst₂ can be assessed. Additional immunostaining for specific hormones (e.g. insulin, glucagon, gastrin or vasoactive intestinal polypeptide) can be performed in a small group of patients with uncommon functional NETs. Also the rate of tumor growth can be estimated using Ki-67 index and/or mitotic count (45).

For staging NETs, current guidelines utilize the tumor-node-metastasis (TNM) classification and the 2010 WHO grading system. The TNM system of NETs is site-specific and describes the stage according to size, lymph node involvement and presence of distant metastasis (46,47). The TNM system is also incorporated in the WHO 2010 classification. The WHO grading system (48) is based on examining tumor-cells and -tissue. A grade 1-3 is given according to the mitotic count or proliferative activity (ki-67), resulting in a NET or NEC, see Table 1. The prognostic validity of both TNM stage and proliferative rate has been demonstrated in several studies (49-51).

Table 1: Pathological grading of Neuroendocrine tumors. Neuroendocrine tumor (NET), Neuroendocrine carcinoma (NEC), High-power field (HPF)

Type of tumour	Degree of differentiation	Grade	Mitotic Count (per 10 HPF)	Ki-67 Index (%)
NET	Well	G1	< 2	< 3
		G2	2 - 20	3 - 20
NEC	Poor	G3	> 20	> 20

TREATMENT

Surgery

Surgery is the only curative treatment option in patients with localized Gastroenteropancreatic Neuroendocrine Tumors (GEP-NETS) (19,52). However, most of the patients often present with tumor-related symptoms and widespread disease. Nonetheless, surgical intervention can be a treatment option in patients with advanced disease. Resection of the primary tumor is associated with an increased overall survival in patients with NETs of pancreatic origin (53,54). Surgery can also be performed for control of hormonal symptoms (55) and can prevent small bowel obstruction or ischemia in patients with mesenteric involvement (56). A combination of surgery, (chemo)embolization and/or radiofrequency ablation (RFA) can be an option for patients with advanced disease (19,56). As for patients without extrahepatic metastasis, liver transplantation can be considered (57).

Interventional radiology

Liver metastases of neuroendocrine tumors are often hypervascular and derive their blood supply mostly from the hepatic artery, as opposed to normal liver parenchyma, which mainly depends on the portal vein. Therefore occlusion of the hepatic arterial branches by (chemo)particles can induce tumor necrosis and volume reduction (58). Transcatheter arterial chemoembolization (TACE) can decrease tumor-related symptoms and has tumor response rates of 33-80% (59). A recent study demonstrated no difference in survival rate for hepatic arterial embolization with or without chemotherapy coated particles (60). Radioembolization of neuroendocrine liver metastases can also be performed with radioactive ⁹⁰Yttrium (⁹⁰Y) microspheres. A median response rate of 63% (range 13-100%) has been reported with this technique (61). Local heating of the tumor with Radio frequency ablation (RFA) is used in patients with limited (< 5 liver lesions) and small tumors (<5 cm) (62). RFA is associated with relief of symptoms and can be used in combination with (partial) hepatic resection (62,63). Other local ablative techniques for neuroendocrine liver metastasis include alcohol ablation or (intraoperative) cryotherapy (63).

Somatostatin analogues

Somatostatin analogues (SSAs) are currently the first line therapy for grade 1-2 GEP-NETs (64). SSAs inhibit hormone production (serotonin and growth hormone) by binding to the sst₂, resulting in symptom control in up to 71% of the patients (65,66). Also an increase in time to progression with SSAs was demonstrated when compared to placebo in patients with NETs (67). Preoperative and perioperative octreotide therapy are essential to protect against carcinoid crises that can arise from anesthesia and/or tumor manipulation (68). However, long-term use of SSAs can desensitize the tumor, resulting in recurrence of hormone-related symptoms.

Molecular targets

Various molecular targeted therapies have been developed for NETs in the past decade. In a recent study, patients treated with the tyrosine kinase inhibitor Sunitinib (Sutent; Pfizer Inc, New York, NY) had a longer median progression free survival (PFS) than placebo, 11.4 versus 5.5 months (69). Also treatment with the mammalian target of rapamycin (mTOR)-inhibitor everolimus (Affinitor; Novartis Pharmaceuticals, Basel, Switzerland) resulted in a longer median PFS compared to placebo (11.0 versus 4.6 months) (70). A phase II study, combining the angiogenesis inhibitor bevacizumab (Avastin) and the antiviral drug interferon alpha-2b (Intron-A), demonstrated that bevacizumab decreased blood flow and had a tumor stabilizing effect (71). However, objective tumor responses with these new targeted therapies are rare (69,70,72), therefore molecular

targeted therapies are currently not first line therapies, despite the fact that sunitinib and everolimus are both registered therapies for pancreatic NETs in the Netherlands.

Interferon- α and chemotherapy

Interferon- α is another targeted therapy and binds specifically to surface receptors of NETs, reducing symptoms in patients with carcinoid syndrome (73). Also antiproliferative effects of Interferon- α in combination with octreotide long-acting release (LAR) have been demonstrated in a prospective randomized study (71). However interferon- α has serious side effects, like fatigue, fever, myelosuppression and auto-immune disorders (74). Other types of Interferon are explored in (future) experimental studies, like Interferon- β , which might be a successor of a more potent anti-tumor agent for NETs (75-77). Poorly differentiated grade 3 neuroendocrine carcinomas (NEC) are usually treated with cisplatin-based chemotherapy regimens, usually a combination of cisplatin and etoposide. Moertel et al. described an overall remission rate of 67% and a median survival of 19 months. A more recent study reported a response rate around 50% for chemotherapy with cisplatin and etoposide (78). An objective response or stabilization was observed in 71% of the NEC patients after temozolomide (with/without Capecitabine (Xeloda)), who failed on first-line chemotherapy (79). Alternatively, streptozocin-based chemotherapies in combination with 5-fluorouracil or doxorubicin result in objective tumor response rates in 35-40% of the patients (78,80). First line temozolomide-based chemotherapy (with or without capecitabine) seems to be promising in pancreatic NETs giving partial remission in 40-70% of the patients (81).

External beam Radiotherapy

External beam radiotherapy (EBRT) has a limited role in the treatment of NETs. EBRT can be performed in case of brain metastases, spinal cord compression or pain due to bone metastases. Furthermore, EBRT can have additional value in localized bronchial NETs (82). Another application of radiotherapy may be its use in combination with chemotherapy (i.e. chemoradiation), which has been performed in a few patients with locally advanced pancreatic NETs (83). Pheochromocytomas and paraganglioma are both a different type of neuroendocrine tumors. In these patients, EBRT can also be considered when the tumor is symptomatic, localized and progressive (84,85).

Peptide Receptor Radionuclide Therapy (PRRT)

Peptide receptor radionuclide therapy (PRRT) with radiolabeled somatostatin analogs plays an increasing role in the treatment of patients with inoperable and/or metastasized NETs.

In PRRT, a cell-targeting protein (or peptide) is combined with a small amount of radioactive material, creating a radiopeptide. When injected into the patient's bloodstream, the radiopeptide binds to the receptor of the tumor cell, delivering a high dose of radiation to the cancer. Various radiopeptides are used in PRRT, such as [^{111}In -DTPA]octreotide (^{111}In -octreotide), [^{90}Y -DOTA, Tyr^3]octreotide (^{90}Y -DOTATOC) and [^{177}Lu -DOTA, Tyr^3]octreotate (^{177}Lu -Octreotate or ^{177}Lu -DOTATATE). In the early days, treatment with ^{111}In -octreotide resulted in relief of symptoms in patients with metastasized NETs, but objective tumor response was rare (86,87). However, complete and partial response in 10-30% of NET patients is obtained after PRRT with ^{90}Y -DOTATOC or ^{177}Lu -Octreotate (88-92). The median time to progression is 29 months for ^{90}Y -DOTATOC (91) and 33 months for ^{177}Lu -octreotate (93).

PRRT: INCLUSION CRITERIA, TREATMENT SCHEMES & ADMINISTERED ACTIVITIES

The studies published in this thesis are part of the ongoing prospective study in patients with neuroendocrine tumors treated with ^{177}Lu -octreotate at the Department of Radiology & Nuclear Medicine in Erasmus MC Rotterdam. General inclusion criteria were: patients with a somatostatin positive tumor and baseline tumor uptake on [^{111}In -DTPA]octreotide scintigraphy (OctreoScan[®]; Mallinckrodt, Petten, The Netherlands) with accumulation in the tumor at least as high as in normal liver tissue; no prior treatment with PRRT; baseline serum hemoglobin (Hb) ≥ 6 mmol/l; white blood cell (WBC) count $\geq 2 \cdot 10^9$ /l; platelet (PLT) count $\geq 75 \cdot 10^9$ /l; serum creatinine ≤ 150 $\mu\text{mol/l}$ or creatinine clearance ≥ 40 ml/min and Karnofsky performance status ≥ 50 .

[DOTA, Tyr^3] octreotate was obtained from BioSynthema (St. Louis, MO). $^{177}\text{LuCl}_3$ was supplied by IDB-Holland (Baarle-Nassau, The Netherlands) and ^{177}Lu -DOTATATE was prepared locally (94). Granisetron 3 mg or ondansetron 8 mg was injected intravenously 30 min before infusion of ^{177}Lu -DOTATATE. Infusion of amino acids (2.5 % arginine and 2.5 % lysine, 1 l) was started 30 min before administration of the radiopharmaceutical and lasted for 4 h. The radiopharmaceutical was coadministered for 30 min using a second pump system. In most patients cycle dosages of 3.7 GBq (100 mCi) and 7.4 GBq (200 mCi) were injected over 30 min. The interval between treatments was 6 – 16 weeks. The initial intended cumulative dose was 29.6 GBq (800 mCi). However, the dose was lowered or discontinued indefinitely if recurrent grade 3/4 hematological toxicity occurred or persistent low blood counts were observed.

COMMON TERMINOLOGY CRITERIA FOR ADVERSE EVENTS (CTCAE)

Over the last 20 years various adverse events grading systems have been developed (95). In 2003 the National Cancer Institute published version (v3.0) of the Common terminology criteria for adverse events (CTCAE) (96). CTCAE provides a grading scale, grades 1 through 5, with unique clinical descriptions of severity for each adverse event. Important clinical adverse events are grade 3 (severe), 4 (life-threatening) and 5 (death). CTCAE was developed for uniform treatment-related toxicity in clinical (chemotherapeutic) trials, but has been generally adopted in the field of nuclear medicine for toxicity assessment. CTCAE version 3.0 provides also criteria concerning late- and acute-effects. The previously used “90-days rule” for acute effects is no longer applied and investigators are encouraged to report all observations by using individual Common terminology criteria (CTC) (95). In CTCAE version 4.0 bone marrow toxicity is further generalized by replacing absolute blood values with relative reduction from normal cellularity (97). Grade 4 toxicity is replaced with life-threatening consequences and aplastic persistence for > 2 weeks. Consequences of this generalization of (hema) toxicity are the difficulties in comparing different studies. Therefore investigators should always clearly specify grade 3 and 4 hematoxicity, also additional toxicity parameters can be specified, e.g. duration of toxicity.

PRRT: TOXICITY

In general the side effects of PRRT with ^{177}Lu -DOTATATE are mild, but possible adverse effects are: Nephrotoxicity (**Chapter 2.1**), (sub)acute hematotoxicity (**Chapter 2.2**), hematological malignancies (**Chapter 2.3**) and spleen volume decrease after PRRT (**Chapter 2.4**). Patients who are treated with ^{177}Lu -DOTATATE may develop radiation-induced hormone disturbances (98). In men ^{177}Lu -octreotate therapy induces transient inhibitory effects on spermatogenesis (temporary infertility) and a gonadotropin decrease in postmenopausal women (98). In general these disturbances in endocrine function are temporary and not severe.

A rare adverse effect after PRRT is carcinoid crisis. Carcinoid crisis is a life-threatening state in patients with hormone producing neuroendocrine tumors (NETs) and is characterized by sudden blood pressure fluctuations, arrhythmias, and bronchospasms. The underlying mechanism is associated with a sudden release of serotonin and other vasoactive substances (99). Stress can trigger a carcinoid crisis, therefore one should be cautious when performing intervention procedures and therapies (100). Hormonal crises after ^{177}Lu -octreotate occur infrequently. In one study, only 6 (1%) of 479 patients had such a crisis (101). The authors found that patients with VIPoma or bronchial

carcinoids are most at risk. Somatostatin analogues have been recommended for prophylactic administration before intervention procedures for functioning NETs (100). In our department, patients with excessive carcinoid syndrome and/or high hormone production were hospitalized before and after treatment with ^{177}Lu -DOTATATE. Also iv somatostatin analogues were resumed directly after PRRT.

REFERENCES

1. Oberndorfer S. Karzinoide Tumoren des Dunndarms, Frankfurt Z. *Pathol.* 1907;7:426-432.
2. Kloppel G, Perren A, Heitz PU. The gastroenteropancreatic neuroendocrine cell system and its tumors: the WHO classification. *Ann NY Acad Sci.* 2004;1014:13-27.
3. Pape UF, Jann H, Muller-Nordhorn J, et al. Prognostic relevance of a novel TNM classification system for upper gastroenteropancreatic neuroendocrine tumors. *Cancer.* 2008;113:256-265.
4. Rindi G, Capella C, Solcia E. Introduction to a revised clinicopathological classification of neuroendocrine tumors of the gastroenteropancreatic tract. *Q J Nucl Med.* 2000;44:13-21.
5. Bosman FT, Carneiro F, Hruban RH, Theise ND. *WHO classification of tumours of the digestive system*: World Health Organization; 2010.
6. Caplin ME, Baudin E, Ferolla P, et al. Pulmonary neuroendocrine (carcinoid) tumors: European Neuroendocrine Tumor Society expert consensus and recommendations for best practice for typical and atypical pulmonary carcinoids. *Ann Oncol.* 2015;26:1604-1620.
7. Kulke MH, Mayer RJ. Carcinoid tumors. *N Engl J Med.* 1999;340:858-868.
8. Reubi JC, Kvols LK, Waser B, et al. Detection of somatostatin receptors in surgical and percutaneous needle biopsy samples of carcinoids and islet cell carcinomas. *Cancer Res.* 1990;50:5969-5977.
9. Patel YC. Somatostatin and its receptor family. *Front Neuroendocrinol.* 1999;20:157-198.
10. Janson ET, Oberg K. Long-term management of the carcinoid syndrome. Treatment with octreotide alone and in combination with alpha-interferon. *Acta Oncol.* 1993;32:225-229.
11. Krenning EP, Kwekkeboom DJ, Bakker WH, et al. Somatostatin receptor scintigraphy with [111In-DTPA-D-Phe1]- and [123I-Tyr3]-octreotide: the Rotterdam experience with more than 1000 patients. *Eur J Nucl Med.* 1993;20:716-731.
12. Krenning EP, Kooij PP, Bakker WH, et al. Radiotherapy with a radiolabeled somatostatin analogue, [111In-DTPA-D-Phe1]-octreotide. A case history. *Ann NY Acad Sci.* 1994;733:496-506.
13. Hemminki K, Li X. Incidence trends and risk factors of carcinoid tumors: a nationwide epidemiologic study from Sweden. *Cancer.* 2001;92:2204-2210.
14. Modlin IM, Lye KD, Kidd M. A 5-decade analysis of 13,715 carcinoid tumors. *Cancer.* 2003;97:934-959.
15. Yao JC, Hassan M, Phan A, et al. One hundred years after "carcinoid": epidemiology of and prognostic factors for neuroendocrine tumors in 35,825 cases in the United States. *J Clin Oncol.* 2008;26:3063-3072.
16. Quaedvlieg PF, Visser O, Lamers CB, Janssen-Heijnen ML, Taal BG. Epidemiology and survival in patients with carcinoid disease in The Netherlands. An epidemiological study with 2391 patients. *Ann Oncol.* 2001;12:1295-1300.
17. Dasari A, Shen C, Halperin D, et al. Trends in the Incidence, Prevalence, and Survival Outcomes in Patients With Neuroendocrine Tumors in the United States. *JAMA Oncol.* 2017.
18. Ter-Minassian M, Chan JA, Hooshmand SM, et al. Clinical presentation, recurrence, and survival in patients with neuroendocrine tumors: results from a prospective institutional database. *Endocr Relat Cancer.* 2013;20:187-196.
19. Modlin IM, Oberg K, Chung DC, et al. Gastroenteropancreatic neuroendocrine tumours. *Lancet Oncol.* 2008;9:61-72.
20. O'Toole D, Grossman A, Gross D, et al. ENETS Consensus Guidelines for the Standards of Care in Neuroendocrine Tumors: biochemical markers. *Neuroendocrinology.* 2009;90:194-202.

21. Lawrence B, Gustafsson BI, Kidd M, Pavel M, Svejda B, Modlin IM. The clinical relevance of chromogranin A as a biomarker for gastroenteropancreatic neuroendocrine tumors. *Endocrinol Metab Clin North Am.* 2011;40:111-134, viii.
22. Janson ET, Holmberg L, Stridsberg M, et al. Carcinoid tumors: analysis of prognostic factors and survival in 301 patients from a referral center. *Ann Oncol.* 1997;8:685-690.
23. Zuetenhorst JM, Bonfrer JM, Korse CM, Bakker R, van Tinteren H, Taal BG. Carcinoid heart disease: the role of urinary 5-hydroxyindoleacetic acid excretion and plasma levels of atrial natriuretic peptide, transforming growth factor-beta and fibroblast growth factor. *Cancer.* 2003;97:1609-1615.
24. Feldman JM, Lee EM, Castleberry CA. Catecholamine and serotonin content of foods: effect on urinary excretion of homovanillic and 5-hydroxyindoleacetic acid. *J Am Diet Assoc.* 1987;87:1031-1035.
25. Velayoudom-Cephise FL, Duvillard P, Foucan L, et al. Are G3 ENETS neuroendocrine neoplasms heterogeneous? *Endocr Relat Cancer.* 2013;20:649-657.
26. Oberg K. Circulating biomarkers in gastroenteropancreatic neuroendocrine tumours. *Endocr Relat Cancer.* 2011;18 Suppl 1:S17-25.
27. Baudin E, Gigliotti A, Ducreux M, et al. Neuron-specific enolase and chromogranin A as markers of neuroendocrine tumours. *Br J Cancer.* 1998;78:1102-1107.
28. Oberg K, Modlin IM, De Herder W, et al. Consensus on biomarkers for neuroendocrine tumour disease. *Lancet Oncol.* 2015;16:e435-446.
29. Khan MS, Kirkwood A, Tsigani T, et al. Circulating tumor cells as prognostic markers in neuroendocrine tumors. *J Clin Oncol.* 2013;31:365-372.
30. Sundin A, Vullierme MP, Kaltsas G, Plockinger U. ENETS Consensus Guidelines for the Standards of Care in Neuroendocrine Tumors: radiological examinations. *Neuroendocrinology.* 2009;90:167-183.
31. Guettier JM, Kam A, Chang R, et al. Localization of insulinomas to regions of the pancreas by intraarterial calcium stimulation: the NIH experience. *J Clin Endocrinol Metab.* 2009;94:1074-1080.
32. Sundin A, Wills M, Rockall A. Radiological Imaging: Computed Tomography, Magnetic Resonance Imaging and Ultrasonography. *Front Horm Res.* 2015;44:58-72.
33. Brandle M, Pfammatter T, Spinass GA, Lehmann R, Schmid C. Assessment of selective arterial calcium stimulation and hepatic venous sampling to localize insulin-secreting tumours. *Clin Endocrinol (Oxf).* 2001;55:357-362.
34. Toumpanakis C, Kim MK, Rinke A, et al. Combination of cross-sectional and molecular imaging studies in the localization of gastroenteropancreatic neuroendocrine tumors. *Neuroendocrinology.* 2014;99:63-74.
35. Bural GG, Muthukrishnan A, Oborski MJ, Mountz JM. Improved Benefit of SPECT/CT Compared to SPECT Alone for the Accurate Localization of Endocrine and Neuroendocrine Tumors. *Mol Imaging Radionucl Ther.* 2012;21:91-96.
36. Kwekkeboom DJ, Krenning EP, Lebtahi R, et al. ENETS Consensus Guidelines for the Standards of Care in Neuroendocrine Tumors: peptide receptor radionuclide therapy with radiolabeled somatostatin analogs. *Neuroendocrinology.* 2009;90:220-226.
37. Antunes P, Ginj M, Zhang H, et al. Are radiogallium-labelled DOTA-conjugated somatostatin analogues superior to those labelled with other radiometals? *Eur J Nucl Med Mol Imaging.* 2007;34:982-993.
38. Poeppel TD, Binse I, Petersenn S, et al. 68Ga-DOTATOC versus 68Ga-DOTATATE PET/CT in functional imaging of neuroendocrine tumors. *J Nucl Med.* 2011;52:1864-1870.

39. Walker RC, Smith GT, Liu E, Moore B, Clanton J, Stabin M. Measured human dosimetry of 68Ga-DOTATATE. *J Nucl Med.* 2013;54:855-860.
40. Menda Y, Ponto LL, Schultz MK, et al. Repeatability of gallium-68 DOTATOC positron emission tomographic imaging in neuroendocrine tumors. *Pancreas.* 2013;42:937-943.
41. Binderup T, Knigge U, Loft A, et al. Functional imaging of neuroendocrine tumors: a head-to-head comparison of somatostatin receptor scintigraphy, 123I-MIBG scintigraphy, and 18F-FDG PET. *J Nucl Med.* 2010;51:704-712.
42. Severi S, Nanni O, Bodei L, et al. Role of 18FDG PET/CT in patients treated with 177Lu-DOTATATE for advanced differentiated neuroendocrine tumours. *Eur J Nucl Med Mol Imaging.* 2013;40:881-888.
43. Oh S, Prasad V, Lee DS, Baum RP. Effect of Peptide Receptor Radionuclide Therapy on Somatostatin Receptor Status and Glucose Metabolism in Neuroendocrine Tumors: Intraindividual Comparison of Ga-68 DOTANOC PET/CT and F-18 FDG PET/CT. *Int J Mol Imaging.* 2011;2011:524130.
44. Kayani I, Bomanji JB, Groves A, et al. Functional imaging of neuroendocrine tumors with combined PET/CT using 68Ga-DOTATATE (DOTA-DPhe1,Tyr3-octreotate) and 18F-FDG. *Cancer.* 2008;112:2447-2455.
45. Takahashi T, Nakano T, Oka K, Ando K. Transitional increase in growth fraction estimated by Ki-67 index after irradiation to human tumor in xenograft. *Anticancer Res.* 2004;24:107-110.
46. Rindi G. The ENETS guidelines: the new TNM classification system. *Tumori.* 2010;96:806-809.
47. Edge SB, Compton CC. The American Joint Committee on Cancer: the 7th edition of the AJCC cancer staging manual and the future of TNM. *Ann Surg Oncol.* 2010;17:1471-1474.
48. Rindi G AR, Bosman FT. Nomenclature and classification of neuroendocrine neoplasms of the digestive system. *WHO classification of tumors of the digestive system.* Lyon: IARC; 2010.
49. Dolcetta-Capuzzo A, Villa V, Albarello L, et al. Gastroenteric neuroendocrine neoplasms classification: comparison of prognostic models. *Cancer.* 2013;119:36-44.
50. Strosberg J, Nasir A, Coppola D, Wick M, Kvols L. Correlation between grade and prognosis in metastatic gastroenteropancreatic neuroendocrine tumors. *Hum Pathol.* 2009;40:1262-1268.
51. Strosberg JR, Cheema A, Weber J, Han G, Coppola D, Kvols LK. Prognostic validity of a novel American Joint Committee on Cancer Staging Classification for pancreatic neuroendocrine tumors. *J Clin Oncol.* 2011;29:3044-3049.
52. Huang LC, Poultsides GA, Norton JA. Surgical management of neuroendocrine tumors of the gastrointestinal tract. *Oncology (Williston Park).* 2011;25:794-803.
53. Tomassetti P, Campana D, Piscitelli L, et al. Endocrine pancreatic tumors: factors correlated with survival. *Ann Oncol.* 2005;16:1806-1810.
54. Norton JA. Surgery for primary pancreatic neuroendocrine tumors. *J Gastrointest Surg.* 2006;10:327-331.
55. Sarmiento JM, Heywood G, Rubin J, Ilstrup DM, Nagorney DM, Que FG. Surgical treatment of neuroendocrine metastases to the liver: a plea for resection to increase survival. *J Am Coll Surg.* 2003;197:29-37.
56. Akerstrom G, Hellman P, Hessman O, Osmak L. Management of midgut carcinoids. *J Surg Oncol.* 2005;89:161-169.
57. van Vilsteren FG, Baskin-Bey ES, Nagorney DM, et al. Liver transplantation for gastroenteropancreatic neuroendocrine cancers: Defining selection criteria to improve survival. *Liver Transpl.* 2006;12:448-456.
58. Garrot C, Stuart K. Liver-directed therapies for metastatic neuroendocrine tumors. *Hematol Oncol Clin North Am.* 2007;21:545-560; ix-x.
59. O'Toole D, Ruszniewski P. Chemoembolization and other ablative therapies for liver metastases of gastrointestinal endocrine tumours. *Best Pract Res Clin Gastroenterol.* 2005;19:585-594.

60. Maire F, Lombard-Bohas C, O'Toole D, et al. Hepatic arterial embolization versus chemoembolization in the treatment of liver metastases from well-differentiated midgut endocrine tumors: a prospective randomized study. *Neuroendocrinology*. 2012;96:294-300.
61. Yang TX, Chua TC, Morris DL. Radioembolization and chemoembolization for unresectable neuroendocrine liver metastases - a systematic review. *Surg Oncol*. 2012;21:299-308.
62. Zappa M, Abdel-Rehim M, Hentic O, Vullierme MP, Ruszniewski P, Vilgrain V. Liver-directed therapies in liver metastases from neuroendocrine tumors of the gastrointestinal tract. *Target Oncol*. 2012;7:107-116.
63. Atwell TD, Charboneau JW, Que FG, et al. Treatment of neuroendocrine cancer metastatic to the liver: the role of ablative techniques. *Cardiovasc Intervent Radiol*. 2005;28:409-421.
64. Toumpanakis C, Caplin ME. Update on the role of somatostatin analogs for the treatment of patients with gastroenteropancreatic neuroendocrine tumors. *Semin Oncol*. 2013;40:56-68.
65. Klibanski A, Melmed S, Clemmons DR, et al. The endocrine tumor summit 2008: appraising therapeutic approaches for acromegaly and carcinoid syndrome. *Pituitary*. 2010;13:266-286.
66. Modlin IM, Pavel M, Kidd M, Gustafsson BI. Review article: somatostatin analogues in the treatment of gastroenteropancreatic neuroendocrine (carcinoid) tumours. *Aliment Pharmacol Ther*. 2010;31:169-188.
67. Rinke A, Muller HH, Schade-Brittinger C, et al. Placebo-controlled, double-blind, prospective, randomized study on the effect of octreotide LAR in the control of tumor growth in patients with metastatic neuroendocrine midgut tumors: a report from the PROMID Study Group. *J Clin Oncol*. 2009;27:4656-4663.
68. Kvols LK, Martin JK, Marsh HM, Moertel CG. Rapid reversal of carcinoid crisis with a somatostatin analogue. *N Engl J Med*. 1985;313:1229-1230.
69. Raymond E, Dahan L, Raoul JL, et al. Sunitinib malate for the treatment of pancreatic neuroendocrine tumors. *N Engl J Med*. 2011;364:501-513.
70. Yao JC, Shah MH, Ito T, et al. Everolimus for advanced pancreatic neuroendocrine tumors. *N Engl J Med*. 2011;364:514-523.
71. Yao JC, Phan A, Hoff PM, et al. Targeting vascular endothelial growth factor in advanced carcinoid tumor: a random assignment phase II study of depot octreotide with bevacizumab and pegylated interferon alpha-2b. *J Clin Oncol*. 2008;26:1316-1323.
72. Pavel ME, Hainsworth JD, Baudin E, et al. Everolimus plus octreotide long-acting repeatable for the treatment of advanced neuroendocrine tumours associated with carcinoid syndrome (RADIANT-2): a randomised, placebo-controlled, phase 3 study. *Lancet*. 2011;378:2005-2012.
73. Di Bartolomeo M, Bajetta E, Zilembo N, et al. Treatment of carcinoid syndrome with recombinant interferon alpha-2a. *Acta Oncol*. 1993;32:235-238.
74. Oberg K. Interferon in the management of neuroendocrine GEP-tumors: a review. *Digestion*. 2000;62 Suppl 1:92-97.
75. Vitale G, van Koetsveld PM, de Herder WW, et al. Effects of type I interferons on IGF-mediated autocrine/paracrine growth of human neuroendocrine tumor cells. *Am J Physiol Endocrinol Metab*. 2009;296:E559-566.
76. Vitale G, de Herder WW, van Koetsveld PM, et al. IFN-beta is a highly potent inhibitor of gastroenteropancreatic neuroendocrine tumor cell growth in vitro. *Cancer Res*. 2006;66:554-562.
77. Booy S, van Eijck CH, Janssen JA, Dogan F, van Koetsveld PM, Hofland LJ. IFN-beta is a potent inhibitor of insulin and insulin like growth factor stimulated proliferation and migration in human pancreatic cancer cells. *Am J Cancer Res*. 2015;5:2035-2046.

- 78.** Eriksson B, Annibale B, Bajetta E, et al. ENETS Consensus Guidelines for the Standards of Care in Neuroendocrine Tumors: chemotherapy in patients with neuroendocrine tumors. *Neuroendocrinology*. 2009;90:214-219.
- 79.** Welin S, Sorbye H, Sebjornsen S, Knappskog S, Busch C, Oberg K. Clinical effect of temozolomide-based chemotherapy in poorly differentiated endocrine carcinoma after progression on first-line chemotherapy. *Cancer*. 2011;117:4617-4622.
- 80.** Kouvaraki MA, Ajani JA, Hoff P, et al. Fluorouracil, doxorubicin, and streptozocin in the treatment of patients with locally advanced and metastatic pancreatic endocrine carcinomas. *J Clin Oncol*. 2004;22:4762-4771.
- 81.** Strosberg JR, Fine RL, Choi J, et al. First-line chemotherapy with capecitabine and temozolomide in patients with metastatic pancreatic endocrine carcinomas. *Cancer*. 2011;117:268-275.
- 82.** Oberg K, Hellman P, Kwekkeboom D, Jelic S. Neuroendocrine bronchial and thymic tumours: ESMO Clinical Practice Guidelines for diagnosis, treatment and follow-up. *Ann Oncol*. 2010;21 Suppl 5:v220-222.
- 83.** Saif MW, Ove R, Ng J, Russo S. Radiotherapy in the management of pancreatic neuroendocrine tumors (PNET): experience at three institutions. *Anticancer Res*. 2013;33:2175-2177.
- 84.** Vogel J, Atanacio AS, Prodanov T, et al. External beam radiation therapy in treatment of malignant pheochromocytoma and paraganglioma. *Front Oncol*. 2014;4:166.
- 85.** Arvold ND, Willett CG, Fernandez-del Castillo C, et al. Pancreatic neuroendocrine tumors with involved surgical margins: prognostic factors and the role of adjuvant radiotherapy. *Int J Radiat Oncol Biol Phys*. 2012;83:e337-343.
- 86.** Valkema R, De Jong M, Bakker WH, et al. Phase I study of peptide receptor radionuclide therapy with [¹¹¹In-DTPA]octreotide: the Rotterdam experience. *Semin Nucl Med*. 2002;32:110-122.
- 87.** Anthony LB, Woltering EA, Espenan GD, Cronin MD, Maloney TJ, McCarthy KE. Indium-111-pentetreotide prolongs survival in gastroenteropancreatic malignancies. *Semin Nucl Med*. 2002;32:123-132.
- 88.** Waldherr C, Pless M, Maecke HR, Haldemann A, Mueller-Brand J. The clinical value of [90Y-DOTA]-D-Phe1-Tyr3-octreotide (90Y-DOTATOC) in the treatment of neuroendocrine tumours: a clinical phase II study. *Ann Oncol*. 2001;12:941-945.
- 89.** Waldherr C, Pless M, Maecke HR, et al. Tumor response and clinical benefit in neuroendocrine tumors after 7.4 GBq (90Y)-DOTATOC. *J Nucl Med*. 2002;43:610-616.
- 90.** Bodei L, Cremonesi M, Zoboli S, et al. Receptor-mediated radionuclide therapy with 90Y-DOTATOC in association with amino acid infusion: a phase I study. *Eur J Nucl Med Mol Imaging*. 2003;30:207-216.
- 91.** Valkema R, Pauwels S, Kvols LK, et al. Survival and response after peptide receptor radionuclide therapy with [90Y-DOTA₀Tyr₃]octreotide in patients with advanced gastroenteropancreatic neuroendocrine tumors. *Semin Nucl Med*. 2006;36:147-156.
- 92.** Kwekkeboom DJ, de Herder WW, Kam BL, et al. Treatment with the radiolabeled somatostatin analog [177 Lu-DOTA₀Tyr₃]octreotate: toxicity, efficacy, and survival. *J Clin Oncol*. 2008;26:2124-2130.
- 93.** Strosberg J, El-Haddad G, Wolin E, et al. Phase 3 Trial of 177Lu-Dotatate for Midgut Neuroendocrine Tumors. *N Engl J Med*. 2017;376:125-135.
- 94.** Kwekkeboom DJ, Bakker WH, Kooij PP, et al. [177Lu-DOTAOTyr₃]octreotate: comparison with [111In-DTPA₀]octreotide in patients. *Eur J Nucl Med*. 2001;28:1319-1325.
- 95.** Trotti A, Colevas A, Setser A, et al. CTCAE v3.0: development of a comprehensive grading system for the adverse effects of cancer treatment. *Seminars in Radiation Oncology*. 2003;13:176-181.

-
- 96.** Common Terminology Criteria for Adverse Events (CTCAE) v3.0. 9 August 2006; http://ctep.cancer.gov/protocolDevelopment/electronic_applications/docs/ctcae3.pdf.
- 97.** Common Terminology Criteria for Adverse Events (CTCAE) v4.03. 14 June 2010; http://evs.nci.nih.gov/ftp1/CTCAE/CTCAE_4.03_2010-06-14_QuickReference_5x7.pdf.
- 98.** Teunissen JJ, Krenning EP, de Jong FH, et al. Effects of therapy with [177Lu-DOTA 0,Tyr 3] octreotate on endocrine function. *Eur J Nucl Med Mol Imaging*. 2009;36:1758-1766.
- 99.** de Vries H, Verschueren RC, Willemse PH, Kema IP, de Vries EG. Diagnostic, surgical and medical aspect of the midgut carcinoids. *Cancer Treat Rev*. 2002;28:11-25.
- 100.** Dierdorf SF. Carcinoid tumor and carcinoid syndrome. *Curr Opin Anaesthesiol*. 2003;16:343-347.
- 101.** de Keizer B, van Aken MO, Feelders RA, et al. Hormonal crises following receptor radionuclide therapy with the radiolabeled somatostatin analogue [177Lu-DOTA0,Tyr3] octreotate. *Eur J Nucl Med Mol Imaging*. 2008;35:749-755.

1.2

DOSIMETRY IN PRRT

Dosimetry is used in the fields of health/medical physics and is concerned with the determination of radiation dose (or a related radiological quantity) that results from the interaction of ionizing radiation with matter. After the discovery of X-rays in 1895, quantification of radiation evolved quickly since harmful effects were discovered after irradiation of the first patients. In the early days, dosimetry was mainly used in external beam radiotherapy (EBRT) (1), but new applications for dosimetry were developed, like in radiation safety (2). In 1941, Saul Hertz gave the first successful therapeutic treatment with a radioactive compound (radioiodine, ^{131}I) to a patient with Graves disease (3). A decade later, Edith Quimby published the mathematical concept of internally administered radioactive isotopes (4). Whereas, Loevinger described the first dose equations for internal dosimetry in 1955 (5) and a decade later the committee on Medical internal radiation dose (MIRD) was founded (6).

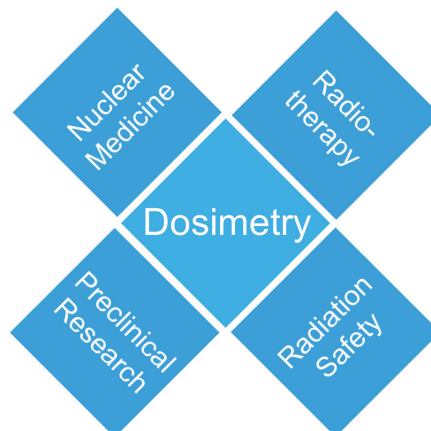


Figure 1: Different fields of dosimetry

EBRT is an example of external exposure, which occurs when a radiation source is outside of the body in contrast to internal exposure. The latter can occur after administration of radioactive isotopes in patients and the nuclear substances inside the body emit radiation. Dosimetry planning for EBRT is relatively straightforward with a homogeneous irradiation field, short exposure, and high-absorbed dose rate, in contrast to PRRT (table 1). Most of the knowledge about radiation effects concerns EBRT and radiobiology, therefore, specific dosimetric aspects for PRRT need to be explored (7).

Table 1: Overview of physical, dosimetrical and radiobiological characteristics of external beam radiotherapy (EBRT) and peptide radionuclide receptor therapy (PRRT).

Characteristics	EBRT	Brachytherapy	PRRT
- Physical			
Type of Irradiation	Homogeneous	Homo- or heterogeneous	Heterogeneous and mixed
Exposure to radioactive source	Short	Short-long	Protracted
Dose rate	High	Low-high	Low
- Dosimetry	Routinely used	Routinely used	Challenging
- Radiobiology			
Absorbed dose and toxicities	Established	Established	Unexplored
Response of irradiated tissues	Known	Known	Different than EBRT?
Dose–effect correlation	Known	Known	Limited data, see Strigari et al. (8)

In this subchapter a theoretical outline is given of dosimetry, imaging aspects and dosimetry of the critical organs in PRRT. In **Chapter 2** we analyze the relationship between the absorbed dose and toxicity for the kidneys, bonemarrow and spleen.

Models

Linear Quadratic Model

Cell survival models were initially developed to compare different dose rates in EBRT and brachytherapy exposures, but their fundamental nature also applies to radionuclide therapy. The linear quadratic model (LQM) represents the surviving fraction (*sf*) of cells after an absorbed dose *D* delivered instantaneously. The equation is:

$$sf(D) = e^{(-\alpha D - \beta D^2)} \quad (1.1)$$

where α and β are tissue specific constants, representing the damage induced by irreparable (i.e. double DNA strand breaks) or reparable (single DNA strand breaks) events. In the model, irreparable events depend on the absorbed dose *D* and they have a probability proportional to *D* by a factor α . At low dose the combined irreparable event is induced by a single electron track. At higher doses two or more independent (separately reparable) ionizing events may be induced by several electron tracks. The DNA damage combination may become irreparable and generate cellular death when occurring within a short time interval and in close distance of the DNA filament. This probability is proportional to the product of D^2 and β . The cell survival curve shows a bended shoulder on a logarithmic scale when this contribution dominates. Early

responding tissue like tumors show a less pronounced “shoulder” in their dose-response curve than late-responding tissue, like the kidneys.

When a dose D is delivered over a period of time (T), the DNA repair process (i.e. by repair enzymes) is initiated during the dose delivery and can then compete more effectively against radiation damage. An additional factor must therefore be introduced into the time-dependent LQ model equation:

$$sf(D(T)) = e^{(-\alpha D(T) - g(T)\beta D(T)^2)} \quad (1.2)$$

$$\text{with } g(T) = \frac{2}{D(T)^2} \int_0^T \dot{D}(t) dt \int_0^t \dot{D}(t') e^{-\mu(t-t')} dt' \quad (1.3)$$

where $g(T)$ is a dimensionless function with a value between 0 and 1, which describes the probability of lethal combinations of reparable events over time (T). When time (T) of the prolonged dose delivery becomes large with consequently a lower dose rate, late-responding normal tissue is saved relatively to the tumor as the lower dose rate reduces the “shoulder” effect which is stronger in normal tissue than in tumor tissue. This relative sparing condition can be compared with fractionated EBRT.

Biological effective dose (BED)

The linear quadratic model mathematically interprets this differential sparing and the BED concept is used to quantify the biological effects induced by different patterns of radiation delivery. BED allows for comparison of different irradiation conditions, producing the same endpoint of cell survival (sf). The BED has physical dimensions of an absorbed dose and is defined as:

$$BED = -\frac{1}{\alpha} \ln(sf) \leftrightarrow sf(BED) = e^{-\alpha BED} \quad (1.4)$$

This equation can be rewritten:

$$BED = D \cdot RE = D \left(1 + \frac{1/N}{\alpha/\beta} D \right) \quad (1.5)$$

Where, RE is the relative effectiveness and N is the number of given fractions. The ratio α/β with the dimension of dose gives an indication of the sensitivity of a tumour or normal tissue in response to changes in dose rate (fractionation). α/β indicates the dose where the linear contribution to cell kill is equal to the quadratic contribution. This ratio is in general higher for early responding tissue like tumours (5-25 Gy) than for late-responding normal tissues (2-5 Gy), e.g. kidneys.

BED values may be used to quantify the impact of a treatment on normal tissue and tumour. Biological effect (efficacy or toxicity) in PRRT can be predicted on the bases of BED by comparison with known EBRT BED values (9). Clinical use of BED in PRRT with ⁹⁰Y has proven to be a reliable predictor for renal toxicity (see section *Kidneys*)

Tumor control probability (TCP)

The expected response rate to radiation treatment can be visualised with the tumour control probability (TCP) for efficacy and normal tissue complication probability (NTCP) for toxicity. TCP and NTCP curves are typically sigmoid in shape.

Different dose response models have resulted in the same sigmoidal shaped curves (figure 2). One of these models is the logistic function:

$$P(D) = \frac{1}{1 + \left(\frac{D_{50}}{D}\right)^k} \tag{1.6}$$

where P is the probability of a clinical effect, D is the radiation absorbed dose and D_{50} is the radiation absorbed dose which leads to 50% cure/complication probability. The parameter k describes the slope of the dose-response curve (10).

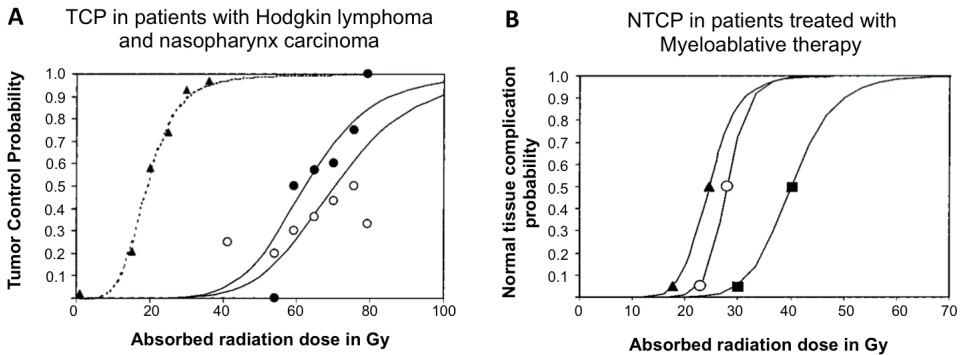


Figure 2: Relationship between tumor control (TCP) or normal tissue complication probability (NTCP) and radiation absorbed dose for representative tumor and normal tissues. **A.** shows representative TCP for Hodgkin’s lymphoma (11) (▲) and carcinoma of the nasopharynx (○ for T1–2 and ● for T3–4) (12). **B.** shows representative NTCP for the three most radiosensitive critical organs for a myeloablative therapy: the lungs (▲), kidneys (○), and liver (■). Complication endpoints are pneumonitis, clinical nephritis, and liver failure. The liver and kidneys are about a factor of two more sensitive than the tumor. Also, the dose-dependent onset of effects is significantly steeper for the normal tissues than for tumor. This is probably due to the greater conformity in dose-response for normal tissues than for tumor. Adapted from Hartmann *et al.* (10).

MIRD scheme

The medical internal radiation dosimetry (MIRD) scheme is the basis for absorbed dose calculations to internal organs, defined as the mean energy imparted to target tissue per unit tissue mass. In EBRT, dose calculations are relatively simple, since a calibrated external source (h) irradiates a target volume (k) within a selected time period. In PRRT, concentrations of radioactivity change over time in different organs (compartments), see figure 3. Therefore the intensity of irradiation to the source (k) by the radioactive sources (h_n) changes over time, there is also irradiation from the source itself (h_k).

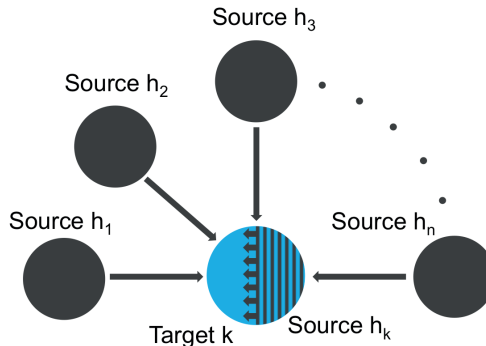


Figure 3: Graphical representation of the MIRD scheme. Sources (h_n) irradiate target (k) including irradiation from the source itself (h_k).

The mean absorbed dose ($D(r_T, T_D)$), to target tissue (r_T) can be calculated over a dose-integration period (T_D) from a uniformly distributed compound within a source tissue (r_S):

$$D(r_T, T_D) = \sum_{r_S} \tilde{A}(r_S, T_D) S(r_T \leftarrow r_S) =$$

$$\tilde{A}_1 \cdot S_{(k \leftarrow h_1)} + \tilde{A}_2 \cdot S_{(k \leftarrow h_2)} + \tilde{A}_3 \cdot S_{(k \leftarrow h_3)} + \dots + \tilde{A}_n \cdot S_{(k \leftarrow h_n)} \quad (1.7)$$

Where $\tilde{A}(r_S, T_D)$ is the time-integrated activity (no. of nuclear transformations) in r_S over T_D and $S(r_T \leftarrow r_S)$ is the absorbed dose rate in r_T per nuclear transformation in r_S .

The pharmacokinetics (PK) compartment model

The pharmacokinetics (PK) compartment model describes the biodistribution of a drug using a series of coupled differential equations for uptake and clearance in organs, which physiologically interact with that drug. This PK compartment model can be solved analytically for 2 or 3 compartments, or otherwise numerically. (e.g. with the SAAMII software Simulation Analysis and Modeling; SAAM Institute, Seattle, Washington State).

Since the peptide is radiolabelled, it is possible to follow the radioactivity at different time points to determine its biodistribution (and clearance). These time dependent measurements, which follow the total injected activity (IA) over time, enable the development of a mathematical description for the molecule uptake and excretion patterns in blood and each organ.

Organs with physiological uptake (kidneys, liver and spleen) are modeled using 2 compartments linked to the central (plasma) compartment, illustrated in figure 4. An additional extracellular fraction (ECF) single compartment was needed to fit the data. The urine data could be modeled by a single compartment linked to the kidney.

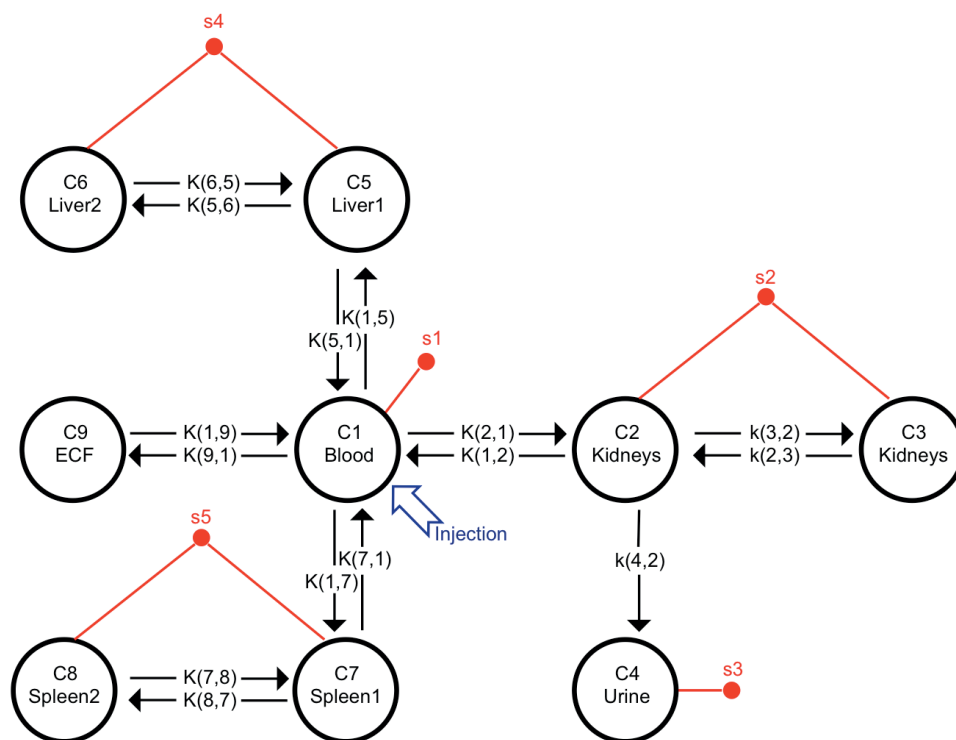


Figure 4: Generalized compartment model for the biodistribution of ^{177}Lu -Octreotate in humans. Abbreviations: Experimental input function; the time of drug administration (defined as T_0); red dots, Sample time points for the indicated compartments (organs); ECF, Extracellular fraction; C^{1-9} , Compartments (or organs) 1 to 9; $k(i,j)$, Kinetic transfer components between the indicated compartments i and j (organs).

The differential equations in the PK compartment model can be solved numerically. To do this, the amount of radioactivity administered to the central plasma compartment at time point 0 (T_0) is normalized to 100%, and assuming that the radioactivity is

uniformly distributed in a plasma distribution volume which is assumed to be constant at 5 L. The radioactivity in plasma is then expressed as a percentage of the total IA. This normalization enables a direct coupling of the plasma time-activity curve with the time-activity curves measured by planar imaging in the kidneys, spleen and liver, which are also normalized to the total IA.

Compartmental models can be utilized for describing the kinetics of the radioactive compound in the source tissue. Each compartment can be mathematically written as a nondifferential equation and can be solved numerically (13). In the model, the time-integrated activity $\tilde{A}(r_S, T_D)$ is the area under the curve for each compartment (organ).

Radionuclide-specific S values are available from calculations using a generic anatomic model (14,15). This Reference man model has some discrepancies in the calculated quantities therefore ICRP adopted radionuclide S values at voxel level for SPECT or PET imaging, published in MIRD pamphlet no. 17 (16). A new reference man phantom has been defined by ICRP based on average patient imagery and several more realistic calculation models have evolved (17,18).

The speed of Monte Carlo calculations have made it as one of the feasible methods for calculation of the absorbed dose to solid organs and tumors (19-21). Patient specific S-values, based on CT/MRI images, have contributed to the accuracy of dose estimates (22-24). Standard S factors can yield mean absorbed doses for normal organs or tumors with a reasonable accuracy (26% for 9 cases studied) as compared with absorbed doses calculated with Monte Carlo, provided that they have been corrected for mass (25).

However, Ljungberg et al. (26) demonstrated limited use of Monte Carlo simulation in post therapy ^{177}Lu -SPECT images since minor improvement in accuracy was found in the dose calculation. This is mainly due to the particle range of ^{177}Lu (2 mm) and the current spatial resolution of SPECT imaging (5 mm).

Most dosimetry models are based on rigid stylized phantoms with a possibility for correcting the dose by the actual organ volumes, but do not allow correction for the actual patient geometry (27). The Olinda/EXM code (15), considers only separate source organs and does not facilitate dose calculations for dispersed radioactivity by wide-spread receptor positive metastases. This technique has limitations for individual patient dosing, because it tends to overestimate organ doses and subsequently leads to conservative limits for the total cumulative dose of administered radioactivity.

Dosimetry in PRRT

PRRT using ^{177}Lu or ^{90}Y radiolabelled somatostatin analogs show similarities to widely used ^{131}I therapy (sodium-iodide Iodine-131) for the treatment of benign and malignant thyroid disorders (28). Table 1 shows the physical characteristics of ^{131}I , ^{90}Y and ^{177}Lu .

Table 3: Physical Characteristics of therapy radionuclides ^{131}I , ^{177}Lu and ^{90}Y (29).

Characteristic	^{131}I	^{90}Y	^{177}Lu
Decay half-life (d)	8.021 d	2.671 d	6.647 d
Mean β -particle energy (keV/decay)	181.9 keV	932.9 keV	133.3 keV
Main γ -rays energy (keV) and abundance (%/decay)	364 keV (81.7%/decay) 637 keV (7.2%/decay)	511 keV (0.00032 %/decay)	113 keV (6.4%/decay) 208 keV (11.0%/decay)
Penetration depth (R_{max})	3.4 mm	11.3 mm	1.8 mm
Mean range in tissue	0.39 mm	4.02 mm	0.23 mm

Early therapeutic dose-escalating studies in patient's demonstrated safe use of ^{90}Y - and ^{177}Lu radiolabelled somatostatin analogues. The radiation toxicity dose estimates in these studies were predominately based on experience and knowledge obtained from external beam radiation. In external beam radiotherapy, recommended radiation toxicity threshold doses are based on empirical data. Over the years, the quality of dosimetry in external beam radiotherapy has improved significantly, and the combination of clinical experience and information on normal organ tolerance doses has resulted in consensus guidelines (30). In external beam radiotherapy, dosimetry-based treatment planning has largely reduced toxicity in normal organs (31). Dosimetry is currently not general practice in PRRT but is developing rapidly.

Biodistribution and dosimetry studies have shown that one of the critical organs in radionuclide therapies (with ^{177}Lu and ^{90}Y) is the bone marrow (see Chapter 2.2 & 2.3). Also a decline in renal function has been observed, particular for radionuclide therapy with ^{90}Y labelled somatostatin analogues. Therefore, co-administration of amino acids is common during PRRT for minimal retention of the radiopeptide in the kidneys (32-34). More detailed information regarding renal toxicity after PRRT with ^{177}Lu -DOTATATE can be found in chapter 2.1.

^{90}Y labelled somatostatin analogues

Imaging and quantification in patients administered with ^{90}Y -labeled peptides is not straightforward since only beta particles are emitted with a maximum energy (E_{max}) of 2.27 MeV. The physical half-life is 2.7 days with a tissue penetration depth (R_{max}) of 12 mm. Four methods have been adopted for ^{90}Y -dosimetry: surrogate SPECT or PET-, bremsstrahlung- and direct PET-imaging.

Surrogate SPECT imaging

Surrogate imaging allows for quantitative analysis of ^{90}Y -therapy, based on the hypothesis that pharmacokinetics and biodistribution are comparable. The receptor-

specific uptake kinetics depends strongly on the amount of peptide used and the specific activity of the surrogate marker should therefore be adjusted to an equimolar to what is being used in the therapy setting (35). This reasoning is hardly fulfilled with most surrogate imaging settings and the resulted effects are not corrected.

In early studies, ^{111}In -DTPA-octreotide was used for simulating therapy with ^{90}Y -labeled compounds (36,37). However ^{111}In -DTPA-octreotide is limited as a surrogate for ^{90}Y -DOTATOC because of the difference in biochemical structure (e.g. different chelator) (37). Scintigraphic images derived from ^{111}In -DOTATOC, ^{111}In -DOTATATE and ^{111}In -Lanreotide reflect higher specific uptake in sst expressing tissue in comparison with ^{111}In -DTPA-octreotide (36-39).

Cremonesi et al. (40) used ^{111}In -DOTATOC for simulation of internal radiotherapy with ^{90}Y -DOTATOC. ^{111}In -DOTATOC showed favorable pharmacokinetics (fast blood clearance and urinary excretion) and biodistribution, as well as high affinity to tumors expressing somatostatin receptors. Though the metal replacement can alter the binding affinity of the radioligand (41).

Surrogate PET imaging

In diagnostic nuclear medicine, ^{68}Ga -labelled peptides are important for diagnoses of somatostatin positive receptors (42). Widely used ^{68}Ga Gallium labeled somatostatin analogues are DOTA-TOC, DOTA-NOC and DOTA-TATE (43). The high quality PET images make it ideal for imaging, but less suitable for pre-therapeutic dosimetry. The washout trend on the time-activity curves cannot be derived due to the short physical half-life (68 minutes). Beauregard et al. (44) demonstrated a tumor sink effect in patients with highly varied burden of somatostatin receptor-positive neuroendocrine tumor on ^{68}Ga -DOTA-octreotate PET. Tumor sequestration of radiopharmaceuticals may lead to a decrease in uptake in healthy tissue, particularly the renal parenchyma. Besides, it is not clear whether the ^{68}Ga Gallium molecule might alter the compound as compared to the ^{90}Y therapeutic agent.

Surrogate Positron Emission Tomography (PET) with ^{86}Y -labelled compounds offers substantial advantages over ^{111}In -labelled radiopeptides. The chemical structure of the compound is preserved and positron emitters allow the use of PET imaging which provides a higher quantitative accuracy and spatial resolution. Jamar et al. studied the pharmacokinetics and biodistribution of ^{86}Y -DOTATOC in 24 patients (45).

Förster et al. compared biodistribution and dosimetry in three patients injected with ^{86}Y -DOTATOC and ^{111}In -DTPA-Otctreotide (46). The authors found that dosimetry based on ^{86}Y -DOTATOC and ^{111}In -DTPA-octreotide yields similar organ doses, whereas there are relevant differences in estimated tumor doses. They stated that dosimetry should be performed with the chemically identical tracer ^{86}Y -DOTATOC. However, Barone et al.

observed an underestimation of the renal dose when using ^{111}In -DTPA-Octreotide in comparison with ^{86}Y -DOTATOC (47). Helisch et al. found an overestimation of doses to kidneys and spleen with ^{111}In -DTPA-Octreotide in comparison with ^{86}Y -DOTA-Phe1-Tyr3-octreotide (48). These contradictory results could be related to the method of imaging for ^{111}In -DTPA-Octreotide (SPECT vs. planar) and the use of amino acid infusion.

Application of ^{86}Y -labelled radioligands is limited, because it requires a PET facility and a high-energy cyclotron. Moreover, the short half-life of ^{86}Y -Yttrium (14.3 h) does not allow acquisitions beyond 48–72 h after tracer administration and overall clearance kinetics can only be estimated by extrapolation (after 48 h). The decay characteristics of ^{86}Y also involve a high number of prompt γ -rays responsible for overestimations of activity in the background and kidneys, when not properly accounted for.

Bremstrahlung imaging

Direct imaging of ^{90}Y can monitor distributions of ^{90}Y in patients after therapy; therefore there has been a great interest in quantitative imaging of ^{90}Y bremsstrahlung using SPECT. In the past, ^{90}Y labeled Selective internal radiation (SIR) spheres have been imaged using SPECT (49), though the quality of the images was relatively poor. The continuous and broad energy distribution of bremsstrahlung photons requires modeling of image degrading factors for accurate quantitative imaging.

Minarik et al. (50) demonstrated the feasibility of ^{90}Y bremsstrahlung quantitative SPECT by modeling the scatter (in a patient receiving ^{90}Y -Ibritumomab tiuxetan (Zevalin)). In whole-body images, the accuracy of the organ activities was most of the time within 15% (Minarik et al. 2009). In three patients, receiving ^{90}Y labeled radio immunotherapy, absorbed doses were calculated based on WB scintigraphy. Differences between absorbed-dose estimates from pre-therapeutic ^{111}In images were within 25%, except for the lungs. Their publications suggest that it is possible to quantify ^{90}Y activity in ROIs with reasonable accuracy using this method. Fabbri et al. (51) demonstrated feasibility of SPECT/CT ^{90}Y -bremsstrahlung imaging in a patient receiving ^{90}Y -DOTATATE (figure 5). Elschot et al. (52) compared quantitative PET and Bremsstrahlung SPECT for imaging the distribution of in vivo Yttrium-90 microsphere. The authors quantitatively demonstrated that the image quality of state-of-the-art PET is superior over Bremsstrahlung SPECT for the assessment of the ^{90}Y microsphere distribution after radio-embolization.

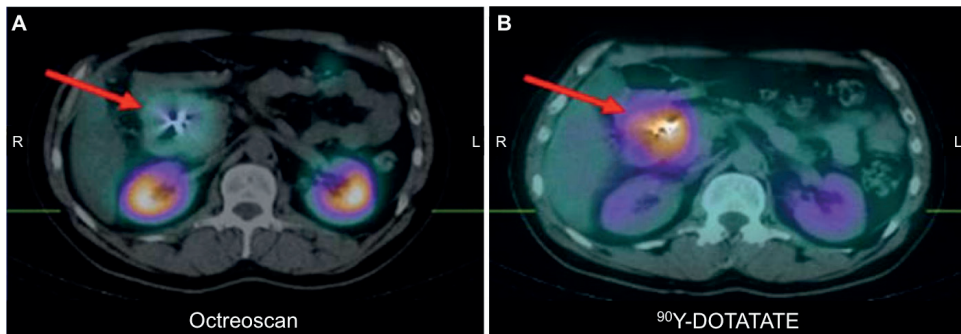


Figure 5 - Coronal slices of fused SPECT-CT, showing uptake in the abdominal lesion (red arrow), the kidneys and the spleen. Images obtained 24 h after the injection of (A) Octreoscan® (185 MBq), (B) ^{90}Y -DOTATATE (1.7 GBq). Images adopted from Fabbri et al. (51).

Direct TOF and non-TOF PET-imaging

Yttrium-90 internal pair production can be imaged by positron emission tomography (PET)/CT with or without time-of-flight capability (53,54). Dosimetry in liver selective internal radiotherapy (SIRT) by direct ^{90}Y time-of-flight (TOF) PET has proven feasible. L'Hommel et al. (55,56) demonstrated high-resolution absorbed dose distribution with a clear correlation with tumor response in one patient after administration of ^{90}Y -labelled SIR-spheres. 3D time of flight PET acquisition was used for imaging. Werner et al. (57) reproduced these results with a non-TOF PET/CT in a patient after selective internal radiotherapy (SIRT).

Walrand et al. (58) evaluated whether ^{90}Y TOF-PET was accurate enough for dosimetry in PRRT with ^{90}Y . The authors used an anthropomorphic fantome with Activities corresponded to typical tissue uptake in a first ^{90}Y -DOTATOC therapy cycle. Although ^{90}Y PET seems feasible in patients receiving radionuclide therapy, no clinical study has been published, so far. In a review article of Wallrand et al. (59) issues concerning ^{86}Y positron emission tomography (PET), ^{90}Y PET and ^{90}Y bremsstrahlung imaging are discussed. The potential imaging capabilities with the radioisotopes ^{87}Y and ^{88}Y are also considered.

Dosimetry with ^{90}Y -labelled peptides is not straightforward, since ^{90}Y decays with essentially no gamma photon emissions. Imaging over time can be done directly after therapy or pre-therapeutic with a surrogate radio peptide. Surrogate imaging results in good quantifiable images but pharmacokinetics and biodistribution could be different from the therapeutic radioligand. On the other hand, direct imaging by PET or bremsstrahlung is time consuming with limited quantification.

¹⁷⁷Lu labeled somatostatin analogues

Peptide receptor radionuclide therapy (PRRT) with ¹⁷⁷Lu-DOTA⁰-Tyr³-Octreotate is a low dose rate radiotherapy (as opposed to external beam radiation) developed for treatment of gastroenteropancreatic neuroendocrine tumors (GEP-NETs) that utilizes the carrier peptide, Octreotate. The radiolabelled peptide contains a DOTA-chelated radionuclide, Lutetium-177 (¹⁷⁷Lu). Octreotate binds with high affinity to somatostatin receptors that are overexpressed on the cell surface of most neuroendocrine tumors. The targeting of radiolabelled somatostatin analogues to tumor cells is the basis of the therapeutic effect of these pharmaceuticals.

The radiation toxicity dose estimates used in PRRT are predominately based on the experience and knowledge obtained from external beam radiation. In external beam radiotherapy, the recommended radiation toxicity threshold doses are based on empirical data. Over the years, the quality of dosimetry in external beam radiotherapy has improved significantly, and the combination of clinical experience and information on normal organ tolerance doses has resulted in consensus guidelines (60). Although the recommendations by Emami (60) contain several limitations and uncertainties, they address a clinical need in external beam radiotherapy, and consequently the incidence of radiation toxicity to normal organs has been reduced by dosimetry-based treatment planning (31).

In addition to the large base of empirical knowledge that has been obtained from external beam radiation research, there is also more than 60 years experience in radionuclide therapy, in particular with ¹³¹I therapy (sodium-iodide Iodine-131) for the treatment of benign and malignant thyroid disorders (28). The most common radiation induced toxicity following ¹³¹I therapy is bone marrow suppression, mainly thrombocytopenia. Limiting the prescribed cumulative administered radioactivity to a radioactivity level where the bone marrow dose remains below 2 Gy has proven to be a successful guideline for preventing hematological side-effects (61,62).

PRRT using ¹⁷⁷Lu-Octreotate shows significant similarities to ¹³¹I therapy. The data in table 3 show that the physical characteristics of ¹³¹I and ¹⁷⁷Lu are similar, except for the high energy γ (gamma)-rays of ¹³¹I, which cause a higher radiation dose to non-target regions (63). Biodistribution and radiation dosimetry studies have shown that the critical organ in both radionuclide therapies (¹³¹I and ¹⁷⁷Lu-Octreotate) is the bone marrow. In both radionuclide therapies, the absorbed dose in the bone marrow can exceed the toxicity threshold dose established with external beam radiotherapy (see data in table 4). ¹⁷⁷Lu-Octreotate treatment results in radiation doses to other organs, such as kidney, spleen and pituitary that may be higher than the doses resulting from ¹³¹I therapy. However, based on clinical experience, the spleen and pituitary are not critical organs in terms of

radiation related damage from PRRT. The kidneys (and the bone marrow) are generally considered to be the critical organs for therapy with ^{177}Lu -Octreotate. Therefore, it is common practice to co-administer amino acids to protect the kidneys (32,33,64,65).

Imaging

The residence time and localization of the Lutetium-177 can be estimated by scanning the patient at various times points post therapy. Siegel et al. described in MIRD pamphlet no. 16 (66), 2-dimensional quantitative planar imaging for calculation of the mean absorbed dose to target organs in patients. Errors of 30-100% have been reported when using this method of internal dose calculations (67). A recent MIRD pamphlet no. 23 (68), describes recommendations for patient-specific dosimetry with quantitative SPECT in internal radionuclide therapy. He et al. (69) compared different image acquisition methods with a phantom population and Monte Carlo simulations. Pure conventional planar images (CPlanar) performed worst with a mean error of 7-159% ($\pm <108\%$) and pure quantitative SPECT (QSPECT) performed best with a mean error of $< 9,9\%$ ($\pm <9,9\%$). The authors suggested hybrid CPlanar/QSPECT imaging (mean error $<19.2\%$ $\pm <22.0\%$) as the method of choice for clinical practice, due to its simplified image acquisition protocol. Garkavij et al. compared the same methods in a clinical setting with 16 NET patients treated with ^{177}Lu -Octreotate (70). Dosimetry based on planar images gave a higher absorbed dose to the kidneys in comparison with the two SPECT-based methods. Sandström et al. investigated the reliability of individualized Planar/SPECT-based dosimetry in 24 patients treated with ^{177}Lu -Octreotate (71). Planar and SPECT dosimetry were comparable in the tumor free areas, but planar dosimetry highly overestimated the absorbed dose in the organs with tumors. Despite the disadvantages of planar image acquisition, it is a widely used and accepted technique in PRRT (72-74). A major cause for the difference between planar imaging and quantitative SPECT is due to the overlap of high activity areas, which gives an overestimation of the organ activity (figure 6).

SPECT-derived images are limited in quantifying small volumes caused by the spatial resolution (5 mm). This partial volume effect underestimates the activity and absorbed dose within a volume of interest (VOI).

Quantitative SPECT can be accurate up to 10% with optimized hybrid SPECT/CT systems using iterative reconstruction algorithms and corrections for image-degrading physical factors. However, a hybrid method (Planar and SPECT/CT) may be better in clinical practice for a good balance between clinical feasibility and accuracy of dosimetric results.

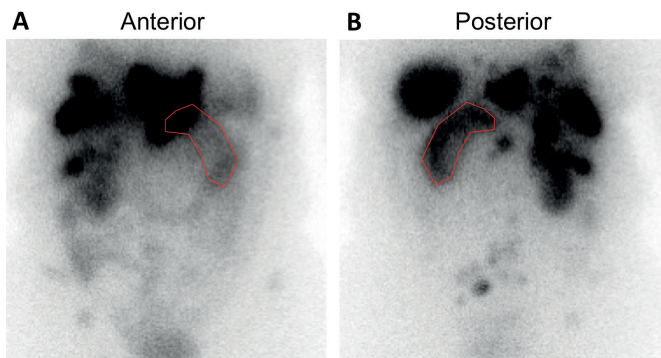


Figure 6 - Planar post therapy scan of a patient with a neuroendocrine tumor. A. anterior and B. posterior images. Red lines are the contour of the left kidney. Notice the overlap of the liver metastasis in the upper region of the kidney contour on the anterior image.

Garske et al. (Garske 2012) demonstrated significant differences in effective half-life during fractionated ^{177}Lu -octreotate therapies, especially in large tumor reductions during during treatment (75). The authors conclude that for most patients it is safe to estimate absorbed doses to kidney, liver and spleen from 24h activity concentration assuming an unchanged effective half-life during therapy. Patients with risk factors for kidney dysfunction or large changes in tumor size during therapy need to be monitored in more detail.

Planar dosimetry is accurate in patient populations to estimate stochastic risks, but inadequate for therapeutic applications, where toxicity and efficacy are the key issues (40). Therefore SPECT/CT should be used as a standard method for dosimetry in PRRT with ^{177}Lu radiolabelled somatostatin analogues (68). In clinical practice, a hybrid method (Planar and SPECT/CT) may be the best solution.

Bone Marrow

Radiation induced bone marrow toxicity results from damage of the hematopoietic tissue (the red marrow) where red blood cells, platelets and white blood cells are produced. The radiation dose to the red bone marrow contributes from β -ray irradiation of ^{131}I or ^{177}Lu in the blood circulating in the bone and from penetrating γ -ray radiation from activity dispersed throughout the remainder of the body. This 'blood dose' bone marrow dosimetry model has been safely employed for decades with ^{131}I therapy. It can also be used to determine the maximum dose that can be safely administered with ^{177}Lu -Octreotate. An overview of the radiation threshold doses to normal organs for external beam radiotherapy and ^{131}I therapy is given in table 4.

Table 4 Overview of radiation threshold doses to normal tissue for external beam radiotherapy and ^{131}I therapy.

Organ	Damage endpoints reported in literature	External beam radiotherapy threshold dose ¹ (Gy)	^{131}I Therapy, 30 GBq ² (Gy)
Thyroid	Ablation	80	Target
Bone marrow	Hypoplasia	2	2~4
Kidneys	Late nephritis	23	2~3
Urinary bladder	Contracture	65	10~15
Liver	Radiation Induced Liver Disease	30	1~2
Testes	Temporary infertility	0.15	0.5~1
Interstitialium (skin)	Temporary baldness	3	1~2
Salivary glands	Xerostomia	14	12~15
Pituitary	Hypopituitarism	45	NR
Spleen	Increased infection	40	NR
Pancreas	Hyperglycemia	NR	1.5
Adrenals	Hypoadrenalism	>60	1~2

¹Data from Marks L et al. (31) and ICRP41 (76); ²Iodine-131 therapy with a cumulative injected radioactivity of 30 GBq (ICRP 53 (77)); NR, Not reported.

Kidneys

Radiation induced kidney toxicity caused by PRRT is due to damage to the nephrons, the basic structural and functional units of the kidney. Nephrons consist of glomeruli and tubuli, which are responsible for filtration and reabsorption, respectively. The threshold dose for radiation damage to the kidneys by PRRT depends on the radionuclide that is used. To date the radionuclides used for PRRT with somatostatin analogues are Indium-111 (78,79), Yttrium-90 (^{90}Y ; (64,72,78,80-83) and Lutetium-177 (^{177}Lu ; (38,72,84,85))

Tubular reabsorption of ^{90}Y labeled peptides leads to a uniform radiation field to the kidney parenchyma that is comparable to that of external beam radiotherapy, despite the lower dose rate of PRRT (86). A correlation was found between the kidney radiation dose and chronic kidney toxicity after treatment with ^{90}Y -Octreotide. The dose at which 50% of the patients will encounter kidney toxicity was established to be $\text{ED}_{50} = 35$ Gy (87). This ED_{50} is 7 Gy higher than the 28 Gy established for external beam radiotherapy (88). Because the β -particles of ^{177}Lu has a shorter range than those from ^{90}Y , there is less damage to nearby non-target tissue (89,90). Moreover, PRRT using a radionuclide with much shorter-range emissions (^{111}In Auger electrons) does not result in kidney damage despite higher cumulative doses to the kidney (78). Therefore, 23 Gy is considered to be a conservative value for the radiation toxicity threshold dose for PRRT using ^{177}Lu -

Octreotide. A summary of previously reported kidney and bone marrow dosimetry findings in studies using ^{177}Lu -Octreotate are provided in Table 5.

Table 5: Overview of peer-reviewed publications on dosimetry for peptide receptor radionuclide therapy with ^{177}Lu -DOTA⁰-Tyr³-Octreotate.

Study	Method	N ¹	IA ² (GBq)	Amino Acids	Kidney dose per IA (Gy/GBq)	Bone marrow dose per IA (Gy/GBq)
Kwekkeboom (33)	Planar	5	1.85	Lys/Arg	0.88 ± 0.19	0.070 ± 0.009
Bodei (72)	Planar	5	3.7 – 5.18	NR	0.9 ± 0.5	NR
Bodei (91)	Planar	12	5.18 – 7.4	Lys/Arg	0.8 ± 0.4	NR
Forrer (92)	Planar	15	7.47 ± 0.10	Lys/Arg	NR	0.02-0.13
Wehrmann (73)	Planar	69	3-7	Lys/Arg	0.9 ± 0.3	0.05 ± 0.02
Sandström (71)	SPECT/CT	24	7.4	VAMIN-14	0.71 ± 0.24	NR
Sandström (93)	SPECT/CT	200	7.4	Vamin 14	1.2 ± 0.6	NR
Garkavij (70)	SPECT/CT	16	7.4	VAMIN-14	0.90 ± 0.21	0.07 ± 0.02
Swärd (74)	Planar	26	8	NR	0.9 ± 0.4	NR
Claringbold (94)	SPECT/CT	33	7.8	Synthamin	0.31 (0.14-0.46)	NR
Svennson (95)	Planar	51	3.5 – 8.2	Lys/Arg	0.8 ± 0.4	NR
This thesis (Chapter 2.1)	Planar	407	7.4	Lys/Arg	0.7 ± 0.2	NR
This thesis (Chapter 2.2)	Planar	24	7.4	Lys/Arg	NR	0.067 ± 0.007

N, Number of patients; IA, Administered radioactivity of ^{177}Lu -DOTA⁰-Tyr³-Octreotate; NR, Not reported.

The dosimetry data analyzed in Chapter 2 is based on planar measurements for dosimetry calculations. Despite the disadvantages of the use of planar image acquisition, it is a widely used and accepted technique in PRRT (72-74). The use of planar data based on conjugate view methods is known to be less accurate for determining kidney and other normal organ radiation doses. Studies, which directly compare SPECT and planar imaging, show that the planar imaging method consistently overestimates organ dosimetry (70,71,94). This is primarily due to the occurrence of overlapping radioactivity that appears on planar images such as from the overprojection of the liver with tumor nodules into the right kidney region of interest, and also from intestinal radioactivity potentially overlapping the left kidney, see figure 6 (73,74). For this reason, in the study reported here, the organ uptake (abdominal region) was not differentiated into separate organs and instead was considered to be a single source region. One issue with this approach, however, is that dosimetry models, like the Olinda/EXM code (15), consider

separate source organs only and do not facilitate dose calculations for dispersed radioactivity by wide-spread receptor positive metastases. Most dosimetry models are based on rigid stylized phantoms with a possibility for correcting the dose by the actual organ volumes, but do not allow correction for the actual patient geometry (96). The technique has limitations for individual patient dosing, because it tends to overestimate organ doses and subsequently leads to conservative limits for the total cumulative dose of administered radioactivity. However, planar imaging based dosimetry with ^{111}In -Octreotide has been of value in determining threshold doses in population studies for ^{90}Y -Octreotide therapy (40).

Studies based on planar measurements for dosimetry calculations were performed by Bodei L et al. (72), Wehrmann C et al. (73), and Swärd C et al. (74). In each of these studies, patients were treated with cumulative doses of approximately 30 GBq (800 mCi) ^{177}Lu -Octreotate given in 4 separate administrations and their findings are in good agreement with the data presented in this report. Bodei and coworkers (72) suggest that for patients without risk factors such as hypertension and diabetes, the threshold for kidney damage is set at a biologically effective dose (BED) of 40 Gy, which would correspond to a MIRD based radiation dose by ^{177}Lu of 36 Gy. In the report by Wehrmann no individual patient doses are given, but with a mean kidney dose per radioactivity of 0.9 ± 0.3 Gy/GBq the cumulative dose to the kidneys will be 27 ± 9 Gy for a cumulative administered radioactivity of 29.6 GBq. There was no indication in their publication of any adjustment of the dosing scheme. In the study by Swärd C et al. (74), the patients were scheduled for 4 administrations of 8 GBq each, unless the total radiation dose to the kidneys was more than 27 Gy. Only 12 out of 26 patients were given the full therapy of 4 administrations. The mean radiation dose to the kidneys was determined to be 24 ± 6 Gy, but no individual dosing schemes were provided. The reported patient-averaged dose per radioactivity is in the same order of magnitude as found by Wehrmann et al. (73) 0.9 ± 0.4 Gy/GBq. Therefore while these studies show general agreement on the radiation dose per unit of administered radioactivity to the kidneys, the lack of long-term follow-up data prevents any conclusions about long-term renal toxicity.

Testes

In men, PRRT with ^{177}Lu -octreotate induces transient inhibitory effects on spermatogenesis (temporary infertility) (97). Also somatostatin scintigraphy, demonstrates uptake in the gonads region (Figure 7). Current radiation models of the testes are simple and cannot predict clinical toxicity (short and late effects). In analogy to the radiation model of the kidneys (89), heterogeneities in radioactivity distribution on a microscopic level might improve the current radiation model of the testes (98).

In order to create a new radiation model of the testis, selective binding of ^{177}Lu -DOTATATE to the sst in the testes has to be demonstrated. Unger et al. (99) used polyclonal rabbit antisera on normal human testis tissue; the expression of ssts within the testis was very heterogenic. Sst type 2A was detected in the basal parts of the tubulus. Fombonne et al. (100) showed SSTR2A receptor expression in Leydig cells in situ from immature pigs using R57 antibody. Detailed cytological analysis demonstrated immunoreactivity to spermatogonia and Leydig Cells. However, both cell types immunostained heterogeneously, i.e. they showed varying intensity of labelling.

We performed several experiments on frozen testes material from 3 patients who underwent orchiectomies. Staining with the antibody SSTR2a (Biotrend, Human) demonstrates minimal staining, which is in lines with results from Unger et al (99). We also performed a hematoxylin-eosin (HE) staining (figure 8A) and autoradiography on testes material with ^{111}In DOTATATE and ^{111}In DOTATATE + block (figure 8B,C).

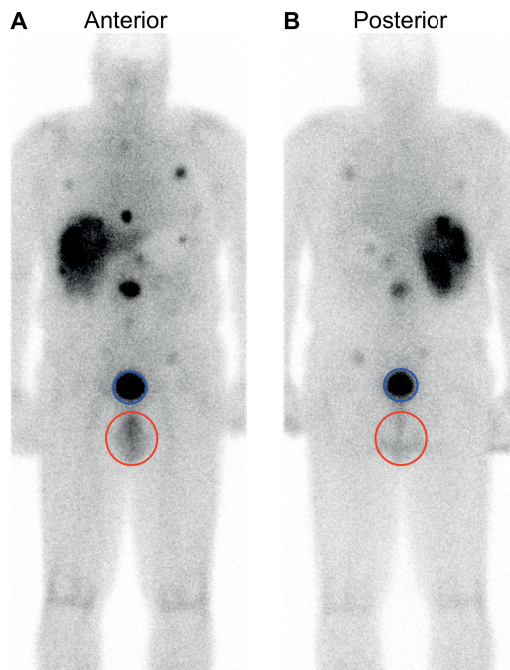


Figure 7. Whole body planar imaging of a male patient, which was performed in the anterior (A) and posterior (B) projections at 4 and 24 hours following the administration of ^{111}In -Octreotide. Blue circle marks the bladder and red circle points out the gonads.

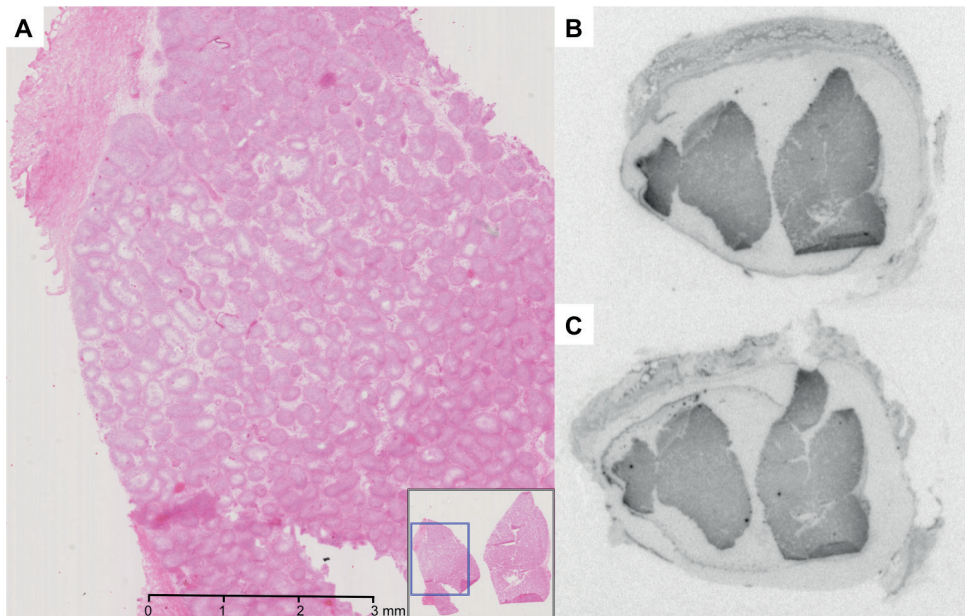


Figure 8 Hematoxylin and eosin stain of normal testes (A). Autoradiography of testis tissue with $1 \cdot 10^{-8}$ M $[^{111}\text{In}]\text{TATE}$ (B) and with block (C). On a visual scale there seems to be no difference between figure B & C, therefore there seems to be no somatostatin receptor selective binding.

On a visual scale, phosphor autoradiography did not show any difference between Block + $[^{111}\text{In}]\text{DOTATATE}$ (somatostatin receptors blocked) vs. $[^{111}\text{In}]\text{DOTATATE}$ (somatostatin receptors not blocked). Quantitative imaging demonstrated no difference in (radioactive) counts. Therefore, there seems to be no somatostatin receptor selective binding with $[^{111}\text{In}]\text{DOTATATE}$ autoradiography on testes tissue (n=3 patients). For this reason, no further enhancement of current dosimetric model for patients receiving $^{177}\text{Lu}\text{-DOTATATE}$ seems necessary.

REFERENCES

1. Thariat J, Hannoun-Levi JM, Sun Myint A, Vuong T, Gerard JP. Past, present, and future of radiotherapy for the benefit of patients. *Nat Rev Clin Oncol*. 2013;10:52-60.
2. Cool DA, Peterson HT, U.S. Nuclear Regulatory Commission. Office of Nuclear Regulatory Research. Division of Regulatory Applications. *Standards for protection against radiation, 10 CFR Part 20 : a comparison of the existing and revised rules*.
3. Fragu P. How the field of thyroid endocrinology developed in France after World War II. *Bulletin of the History of Medicine*. 2003;77:393-414.
4. Quimby EH. Dosimetry of internally administered radioactive isotopes. *A Manual of artificial radioisotope therapy*. 1951:46.
5. Loevinger R. CALCULATION OF RADIATION DOSAGE IN INTERNAL THERAPY WITH I-131. *Int: Radioisotopes in Medicine Sep-tember*. 1953:91.
6. Loevinger R, Berman M. A schema for absorbed-dose calculations for biologically-distributed radionuclides. MIRDO Pamphlet No. 1. *J Nucl Med*. 1968;9:7-14.
7. Pouget JP, Lozza C, Deshayes E, Boudousq V, Navarro-Teulon I. Introduction to radiobiology of targeted radionuclide therapy. *Front Med (Lausanne)*. 2015;2:12.
8. Strigari L, Konijnenberg M, Chiesa C, et al. The evidence base for the use of internal dosimetry in the clinical practice of molecular radiotherapy. *Eur J Nucl Med Mol Imaging*. 2014;41:1976-1988.
9. Dale R. Use of the Linear-Quadratic Radiobiological Model for Quantifying Kidney Response in Targeted Radiotherapy. *Cancer Biother. Radiopharm*. Vol 19; 2004:363-370.
10. Hartmann Siantar CL, Vetter K, DeNardo GL, DeNardo SJ. Treatment Planning for Molecular Targeted Radionuclide Therapy. *Cancer Biother Radiopharm*. Vol 17: Mary Ann Liebert, Inc. ; 2002:267-280.
11. Fletcher GH, Shukovsky LJ. The interplay of radiocurability and tolerance in the irradiation of human cancers. *J Radiol Electrol Med Nucl*. 1975;56:383-400.
12. Agren Cronqvist AK, Kallman P, Turesson I, Brahme A. Volume and heterogeneity dependence of the dose-response relationship for head and neck tumours. *Acta Oncol*. 1995;34:851-860.
13. MIRDO no. 12 - Kinetic Models for Absorbed Dose Calculations [computer program]. Version; 1977.
14. Snyder WS, Ford MR, Warner GG, Watson SB. "S"; absorbed dose per unit cumulated activity for selected radionuclides and organs. MIRDO Pamphlet No. 11. *Society of Nuclear ...*; 1975.
15. Stabin MG, Sparks RB, Crowe E. OLINDA/EXM: the second-generation personal computer software for internal dose assessment in nuclear medicine. *J Nucl Med*. 2005;46:1023-1027.
16. Bolch WE, Bouchet LG, Robertson JS, et al. MIRDO pamphlet No. 17: the dosimetry of nonuniform activity distributions--radionuclide S values at the voxel level. Medical Internal Radiation Dose Committee. *J Nucl Med*. Vol 40; 1999:115-365.
17. Stabin MG, Xu XG, Emmons MA, Segars WP, Shi C, Fernald MJ. RADAR reference adult, pediatric, and pregnant female phantom series for internal and external dosimetry. *J Nucl Med*. 2012;53:1807-1813.
18. Menzel HG, Clement C, DeLuca P. ICRP Publication 110. Realistic reference phantoms: an ICRP/ICRU joint effort. A report of adult reference computational phantoms. *Ann ICRP*. 2009;39:1-164.
19. Dieudonne A, Hobbs RF, Bolch WE, Sgouros G, Gardin I. Fine-resolution voxel S values for constructing absorbed dose distributions at variable voxel size. *J Nucl Med*. 2010;51:1600-1607.

20. Ljungberg M, Frey E, Sjögren K, Liu X, Dewaraja Y, Strand S-E. 3D absorbed dose calculations based on SPECT: evaluation for 111-In/90-Y therapy using Monte Carlo simulations. *Cancer Biother. Radiopharm.* Vol 18; 2003:99-107.
21. Wilderman SJ, Dewaraja YK. Method for Fast CT/SPECT-Based 3D Monte Carlo Absorbed Dose Computations in Internal Emitter Therapy. *IEEE Trans Nucl Sci.* 2007;54:146-151.
22. Tsougos I, Loudos G, Georgoulas P, Theodorou K, Kappas C. Patient-specific internal radionuclide dosimetry. *Nucl Med Commun.* 2010;31:97-106.
23. Dewaraja YK, Schipper MJ, Roberson PL, et al. 131I-tositumomab radioimmunotherapy: initial tumor dose-response results using 3-dimensional dosimetry including radiobiologic modeling. *J Nucl Med.* 2010;51:1155-1162.
24. Sgouros G, Squeri S, Ballangrud AM, et al. Patient-specific, 3-dimensional dosimetry in non-Hodgkin's lymphoma patients treated with 131I-anti-B1 antibody: assessment of tumor dose-response. *Journal of Nuclear Medicine.* Vol 44; 2003:260-268.
25. Divoli A, Chiavassa S, Ferrer L, Barbet J, Flux GD, Bardies M. Effect of patient morphology on dosimetric calculations for internal irradiation as assessed by comparisons of Monte Carlo versus conventional methodologies. *J Nucl Med.* 2009;50:316-323.
26. Ljungberg M, Sjogren-Gleisner K. The accuracy of absorbed dose estimates in tumours determined by quantitative SPECT: a Monte Carlo study. *Acta Oncol.* 2011;50:981-989.
27. Stabin MG. Uncertainties in internal dose calculations for radiopharmaceuticals. *Journal of Nuclear Medicine.* Vol 49; 2008:853-860.
28. Lassmann M, Hänscheid H, Chiesa C, et al. EANM Dosimetry Committee series on standard operational procedures for pre-therapeutic dosimetry I: blood and bone marrow dosimetry in differentiated thyroid cancer therapy. Vol 35; 2008:1405-1412.
29. Eckerman KF, Endo A, Medicine SoN, Committee SoNMMIRD. *MIRD: Radionuclide Data and Decay Schemes*: Society of Nuclear Medicine; 2007.
30. Emami B, Lyman J, Brown A, et al. Tolerance of normal tissue to therapeutic irradiation. *International Journal of Radiation Oncology*Biophysics*. Vol 21; 1991:109-122.
31. Marks LB, Yorke ED, Jackson A, et al. Use of normal tissue complication probability models in the clinic. *Int J Radiat Oncol Biol Phys.* 2010;76:S10-19.
32. Hammond PJ, Wade AF, Gwilliam ME, et al. Amino acid infusion blocks renal tubular uptake of an indium-labelled somatostatin analogue. *Br J Cancer.* 1993;67:1437-1439.
33. Kwekkeboom D, Bakker W, Kooij P, et al. [177 Lu-DOTA 0 ,Tyr 3]octreotate: comparison with [111 In-DTPA 0]octreotide in patients. *Eur. J. Nucl. Med. Mol. Imaging.* Vol 28; 2001:1319-1325.
34. Melis M, Krenning EP, Bernard BF, Barone R, Visser TJ, de Jong M. Localisation and mechanism of renal retention of radiolabelled somatostatin analogues. *Eur J Nucl Med Mol Imaging.* 2005;32:1136-1143.
35. Kletting P, Kull T, Maass C, et al. Optimized Peptide Amount and Activity for (9)(0)Y-Labeled DOTATATE Therapy. *J Nucl Med.* 2016;57:503-508.
36. Kwekkeboom D, Kooij P, Bakker W, Mäcke H, Krenning E. Comparison of 111In-DOTA-Tyr3-octreotide and 111In-DTPA-octreotide in the same patients: biodistribution, kinetics, organ and tumor uptake. *Journal of Nuclear Medicine.* Vol 40; 1999:762-767.
37. Pauwels S, Barone R, Walrand S, et al. Practical dosimetry of peptide receptor radionuclide therapy with (90)Y-labeled somatostatin analogs. *J Nucl Med.* 2005;46 Suppl 1:92S-98S.
38. Kwekkeboom DJ, Teunissen JJ, Bakker WH, et al. Radiolabeled somatostatin analog [177Lu-DOTA0,Tyr3]octreotate in patients with endocrine gastroenteropancreatic tumors. *J Clin Oncol.* 2005;23:2754-2762.

39. Virgolini I, Britton K, Buscombe J, Moncayo R, Paganelli G, Riva P. In- and Y-DOTA-¹¹¹In-reotide: results and implications of the MAURITIUS trial. *Semin Nucl Med.* 2002;32:148-155.
40. Cremonesi M, Ferrari M, Zoboli S, et al. Biokinetics and dosimetry in patients administered with (¹¹¹In)-DOTA-Tyr(3)-octreotide: implications for internal radiotherapy with (⁹⁰Y)-DOTATOC. *Eur J Nucl Med.* 1999;26:877-886.
41. Reubi J, Schär J, Waser B, Wenger S. Affinity profiles for human somatostatin receptor subtypes SSTR1–SSTR5 of somatostatin radiotracers selected for scintigraphic and radiotherapeutic use. *European journal of*; 2000:1-10.
42. Buchmann I, Henze M, Engelbrecht S, et al. Comparison of ⁶⁸Ga-DOTATOC PET and ¹¹¹In-DTPAOC (Octreoscan) SPECT in patients with neuroendocrine tumours. *Eur J Nucl Med Mol Imaging.* 2007;34:1617-1626.
43. Breeman WA, de Blois E, Sze Chan H, Konijnenberg M, Kwekkeboom DJ, Krenning EP. (⁶⁸Ga)-labeled DOTA-peptides and (⁶⁸Ga)-labeled radiopharmaceuticals for positron emission tomography: current status of research, clinical applications, and future perspectives. *Semin Nucl Med.* 2011;41:314-321.
44. Beaugard JM, Hofman MS, Kong G, Hicks RJ. The tumour sink effect on the biodistribution of ⁶⁸Ga-DOTA-octreotate: implications for peptide receptor radionuclide therapy. *Eur J Nucl Med Mol Imaging.* 2012;39:50-56.
45. Jamar F, Barone R, Mathieu I, et al. ⁸⁶Y-DOTA(0)-D-Phe1-Tyr3-octreotide (SMT487)—a phase 1 clinical study: pharmacokinetics, biodistribution and renal protective effect of different regimens of amino acid co-infusion. *Eur J Nucl Med Mol Imaging.* 2003;30:510-518.
46. Forster GJ, Engelbach MJ, Brockmann JJ, et al. Preliminary data on biodistribution and dosimetry for therapy planning of somatostatin receptor positive tumours: comparison of (⁸⁶Y)-DOTATOC and (¹¹¹In)-DTPA-octreotide. *Eur J Nucl Med.* 2001;28:1743-1750.
47. Barone R, Jamar F, Walrand D. Can ¹¹¹In-DTPA-Octreotide (IN-OC) predict kidney and tumor exposure during treatment with ⁹⁰Y-SMT487 (OctreoThetm)? *J Nucl Med.* 2000;41(5,suppl.):110P.
48. Helisch A, Forster GJ, Reber H, et al. Pre-therapeutic dosimetry and biodistribution of ⁸⁶Y-DOTA-Phe1-Tyr3-octreotide versus ¹¹¹In-pentetreotide in patients with advanced neuroendocrine tumours. *Eur J Nucl Med Mol Imaging.* 2004;31:1386-1392.
49. Mansberg R, Sorensen N, Mansberg V, Van der Wall H. Yttrium ⁹⁰ Bremsstrahlung SPECT/CT scan demonstrating areas of tracer/tumour uptake. *Eur J Nucl Med Mol Imaging.* 2007;34:1887.
50. Minarik D, Gleisner KS, Ljungberg M. Evaluation of quantitative (⁹⁰Y) SPECT based on experimental phantom studies. *Physics in medicine and biology.* Vol 53; 2008:5689-5703.
51. Fabbri C, Sarti G, Agostini M, Di Dia A, Paganelli G. SPECT/CT ⁹⁰Y-Bremsstrahlung images for dosimetry during therapy. *Ecancermedicalscience.* 2008;2:106.
52. Elschot M, Vermolen BJ, Lam MG, de Keizer B, van den Bosch MA, de Jong HW. Quantitative comparison of PET and Bremsstrahlung SPECT for imaging the in vivo yttrium-90 microsphere distribution after liver radioembolization. *PLoS One.* 2013;8:e55742.
53. Carlier T, Eugène T, Bodet-Milin C, et al. Assessment of acquisition protocols for routine imaging of Y-90 using PET/CT. *EJNMMI Res.* Vol 3; 2013:11.
54. Willowson K, Forwood N, Jakoby BW, Smith AM, Bailey DL. Quantitative (⁹⁰Y) image reconstruction in PET. *Medical Physics.* Vol 39; 2012:7153-7159.
55. Lhommel R, Goffette P, Van den Eynde M, et al. Yttrium-90 TOF PET scan demonstrates high-resolution biodistribution after liver SIRT. *Eur J Nucl Med Mol Imaging.* 2009;36:1696.

56. Lhommel R, van Elmbt L, Goffette P, et al. Feasibility of 90Y TOF PET-based dosimetry in liver metastasis therapy using SIR-Spheres. *Eur J Nucl Med Mol Imaging*. 2010;37:1654-1662.
57. Werner MK, Brechtel K, Beyer T, Dittmann H, Pfannenberger C, Kupferschlag J. PET/CT for the assessment and quantification of (90)Y biodistribution after selective internal radiotherapy (SIRT) of liver metastases. *Eur J Nucl Med Mol Imaging*. 2010;37:407-408.
58. Walrand S, Jamar F, van Elmbt L, Lhommel R, Bekonde EB, Pauwels S. 4-Step renal dosimetry dependent on cortex geometry applied to 90Y peptide receptor radiotherapy: evaluation using a fillable kidney phantom imaged by 90Y PET. *J Nucl Med*. 2010;51:1969-1973.
59. Walrand S, Flux GD, Konijnenberg MW, et al. Dosimetry of yttrium-labelled radiopharmaceuticals for internal therapy: 86Y or 90Y imaging? *Eur J Nucl Med Mol Imaging*. 2011;38 Suppl 1:S57-68.
60. Emami B, Purdy JA, Manolis J, et al. Three-dimensional treatment planning for lung cancer. *Int J Radiat Oncol Biol Phys*. 1991;21:217-227.
61. Benua RS, Cicale NR, Sonenberg M, Rawson RW. The relation of radioiodine dosimetry to results and complications in the treatment of metastatic thyroid cancer. *Am J Roentgenol Radium Ther Nucl Med*. 1962;87:171-182.
62. Verburg FA, Hanscheid H, Biko J, et al. Dosimetry-guided high-activity (131)I therapy in patients with advanced differentiated thyroid carcinoma: initial experience. *Eur J Nucl Med Mol Imaging*. 2010;37:896-903.
63. Eckerman K, Endo A. ICRP Publication 107. Nuclear decay data for dosimetric calculations. *Ann ICRP*. 2008;38:7-96.
64. Valkema R, De Jong M, Bakker WH, et al. Phase I study of peptide receptor radionuclide therapy with [¹¹¹In-DTPA]octreotide: the Rotterdam experience. *Semin Nucl Med*. 2002;32:110-122.
65. Bodei L, Cremonesi M, Zoboli S, et al. Receptor-mediated radionuclide therapy with 90Y-DOTATOC in association with amino acid infusion: a phase I study. *Eur J Nucl Med Mol Imaging*. 2003;30:207-216.
66. Siegel JA, Thomas SR, Stubbs JB, et al. MIRD pamphlet no. 16: Techniques for quantitative radiopharmaceutical biodistribution data acquisition and analysis for use in human radiation dose estimates. *Journal of Nuclear Medicine*. Vol 40; 1999:375-615.
67. Flux G, Bardies M, Monsieurs M, et al. The impact of PET and SPECT on dosimetry for targeted radionuclide therapy. *Z Med Phys*. 2006;16:47-59.
68. Dewaraja YK, Frey EC, Sgouros G, et al. MIRD pamphlet No. 23: quantitative SPECT for patient-specific 3-dimensional dosimetry in internal radionuclide therapy. *J Nucl Med*. 2012;53:1310-1325.
69. He B, Du Y, Segars WP, et al. Evaluation of quantitative imaging methods for organ activity and residence time estimation using a population of phantoms having realistic variations in anatomy and uptake. *Med Phys*. 2009;36:612-619.
70. Garkavij M, Nickel M, Sjogreen-Gleisner K, et al. 177Lu-[DOTA0,Tyr3] octreotate therapy in patients with disseminated neuroendocrine tumors: Analysis of dosimetry with impact on future therapeutic strategy. *Cancer*. 2010;116:1084-1092.
71. Sandstrom M, Garske U, Granberg D, Sundin A, Lundqvist H. Individualized dosimetry in patients undergoing therapy with (177)Lu-DOTA-D-Phe (1)-Tyr (3)-octreotate. *Eur J Nucl Med Mol Imaging*. 2010;37:212-225.
72. Bodei L, Cremonesi M, Ferrari M, et al. Long-term evaluation of renal toxicity after peptide receptor radionuclide therapy with 90Y-DOTATOC and 177Lu-DOTATATE: the role of associated risk factors. *Eur J Nucl Med Mol Imaging*. 2008;35:1847-1856.

- 73.** Wehrmann C, Senftleben S, Zachert C, Muller D, Baum RP. Results of individual patient dosimetry in peptide receptor radionuclide therapy with ¹⁷⁷Lu DOTA-TATE and ¹⁷⁷Lu DOTA-NOC. *Cancer Biother Radiopharm.* 2007;22:406-416.
- 74.** Sward C, Bernhardt P, Ahlman H, et al. [¹⁷⁷Lu-DOTA 0-Tyr 3]-octreotate treatment in patients with disseminated gastroenteropancreatic neuroendocrine tumors: the value of measuring absorbed dose to the kidney. *World J Surg.* 2010;34:1368-1372.
- 75.** Garske U, Sandstrom M, Johansson S, et al. Minor changes in effective half-life during fractionated ¹⁷⁷Lu-octreotate therapy. *Acta Oncol.* 2012;51:86-96.
- 76.** International Commission on Radiological Protection. Committee 1. *Nonstochastic effects of ionizing radiation : a report.* 1st ed. Oxford: New York : Published for the International Commission on Radiological Protection by Pergamon Press; 1984.
- 77.** International Commission on Radiological Protection. Committee 2., International Commission on Radiological Protection., Task Group of ICRP Committee 2 on Absorbed Dose to Patients from Radiopharmaceuticals. *Radiation dose to patients from radiopharmaceuticals : a report of a task group of Committee 2 of the International Commission on Radiological Protection.* 1st ed. Oxford ; New York: Published for the International Commission on Radiological Protection by Pergamon Press; 1988.
- 78.** Valkema R, Pauwels SA, Kvols LK, et al. Long-term follow-up of renal function after peptide receptor radiation therapy with (90)Y-DOTA(0),Tyr(3)-octreotide and (177)Lu-DOTA(0), Tyr(3)-octreotate. *J Nucl Med.* 2005;46 Suppl 1:835-915.
- 79.** Barone R, Walrand S, Konijnenberg M, et al. Therapy using labelled somatostatin analogues: comparison of the absorbed doses with ¹¹¹In-DTPA-D-Phe1-octreotide and yttrium-labelled DOTA-D-Phe1-Tyr3-octreotide. *Nucl Med Commun.* 2008;29:283-290.
- 80.** Waldherr C, Pless M, Maecke HR, Haldemann A, Mueller-Brand J. The clinical value of [90Y-DOTA]-D-Phe1-Tyr3-octreotide (90Y-DOTATOC) in the treatment of neuroendocrine tumours: a clinical phase II study. *Ann Oncol.* 2001;12:941-945.
- 81.** Paganelli G, Zoboli S, Cremonesi M, et al. Receptor-mediated radiotherapy with 90Y-DOTA-D-Phe1-Tyr3-octreotide. *Eur J Nucl Med.* Vol 28; 2001:426-434.
- 82.** Valkema R, Pauwels S, Kvols LK, et al. Survival and response after peptide receptor radionuclide therapy with [90Y-DOTA0,Tyr3]octreotide in patients with advanced gastroenteropancreatic neuroendocrine tumors. *Semin Nucl Med.* 2006;36:147-156.
- 83.** Bodei L, Cremonesi M, Grana C, et al. Receptor radionuclide therapy with 90Y-[DOTA]0-Tyr3-octreotide (90Y-DOTATOC) in neuroendocrine tumours. *Eur J Nucl Med Mol Imaging.* 2004;31:1038-1046.
- 84.** Kwekkeboom DJ, Bakker WH, Kam BL, et al. Treatment of patients with gastro-enteropancreatic (GEP) tumours with the novel radiolabelled somatostatin analogue [¹⁷⁷Lu-DOTA(0),Tyr3]octreotate. *Eur J Nucl Med Mol Imaging.* 2003;30:417-422.
- 85.** Kwekkeboom DJ, de Herder WW, Kam BL, et al. Treatment with the radiolabeled somatostatin analog [¹⁷⁷ Lu-DOTA 0,Tyr3]octreotate: toxicity, efficacy, and survival. *J Clin Oncol.* 2008;26:2124-2130.
- 86.** Barone R, Borson-Chazot F, Valkema R, et al. Patient-specific dosimetry in predicting renal toxicity with (90)Y-DOTATOC: relevance of kidney volume and dose rate in finding a dose-effect relationship. *J Nucl Med.* 2005;46 Suppl 1:995-1065.
- 87.** Wessels BW, Konijnenberg MW, Dale RG, et al. MIRD pamphlet No. 20: the effect of model assumptions on kidney dosimetry and response-implications for radionuclide therapy. *J Nucl Med.* 2008;49:1884-1899.
- 88.** Dawson LA, Kavanagh BD, Paulino AC, et al. Radiation-associated kidney injury. *Int J Radiat Oncol Biol Phys.* 2010;76:S108-115.

89. Konijnenberg M, Melis M, Valkema R, Krenning E, de Jong M. Radiation dose distribution in human kidneys by octreotides in peptide receptor radionuclide therapy. *J Nucl Med*. 2007;48:134-142.
90. De Jong M, Valkema R, Van Gameren A, et al. Inhomogeneous localization of radioactivity in the human kidney after injection of [(111)In-DTPA]octreotide. *J Nucl Med*. 2004;45:1168-1171.
91. Bodei L, Cremonesi M, Grana CM, et al. Peptide receptor radionuclide therapy with (1)(7)(7)Lu-DOTATATE: the IEO phase I-II study. *Eur J Nucl Med Mol Imaging*. 2011;38:2125-2135.
92. Forrer F, Krenning EP, Kooij PP, et al. Bone marrow dosimetry in peptide receptor radionuclide therapy with [177Lu-DOTA(0),Tyr(3)]octreotate. *Eur J Nucl Med Mol Imaging*. 2009;36:1138-1146.
93. Sandstrom M, Garske-Roman U, Granberg D, et al. Individualized dosimetry of kidney and bone marrow in patients undergoing 177Lu-DOTA-octreotate treatment. *J Nucl Med*. 2013;54:33-41.
94. Claringbold PG, Brayshaw PA, Price RA, Turner JH. Phase II study of radiopeptide 177Lu-octreotate and capecitabine therapy of progressive disseminated neuroendocrine tumours. *Eur J Nucl Med Mol Imaging*. 2011;38:302-311.
95. Svensson J, Berg G, Wangberg B, Larsson M, Forssell-Aronsson E, Bernhardt P. Renal function affects absorbed dose to the kidneys and haematological toxicity during (1)(7)(7)Lu-DOTATATE treatment. *Eur J Nucl Med Mol Imaging*. 2015;42:947-955.
96. Stabin MG. Uncertainties in internal dose calculations for radiopharmaceuticals. *J Nucl Med*. 2008;49:853-860.
97. Teunissen JJ, Krenning EP, de Jong FH, et al. Effects of therapy with [177Lu-DOTA 0,Tyr 3] octreotate on endocrine function. *Eur J Nucl Med Mol Imaging*. 2009;36:1758-1766.
98. Larsson E, Meerkhan SA, Strand SE, Jonsson BA. A small-scale anatomic model for testicular radiation dosimetry for radionuclides localized in the human testes. *J Nucl Med*. 2012;53:72-81.
99. Unger N, Ueberberg B, Schulz S, Saeger W, Mann K, Petersenn S. Differential expression of somatostatin receptor subtype 1-5 proteins in numerous human normal tissues. *Exp Clin Endocrinol Diabetes*. 2012;120:482-489.
100. Fombonne J, Csaba Z, von Boxberg Y, et al. Expression of somatostatin receptor type-2 (sst2A) in immature porcine Leydig cells and a possible role in the local control of testosterone secretion. *Reprod Biol Endocrinol*. 2003;1:19.

1.3

PEPTIDE RECEPTOR RADIONUCLIDE THERAPY FOR GEP-NETS

Hendrik Bergsma^a, Esther I. van Vliet^a, Jaap J.M. Teunissen^a, Boen L.R. Kam^a, Wouter W. de Herder^b, Robin P. Peeters^b, Eric P. Krenning^a, Dik J. Kwekkeboom^a

^a Department of Radiology & Nuclear Medicine,

^b Section of Endocrinology, Department of Internal Medicine, Erasmus MC, University Medical Center, Rotterdam, The Netherlands

ABSTRACT

Peptide receptor radionuclide therapy (PRRT) with radiolabelled somatostatin analogues plays an increasing role in the treatment of patients with inoperable or metastasised gastroenteropancreatic neuroendocrine tumors (GEP-NETs). ^{90}Y -DOTATOC and ^{177}Lu -DOTATATE are the most used radiopeptides for PRRT with comparable tumor response rates (about 15–35%). The side effects of this therapy are few and mild. However, amino acids should be used for kidney protection, especially during infusion of ^{90}Y -DOTATOC. Options to improve PRRT may include combinations of radioactive labeled somatostatin analogues and the use of radio-sensitizing drugs combined with PRRT. Other therapeutic applications of PRRT may include intra-arterial administration, neoadjuvant treatment and additional PRRT cycles in patients with progressive disease, who have benefited from initial therapy. Considering the mild side-effects, PRRT may well become the firstline therapy in patients with metastasized or inoperable GEP-NETs if more widespread use of PRRT can be accomplished.

Keywords:

Neuroendocrine tumors, Lutetium, Yttrium, Peptide receptor radionuclide therapy, PRRT, Somatostatin analogues

INTRODUCTION

In patients with inoperable metastasized gastroenteropancreatic neuroendocrine tumors (GEP-NETs), therapeutic options are limited. Treatment with somatostatin analogues such as octreotide and lanreotide reduces hormonal overproduction and can relieve symptoms in patients with GEP-NETs [1–3]. Furthermore, the long acting formula of the somatostatin Octreotide LAR significantly lengthens time to tumor progression in patients with metastatic midgut neuroendocrine tumors (NETs) [4].

The majority of GEP-NETs express somatostatin receptors, mainly somatostatin receptor subtype (1) 2 and 5 [5]. These can be visualized using radiolabelled somatostatin analogues. The first commercially available diagnostic somatostatin receptor analogues were [^{111}In -DTPA 0]octreotide (^{111}In -octreotide or Octreoscan) [6] and $^{99\text{m}}\text{Tc}$ -depreotide (NEOSPECT or NEOTECT). Nowadays newer positron emission tomography (PET) radiopharmaceuticals have been developed, such as [^{68}Ga -DOTA-Tyr 3]octreotide [7] and [^{68}Ga -DOTA-Tyr 3]octreotate [8].

After the introduction of ^{111}In -octreotide, the therapeutic application of high dose ^{111}In -octreotide showed promising results on symptomatology in patients with neuroendocrine tumors [9]. However, the reported number of objective responses was rather disappointing with a relatively low percentage of patients with tumor shrinkage. In subsequent studies, severe hematological toxicity (myelodysplastic syndrome (MDS) or leukemia) was observed in a few patients [10,11].

The use of beta-emitters, such as Yttrium-90 (^{90}Y) and Lutetium-177 (^{177}Lu) was made possible with the introduction of the chelator DOTA (1,4,7,10-tetraazacyclodecane-1,4,7,10-tetraacetic acid). Newer, more efficient, radiolabelled somatostatin analogues were developed with high affinity to the somatostatin receptor, such as [^{90}Y -DOTA 0 , Tyr 3]octreotide (^{90}Y -DOTATOC) and [^{177}Lu -DOTA 0 , Tyr 3]octreotate (^{177}Lu -DOTATATE). The main focus of this review is on this next generation of somatostatin analogues, labeled with ^{177}Lu and ^{90}Y .

Chelator and peptides

The structure of somatostatin analogues that are used for diagnostic and therapeutic purposes consists of three parts: a radionuclide, a chelator and a cyclic octapeptide (Figure 1).

DTPA (diethylene triamine penta-acetic acid) and DOTA (1,4,7,10-tetraazacyclododecane-1,4,7,20-tetra-acetic acid) are commonly used as chelators for PRRT. The most widely used combinations of peptide-chelators are [DOTA 0 ,Tyr 3]octreotide (DOTATOC) and [DOTA 0 ,Tyr 3]octreotate (DOTATATE). Other complexes include [DOTA 0 -1-Nal 3]octreotide (DOTANOC), ^{111}In -DOTA-lanreotide

(Lanreotide) and DTPA-octreotide. Changes in radionuclide and chelator can considerably alter compound characteristics, e.g. biochemical stability, excretion and receptor affinity. Reubi et al [12] reported affinity profiles (Table 1) for different somatostatin analogues in cell lines transfected with somatostatin receptor subtypes (sst_1 - sst_5). They concluded that small structural modifications, chelator substitution or metal replacement can considerably affect the binding affinity.

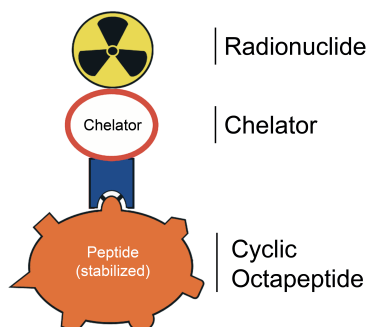


Figure 1 - Structure of Somatostatin Analogue: Radionuclide, Chelator and Cyclic Octapeptide (adapted from Eberle et al. [63]).

Table 1 - Affinity profile (IC_{50}) for human sst_1 - sst_5 receptors of a series of somatostatin analogues. Adapted from Reubi et al [12]

Peptides	Somatostatin receptor				
	Subtype 1	Subtype 2	Subtype 3	Subtype 4	Subtype 5
Somatostatin-28	5.2 (0.3)	2.7 (0.3)	7.7 (0.9)	5.6 (0.4)	4.0 (0.3)
Octreotide	> 10,000	2.0 (0.7)	187 (55)	>1,000	22 (6)
DTPA-octreotide	> 10,000	12 (4)	376 (84)	>1,000	299 (50)
^{111}In -DTPA-octreotide	> 10,000	22 (3.6)	182 (13)	>1,000	237 (52)
^{111}In -DTPA-[Tyr ³]octreotate	> 10,000	1.3 (0.2)	> 10,000	433 (16)	>1,000
DOTA-[Tyr ³]octreotide	> 10,000	14 (2.6)	880 (324)	>1,000	393 (84)
DOTA-[Tyr ³]octreotate	> 10,000	1.5 (0.4)	>1,000	453 (176)	547 (160)
DOTA- <i>lanreotide</i>	> 10,000	26 (3.4)	771 (229)	> 10,000	73 (12)
^{90}Y -DOTA-[Tyr ³]octreotide	> 10,000	11 (1.7)	389 (135)	> 10,000	114 (29)
^{90}Y -DOTA-[Tyr ³]octreotate	> 10,000	1.6 (0.4)	>1,000	523 (239)	187 (50)
^{90}Y -DOTA- <i>lanreotide</i>	> 10,000	23 (5)	290 (105)	> 10,000	16 (3.4)
^{90}Y -DOTA- <i>vapreotide</i>	> 10,000	12 (4)	102 (25)	778 (225)	20 (2.3)
^{68}Ga -DOTA-[Tyr ³]octreotide	> 10,000	2.5 (0.5)	613 (140)	>1,000	73 (21)
^{68}Ga -DOTA-[Tyr ³]octreotate	> 10,000	0.2 (0.04)	>1,000	300 (140)	377 (18)

All values are IC_{50} (Standard Error Mean) in nanometer.

No data are available for ^{177}Lu labeled somatostatin analogs.

Table 2 - Summary of PRRT clinical trials with ⁹⁰Y or ¹⁷⁷Lu-labelled somatostatin analogues in patients with GEP-NETs.

Reference	No. of patients	Progression at inclusion (%)	Reported Response					Criteria of Tumor Response	
			CR	PR	MR*	SD	PD		
[⁹⁰Y-DOTA⁰,Tyr³]octreotide									
Otte <i>et al.</i> 1999 [17]	16	NA	0	2(13%)	NA	13(81%)	1(6%)	2 / 16 (13%)	NA
Waldherr <i>et al.</i> 2001 [18]	37	76	1(3%)	9(24%)	N/I	23(62%)	4(11%)	10 / 37 (27%)	WHO
Waldherr <i>et al.</i> 2002 [25]	37	100	1(3%)	7(19%)	N/I	6(70%)	3(8%)	8 / 37 (22%)	WHO
Bodei <i>et al.</i> 2003 [65]	21	N/I	0	6(29%)	N/I	11(52%)	4(19%)	6 / 21 (29%)	WHO
Valkema <i>et al.</i> 2006 [19]	58	81	0	5(9%)	7(12%)	29(50%)	14(24%)	5 / 58 (9%)	SWOG
Bushnell <i>et al.</i> 2010 [20]	90	100	0	4(4%)	N/I	63 (70%)	15 (17%)	4 / 90 (4%)	SWOG
Pfeifer <i>et al.</i> 2011 ^b [22]	53	77	2 (4%)	10(19%)	N/I	34 (64%)	7 (13%)	12 / 53 (23%)	RECIST
[⁹⁰Y-DOTA]lanreotide									
Virgolini <i>et al.</i> 2002 [21]	39	100	0	0	8(20%)	17(44%)	14(36%)	0 / 39 (0%)	WHO
[⁹⁰Y-DOTA0, D-Phe1, Tyr3]octreotate									
Cwikla <i>et al.</i> 2010 [23]	60	100	0	13(23%)	N/I	44(77%)	3(5%)	13 / 60 (23%)	RECIST
[¹⁷⁷Lu-DOTA⁰,Tyr³]octreotate									
Kwekkeboom <i>et al.</i> 2008 [32]	310	38	5(2%)	86(28%)	51(16%)	107(35%)	61(20%)	91 / 310 (29%)	SWOG
Sward <i>et al.</i> 2010 [40]	16	N/I	0	6(38%)	N/I	8(50%)	2(13%)	6 / 16 (38%)	RECIST
Garkavij <i>et al.</i> 2010 [66]	12	N/I	0	2(17%)	3 (25%)	5(42%)	2(17%)	2 / 12 (17%)	RECIST
Bodei <i>et al.</i> 2011 [33]	39	N/I	1 (3%)	12(31%)	7(18%)	10(26%)	9(23%)	13 / 39 (33%)	RECIST

a. modification of the Southwest Oncology Group (SWOG) criteria including MR (minor remission), between 25 and 50% reduction of tumor size. b. We included another 4 patients to the PD group who died during the study.

* Response Evaluation Criteria In Solid Tumors (RECIST): PR (partial remission), ≥ 30% reduction in tumor size; MR (minor remission), 30% reduction or increase of SD (stable disease), < 30% reduction or increase of < 20% of tumor size; PD (progressive disease), ≥ 20% increase of tumor size or new lesion(s). Measurements: bidimensional

* World Health Organization (WHO): PR (Partial Remission) ≥ 50% reduction of tumor size; SD (Stable Disease), < 50% reduction or increase of < 25% of tumor size; PD (Progressive Disease), ≥ 25% increase of tumor size or new lesion(s). Bidimensional

* Southwest Oncology Group (SWOG): PR (partial remission), ≥ 50% reduction of tumor size; SD, Not qualifying for CR/PR/PD; PD, > 50% increase of tumor size. Measurements: unidimensional

* NA, Not Applicable or Non-Available

Radionuclide characteristics

Over the past two decades, different radionuclides have been used for PRRT. Indium-111 (^{111}In), with its auger electrons caused by gamma-emission, was used in early studies [10,11]. Besides encouraging results with regard to symptom relief, the reported number of objective responses was rather disappointing. Furthermore, ^{111}In -coupled peptides are not ideal for PRRT due to the small particle range and therefore low tissue penetration.

^{90}Y has high tissue penetration (12 mm) due to beta particles with a maximum energy of 2.27 MeV. The half-life of ^{90}Y 2.5 days is about the same in comparison with ^{111}In (2.8 days). Imaging is limited with ^{90}Y because no direct gamma-radiation is emitted. Only indirect gamma-radiation by deceleration of a charged particle, Bremsstrahlung, can be used for imaging [13]. ^{177}Lu with beta- and gamma-emission has a half-life of 6.7 days. The beta radiation of ^{177}Lu with an energy of 0.5 MeV has a tissue penetration depth of 2 mm. Gamma-rays at 208 and 113 keV, with yields of 10% and 6% respectively can be used for imaging purposes. In theory, the shorter beta-range of ^{177}Lu provides better irradiation of small tumors, in contrast to the longer beta-range of ^{90}Y which allows more uniform irradiation in large tumors with heterogeneous uptake [14]. De Jong et al [15] confirmed these findings in a preclinical study.

^{90}Y -labeled somatostatin analogues

Early studies with ^{90}Y labeled somatostatin analogues were done in Basel by Otte et al [16,17]. In their pilot study, 29 patients with mostly neuroendocrine tumors were treated with ^{90}Y -DOTATOC in a mean cumulative administered activity of 6120 ± 1347 MBq/m² given in four or more single injections. Sixteen patients were diagnosed with inoperable or metastasized GEP-NETs. Disease stabilization (2) was reported in 14 (88%) GEP-NET patients and one (6%) patient had a partial remission (PR). One (6%) patient had progressive disease (3).

Waldherr et al [18] reported overall tumor response rate (CR and PR) of 24% in 41 NET patients treated with four intravenous injections of a total of 6000 MBq/m² ^{90}Y -DOTATOC. The median follow up was 15 months (range 1–36 months).

In a multicenter dose escalating study [19], 58 GEP-NET patients received up to 14.8 GBq/m² of ^{90}Y -DOTATOC in four cycles or up to 9.3 GBq/m² in a single administration, without reaching the maximum tolerated single dose. The maximum cumulative radiation dose to the kidneys, estimated with planar scintigraphy, was limited to 27 Gy. Amino acids were given during infusion for renal protection. Three (5%) patients had dose-limiting toxicity: one liver toxicity, one thrombocytopenia grade 4 ($<25 \times 10^9/l$), and one MDS. Five (9%) out of 58 patients had PR, and seven (12%) patients had a minor

response (MR; 25–50% tumor volume reduction). The median time to progression was 29 months.

In a multicenter trial, 90 NET patients were treated with ⁹⁰Y-DOTATOC in fixed doses of three times 4.4 GBq [20]. Four (4.4%) patients had PD, whereas 63 (70%) out of 90 patients had SD. All patients had proven progression at baseline. Reversible renal toxicity (according to Common Toxicity Criteria (CTC) v2.0), grade 3 and 4, in three (3.3%) patients was reported, despite coadministration of amino acids. The median progression-free survival (PFS) was 16 months and the median overall survival (OS) was 27 months.

In the European Mauritius trial [21], 154 patients with different tumors were treated with [⁹⁰Y-DOTA]lanreotide (⁹⁰Y-DOTALAN) with cumulative doses up to 8.6 GBq. Within the GEP-NETs subgroup (39 patients), none showed PR and eight (20%) out of 39 patients demonstrated MR.

In a Danish cohort [22], 69 patients with mainly GEP-NETs were treated with ⁹⁰Y-DOTATOC and/or ¹⁷⁷Lu-DOTATOC. In one group (of 53 patients), ⁹⁰Y-DOTATOC was given in two cycles with cumulative doses of 9.62–15.54 GBq. Two (4%) patients had complete remission (CR) and PR was reported in ten (19%) patients.

Cwikla et al [23] described the results of treatment with ⁹⁰Y-DOTATATE in 60 GEP-NET patients. The cumulative dose was 11.2 GBq given in four therapy cycles. Three (5%) patients died after the second cycle due to extensive progressive disease. PR was reported in 13 (22%) out of 60 patients. The median PFS was 17 months and median OS was 22 months (with exclusion of the three deceased patients). Twelve months after the completion of the therapy, three (7%) out of 43 patients had grade 2 and two (5%) patients had grade 3 World Health Organization (WHO) renal toxicity.

Imhof et al [24] published the effects of treatment with ⁹⁰Y-DOTATOC in a large group of 1109 patients with NETs. Results in a smaller number of patients were also reported earlier [17,18,22,25]. After the first treatment cycle, response was evaluated and defined as clinical, biochemical or morphologic disease control. Morphologic response was assessed by computed tomography (CT), magnetic resonance imaging (MRI), or ultrasound. Tumor response was defined as any measurable decrease in the sum of the longest diameters of all pretherapeutically detected tumor lesions. Additional treatment cycles were given if no stop criteria were met: tumor progression during ⁹⁰Y-DOTATOC treatment or severe toxicity (grade 3–4 hematological toxicity and/or grade 4–5 renal toxicity according to CTC v3.0). Of 1109 patients, 378 (34%) had a morphologic response. Fifty-eight (5%) of these patients had SD. However response evaluation was not based on Response Evaluation Criteria In Solid Tumors (RECIST), Southwest Oncology Group (SWOG) or WHO criteria. The median survival from diagnosis was 95 months. No data on median PFS was available. Two (0.2%) patients developed myeloproliferative diseases.

One patient developed MDS after two cycles; one patient developed acute myeloid leukemia after four cycles. Despite infusion of amino acids for renal protection, 102 (9%) patients had severe permanent renal toxicity. Sixty-seven (6%) patients developed grade 3 (GFR 15–29 ml/min/1.73 m²) and 35 (3%) grade 4 (GFR < 15 ml/min/1.73 m²) renal toxicity. This relatively high incidence could be related to relatively high activities administered per cycle and to the fact that patients with pre-existing reduced kidney function were not excluded from treatment. The possible lack of use of amino acids in the first years of this study [17,18] must also be taken into account.

Table 2 summarizes the reported tumor outcome in different clinical trials using ⁹⁰Y labeled somatostatin analogues. Differences in outcome, despite using the same compound (⁹⁰Y-DOTATOC). This may be due to several factors. An important factor is the variety in administered doses (fixed or dose-escalating) and the number of therapy cycles. Furthermore, patient and tumor characteristics also differ between the studies mentioned, possibly contributing to the differences in radiological response.

¹⁷⁷Lu-labeled somatostatin analogues

De Jong et al [26] compared different radiolabelled somatostatin analogues in a preclinical setting. ¹¹¹In-octreotide, ⁹⁰Y-DOTATOC and ¹⁷⁷Lu-DOTATATE were injected in rats bearing Somatostatin receptor subtype 2 (sst₂) tumors. ¹⁷⁷Lu-DOTATATE demonstrated the highest tumor uptake together with excellent tumor-to-kidney ratios. Forrer et al [27] injected 222 MBq ¹¹¹In-DOTATOC and ¹¹¹In-DOTATATE within two weeks in five patients with metastatic neuroendocrine tumors. They examined whether one of the ¹¹¹In labeled peptides had a more favorable biodistribution and used ¹¹¹In as a surrogate for ⁹⁰Y and ¹⁷⁷Lu. The mean absorbed dose was calculated for tumors, kidney, liver, spleen and bone marrow. In all cases ¹¹¹In-DOTATATE showed a higher percentage of injected activity (%IA) in kidney and liver. ¹¹¹In-DOTATOC showed a higher tumor-to-kidney absorbed dose ratio in seven (78%) out of nine evaluated tumors. They concluded that the two peptides appear to be nearly equivalent for PRRT in neuroendocrine tumors, with minor advantages for ¹¹¹In-DOTATOC.

In an earlier study, Esser et al [28] compared ¹⁷⁷Lu-DOTATOC with ¹⁷⁷Lu-DOTATATE in seven patients. In the same patients 3.7 GBq of each compound was administered in separate therapy sessions (Figure 2). The residence times in the spleen and the kidneys were significantly longer after ¹⁷⁷Lu-DOTATATE injection. Also tumor uptake over time was longer after ¹⁷⁷Lu-DOTATATE, which resulted in a higher tumor dose. They concluded that ¹⁷⁷Lu-DOTATATE is the radiolabelled Somatostatin analogue of choice for PRRT.

Kwekkeboom et al [29] reported the first clinical results of ¹⁷⁷Lu-DOTATATE (cumulative dose 22.2–29.6 GBq) in 34 GEP-NET patients. Three months after the final administration, CR was found in one (3%) patient, partial remission in 12 (35%), stable disease in 14

(41%) and progressive disease in seven (21%) patients. Teunissen et al [30] evaluated the Quality of Life (QoL) in 50 Dutch patients before therapy and at follow-up visit six-weeks after the last cycle. A significant improvement in the global health status/QoL scale was observed after therapy with ^{177}Lu -DOTATATE. In the study that followed, Khan et al [31] concluded that ^{177}Lu -DOTATATE therapy not only can reduce tumor size and can prolong overall survival but also led to an improvement in symptoms. Two hundred and sixty-five (94%) out of 282 Dutch patients completed the Quality of Life (QoL) questionnaire at fixed times points: six weeks, three months and six months after therapy with ^{177}Lu -DOTATATE. In 40–70% of the patients, symptoms improved after ^{177}Lu -DOTATATE therapy and no significant decrease in QoL was observed in patients who had no symptoms before therapy.

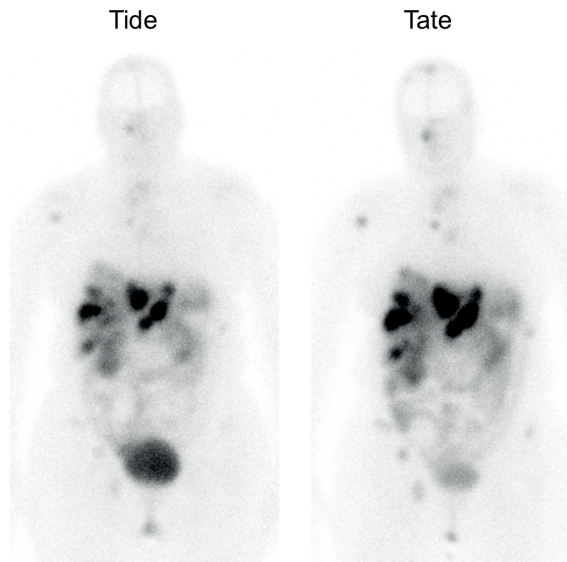


Figure 2 - Planar anterior scans of a patient with a GEP-NET after ^{177}Lu -DOTATOC (left) and ^{177}Lu -DOTATATE (right) injection. A longer mean residence time is observed on the ^{177}Lu -DOTATATE scan (right) in comparison with ^{177}Lu -DOTATOC (left). (Adapted from Esser et al.[28]).

Analysis of a large group of a total of 310 GEP-NET patients was published in 2008 [32]. Patients were treated with ^{177}Lu -DOTATATE up to 27.8–29.6 GBq, usually in four treatment cycles. Complete and partial tumor remissions (CR and PR) occurred in five (2%) and 86 (28%) of 310 GEP-NET patients, respectively. A reduced tumour uptake after the second, third or fourth therapy in comparison with first post-therapy scan was frequently seen in patients with PR during follow-up (Figure 3). The median PFS was 33 months. The most important factor predicting increased survival was treatment outcome. Patients with

PD had a significantly shorter survival in comparison with SD, CR, PR and MR. Compared with historical controls, there was a survival benefit of 40–72 months.

In a recent dose escalating study with ^{177}Lu -DOTATATE, Bodei et al [33] treated 51 patients with sst_2 receptor positive tumors. Forty-two (82%) patients were diagnosed with GEP-NETs. One patient (2%) had CR, 12 (29%) patients showed PR after the last administration of ^{177}Lu -DOTATATE. Three year overall survival was 68%. The median time to progression was 36 months, which is in accordance with results of the Kwekkeboom et al [32].

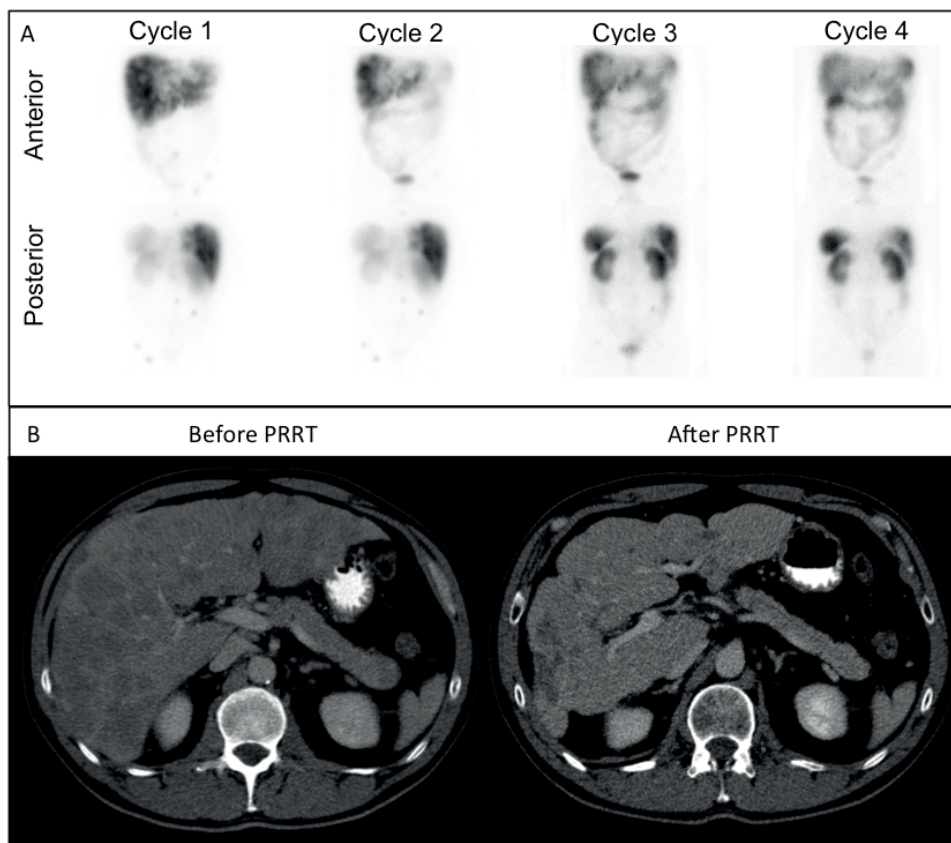


Figure 3 - A. Posterior and anterior post-therapy scans after each cycle of PRRT with 7400 MBq ^{177}Lu -DOTATATE in a patient with neuroendocrine tumor (primary in rectum) with liver metastasis who eventually had partial remission (PR) as tumor outcome. Note the decrease of uptake in the lesion of liver segment 8 compared to physiological liver uptake.

B. CT of abdomen of the same patient before PRRT (left panel) and 3 months after PRRT (right panel). (Adapted from Teunissen et al. [64])

Side effects

The kidneys are the dose-limiting organs for PRRT, when ^{90}Y labeled somatostatin analogues are used. Valkema et al [34] compared the decline in creatinine clearance after treatment with ^{90}Y -DOTATOC or ^{177}Lu -DOTATATE. A median decline in creatinine of 7.3% per year was observed in 28 patients treated with ^{90}Y -DOTATOC with a median follow-up of 2.9 years [35]. The median decline in creatinine was 3.8% per year in 37 patients treated with ^{177}Lu -DOTATATE (cumulative administered activity of 27.8–29.6 GBq) [29]. Two (7%) out of 28 patients treated with ^{90}Y -DOTATOC developed grade 3 renal toxicity. All patients treated with ^{90}Y -DOTATOC received concomitant amino acids for kidney protection, since high amounts of lysine lead to a greater reduction in renal uptake of radiopeptides [36]. The mean cumulative renal dose was higher in patients treated with ^{90}Y -DOTATOC than in patients treated with ^{177}Lu -DOTATATE (27 vs. 20 Gy). Age, hypertension and diabetes were probable risk factors contributing to a further decline of creatinine clearance after PRRT. Bodei et al [37] reported age, hypertension, diabetes and renal morphological abnormalities as contributing risk factors to a further decline of creatinine clearance. In the study of Bodei et al [37], who treated patient with ^{90}Y -DOTATOC, WHO grade 1–3 creatinine toxicity was reported in nine (3%) out of 23 patients. These patients were selected for further dosimetric studies out of a group of 211 patients. One of these nine patients developed a grade 3 (3–6 Upper Limit of Normal, ULN) renal toxicity. Patients were followed up for renal toxicity by measuring creatinine and creatinine clearance according to the Cockcroft–Gault formula.

In the study of Valkema et al [19], 58 patients were treated with ^{90}Y -DOTATOC with cumulative doses of 1.7 GBq up to 32.8 GBq. Two (4%) patients had dose-limiting toxicity unrelated to renal function: one patient had transient grade 3 liver toxicity and one patient had grade 4 thrombocytopenia. One (2%) patient developed MDS, two years after the start of PRRT. Nine (16%) patients had a more than 15% per year decline in creatinine clearance with end-stage renal disease in one patient.

Side effects of ^{177}Lu -DOTATATE were analyzed in 504 patients with GEP-NETs [32]. Subacute hematological toxicity (WHO grade 3 or 4) occurred four–eight weeks after at least one of several treatments in 48 (9.5%) patients. Factors associated with a higher frequency of hematological toxicity grade 3 or 4 were: age over 70 years, previous chemotherapy, creatinine clearance (calculated with Cockcroft–Gault formula) 60 ml/min, and the presence of bone metastasis. Serious delayed toxicities were observed in nine (2%) out of 504 patients. Two (0.4%) patients developed renal insufficiency, which was probably unrelated to treatment with ^{177}Lu -DOTATATE in both patients. Three (0.6%) patients had serious liver toxicity, two (0.4%) of whom were probably related to the treatment. MDS was found in four (0.8%) patients, which was potentially treatment related in three (0.6%) patients. In six patients with a hormonally highly active NET

(mostly VIPomas), a hormone-related crisis occurred after administration due to massive release of bioactive substances [38].

Bodei et al [33] reported in their dose escalating study with ^{177}Lu -DOTATE (Cumulative activities 3.7–29.2 GBq) of 51 patients, only one (2%) patient with both grade 3 leukopenia and thrombocytopenia.

Retreatment

Van Essen et al [39] reported successful retreatment with ^{177}Lu -DOTATATE in 33 NET patients. All patients had benefit from prior therapy with 18.5–29.6 GBq of ^{177}Lu -DOTATATE and later again experienced progressive disease, documented by CT or somatostatin receptor scintigraphy (SRS). Two additional cycles of 7.4 GBq ^{177}Lu -DOTATATE were given. Tumor response was evaluated using SWOG criteria. Two (6%) patients had PR, six (18%) patients responded with MR, SD was reported in ten (30%) patients and 15 (45%) patients had PD. No kidney failure or MDS was observed during a median follow-up of 16 months.

Forrer et al [36] also retreated 27 patients with ^{177}Lu -DOTATATE who had initially been treated with ^{90}Y -DOTATOC. The mean time between the initial treatment and retreatment was 15.4 months. All patients were injected with a single dose of 7.400 MBq ^{177}Lu -DOTATATE. In two (7%) patients PR was found, in five (19%) minor response, in 12 (44%) patients SD and PD in eight (30%) patients. ^{177}Lu -DOTATATE therapy was well tolerated and no severe toxicities (grade 3–4) occurred.

From these studies it can be concluded that patients with good response after initial therapy with PRRT are eligible for retreatment, but tumor response rates of retreatment are less favorable than for the initial treatment.

Dosimetry

In the first PRRT biodistribution and therapy studies, it was found that the kidneys and bone marrow are the critical organs for PRRT. The current role of dosimetry is that of a guide with respect to safety, especially to prevent kidney damage.

In a recent ^{177}Lu -DOTATATE dose escalating study of Bodei et al [33], evaluation of pharmacokinetics, activity biodistribution and absorbed dose to normal organs and tumors was performed. Fifty-one patients with metastatic sst₂-positive tumors (mainly NETs) were divided into two groups. Group 1 received escalating activities of 3.7–5.18 GBq/cycle and group 2 received escalating activities of 5.18–7.4 GBq/cycle. No major acute or delayed renal or hematological toxicity occurred. Cumulative renal absorbed doses were 8–37 Gy. A median decrease of creatinine clearance of 27.6% after two years was observed.

Cumulative bone marrow doses were <1.5 Gy. Blood cell counts showed a progressive mild drop during cycles and recovered during follow-up (median 30 months). The authors concluded that the maximum tolerated dose/cycle of ¹⁷⁷Lu-DOTATATE was not reached and therefore 7.4 GBq, as a maximum activity per cycle, can be used safely.

Sward et al [40] analyzed the clinical impact of dosimetry by using the absorbed dose to the kidneys as a limiting factor in treatments with ¹⁷⁷Lu-DOTATATE. Twenty-six patients with GEP-NETs were treated with 8 GBq/cycle in up to five cycles with a dose limit of 27 Gy to the kidneys. Ten (39%) out of 26 patients did not receive the planned four treatments due to dosimetric calculations to prevent overtreatment. Four patients had the potential to receive additional treatment without exceeding the dose limit. Three (12%) patients experienced CTC grade 3 hematologic with low platelet counts. A significant difference in glomerular filtration rate (GFR) was observed before treatment (80 ml/ 1.73 m²/min) in comparison with mean GFR at follow-up (70 ml/1.73 m²/min). The authors conclude that by using the absorbed dose to the kidneys as a limiting factor, treatment with ¹⁷⁷Lu-DOTATATE can be individualized. Overtreatment can be avoided and patients with the potential to receive additional treatment can be identified.

Dosimetry is currently used as a tool for risk assessment in critical organs. Dosimetric analysis can help maximize full potential of PRRT in regards of maximum activity per treatment cycle. In the future, individual dosimetry could be used for treatment planning of PRRT on a patient level.

Options to improve PRRT

Combination of compounds

A preclinical study by de Jong et al [15] compared the antitumoral effects of the combination of ¹⁷⁷Lu- and ⁹⁰Y-labelled somatostatin analogues with either ⁹⁰Y- or ¹⁷⁷Lu-analogue alone in animals bearing tumors of various sizes. The combination of both compounds was best for tumor control of both large and small tumors and resulted in the longest survival of the animals. The tumor in this rat model was rapidly growing and this may led to necrosis in parts of the tumor, therefore causing a heterogeneous expression of the somatostatin receptor. In contrast, neuroendocrine tumors in humans have a homogeneous receptor distribution and grow slowly. Extrapolation of preclinical results to neuroendocrine tumors in humans is limited, as has been reviewed by de Jong and Maina [41].

In a clinical setting, Frilling et al [42] treated 20 patients suffering from metastatic non-resectable NETs. All patients received ⁹⁰Y-DOTATOC as an initial treatment and additional sessions with ¹⁷⁷Lu- DOTATATE took place in six individuals. They concluded that it is safe to administer ⁹⁰Y-DOTATOC and additional ¹⁷⁷Lu-DOTATATE within a reasonable time in patients with NETs.

Villard et al [43] compared the efficacy of ^{90}Y -DOTATOC with a combination of ^{90}Y -DOTATOC and ^{177}Lu -DOTATATE in 486 patients with NETs. Patients receiving ^{90}Y -DOTATOC plus ^{177}Lu -DOTATATE had a significantly longer survival than patients receiving ^{90}Y -DOTATOC alone, 5.5 and 4.0 years respectively. This is a good result although a large discrepancy between the two treatment arms was observed. In this retrospective study 1396 patients were enrolled initially, but only patients who received more than two treatment cycles were included in the analysis. In order to be a candidate for a next treatment cycle, a patient had to benefit (clinically, biochemically or on tomographic imaging) from the previous treatment cycles. Thirty-eight (13%) out of 287 patients in the combination arm were not analyzed because they received two or less treatment cycles. On the other hand, 872 (71%) out of 1109 patients in the ^{90}Y -DOTATOC arm were not analyzed. A higher percentage of patients in ^{90}Y -DOTATOC group were not analyzed, which could imply that patients were in a poorer clinical condition than those treated with the combination of radiopharmaceuticals. This selection bias could influence trial outcome dramatically.

Kunikowska et al [44] published results of a retrospective, non-randomized study in 50 patients (25 per arm) with NETs. Candidates were treated with a combination of ^{90}Y -DOTATOC and ^{177}Lu -DOTATATE or with ^{90}Y -DOTATOC as a monotherapy. The investigators found that the median PFS was not significantly different between the groups, but that overall survival was longer in patients who were treated with the combination of radiopharmaceuticals. However, the median concentration of the serum tumour marker chromogranin A (CgA) was 179 microgram per liter in patients treated with the combination of radiopharmaceuticals, whereas it was 423 microgram per liter in the patients treated with ^{90}Y -DOTATOC only, suggesting a higher tumor load. This selection bias could have influenced outcome of this study.

Seregni et al [45] described a study protocol using a dual treatment with ^{90}Y -DOTATOC and ^{177}Lu -DOTATATE. Patients with NETs were treated with an intended dose of 5.6 GBq ^{177}Lu -DOTATATE alternating with 2.6 GBq ^{90}Y -DOTATOC with a total of four administrations. Nine (69%) out of 13 patients had progressive disease before treatment. Tumor response was PR in eight (62%) out of 13 patients with GEP-NETs. However, two patients who had a deterioration of their health condition during treatment were excluded from the analysis, thus resulting in a more favorable treatment outcome.

Despite these promising results from the studies mentioned above, doubts remain about the selection bias [46]. A proper randomized trial with long-term follow-up is necessary for final confirmation regarding PRRT with combined compounds.

Neo-adjuvant use of PRRT

In a case report, Kaemmerer et al [47] described the neoadjuvant use of ^{90}Y -DOTATATE in a patient with an initially inoperable malignant neuroendocrine tumor of the pancreas. In a Dutch cohort [32], four patients had inoperable pancreatic NETs that had not metastasized. Tumor shrinkage subsequent to treatment with ^{177}Lu -DOTATATE made these patients candidates for surgery (Figure 4).

Sowa-staszczak et al [48] treated 47 inoperable NET patients with ^{90}Y -DOTATOC. Six patients were selected for neoadjuvant treatment. Stabilization of the disease was observed in four (66%) patients and partial responses in two (33%) patients. Tumor response was evaluated by RECIST criteria. In two patients, reduction of the tumor size enabled surgical intervention.

Barber et al [49] treated five inoperable pancreatic and duodenal NET patients without distant metastatic disease with ^{177}Lu -DOTATATE and concurrent Fluorouracil (5-FU) chemotherapy. Patients were followed up three months post-treatment with SRS, radiology, biochemical markers and clinical assessment. All five patients had an ongoing treatment response beyond three months. One (20%) patient with localized pancreatic NET encasing the portal vein before PRRT was reconsidered for curative surgery. A complete resection was performed and histopathological evaluation confirmed surgical margins free of tumor.

In conclusion, PRRT can be effective in patients with inoperable GEP-NETs without other sites of unresectable metastatic disease. The neoadjuvant use of PRRT, though applicable in select cases only, may potentially cure such patients.

Intra-arterial administration

Selective hepatic intra-arterial injection of ^{90}Y -DOTA-lanreotide (DOTALAN) was safely used as a palliative therapy in 23 patients with large volume liver metastasis from NETs [50]. Selective hepatic intra-arterial injection of ^{90}Y -DOTALAN (36 treatments; median activity per dose, 1 GBq) was administered with or without embolization. Objective tumor response was classified according to WHO response criteria. PR after the treatment was accomplished in three (16%) out of 19 patients and stable disease was achieved in 12 (63%) patients. The authors concluded that hepatic intra-arterial injection of ^{90}Y -DOTALAN is a safe and effective palliative treatment.

Kratochwil et al [51] investigated the effectiveness of infusion into the hepatic artery of ^{90}Y -DOTATOC and/or ^{177}Lu -DOTATOC in 15 patients with liver metastases arising from GEP-NETs. Response was assessed using ^{68}Ga -DOTATOC PET, multiphase contrast enhanced CT, MRI and chromogranin A. CR was achieved in one (7%) patient and PR was observed in eight (53%) patients, six (40%) patients were classified as SD.

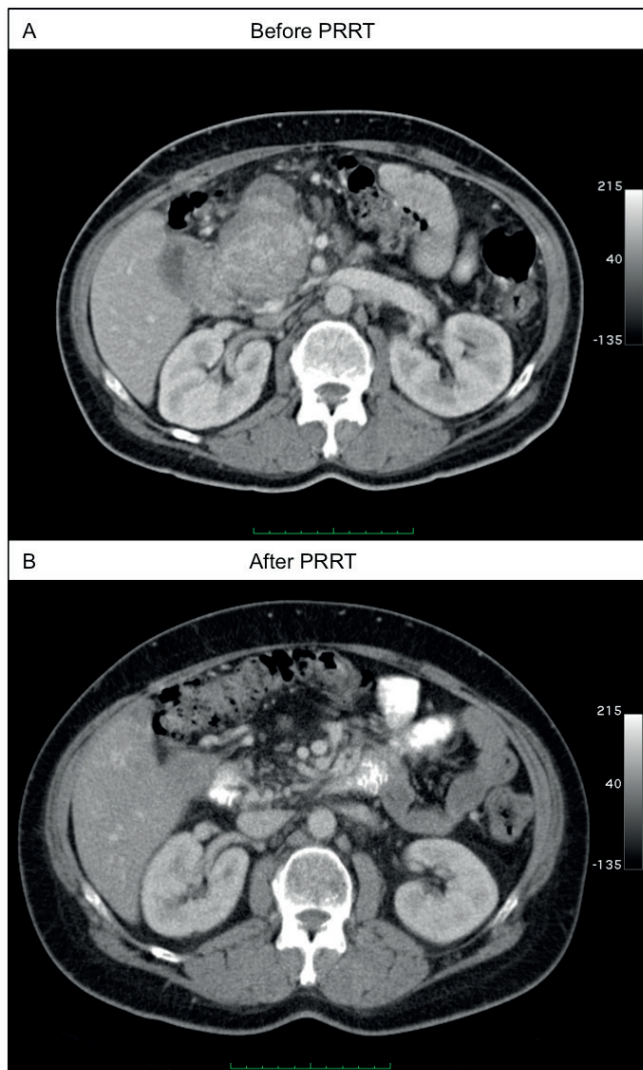


Figure 4 - Initially inoperable NET of the pancreas. CT of abdomen before (A) and 3 months after (B) PRRT in 4 cycles with cumulative 29.6 GBq of ^{177}Lu -DOTATATE. This patient had eventually partial remission (PR) as tumor outcome. A successful Whipple procedure plus reconstruction of the portal vein was performed 7 months after the last treatment. Resection edges and lymphnodes were free of tumor.

Limouris et al [52] evaluated the effectiveness of ^{111}In -octreotide after selective catheterization of the hepatic artery in 16 GEPNET patients with liver metastasis. These patients received a mean cumulative dose of 58 GBq ^{111}In -octreotide in a mean number of 11 treatments. Tumor response was CR in one (6%) patient and PR in eight (50%)

patients. Median survival time was 32 months for the patients with CR, PR or SD as a tumor response. Minimal hematological toxicity was observed in this study. WHO toxicity grade 1 anemia occurred in five (31%) patients and grade 1 leucocytopenia and thrombocytopenia in three (20%) patients.

The results of intra-arterial administration of PRRT is promising, though only GEPNET patients with a predominant tumor load in the liver can benefit. Furthermore intra-arterial administration makes PRRT more complex with additional risks (e.g. infection, bleeding).

Radiosensitising drugs and PRRT

A way to improve PRRT may be to combine the treatment with radiosensitizing chemotherapeutical agents (Cisplatin, 5-FU, capecitabine, etc.). Intravenous 5-FU was used in different trials to investigate the effects of (fractionated) external beam radiation on various tumor types. On a biochemical level, the enzyme thymidine phosphorylase (TP) converts the inactive form (capecitabine) into its active form (5-FU). Many tumors have a higher amount of TP and this results in an increased concentration of the active form in such tumors than in normal tissue. In addition, irradiation induces upregulation of TP in the tumor cell [53]. With the combination of external beam radiotherapy and capecitabine, an increased efficacy in terms of tumour growth control was reported, when compared to external beam radiotherapy as single treatment modality for a variety of tumors [54]. These results led to the hypothesis that PRRT in combination with capecitabine could be more effective than PRRT without capecitabine.

Van Essen et al [55] reported the safe use of ¹⁷⁷u-DOTATATE and capecitabine in seven patients with GEP-NETs. A clinical randomized controlled trial was started in our institution in 2008 to compare this combination with ¹⁷⁷Lu-DOTATATE as a single agent with regard to anti-tumor effects and side effects.

In a recent non-randomized study [56], 33 GEP-NET patients were treated with ¹⁷⁷Lu-DOTATATE in combination with capecitabine. The cumulative intended administered activity was 31.2 GBq with 14 days of 1.650 mg/m² capecitabine per day per treatment cycle. Three patients discontinued capecitabine use due to transient angina. Objective response rates (ORR) were: eight (24%) out of 33 patients had PR, and 23 (70%) out of 33 had SD according to the revised RECIST (version 1.1) criteria. The authors defined an increase of >30% in target lesions as PD, but in the revised RECIST guideline PD is defined as an increase of >20% in target lesions. This modified RECIST criteria could have influenced the outcome of PD in a positive way. A proper randomized control trial comparing treatment with ¹⁷⁷Lu-DOTATATE with and without capecitabine will demonstrate if capecitabine has an additive effect in NET patients treated with PRRT.

Targeted alpha-particle therapy

Alpha particles have a short path length and are potentially ideal to treat small tumor-volumes effectively. Several oncological studies with alpha-particle-emitting radionuclides have been reported, including the treatment of myeloid leukemia with an anti-CD33 monoclonal antibody labeled with ^{213}Bi [57], the therapy of patients with bone metastases from hormone- refractory prostate cancer with ^{223}Ra [58] and the loco-regional targeted radiotherapy with ^{211}At -labelled antitenascin monoclonal antibody in patients with recurrent malignant brain tumors [59].

Only limited research has been done on somatostatin analogues labeled with alpha-emitters. Nayak et al demonstrated in two preclinical studies [60,61] the advantages of ^{213}Bi -[DOTA⁰-Tyr³]-octreotide (^{213}Bi -DOTATATE) over ^{177}Lu -DOTATATE in somatostatin receptor-positive cell line (Capan-2).

In a clinical study, Kratochwil et al [62] reported preliminary data on the therapeutic application of the intra-arterial administration of alpha-emitter with ^{213}Bi -DOTATATE. Ten patients with neuroendocrine liver metastases were injected intra-arterially with ^{213}Bi -DOTATATE. No acute kidney, endocrine or hematologic toxicity (>grade 1) was observed during the first dose-escalating steps (2.5 GBq cumulative activity, 1.5 GBq per cycle).

Despite the conceptual appeal and the theoretical advantages, the translation of targeted alpha particle therapy into the clinical domain has been slow, in part because of limited radionuclide availability and the lack of alpha emitters with physical half-lives that can be implemented in the daily clinical practice.

SUMMARY

Peptide receptor radionuclide therapy (PRRT) with radiolabelled somatostatin analogues plays an increasing role in the treatment of patients with inoperable or metastasised gastroenteropancreatic neuroendocrine tumors (GEP-NETs). ^{90}Y -DOTATOC and ^{177}Lu -DOTATATE are the most used radio- peptides for PRRT with comparable tumor response rates (about 15–35%). The side effects of this therapy are few and mild. However, amino acids should be used for kidney protection, especially during infusion of ^{90}Y -DOTATOC. PRRT based on dosimetry could monitor and even prevent damage to normal organs on an individual level, especially when different 'cocktails' of radiopeptides are used.

Options to improve PRRT may include combinations of radioactive labeled somatostatin analogues and the use of radiosensitising drugs combined with PRRT. Other therapeutic applications of PRRT are neo-adjuvant treatment and additional therapy cycles in patients with progressive disease, after benefit from initial therapy. Intra-arterial administration could enhance tumor response rates with current radioactive compounds and can locally administer radiopeptides labeled with alpha-emitters.

If more widespread use of PRRT can be accomplished, PRRT may well become the therapy of first choice in patients with metastasized or inoperable GEP-NETs.

REFERENCES

1. Arnold R, Benning R, Neuhaus C, Rolwage M, Trautmann ME. Gastroenteropancreatic endocrine tumours: effect of Sandostatin on tumour growth. The German Sandostatin Study Group. *Digestion*. 1993;54 Suppl 1:72-75.
2. Janson ET, Oberg K. Long-term management of the carcinoid syndrome. Treatment with octreotide alone and in combination with alpha-interferon. *Acta Oncol*. 1993;32:225-229.
3. Ducreux M, Ruzsniowski P, Chayvialle JA, et al. The antitumoral effect of the long-acting somatostatin analog lanreotide in neuroendocrine tumors. *Am J Gastroenterol*. 2000;95:3276-3281.
4. Rinke A, Müller H-H, Schade-Brittinger C, et al. Placebo-controlled, double-blind, prospective, randomized study on the effect of octreotide LAR in the control of tumor growth in patients with metastatic neuroendocrine midgut tumors: a report from the PROMID Study Group. *J Clin Oncol*. 2009;27:4656-4663.
5. Reubi JC, Waser B, Schaer JC, Laissue JA. Somatostatin receptor sst1-sst5 expression in normal and neoplastic human tissues using receptor autoradiography with subtype-selective ligands. *Eur J Nucl Med*. 2001;28:836-846.
6. Balon HR, Goldsmith SJ, Siegel BA, et al. Procedure guideline for somatostatin receptor scintigraphy with (111)In-pentetreotide. *J Nucl Med*. Vol 42; 2001:1134-1138.
7. Gabriel M, Decristoforo C, Kendler D, et al. 68Ga-DOTA-Tyr3-octreotide PET in neuroendocrine tumors: comparison with somatostatin receptor scintigraphy and CT. *J Nucl Med*. 2007;48:508-518.
8. Kayani I, Bomanji JB, Groves A, et al. Functional imaging of neuroendocrine tumors with combined PET/CT using 68Ga-DOTATATE (DOTA-DPhe1,Tyr3-octreotate) and 18F-FDG. *Cancer*. 2008;112:2447-2455.
9. Krenning EP, Kooij PP, Bakker WH, et al. Radiotherapy with a radiolabeled somatostatin analogue, [111In-DTPA-D-Phe1]-octreotide. A case history. *Ann N Y Acad Sci*. 1994;733:496-506.
10. Valkema R, de Jong M, Bakker WH, et al. Phase I study of peptide receptor radionuclide therapy with [111In-DTPA]octreotide: the Rotterdam experience. *Semin Nucl Med*. 2002;32:110-122.
11. Anthony LB, Woltering EA, Espenan GD, Cronin MD, Maloney TJ, McCarthy KE. Indium-111-pentetreotide prolongs survival in gastroenteropancreatic malignancies. *Semin Nucl Med*. 2002;32:123-132.
12. Reubi JC, Schär JC, Waser B, et al. Affinity profiles for human somatostatin receptor subtypes SST1-SST5 of somatostatin radiotracers selected for scintigraphic and radiotherapeutic use. *Eur J Nucl Med*. 2000;27:273-282.
13. Walrand S, Barone R, Pauwels S, Jamar F. Experimental facts supporting a red marrow uptake due to radiometal transchelation in 90Y-DOTATOC therapy and relationship to the decrease of platelet counts. *Eur J Nucl Med Mol Imaging*. 2011;38:1270-1280.
14. O’Donoghue JA, Bardiès M, Wheldon TE. Relationships between tumor size and curability for uniformly targeted therapy with beta-emitting radionuclides. *J Nucl Med*. 1995;36:1902-1909.
15. de Jong M, Breeman WAP, Valkema R, Bernard BF, Krenning EP. Combination radionuclide therapy using 177Lu- and 90Y-labeled somatostatin analogs. *J Nucl Med*. 2005;46 Suppl 1:135-175.
16. Otte A, Jermann E, Behe M, et al. DOTATOC: a powerful new tool for receptor-mediated radionuclide therapy. *Eur J Nucl Med*. 1997;24:792-795.
17. Otte A, Herrmann R, Heppeler A, et al. Yttrium-90 DOTATOC: first clinical results. *Eur J Nucl Med*. 1999;26:1439-1447.

18. Waldherr C, Pless M, Maecke HR, Haldemann A, Mueller-Brand J. The clinical value of [90Y-DOTA]-D-Phe1-Tyr3-octreotide (90Y-DOTATOC) in the treatment of neuroendocrine tumours: a clinical phase II study. *Ann Oncol.* 2001;12:941-945.
19. Valkema R, Pauwels S, Kvols LK, et al. Survival and response after peptide receptor radionuclide therapy with [90Y-DOTA0,Tyr3]octreotide in patients with advanced gastroenteropancreatic neuroendocrine tumors. *Semin Nucl Med.* 2006;36:147-156.
20. Bushnell DL, O'Doriso TM, O'Doriso MS, et al. 90Y-edotreotide for metastatic carcinoid refractory to octreotide. *J Clin Oncol.* 2010;28:1652-1659.
21. Virgolini I, Britton K, Buscombe J, Moncayo R, Paganelli G, Riva P. In- and Y-DOTA-Ianreotide: results and implications of the MAURITIUS trial. *Semin Nucl Med.* 2002;32:148-155.
22. Pfeifer AK, Gregersen T, Grønbaek H, et al. Peptide receptor radionuclide therapy with Y-DOTATOC and (177)Lu-DOTATOC in advanced neuroendocrine tumors: results from a Danish cohort treated in Switzerland. *Neuroendocrinology.* 2011;93:189-196.
23. Cwikla JB, Sankowski A, Seklecka N, et al. Efficacy of radionuclide treatment DOTATATE Y-90 in patients with progressive metastatic gastroenteropancreatic neuroendocrine carcinomas (GEP-NETs): a phase II study. *Ann Oncol.* 2010;21:787-794.
24. Imhof A, Brunner P, Marincek N, et al. Response, survival, and long-term toxicity after therapy with the radiolabeled somatostatin analogue [90Y-DOTA]-TOC in metastasized neuroendocrine cancers. *J Clin Oncol.* 2011;29:2416-2423.
25. Waldherr C, Pless M, Maecke HR, et al. Tumor response and clinical benefit in neuroendocrine tumors after 7.4 GBq (90)Y-DOTATOC. *J Nucl Med.* 2002;43:610-616.
26. de Jong M, Valkema R, Jamar F, et al. Somatostatin receptor-targeted radionuclide therapy of tumors: preclinical and clinical findings. *Semin Nucl Med.* 2002;32:133-140.
27. Forrer F, Uusijärvi H, Waldherr C, et al. A comparison of (111)In-DOTATOC and (111)In-DOTATATE: biodistribution and dosimetry in the same patients with metastatic neuroendocrine tumours. *Eur J Nucl Med Mol Imaging.* 2004;31:1257-1262.
28. Esser JP, Krenning EP, Teunissen JJM, et al. Comparison of [(177)Lu-DOTA(3),Tyr(3)] octreotate and [(177)Lu-DOTA(3),Tyr(3)] octreotide: which peptide is preferable for PRRT? *Eur J Nucl Med Mol Imaging.* 2006;33:1346-1351.
29. Kwekkeboom DJ, Bakker WH, Kam BL, et al. Treatment of patients with gastro-entero-pancreatic (GEP) tumours with the novel radiolabelled somatostatin analogue [177Lu-DOTA(3),Tyr3]octreotate. *Eur J Nucl Med Mol Imaging.* 2003;30:417-422.
30. Teunissen JJM, Kwekkeboom DJ, Krenning EP. Quality of life in patients with gastroenteropancreatic tumors treated with [177Lu-DOTA0,Tyr3]octreotate. *J Clin Oncol.* 2004;22:2724-2729.
31. Khan S, Krenning EP, van Essen M, Kam BL, Teunissen JJ, Kwekkeboom DJ. Quality of Life in 265 Patients with Gastroenteropancreatic or Bronchial Neuroendocrine Tumors Treated with [177Lu-DOTA0,Tyr3]Octreotate. *J Nucl Med.* 2011;52:1361-1368.
32. Kwekkeboom DJ, de Herder WW, Kam BL, et al. Treatment with the radiolabeled somatostatin analog [177 Lu-DOTA 0,Tyr3]octreotate: toxicity, efficacy, and survival. *J Clin Oncol.* 2008;26:2124-2130.
33. Bodei L, Cremonesi M, Grana CM, et al. Peptide receptor radionuclide therapy with ¹⁷⁷Lu-DOTATATE: the IEO phase I-II study. *Eur J Nucl Med Mol Imaging.* 2011;38:2125-2135.
34. Valkema R, Pauwels SA, Kvols LK, et al. Long-term follow-up of renal function after peptide receptor radiation therapy with (90)Y-DOTA(3),Tyr(3)-octreotide and (177)Lu-DOTA(3), Tyr(3)-octreotate. *J Nucl Med.* 2005;46 Suppl 1:83S-91S.

35. Smith MC, Liu J, Chen T, et al. OctreoTher: ongoing early clinical development of a somatostatin-receptor-targeted radionuclide antineoplastic therapy. *Digestion*. 2000;62 Suppl 1:69-72.
36. Forrer F, Uusijärvi H, Storch D, Maecke HR, Mueller-Brand J. Treatment with 177Lu-DOTATOC of patients with relapse of neuroendocrine tumors after treatment with 90Y-DOTATOC. *J Nucl Med*. 2005;46:1310-1316.
37. Bodei L, Cremonesi M, Ferrari M, et al. Long-term evaluation of renal toxicity after peptide receptor radionuclide therapy with 90Y-DOTATOC and 177Lu-DOTATATE: the role of associated risk factors. *Eur J Nucl Med Mol Imaging*. 2008;35:1847-1856.
38. de Keizer B, van Aken MO, Feelders RA, et al. Hormonal crises following receptor radionuclide therapy with the radiolabeled somatostatin analogue [177Lu-DOTA0,Tyr3]octreotate. *Eur J Nucl Med Mol Imaging*. 2008;35:749-755.
39. van Essen M, Krenning EP, Kam BLR, de Herder WW, Feelders RA, Kwekkeboom DJ. Salvage therapy with (177)Lu-octreotate in patients with bronchial and gastroenteropancreatic neuroendocrine tumors. *J Nucl Med*. 2010;51:383-390.
40. Swärd C, Bernhardt P, Ahlman H, et al. [177Lu-DOTA 0-Tyr 3]-octreotate treatment in patients with disseminated gastroenteropancreatic neuroendocrine tumors: the value of measuring absorbed dose to the kidney. *World J Surg*. 2010;34:1368-1372.
41. de Jong M, Maina T. Of mice and humans: are they the same?--Implications in cancer translational research. *J Nucl Med*. 2010;51:501-504.
42. Frilling A, Weber F, Saner F, et al. Treatment with 90Y- and 177Lu-DOTATOC in patients with metastatic neuroendocrine tumors. *Surgery*. 2006;140:968-977.
43. Villard L, Romer A, Marincek N, et al. Cohort study of somatostatin-based radiolabeled peptide therapy with [(90)Y-DOTA]-TOC versus [(90)Y-DOTA]-TOC plus [(177)Lu-DOTA]-TOC in neuroendocrine cancers. *Journal of Clinical Oncology*. 2012;30:1100-1106.
44. Kunikowska J, Królicki L, Hubalewska-Dydejczyk A, Mikołajczak R, Sowa-Staszczak A, Pawlak D. Clinical results of radionuclide therapy of neuroendocrine tumours with 90Y-DOTATATE and tandem 90Y/177Lu-DOTATATE: which is a better therapy option? *Eur J Nucl Med Mol Imaging*. 2011;38:1788-1797.
45. Seregni E, Maccauro M, Coliva A, et al. Treatment with tandem [(90)Y]DOTA-TATE and [(177)Lu]DOTA-TATE of neuroendocrine tumors refractory to conventional therapy: preliminary results. *Q J Nucl Med Mol Imaging*. 2010;54:84-91.
46. Kwekkeboom DJ. Therapy: Neuroendocrine cancer--are two radionuclides better than one? *Nat Rev Endocrinol*. Jul, 2012: 326-328.
47. Kaemmerer D, Prasad V, Daffner W, et al. Neoadjuvant peptide receptor radionuclide therapy for an inoperable neuroendocrine pancreatic tumor. *World J Gastroenterol*. 2009;15:5867-5870.
48. Sowa-Staszczak A, Pach D, Chrzan R. Peptide receptor radionuclide therapy as a potential tool for neoadjuvant therapy in patients with inoperable neuroendocrine tumours (NETs). *European journal of ...* 2011.
49. Barber TW, Hofman MS, Thomson BNJ, Hicks RJ. The potential for induction peptide receptor chemoradionuclide therapy to render inoperable pancreatic and duodenal neuroendocrine tumours resectable. *Eur J Surg Oncol*. 2012;38:64-71.
50. McStay MKG, Maudgil D, Williams M, et al. Large-Volume Liver Metastases from Neuroendocrine Tumors: Hepatic Intraarterial 90Y-DOTA-Lanreotide as Effective Palliative Therapy. *Radiology*. 2005.

51. Kratochwil C, López-Benítez R, Mier W, et al. Hepatic arterial infusion enhances DOTATOC radiopeptide therapy in patients with neuroendocrine liver metastases. *Endocr Relat Cancer*. 2011;18:595-602.
52. Limouris GS, Chatziioannou A, Kontogeorgakos D, et al. Selective hepatic arterial infusion of In-111-DTPA-Phe1-octreotide in neuroendocrine liver metastases. *Eur J Nucl Med Mol Imaging*. 2008;35:1827-1837.
53. Sawada NN, Ishikawa TT, Sekiguchi FF, Tanaka YY, Ishitsuka HH. X-ray irradiation induces thymidine phosphorylase and enhances the efficacy of capecitabine (Xeloda) in human cancer xenografts. *Clin Cancer Res*. 1999;5:2948-2953.
54. Rich TA, Shepard RC, Mosley ST. Four decades of continuing innovation with fluorouracil: current and future approaches to fluorouracil chemoradiation therapy. *J Clin Oncol*. 2004;22:2214-2232.
55. van Essen M, Krenning EP, Kam BL, de Herder WW, van Aken MO, Kwekkeboom DJ. Report on short-term side effects of treatments with 177Lu-octreotate in combination with capecitabine in seven patients with gastroenteropancreatic neuroendocrine tumours. *Eur J Nucl Med Mol Imaging*. 2008;35:743-748.
56. Claringbold PG, Brayshaw PA, Price RA, Turner JH. Phase II study of radiopeptide 177Lu-octreotate and capecitabine therapy of progressive disseminated neuroendocrine tumours. *Eur J Nucl Med Mol Imaging*. 2011;38:302-311.
57. Jurcic JG, Larson SM, Sgouros G, et al. Targeted alpha particle immunotherapy for myeloid leukemia. *Blood*. 2002;100:1233-1239.
58. Nilsson S, Franzén L, Parker C, et al. Bone-targeted radium-223 in symptomatic, hormone-refractory prostate cancer: a randomised, multicentre, placebo-controlled phase II study. *Lancet Oncol*. 2007;8:587-594.
59. Zalutsky MR, Reardon DA, Akabani G, et al. Clinical experience with alpha-particle emitting 211At: treatment of recurrent brain tumor patients with 211At-labeled chimeric antitenascin monoclonal antibody 81C6. *J Nucl Med*. 2008;49:30-38.
60. Nayak T, Norenberg J, Anderson T, Atcher R. A Comparison of High- Versus Low-Linear Energy Transfer Somatostatin Receptor Targeted Radionuclide Therapy In Vitro. *Cancer Biother Radiopharm*. 2005;20:52-57.
61. Nayak TK, Norenberg JP, Anderson TL, Prossnitz ER, Stabin MG, Atcher RW. Somatostatin-receptor-targeted alpha-emitting 213Bi is therapeutically more effective than beta(-)-emitting 177Lu in human pancreatic adenocarcinoma cells. *Nucl Med Biol*. 2007;34:185-193.
62. Kratochwil C, Giesel FL, Morgenstern A, et al. Regional 213Bi-DOTATOC peptide receptor alpha-therapy in patients with neuroendocrine liver metastases refractory to beta-radiation. *J Nucl Med*. 2011;29 (abstract).
63. Eberle AN, Mild G. Receptor-mediated tumor targeting with radiopeptides. *Journal of Receptors and Signal Transduction*. 2009;29:1-37.
64. Teunissen JJM, Kwekkeboom DJ, Valkema R, Krenning EP. Nuclear medicine techniques for the imaging and treatment of neuroendocrine tumours. *Endocr Relat Cancer*. 2011;18 Suppl 1:S27-51.
65. Bodei L, Cremonesi M, Zoboli S, et al. Receptor-mediated radionuclide therapy with 90Y-DOTATOC in association with amino acid infusion: a phase I study. *Eur J Nucl Med Mol Imaging*. 2003;30:207-216.
66. Garkavij M, Nickel M, Sjogreen-Gleisner K, et al. 177Lu-[DOTA0,Tyr3] octreotate therapy in patients with disseminated neuroendocrine tumors: Analysis of dosimetry with impact on future therapeutic strategy. *Cancer*. 2010;116:1084-1092.



2

TOXICITY
AFTER PRRT

2.1

NEPHROTOXICITY AFTER PRRT WITH ^{177}Lu - DOTA-OCTREOTATE

Hendrik Bergsma¹ & Mark W. Konijnenberg¹, Wouter A. van der Zwan¹, Boen L. R. Kam¹, Jaap J. M. Teunissen¹, Peter P. Kooij¹, Katya A. L. Mauff², Eric P. Krenning¹, Dik J. Kwekkeboom¹

¹ Department of Radiology & Nuclear Medicine,

² Department of Biostatistics, Erasmus MC, University Medical Center, Rotterdam, The Netherlands

ABSTRACT

After peptide receptor radionuclide therapy (PRRT), renal toxicity may occur, particular in PRRT with ^{90}Y -labelled somatostatin analogues. Risk factors have been identified for increased probability of developing renal toxicity after PRRT, including hypertension, diabetes and age. We investigated the renal function over time, the incidence of nephrotoxicity and associated risk factors in patients treated with PRRT with [^{177}Lu -DOTA⁰,Tyr³]-Octreotate (^{177}Lu -Octreotate). Also, radiation dose to the kidneys was evaluated and compared with the accepted dose limits in external beam radiotherapy and PRRT with ^{90}Y -radiolabelled somatostatin analogues.

Methods:

The annual decrease in creatinine clearance (CLR) was determined in 209 Dutch patients and the incidence of grade 3 or 4 renal toxicity (according to CTCAE v4.03) was evaluated in 323 patients. Risk factors were analyzed using a nonlinear mixed effects regression model. Also, radiation doses to the kidneys were calculated and their association with high annual decrease in renal function were analyzed.

Results:

Of the 323 patients, 3 (1 %) developed (subacute) renal toxicity grade 2 (increase in serum creatinine $>1.5 - 3.0$ times baseline or upper limit of normal). No subacute grade 3 or 4 nephrotoxicity was observed. The estimated average baseline CLR (\pm SD) was 108 ± 5 ml/min and the estimated average annual decrease in CLR (\pm SD) was 3.4 ± 0.4 %. None of the risk factors (hypertension, diabetes, high cumulative injected activity, radiation dose to the kidneys and CTCAE grade) at baseline had a significant effect on renal function over time. The mean absorbed kidney dose in 228 patients was 20.1 ± 4.9 Gy.

Conclusion:

Nephrotoxicity in patients treated with ^{177}Lu - octreotate was low. No (sub)acute grade 3 or 4 renal toxicity occurred and none of the patients had an annual decrease in renal function of >20 %. No risk factors for renal toxicity could be identified. Our data support the idea that the radiation dose threshold, adopted from external beam radiotherapy and PRRT with ^{90}Y -labelled somatostatin analogues, does not seem valid for PRRT with ^{177}Lu -octreotate.

Keywords:

PRRT, ^{177}Lu -Octreotate, Kidneys, Renal function, Toxicity, Dosimetry, Nephrotoxicity

INTRODUCTION

Peptide receptor radionuclide therapy (PRRT) with radiolabelled somatostatin analogues is increasingly being used in patients with neuroendocrine tumors. Frequently used somatostatin analogues are [⁹⁰Y-DOTA⁰,Tyr³]- octreotide (⁹⁰Y-DOTATOC) and [¹⁷⁷Lu-DOTA⁰,Tyr³]- octreotate (¹⁷⁷Lu-Octreotate). Although the side effects of this therapy are mild, renal toxicity has been observed, particularly in PRRT with ⁹⁰Y-DOTATOC with an average annual decrease in creatinine clearance (CLR) of 7 % in contrast to 3 % for ¹⁷⁷Lu-Octreotate [1–4]. Also several risk factors have been identified for developing renal toxicity after PRRT: poor renal function, hypertension, and diabetes at baseline [2,5].

In the kidneys, radiolabelled somatostatin analogues are reabsorbed in the renal proximal tubules [6]. A decrease in renal uptake can be achieved by coinfusion of amino acids during PRRT [7,8]. Despite this renoprotection, there is still a significant radiation dose to the kidneys. In the past, the threshold dose for late-stage kidney radiation damage was set at 23 Gy, which was the dose adopted from external beam radiation therapy (EBRT) [9]. According to new consensus guidelines, the limit for fractionated EBRT is set at 18 Gy that results in late radiation damage to the kidneys in 5 % of a treated population [10]. However, doses higher than 23 Gy are safely given to patients receiving PRRT with (mainly) ⁹⁰Y-based somatostatin analogues [2,11]. Here we present our dosimetric results and long-term follow-up of a large number of patients treated with ¹⁷⁷Lu-Octreotate. We also analyzed the association between known risk factors that have been indicated for PRRT with ⁹⁰Y-based somatostatin analogues [2,5] and change in renal function, including hypertension, diabetes, cumulative injected activity, age, previous therapies and poor renal function at baseline. In addition, radiation doses to the kidneys were calculated and analyzed.

MATERIALS AND METHODS

Patients

A total of 615 patients, who were treated from January 2000 to December 2007 were studied. Inclusion criteria for the study were: patients with somatostatin positive tumors and baseline tumor uptake on [¹¹¹In-DTPA⁰]Octreotide scintigraphy (Octreoscan®; Mallinckrodt, Petten, The Netherlands) with accumulation in the tumor at least as high as in normal liver tissue; no prior treatment with PRRT; baseline serum hemoglobin (Hb) ≥6 mmol/l; white blood cells ≥2 10⁹/l; platelets ≥75 10⁹/l; Karnofsky performance status ≥50; serum creatinine ≤150 μmol/l; and 24-h CLR ≥40 ml/min. Of the 615 patients, 323 Dutch patients were selected for this long-term evaluation, because loss to follow-up is limited in these patients.

This study was part of an ongoing prospective study in patients with neuroendocrine tumors treated with ^{177}Lu - Octreotate at the Department of Nuclear Medicine, Erasmus University Medical Center Rotterdam. The hospital's medical ethics committee approved the study. All patients gave written informed consent for participation in the study.

Treatment

[DOTA⁰,Tyr³]Octreotate was obtained from BioSynthema (St. Louis, MO). $^{177}\text{LuCl}_3$ was supplied by IDB-Holland (Baarle-Nassau, The Netherlands) and ^{177}Lu -Octreotate was locally prepared [12].

Granisetron 3 mg or ondansetron 8 mg was injected intravenously 30 min before infusion of ^{177}Lu -Octreotate. Infusion of amino acids (2.5 % arginine and 2.5 % lysine, 1 l) was started 30 min before administration of the radiopharmaceutical and lasted for 4 h. The radiopharmaceutical was coadministered for 30 min using a second pump system. The interval between treatments was 6 – 16 weeks. The intended cumulative activity was 29.6 GBq (800 mCi). Median cumulative activity was 29.6 GBq (range 7.4 – 29.6 GBq) and the median number of therapy cycles was four (range one to eight). However, the total administered activity was lowered if the calculated kidney dose was higher than 23 Gy. Other reasons for dose reduction or cessation of further therapy were recurrent grade 3 or 4 hematological toxicity and persistently low blood cell counts.

Toxicity, risk factor assessment and follow-up

Hematology, liver and renal function tests were performed during the 6 weeks before the first therapy, 4 and 6 weeks after each therapy, and at follow-up visits. Acute and long-term renal toxicity assessment was done according to Common Terminology Criteria for Adverse Events (CTCAE v4.0) [13].

Hypertension was defined as the use of antihypertensive drugs (thiazide diuretics, beta blockers, ACE inhibitors, angiotensin II receptor antagonists and calcium channel blockers). Diabetes mellitus was defined as an HbA1c of ≥ 6.0 % and/or the use of antidiabetic medication (insulin and insulin sensitizers). CLR in milliliters per minute was used as an estimate of glomerular filtration rate (GFR). Four serum-based methods were used to determine baseline 24-h urine CLR, and the results compared (see Supplementary material). The Cockcroft-Gault (CG) formula had the highest Spearman's rank correlation coefficient. Therefore, changes in renal function during follow-up were assessed in terms of CLR determined using the CG formula:

$$CLR(ml/min) = \frac{(140 - age[y] \cdot weight(kg))}{s\text{-creat}(\mu mol/L)} \cdot [0.85 \text{ if female}] \quad (2.1)$$

Statistical analysis

SPSS (SPSS 19; IBM, Armonk, NY) and R (R 3.2.2; R Foundation for Statistical Computing, Vienna, Austria) software was used for statistical analysis. The Shapiro-Wilk test was used to assess the normality of the response. The primary outcome was CLR predicted by a nonlinear mixed effects regression model with independent factors (hypertension, diabetes, cumulative injected activity, radiation dose to the kidneys, age and CTAEC at baseline). Various functional model forms (linear, nonlinear, polynomial and spline) were fitted to the CLR data (see Supplementary material). The nonlinear model with the monoexponential function performed best:

$$\widehat{CLR}(ml/min) = \widehat{b}_0 \cdot factor_1 \cdot \exp(\widehat{b}_1 \cdot factor_2 \cdot time(weeks)) \quad (2.2)$$

where b_0 is the estimated average CLR at time 0 when all other covariates are zero, and b_1 is the estimated average change in CLR in percent/time. Time is expressed in weeks and $factor_1$ and $factor_2$ are constants, given specific values of the covariates included in the mixed model. The combined term $(\widehat{b}_0 \cdot factor_1)$ represents the estimated average CLR at time = 0 for a specific covariate pattern, whereas $(\widehat{b}_1 \cdot factor_2)$ is the estimated average percentage decrease/increase in CLR per week. Random effects were included on both the intercept and slope parameters, and a diagonal covariance matrix was assumed.

Dosimetry

Uptake of radioactivity in the kidneys was determined by planar imaging at 1, 3–4 and 7 days after administration of ¹⁷⁷Lu-Octreotate. Extensive information regarding the dosimetric method is provided in an earlier paper [12]. Dosimetry values were computed with S-factors for ¹⁷⁷Lu derived from the Radiation Dose Assessment Resource (RADAR) website [14, 15]. The general scheme for calculating radiation dosimetry with radionuclides has been defined by the MIRD scheme dosimetry formula [16]:

$$D(r_t) = \sum_S \int A_S(t) dt \cdot S(r_t \leftarrow r_s) = \sum_S \tilde{A}_S \cdot S(r_t \leftarrow r_s) \quad (2.3)$$

$$\Rightarrow D_{kidneys} \approx \tilde{A}_{kidneys} \cdot S(kidneys \leftarrow kidneys) \quad (2.4)$$

The dose to the target organ ($D_{kidneys}$) is calculated as the product of the number of decays in a source organ (\tilde{A}_s) and the S-value, which expresses the dose rate per radioactivity for a source (r_s) to target (r_t) combination. With moderately weak β -particle-emitting radionuclides such as ¹⁷⁷Lu, only the self-dose needs to be considered ($r_s = r_t$). The radioactivity uptake and clearance kinetics of ¹⁷⁷Lu-Octreotate $A(t)$ in the kidneys is

needed for calculation of the radiation dose to the kidneys, together with the S-value for the kidney self-dose. The ^{177}Lu S-values were taken from the RADAR website [15]: for adult male kidneys (with a mass of 299 g) the S-value is 0.289 mGy/ MBq.h and for a adult female kidneys (with a mass of 275 g) the S-value is 0.314 mGy/MBq.h. In a subgroup of patients, the kidney volume was determined based on baseline CT images, since complete kidney imaging was not always available. A correction factor and adjusted dose were calculated in these patients, using OsiriX 5.9 (Pixmeo Sàrl, Bernex, Switzerland). A polygonal region of interest was (semi)automatically drawn on each CT slice and the slices were summed for calculation of the total kidney volume.

RESULTS

In 554 patients the inclusion criteria were met. In-depth evaluation was done in 322 Dutch patients (excluding one patient with no baseline CLR). Patient characteristics are summarized in Table 1. A Spearman's correlation coefficient of 0.76 was found between baseline 24-h urine and serum-based CLR (Figure 1).

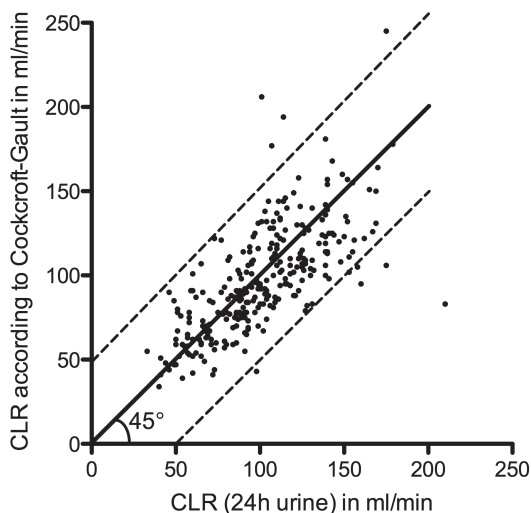


Figure 1 - Baseline 24-h urine creatinine clearance (CLR) versus serum-based CLR according to the Cockcroft-Gault formula in 281 of 323 patients. The solid line is the linear regression line with a slope of 1 with 95 % confidence intervals (dotted lines).

Table 1 - Baseline characteristics of 323 Dutch patients

Characteristic	no.
Gender	
Male	158 (49 %)
Female	165 (51 %)
Age (years)	
≥70	63 (20 %)
<70	260 (80 %)
Karnofsky performance status	
≤70	46 (14 %)
>70	277 (86 %)
Diabetes	
Yes	104 (32 %)
No	219 (68 %)
Hypertension	
Yes	77 (24 %)
No	246 (76 %)
Solitary kidney	
Yes	10 (3 %)
No	313 (97 %)
Previous therapy	
Radiotherapy (external)	
Yes	32 (10 %)
No	291 (90 %)
Chemotherapy	39 (12 %)
Cisplatin	5 (13 %)
Other	34 (87 %)
Tumour type	
Neuroendocrine tumour	281 (87 %)
Other	42 (13 %)
Dosimetry	
Dosimetric data available	228 (71 %)
Limit 23 Gy to the kidneys	
Yes	55 (24 %)
No	173 (76 %)
Volume of kidneys available	
Yes	119 (52 %)
No	109 (48 %)
Cumulative activity (GBq)	
Up to 22.2	106 (33 %)
Up to 29.6 Kidneys	217 (66 %)
Baseline creatinine clearance	
<60 ml/min/1.73 m ²	37 (11 %)
≥60 ml/min/1.73 m ²	286 (89 %)
Baseline Cockcroft-Gault	
creatinine clearance (ml/ min), median (range)	95 (34 – 245)
Follow-up (months), median (range)	25 (0 – 142)

Kidney toxicity

Of the 323 patients, 14 (4 %) had a (sub)acute toxicity grade 1 (creatinine increase >26.5 $\mu\text{mol/l}$). Three patients (1 %) developed (subacute) toxicity grade 2 (creatinine increase $>1.5 - 3.0 \times$ baseline or upper limit of normal). These were judged not related to therapy: one patient had received prolonged antibiotics due to an infection and developed temporary renal insufficiency, one patient was dehydrated because of diarrhea, and one patient showed progression of disease with hypoalbuminaemia and forward heart failure resulting in death 2 weeks after the first treatment. No grade 3 or 4 (sub)acute nephrotoxicity was observed.

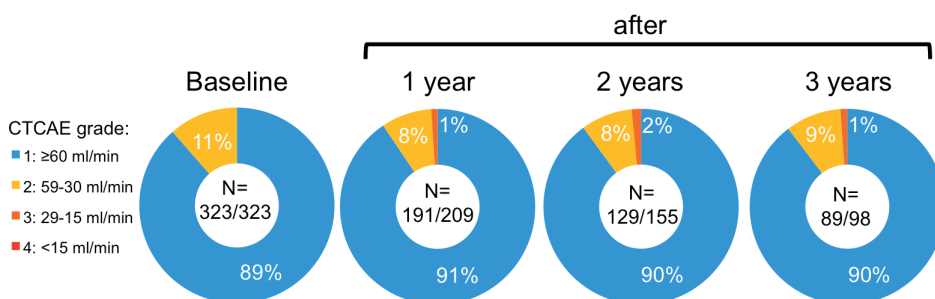


Figure 2 - Distribution of creatinine clearance in 323 patients according to Common Terminology Criteria for Adverse Events (CTCAE) classification at baseline, and at 1, 2 and 3 years after inclusion. Number (N) of patients with serum creatinine available / total number of patients in follow-up. No CTCAE grade 4 was observed.

Table 2 - Cumulative numbers of 323 Dutch patients lost to follow-up 1, 2 and 3 years after the last PRRT with ^{177}Lu -Octreotate.

Reason lost to follow-up	after 1 year	after 2 years	after 3 years
Progressive Disease	43	47	56
Death	8	9	12
Follow-up elsewhere (patient request)	18	23	32
Complications (e.g. bleeding, infection, ileus, dyspnea)	11	13	19
Bone marrow depression	4	7	9
Liver failure	2	2	2
Other therapy	23	28	40
Octreoscan negative lesions during follow-up	2	2	3
Retreatment with ^{177}Lu -DOTATATE	3	37	51
Kidney failure (see text)	0	0	1
Total number of patients	114	168	225

Follow-up data for 1, 2 and 3 years after the last therapy were available in 209, 155 and 98 patients, respectively. Grade 3 kidney toxicity was observed in 5 out of the 323 patients during this follow-up. Toxicity was not related to PRRT since all five patients had a baseline CLR of <60 ml/min (i.e. grade 2), making them more prone to more severe renal function impairment. However, the annual decrease in CLR was <12 %. The distribution of CLR at baseline and during follow-up (1, 2 and 3 years after inclusion) is shown in Figure 2. Reasons for loss to follow-up after 1, 2 and 3 years are summarized in Table 2. One patient was lost to follow-up after 2 years, due to kidney failure resulting in dialysis based on preexisting kidney disease.

Long-term change in renal function

Follow-up of more than 1 year was available in 209 of the 323 patients. One patient with an incomplete set of risk factors was excluded; thus the analysis included 208 patients. The estimated average annual decrease in CLR (\pm SD) was 3.4 ± 0.4 %, and the estimated average baseline CLR (b_0) was 108 ± 5 ml/min (Figure 3). The time course of CLR and the fitted nonlinear model in an example patient are shown in Figure 4. In 203 out of 208 patients, the annual decrease in renal function was <10 %. Five patients had an annual decrease in CLR of ≥ 10 %, and two patients had an annual decrease of ≥ 15 % (Figure 5). In 29 (14 %) of 208 patients, a positive annual change in CLR (improvement in renal function) was observed. No patient showed an annual decrease in renal function of ≥ 20 %.

Risk factor assessment

Age and baseline CTCAE had significant effects on the baseline CLR (both $p < 0.0001$). With all other factors held constant, the estimated average baseline CLR showed a significant decrease in patients older than 70 years or with baseline CTCAE grade 2. None of the risk factors considered for inclusion in the model (hypertension, diabetes, age >70 years, cumulative injected activity >22.2 GBq, high radiation dose to the kidneys and CTCAE grade at baseline) had a significant effect on the estimated rate of change in CLR over time, and were thus not included in the final model.

Dosimetry

Dosimetric data for kidney dose calculations was available in 407 of the 554 on-protocol patients. In 147 patients no radiation dose to the kidneys could be calculated due to incomplete dosimetric data and/or over-projection of tumour nodules on planar images of the kidney region of interest. Clearance of radioactivity from the kidneys proceeded with a median effective half-life of 58 h (range: 27 – 135 h) in 407 patients.

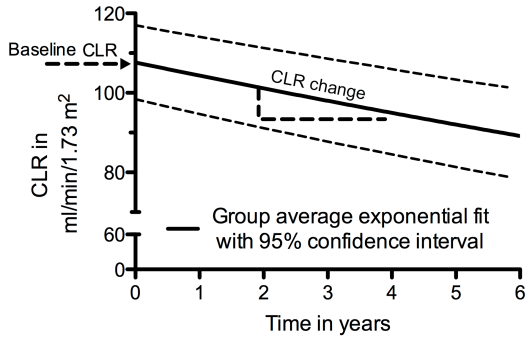


Figure 3 - Nonlinear model of creatinine clearance (CLR) over time based on 208 patients. Solid line is the exponential function with 95 % confidence interval (dashed lines). The estimated average baseline CLR (\pm SD) is 108 ± 5 ml/min and the estimated average annual change in CLR (\pm SD) is 3.4 ± 0.4 %

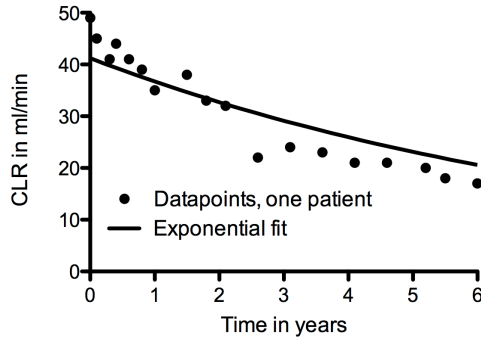


Figure 4 - Time-course of creatinine clearance (CLR) and fitted monoexponential decay (solid line) in a 71-year-old patient with a neuroendocrine tumor, hypertension and diabetes, who received 4×7.4 GBq ^{177}Lu -Octreotate. The estimated decrease in CLR is 11.4 % per year

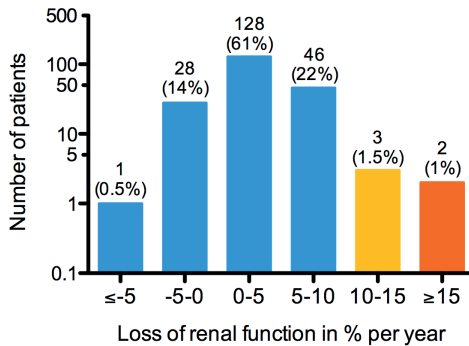


Figure 5 – Distribution of the change in creatinine clearance per year in 208 patients with long-term follow-up. Note the log scale on the y-axis. Coloured bars represent annual loss of renal function < 10% (blue), 10-15% (yellow) and >15% (orange).

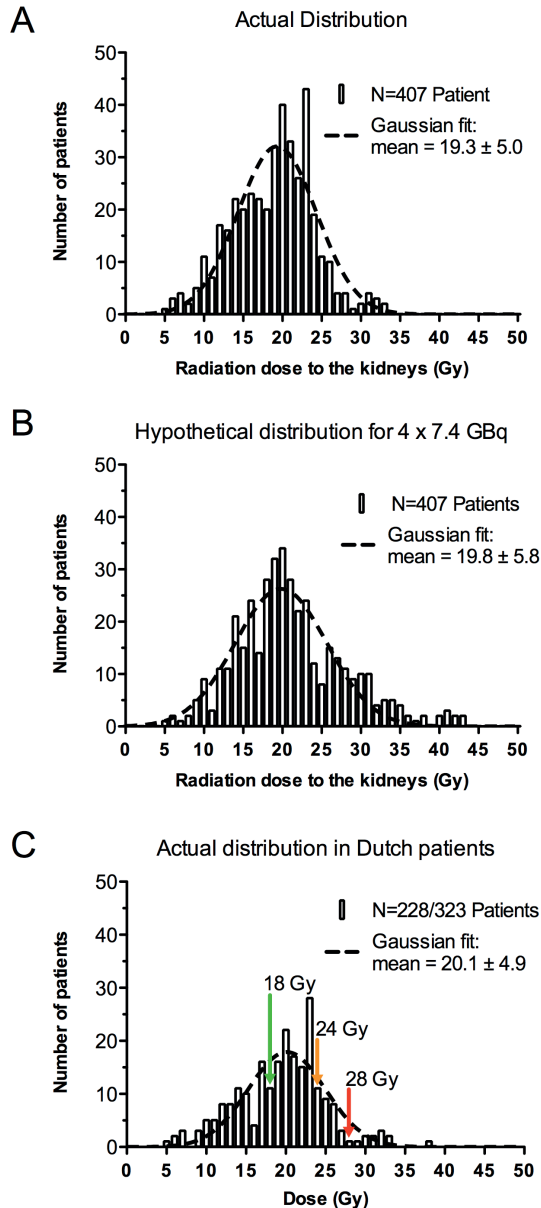


Figure 6 - Distribution in 1-Gy increments of the radiation dose to the kidneys for 407 patients and in 228 patients with quantifiable kidney uptake: a actual distribution in 407 patients; b hypothetical distribution for 4×7.4 GBq of ^{177}Lu -Octreotate; c actual distribution in 228 Dutch patients. Gaussian fits (dashed lines) are overlain on the histograms. The green arrow indicates the kidney threshold dose (18 Gy) according to current EBRT guidelines [10]. The orange arrow (24 Gy) and red arrow (28 Gy) correspond to the PRRT dose limits for kidney damage according to Wessels et al. [11] and Bodei et al. [2], respectively, for therapies given in four cycles.

The mean radiation dose to the kidneys was 19.3 ± 5.0 Gy (Figure 6a). The mean kidney absorbed dose for a hypothetical dose distribution of 4×7.4 GBq of ^{177}Lu -Octreotate was 19.8 ± 5.8 Gy (Figure 6b). The mean calculated radiation dose to the kidneys in 228 of the 323 Dutch patients in whom it could be calculated was 20.1 ± 4.9 Gy (Figure 6c), and 11 (5 %) of these 228 patients had a calculated kidney absorbed dose of more than 28 Gy. The total administered injected activity was reduced in 55 of the 228 patients because the calculated kidney dose was more than 23 Gy. The average measured kidney volume (with corresponding mass) in 119 (49 %) of the 228 patients in whom it could be measured was a factor of 0.95 (range 0.49 – 1.71) less than the fixed phantom-based kidney mass.

DISCUSSION

After PRRT with ^{177}Lu -Octreotate, the average annual decrease in CLR was 3 % and no patient showed a decrease of more than 20 %, which is in line with the results of other studies with ^{177}Lu -Octreotate [2, 5, 17, 18]. Of the patients treated with ^{177}Lu -Octreotate, 14 % showed an annual improvement in CLR. Tumor response and improvement in clinical condition could explain the increase in CLR in these patients, since a rapid weight gain with stable serum creatinine values results in a higher CLR. Therefore, we suspect that the improvement in CLR did not reflect a true improvement in renal function.

In practice, an annual decrease of 3 % means a CLR of 91 ml/min after 3 years in a patient with normal renal function at baseline (Table 3). Five of our patients had an annual decrease in renal function of more than 10 %, translating to a CLR after 3 years of 74 ml/min in an individual with normal renal function at the start. Since the overall survival following PRRT with ^{177}Lu -octreotate is 3 to 4 years [19], it is unlikely that the kidneys are the long-term limiting factor. A decrease in renal function to CTCAE grade 2 or higher occurs after 7 years in a patient with normal renal function at the start and an annual decrease of 10 % (Table 3). In our study, only 1 % of the patients developed therapy-unrelated severe (grade 3) renal toxicity after 1 year. Furthermore, the CTCAE distribution of CLR over time did not change, confirming the low nephrotoxicity of PRRT with ^{177}Lu -Octreotate.

Several risk factors for kidney toxicity after PRRT with mainly ^{90}Y -labelled somatostatin analogues have been identified, including age (>60 years), diabetes, hypertension, previous chemotherapy and poor baseline renal function [1, 2, 4]. In a recent study [5], renal function was analyzed in 807 patients treated with ^{177}Lu -Octreotate and/or ^{90}Y -Octreotide. Hypertension was identified as a main risk factor for (persistent) nephrotoxicity. However, nephrotoxicity was defined as a categorical outcome according to CTCAE, neglecting the change in renal function over time. This can lead to a simplified representation of kidney toxicity after PRRT and false identification of

risk factors. Valkema et al. analyzed renal function in 37 patients treated with ¹⁷⁷Lu-Octreotate by taking the subject-specific annual decrease in CLR extracted from fitted monoexponential curves [1]. Hypertension was also found to be a possible factor contributing to the rate of decrease in CLR after PRRT. Although the authors did take into account the change in renal function over time, they were unable to determine the impact of covariates on the change over time but only on summary measurements obtained from individually fitted curves.

Table 3 - Creatinine clearance in hypothetical patients with a baseline renal function of 100 ml/min and annual decreases of 3 %, 10 % and 20 %.

Year	Creatinine clearance in ml/min		
	3% annual decrease	10% annual decrease	20% annual decrease
0	100	100	100
3	91	74	55
5	86	61	37
7	81	50	25

*red highlighted number are Creatinine clearance of CTCAE grade 2 or higher

Given the repeated measurement structure of the data and the need to assess the effect of risk factors on both baseline CLR and change in CLR over time, a more advanced approach is required. We therefore used a mixed effects regression model. Mixed effects models are the standard modeling framework for the analysis of longitudinal data. These models explicitly account for differences in correlation structure of the data within/between patients and deal well with unbalanced data (varying times of measurement in each subject and un- equal numbers of follow-up measurements among subjects).

In our present analysis, age >70 years and baseline CTCAE grade influenced the nonlinear model. However, the two risk factors only changed the estimated average baseline CLR component in our model, meaning that patients older than 70 years and/or patients with baseline CTCAE grade 2 had a lower estimated average CLR at baseline. None of the evaluated risk factors modified the percentage CLR change component significantly, implying that the percentage change in CLR over time in patients with risk factors was not different from that in patients without risk factors.

An explanation for our results could be that the frequency of nephrotoxicity after PRRT with ¹⁷⁷Lu-Octreotate is low and a higher number of patients would be required to show statistical significance of the risk factors. For the same reason, we were not able to compare patient's with/without a solitary kidney and with/without alkylating chemotherapy (e.g. cisplatin). The relatively low numbers of patients resulted in low statistical power for testing these risk factors.

GFR measurement with inulin is the gold standard for measuring renal function, but practical implementation is difficult [20]. Other radionuclide-based filtration markers such as ^{99m}Tc -MAG3 (mercaptoacetyltriglycine) are used for accurate assessment of renal function in clinical practice [21]. However, these methods are expensive and time-consuming in the follow-up of large patient groups. We used CLR as an indirect marker for estimating GFR since serum creatinine is widely available. Also most of our patients had normal baseline renal function, making CLR a reasonable estimator for GFR. However, different formulas for calculation of renal function are available: the (body surface area-corrected) CG formula and the (abbreviated) modification of diet in renal disease (MDRD) equations. The CG formula estimates CLR [22], whereas the MDRD equations estimate GFR [23]. All formulas have different performance in various subgroups of patients depending on age, sex, weight and range of renal function [24]. Therefore, we calculated Spearman's rank correlation coefficients for different equations versus 24-h urine CLR in our patient group. The CG formula had the best correlation (Figure 1). Our results are in line with those of other studies indicating that CG is more precise than MDRD [24], meaning that individual changes in renal function over time are more reliable.

Radiation toxicity dose effect models used in PRRT are pre-dominantly based on the experience and knowledge obtained from EBRT. In the past, the threshold dose for late-stage kidney radiation damage for EBRT was set at 23 Gy [9]. However, the tolerable dose in current guidelines for radiotherapy-associated kidney injury are lower at 18 Gy [10]. Kidney radiation doses of 18 Gy given in a fractionation scheme of 2 Gy per fraction are considered to result in a 5 % probability of developing radiation nephropathy during the 5 years after EBRT.

For PRRT with ^{90}Y -DOTATOC, a correlation was found between the kidney absorbed dose and chronic kidney toxicity. The dose at which 5 % of patients will show kidney toxicity has been estimated at 24 Gy for ^{90}Y -DOTATOC [11]. Another study has confirmed this dose limit in 22 of 50 patients treated with ^{90}Y -DOTANOC [25]. The absorbed dose limit after ^{90}Y irradiation and that for fractionated EBRT can be compared using the concept of the biologically effective dose (BED). BED is a measure of the true biological dose delivered at a particular dose rate and fractionation pattern, tissue-specific for a relevant biological end-point (in this case late-stage renal disease). It takes the protracted nature of the absorbed dose delivery by radionuclides into account by adjusting the kidney's radiation sensitivity for the repair of sublethal radiation damage during the absorbed dose buildup according to the linear quadratic (LQ) model. The BED concept is thought to explain the 6-Gy higher dose limit than the 18 Gy accepted for EBRT [10]. Bodei et al. proposed a BED limit of 40 Gy to the kidneys in patients without risk factors and a BED of 28 Gy in patients with risk factors, corresponding to absorbed doses of 28 and 24 Gy,

respectively (both given in four fractions) [2]. A summary of previously reported kidney dosimetry findings in studies using ¹⁷⁷Lu-Octreotate is provided in Table 4.

Table 4 - Reported data on kidney dosimetry for PRRT with ¹⁷⁷Lu-Octreotate

Reference	Method	No. of patients	Administered Activity (GBq)	Amino acids	Dose to kidneys	
					Per activity administered (Gy/GBq)	For 4×7.4 GBq (Gy)
[12]	Planar	5	1.85	Lys/Arg	0.9 ± 0.2	26.6 ± 5.3
[2]	Planar	5	3.7 – 5.18	NR	0.9 ± 0.5	26.6 ± 13.3
[32]	Planar	69	3 – 7	Lys/Arg	0.9 ± 0.3	26.6 ± 8.0
[33]	SPECT/CT	24	7.4	VAMIN-14	0.7 ± 0.3	20.7 ± 6.2
[34]	SPECT/CT	16	7.4	VAMIN-14	0.9 ± 0.3	26.6 ± 8.0
[35]	Planar	26	8	NR	0.9 ± 0.4	26.6 ± 10.6
[36]	SPECT/CT	33	7.8	Synthamin	0.3 (0.1-0.5)	9.2 (4.1-13.6)
[18]	Planar	12	5.18 – 7.4	Lys/Arg	0.8 ± 0.4	23.7 ± 9.5
[37]	SPECT/CT	200	7.4	VAMIN-14	1.2 ± 0.6	36.3 ± 16.0
[28]	Planar	51	3.5 – 8.2	Lys/Arg	0.8 ± 0.4	23.7 ± 9.5
This study	Planer	407	7.4	Lys/Arg	0.7 ± 0.2	19.8 ± 5.8

Values are means ± SD, or median (range)

Lys/Arg Lysine 2.5 % and arginine 2.5 %, Lys Lysine 2.5 %

In this study, we did not find a significant difference in the effect of kidney dose on renal function. Most patients received a kidney dose of less than 28 Gy (Figure 6c). However, in a small number of patients the kidney dose exceeded this limit. In our long-term follow-up group, 11 patients received a kidney dose that exceeded 28 Gy. None of these patients developed grade 3 or 4 nephrotoxicity and/or had an annual decrease in CLR of more than 10 %. Therefore, the 28 Gy dose limit seems to be a conservative value for PRRT with ¹⁷⁷Lu-Octreotate. Another argument for a higher dose limit is that ¹⁷⁷Lu has shorter-range β-particles than ⁹⁰Y. This results in less damage to nearby non-target tissue and (theoretically) in fewer cases of nephrotoxicity at a fixed kidney dose [26–28]. In PRRT studies, the LQ model concept of BED was first introduced with dosimetric data from 18 patients who received ⁹⁰Y-DOTATOC [29]. A stronger correlation was observed with the decrease in CLR when applying this model, compared with using absorbed renal dose alone. Also, a comparison between the relatively high dose-rate of EBRT and low dose-rate irradiation of radionuclide therapy is possible using BED. The LQ model can be used to analyze the effects of dose rate, number of therapy cycles in EBRT/PRRT and the type of radionuclide in PRRT. The LQ model-based BED for PRRT has been adopted by the Committee on Medical Internal Radiation Dose (MIRD) for late kidney damage [11]. In PRRT little scientific evidence is available for the choice of α/β ratio and

repair $T_{1/2}$, which represents the damage and repair half-life in the BED model, however the two variables have an important effect on the dosimetric outcome [30, 31]. Also, since no severe renal toxicity was observed in the present study with an intended dose scheme of 4×7.4 GBq, reporting the BED did not seem appropriate. Moreover, in the present study the factor relating absorbed dose and BED was low: median 1.09 (range 1.02 – 1.21).

Our results demonstrate that the kidneys are not the dose- limiting organ in patients treated with ^{177}Lu -Octreotate. Therefore, in clinical practice, kidney dosimetry does not currently have a prominent place in PRRT with 4×7.4 GBq ^{177}Lu -Octreotate. However, (serum-based) assessment of renal function during and after PRRT is mandatory since renal toxicity unrelated to PRRT could occur. Also measurement of renal function at baseline is required since low GFR is a risk factor for development of (sub)acute haematotoxicity after PRRT.

CONCLUSION

The number of patients with nephrotoxicity after PRRT with ^{177}Lu -Octreotate is low. No patient showed (sub)acute grade 3 or 4 nephrotoxicity or an annual decrease in renal function of $>20\%$. No risk factors (e.g. hypertension, diabetes) leading to an additional annual decrease in renal function could be identified. Our study showed that the maximum radiation dose to the kidney adopted from EBRT and PRRT with ^{90}Y -labelled analogues does not seem to apply to PRRT with ^{177}Lu -Octreotate.

SUPPLEMENTAL DATA

Follow-up and data analyses

Creatinine clearance (CLR) was used as an estimate of the glomerular filtration rate (GFR). Baseline 24hr urine creatinine was collected and compared with different serum based creatinine clearance methods (Supplemental figure 1 and 2). We estimated the serum CLR with four formulas (see below) in comparison to 24-h urine CLR at baseline.

24hr urine collection:

$$GFR = C_x = \frac{U_{creatinine} \cdot V}{s-creat(\mu\text{mol/L})} \quad (2.5)$$

Cockcroft-Gault (C-G):

$$c-CLR = \frac{(140 - \text{age}[y] \cdot \text{weight}(kg))}{s-creat(\mu\text{mol/L})} \cdot [0.85 \text{ if female}] \quad (2.6)$$

Cockcroft-Gault (C-G) correct for body surface area (BSA):

$$c-CLR = \frac{(140 - \text{age}[y] \cdot \text{weight}(kg) \cdot [0.85 \text{ if female}])}{s-creat\left(\frac{\mu\text{mol}}{L}\right)} \cdot \frac{1.73}{BSA} \quad (2.7)$$

Body surface area (BSA) according to Du Bois and Du Bois:

$$BSA = (\text{body-weight}^{0.425} [\text{in kg}] \cdot \text{height}^{0.725} [\text{in cm}]) \cdot 0.007184 \quad (2.8)$$

Modification of Diet in Renal Disease (MDRD):

$$GFR = 186 \cdot (s-creat \cdot 0.0113)^{-1.154} \cdot \text{Age}^{-0.203} \cdot 0.742 \text{ (if female)} \quad (2.9)$$

or

$$GFR = 186 \cdot (s-creat \cdot 0.0113)^{-1.154} \cdot \text{Age}^{-0.203} \cdot 1.21 \text{ (if black)} \quad (2.10)$$

Extended Modification of Diet in Renal Disease (extMDRD):

$$GFR = 170 \cdot (s-creat \cdot 0.0113)^{-0.999} \cdot \text{Age}^{-0.176} \cdot (\text{BUN} \cdot 2.80)^{-0.170} \cdot (\text{Alb} \cdot 0.1)^{0.318} \cdot (0.762 \text{ if female}) \quad (2.11)$$

or

$$GFR = 170 \cdot (s-creat \cdot 0.0113)^{-0.999} \cdot \text{Age}^{-0.176} \cdot (\text{BUN} \cdot 2.80)^{-0.170} \cdot (\text{Alb} \cdot 0.1)^{0.318} \cdot (1.18 \text{ if black}) \quad (2.12)$$

where BUN is the blood urea nitrogen in mmol/l and Alb is the albumin in g/l.

The difference between estimated and measured CLR from 24h-urine was the smallest in the C-G formula (Supplemental figure 1). Also the spearman rank correlation coefficient was the best in the latter (Supplemental figure 2).

Dosimetry

All patients underwent planar imaging to determine kidney dosimetry. Dosimetry was performed minimally after the first treatment to determine if the 4th treatment with 7.4 GBq of ¹⁷⁷Lu-Octreotate would result in a kidney radiation dose that would not exceed the 23 Gy threshold limit. 407 of the 554 on-protocol patients had quantifiable kidney uptake, which enabled kidney dosimetry. The lack of accurate dosimetry data for the remaining patients is largely due to overlapping radioactivity from tumours in the abdominal region obscuring organ delineation.

The ¹⁷⁷Lu S-values were taken from the Radiation Dose Assessment Resource (RADAR) website [15]: for a male adult (with 300g kidneys) the S-value is 0.289 mGy/MBq.h and for a female adult (with 275 g kidneys) the S-value is 0.314 mGy/MBq.h. These can be adjusted with the actual patient's kidney volume, derived from CT imaging [38]. A correction factor and adjusted dose was calculated in patients with CT scan available before the first treatment, using OsiriX 5.9 (Pixmeo SARL, Bernex – Swiss). A polygon region of interest (ROI) was (semi)automatic drawn on each CT slice and each slice was summed up for calculation of the total kidney volume.

Imaging

Planar spot images of the upper abdomen, chest, and the head and neck region were obtained with a double head camera (Picker Prism 2000) at regular intervals. For the first administration in Group-1, the imaging time points were 4 h, and 1, 3, 10 and 17 days after administration. After the second administration in Group-1 (with amino acid co-infusion) and in all other groups, the imaging time points were 1, 3 or 4 and 7 or 10 days after administration. Counts from both gamma-peaks (208 and 113 keV) were collected in separate windows (width 20%). Acquisition time was 15 min/view at maximum. A standard with a known aliquot of the infused radioactivity was also counted for dosimetry calibration.

Regions of Interest

For biodistribution studies the percentage of infused radioactivity (%IA) accumulated in each organ was measured by manually contouring and selecting the regions of interest (ROIs) for the whole body, bone marrow, kidney, liver, spleen, total abdomen, thyroid,

gonads, pituitary, adrenals and pancreas. The geometric means of the regions were computed and these values were used to calculate the %IA based on a comparison to an aliquot of the administered dose [3, 4].

Dosimetry Calculations

Dosimetry values were computed with a MIRDOSE software package, version 3.0, and using S-factors for ¹⁷⁷Lu [5]. The general scheme for calculating radiation dosimetry with radionuclides has been defined by the MIRD scheme dosimetry formula [16].

$$D(r_t) = \sum_S \int A_S(t) dt \cdot S(r_t \leftarrow r_S) = \sum_S \tilde{A}_S \cdot S(r_t \leftarrow r_S) \quad (2.3)$$

$$D_{kidneys} \approx \tilde{A}_{kidneys} \cdot S(kidneys \leftarrow kidneys) \quad (2.4)$$

The dose to the target organ (D; kidney or bone marrow) is calculated by the product of the number of decays in a source organ (\tilde{A}_S) and the S-value, which expresses the dose rate per radioactivity for a source (r_S) to target (r_t) combination. With moderately weak beta-particle emitting radionuclides like ¹⁷⁷Lu, only the self-dose needs to be considered ($r_S=r_t$). The radioactivity uptake and clearance kinetics of ¹⁷⁷Lu-DOTA⁰-Tyr³-Octreotate $A_S(t)$ in the kidneys is needed for calculation of the radiation dose to the kidneys, together with the S-value for the kidney self-dose. The ¹⁷⁷Lu S-values were taken from the Radiation Dose Assessment Resource (RADAR) website [15]: for a male adult (with 300g kidneys) the S-value is 0.289 mGy/MBq.h and for a female adult (with 275 g kidneys) the S-value is 0.314 mGy/MBq.h. These can be adjusted with the actual patient's kidney volume, derived from CT imaging [38], this was not done in a select number of patients.

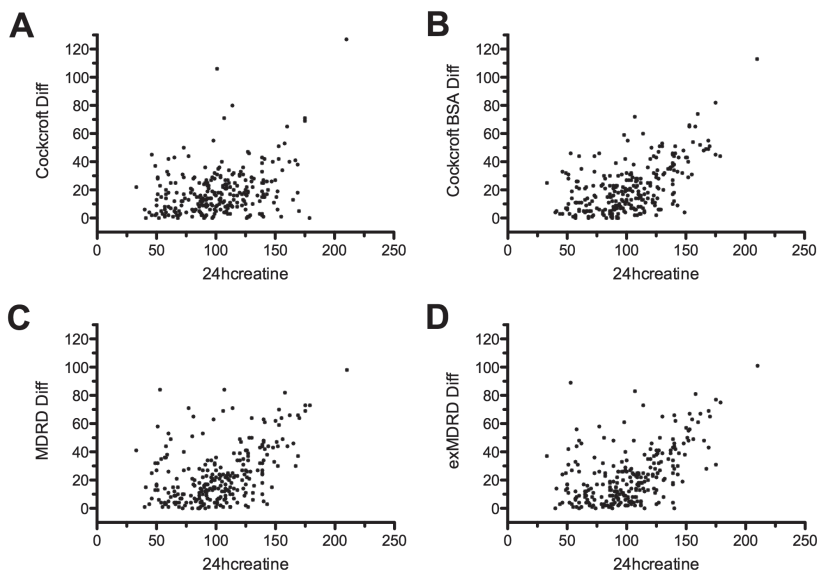
Results

Statistical analysis

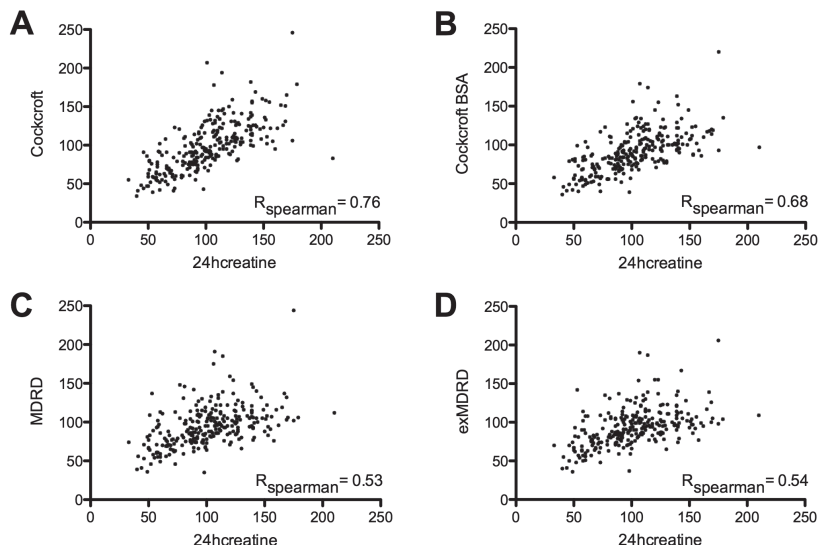
Baseline 24hr urine CLR was compared with 4 serum based CLR methods (Appendix A). The Cockcroft-Gault (CG) formula had the highest Spearman rank correlation coefficient (see figure 7 & 8).

Dosimetry

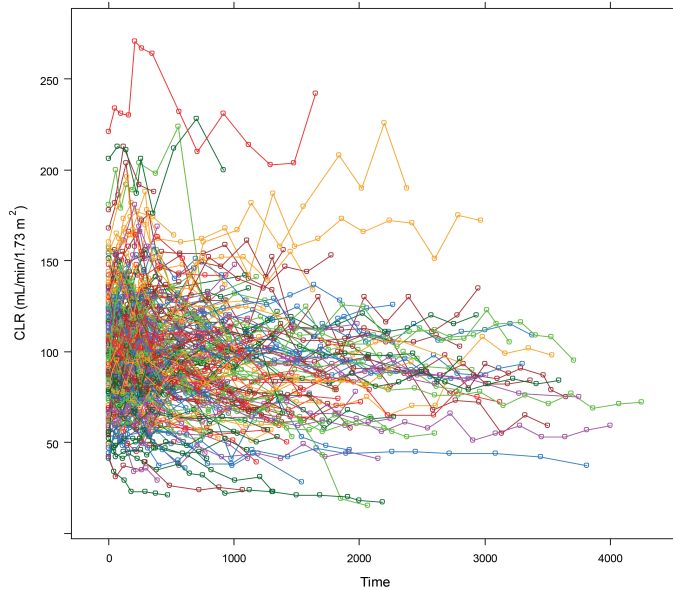
In 228 out of 323 Dutch patients the radiation dose to the kidneys (and SD) was 20.1 ± 4.9 Gy (figure 6C), calculated with standard kidney mass. In 119 out of 323 Dutch patients the radiation dose to the kidneys was 19.9 ± 5.4 Gy with standard kidney volume and 16.9 ± 5.2 Gy with individual CT-based kidney volume.



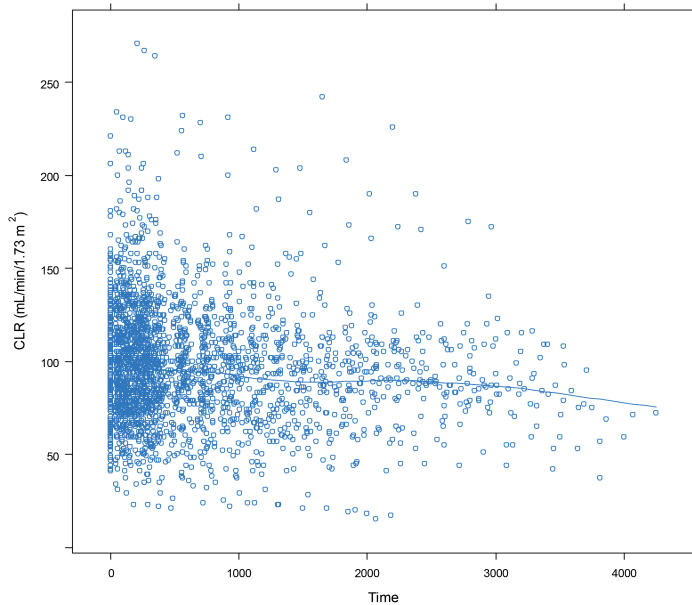
Supplemental figure 1 – The difference between estimated and measured CLR from 24h-urine for Cockcroft (A), Cockcroft-Gault (C-G) correct for body surface area (BSA) (B), Modification of Diet in Renal Disease (MDRD) and Extended Modification of Diet in Renal Disease (extMDRD).



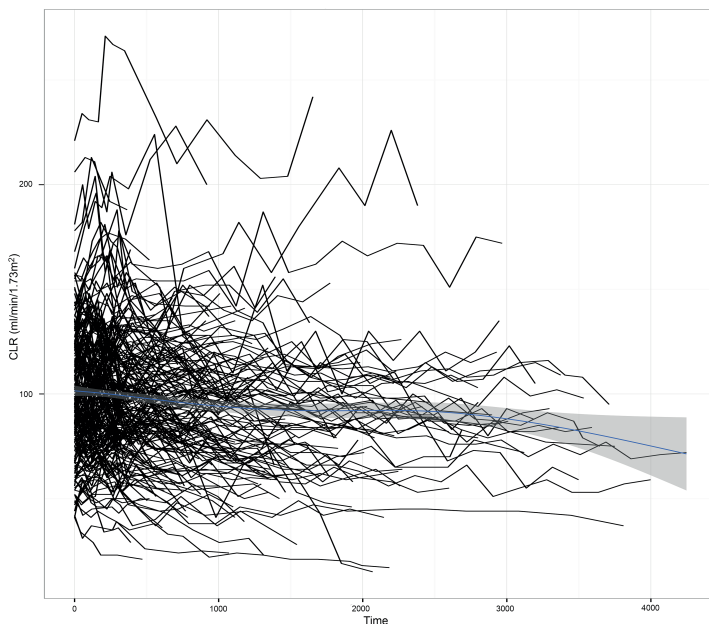
Supplemental figure 2 – Absolute estimated and measured CLR from 24h-urine for Cockcroft (A), Cockcroft-Gault (C-G) correct for body surface area (BSA) (B), Modification of Diet in Renal Disease (MDRD) and Extended Modification of Diet in Renal Disease (extMDRD). Also Spearman’s rank correlation coefficient (R_{spearman}) is given per graph.



Supplemental figure 3 - Evolution of renal function (Cockcroft-Gault) over time overlaid on the same plot in 209 Dutch patients.



Supplemental figure 4 - Smooth average longitudinal renal function (Cockcroft-Gault) for 209 Dutch patients is indicated by blue line. Dots are single measurement of Creatinine clearance (CLR).



Supplemental figure 5 - Smooth average longitudinal profile of all patients indicated by blue line (loess plus confidence band):

Supplemental Table 1 – Comparison of different models

Model	AICc	BIC	df
Linear	18983.36	19012.45	5
Polynomial	18974.54	19015.76	7
Spline	18960.14	19018.28	10
Nonlinear with plateau	19606.72	19641.63	6
Nonlinear without plateau	19000.84	19029.94	5

Subset Analysis: Model	AICc	BIC	df
Nonlinear without plateau	15281.36	15337.47	10
- including Kdose	15281.93	15343.64	11
-including BED	15282.3	15344.01	11

Akaike Information Criterion (AIC), Bayesian information criterion (BIC)

Supplemental Table 2 – Final Model output - Nonlinear mixed-effects model fit by REML:

Fixed effects	Coefficient	Std Err.	Df	t-value	p-value
Intercept	107.745	4.665	2284	23.097	0.0000
Age >70 vs. Age <=70	-24.492	5.411	2284	-4.526	0.0000
HT (yes vs. no)	0.932	4.466	2284	0.209	0.8346
Diabetes (yes vs. no)	3.299	3.933	2284	0.839	0.4017
Baseline CTCAE	-46.190	6.552	2284	-7.050	0.0000
Newdosis > 600 vs. Newdosis <=600	0.868	4.582	2284	0.189	0.8498
Decay rate	0.001	0.000	2284	9.374	0.0000

Output random effects:

Diagonal covariate matrix: estimated standard deviation of 26.17 and 0.001 for b_0 and b_1 respectively.

#Note; interactions tried between Time in weeks and Age, BasCTCAE, HT, Diabetes and NewDosis, do not improve model fit. Use of DMMed/HBA1c60 does not improve model fit over use of Diabetes.

REFERENCES

1. Valkema R, Pauwels SA, Kvols LK, Kwekkeboom DJ, Jamar F, de Jong M, et al. Long-term follow-up of renal function after peptide receptor radiation therapy with (90)Y-DOTA(0), Tyr(3)-octreotide and (177)Lu-DOTA(0), Tyr(3)-octreotate. *J Nucl Med*. 2005;46 Suppl 1:835–91S.
2. Bodei L, Cremonesi M, Ferrari M, Pacifici M, Grana CM, Bartolomei M, et al. Long-term evaluation of renal toxicity after peptide receptor radionuclide therapy with 90Y-DOTATOC and 177Lu-DOTATATE: the role of associated risk factors. *Eur J Nucl Med Mol Imaging*. 2008;35:1847–56. doi:10.1007/s00259-008-0778-1.
3. Rolleman EJ, Melis M, Valkema R, Boerman OC, Krenning EP, de Jong M. Kidney protection during peptide receptor radionuclide therapy with somatostatin analogues. *Eur J Nucl Med Mol Imaging*. 2010;37:1018–31. doi:10.1007/s00259-009-1282-y.
4. Imhof A, Brunner P, Marinček N, Briel M, Schindler C, Rasch H, et al. Response, survival, and long-term toxicity after therapy with the radiolabeled somatostatin analogue [90Y-DOTA]-TOC in metastasized neuroendocrine cancers. *J Clin Oncol*. 2011;29:2416–23. doi: 10.1200/JCO.2010.33.7873.
5. Bodei L, Kidd M, Paganelli G, Grana CM, Drozdov I, Cremonesi M, et al. Long-term tolerability of PRRT in 807 patients with neuroendocrine tumours: the value and limitations of clinical factors. *Eur J Nucl Med Mol Imaging*. 2015;42:5–19. doi:10.1007/s00259-014-2893-5.
6. Melis M, Krenning EP, Bernard BF, Barone R, Visser TJ, de Jong M. Localisation and mechanism of renal retention of radiolabelled somatostatin analogues. *Eur J Nucl Med Mol Imaging*. 2005;32: 1136–43. doi:10.1007/s00259-005-1793-0.
7. Jamar F, Barone R, Mathieu I, Walrand S, Labar D, Carlier P, et al. 86Y-DOTA(0)-D-Phe1-Tyr3-octreotide (SMT487) – a phase 1 clinical study: pharmacokinetics, biodistribution and renal protective effect of different regimens of amino acid co-infusion. *Eur J Nucl Med Mol Imaging*. 2003;30:510–8. doi:10.1007/s00259-003-1117-1.
8. Rolleman EJ, Valkema R, de Jong M, Kooij PP, Krenning EP. Safe and effective inhibition of renal uptake of radiolabelled octreotide by a combination of lysine and arginine. *Eur J Nucl Med Mol Imaging*. 2003;30:9–15. doi:10.1007/s00259-002-0982-3.
9. Emami B, Purdy JA, Manolis J, Barest G, Cheng E, Coia L, et al. Three-dimensional treatment planning for lung cancer. *Int J Radiat Oncol Biol Phys*. 1991;21:217–27.
10. Marks LB, Yorke ED, Jackson A, Ten Haken RK, Constine LS, Eisbruch A, et al. Use of normal tissue complication probability models in the clinic. *Int J Radiat Oncol*. 2010;76:S10–S9. doi:10.1016/j.ijrobp.2009.07.1754.
11. Wessels BW, Konijnenberg MW, Dale RG, Breitz HB, Cremonesi M, Meredith RF, et al. MIRDP pamphlet No. 20: the effect of model assumptions on kidney dosimetry and response – implications for radionuclide therapy. *J Nucl Med*. 2008;49:1884–99. doi:10.2967/jnumed.108.053173.
12. Kwekkeboom DJ, Bakker WH, Kooij PP, Konijnenberg MW, Srinivasan A, Erion JL, et al. [177Lu-DOTA0, Tyr3]octreotate: comparison with [111In-DTPA0]octreotide in patients. *Eur J Nucl Med*. 2001;28:1319–25. doi:10.1007/s002590100574.
13. US Department of Health and Human Services, National Institutes of Health, National Cancer Institute. Common Terminology Criteria for Adverse Events (CTCAE), version 4.0. Bethesda, MD: US Department of Health and Human Services; 2010.
14. Konijnenberg MW, Bijster M, Krenning EP, De Jong M. A stylized computational model of the rat for organ dosimetry in support of preclinical evaluations of peptide receptor radionuclide therapy with (90)Y, (111)In, or (177)Lu. *J Nucl Med*. 2004;45:1260–9.
15. Stabin MG, Siegel JA. Physical models and dose factors for use in internal dose assessment. *Health Phys*. 2003;85:294–310. doi:10.1097/00004032-200309000-00006.

16. Sgouros G. Dosimetry of internal emitters. *J Nucl Med.* 2005;46 Suppl 1:18S–27S.
17. Sabet A, Ezziddin K, Pape UF, Reichman K, Haslerud T, Ahmadzadehfar H, et al. Accurate assessment of long-term nephrotoxicity after peptide receptor radionuclide therapy with (177)Lu-octreotate. *Eur J Nucl Med Mol Imaging.* 2014;41:505–10. doi:10.1007/s00259-013-2601-x.
18. Bodei L, Cremonesi M, Grana CM, Fazio N, Iodice S, Baio SM, et al. Peptide receptor radionuclide therapy with (177)Lu-DOTATATE: the IEO phase I-II study. *Eur J Nucl Med Mol Imaging.* 2011;38:2125–35. doi:10.1007/s00259-011-1902-1.
19. Kwekkeboom DJ, de Herder WW, Kam BL, van Eijck CH, van Essen M, Kooij PP, et al. Treatment with the radiolabeled somatostatin analog [177Lu-DOTA 0, Tyr3]octreotate: toxicity, efficacy, and survival. *J Clin Oncol.* 2008;26:2124–30. doi:10.1200/JCO.2007.15.2553.
20. Sterner G, Frennby B, Mansson S, Nyman U, Van Westen D, Almen T. Determining 'true' glomerular filtration rate in healthy adults using infusion of inulin and comparing it with values obtained using other clearance techniques or prediction equations. *Scand J Urol Nephrol.* 2008;42:278–85. doi: 10.1080/00365590701701806.
21. Murray AW, Barnfield MC, Waller ML, Telford T, Peters AM. Assessment of glomerular filtration rate measurement with plasma sampling: a technical review. *J Nucl Med Technol.* 2013;41:67–75. doi:10.2967/jnmt.113.121004.
22. Cockcroft DW, Gault MH. Prediction of creatinine clearance from serum creatinine. *Nephron.* 1976;16:31–41.
23. Levey AS, Coresh J, Greene T, Stevens LA, Zhang YL, Hendriksen S, et al. Using standardized serum creatinine values in the modification of diet in renal disease study equation for estimating glomerular filtration rate. *Ann Intern Med.* 2006;145:247–54.
24. Michels WM, Grootendorst DC, Verduijn M, Elliott EG, Dekker FW, Krediet RT. Performance of the Cockcroft-Gault, MDRD, and new CKD-EPI formulas in relation to GFR, age, and body size. *Clin J Am Soc Nephrol.* 2010;5:1003–9. doi:10.2215/CJN.06870909.
25. Van Binnebeek S, Baete K, Vanbilloen B, Terwinghe C, Koole M, Mottaghy FM, et al. Individualized dosimetry-based activity reduction of (90)Y-DOTATOC prevents severe and rapid kidney function deterioration from peptide receptor radionuclide therapy. *Eur J Nucl Med Mol Imaging.* 2014;41:1141–57. doi:10.1007/s00259-013-2670-x.
26. Konijnenberg M, Melis M, Valkema R, Krenning E, de Jong M. Radiation dose distribution in human kidneys by octreotides in peptide receptor radionuclide therapy. *J Nucl Med.* 2007;48:134–42.
27. De Jong M, Valkema R, Van Gameren A, Van Boven H, Bex A, Van De Weyer EP, et al. Inhomogeneous localization of radioactivity in the human kidney after injection of [(111)In-DTPA]octreotide. *J Nucl Med.* 2004;45:1168–71.
28. Svensson J, Berg G, Wangberg B, Larsson M, Forssell-Aronsson E, Bernhardt P. Renal function affects absorbed dose to the kidneys and haematological toxicity during (177)Lu-DOTATATE treatment. *Eur J Nucl Med Mol Imaging.* 2015;42:947–55. doi:10.1007/s00259-015-3001-1. 29.
29. Barone R, Borson-Chazot F, Valkema R, Walrand S, Chauvin F, Gogou L, et al. Patient-specific dosimetry in predicting renal toxicity with (90)Y-DOTATOC: relevance of kidney volume and dose rate in finding a dose-effect relationship. *J Nucl Med.* 2005;46 Suppl 1:99S–106S.
30. Thames HD, Ang KK, Stewart FA, van der Schueren E. Does incomplete repair explain the apparent failure of the basic LQ model to predict spinal cord and kidney responses to low doses per fraction? *Int J Radiat Biol.* 1988;54:13–9.

- 31.** Gustafsson J, Nilsson P, Gleisner KS. On the biologically effective dose (BED) – using convolution for calculating the effects of repair: II. Numerical considerations. *Phys Med Biol.* 2013;58:1529–48. doi:10.1088/0031-9155/58/5/1529.
- 32.** Wehrmann C, Senftleben S, Zachert C, Muller D, Baum RP. Results of individual patient dosimetry in peptide receptor radionuclide therapy with ¹⁷⁷Lu DOTA-TATE and ¹⁷⁷Lu DOTA-NOC. *Cancer Biother Radiopharm.* 2007;22:406–16. doi:10.1089/cbr.2006.325.
- 33.** Sandstrom M, Garske U, Granberg D, Sundin A, Lundqvist H. Individualized dosimetry in patients undergoing therapy with (¹⁷⁷)Lu-DOTA-D-Phe (1)-Tyr (3)-octreotate. *Eur J Nucl Med Mol Imaging.* 2010;37:212–25. doi:10.1007/s00259-009-1216-8.
- 34.** Garkavij M, Nickel M, Sjogreen-Gleisner K, Ljungberg M, Ohlsson T, Wingardh K, et al. ¹⁷⁷Lu-[DOTA0,Tyr3] octreotate therapy in patients with disseminated neuroendocrine tumors: Analysis of dosimetry with impact on future therapeutic strategy. *Cancer.* 2010;116:1084–92. doi:10.1002/cncr.24796.
- 35.** Sward C, Bernhardt P, Ahlman H, Wangberg B, Forssell-Aronsson E, Larsson M, et al. [¹⁷⁷Lu-DOTA 0-Tyr3]-octreotate treatment in patients with disseminated gastroenteropancreatic neuroendocrine tumors: the value of measuring absorbed dose to the kidney. *World J Surg.* 2010;34:1368–72. doi:10.1007/s00268-009-0387-6.
- 36.** Claringbold PG, Brayshaw PA, Price RA, Turner JH. Phase II study of radiolabeled peptide ¹⁷⁷Lu-octreotate and capecitabine therapy of progressive disseminated neuroendocrine tumours. *Eur J Nucl Med Mol Imaging.* 2011;38:302–11. doi:10.1007/s00259-010-1631-x.
- 37.** Sandstrom M, Garske-Roman U, Granberg D, Johansson S, Widstrom C, Eriksson B, et al. Individualized dosimetry of kidney and bone marrow in patients undergoing ¹⁷⁷Lu-DOTA-octreotate treatment. *J Nucl Med.* 2013;54:33–41. doi:10.2967/jnumed.112.107524.
- 38.** Stabin MG, Sparks RB, Crowe E. OLINDA/EXM: the second-generation personal computer software for internal dose assessment in nuclear medicine. *J Nucl Med.* 2005;46(6):1023-7.
- 39.** Bakker WH, Albert R, Bruns C, Breeman WA, Hofland LJ, Marbach P et al. [¹¹¹In-DTPA-D-Phe1]-octreotide, a potential radiopharmaceutical for imaging of somatostatin receptor-positive tumors: synthesis, radiolabeling and in vitro validation. *Life Sci.* 1991;49(22):1583-91.
- 40.** Bakker WH, Krenning EP, Reubi JC, Breeman WA, Setyono-Han B, de Jong M et al. In vivo application of [¹¹¹In-DTPA-D-Phe1]-octreotide for detection of somatostatin receptor-positive tumors in rats. *Life Sci.* 1991;49(22):1593-601.

2.2

SUBACUTE HAEMATOTOXICITY AFTER PRRT WITH ¹⁷⁷LU- DOTA-OCTREOTATE: PROGNOSTIC FACTORS, INCIDENCE AND COURSE

Hendrik Bergsma¹, Mark W. Konijnenberg¹, Boen L. R. Kam¹, Jaap J. M. Teunissen¹, Peter P. Kooij¹,
Wouter W. de Herder², Gaston J. H. Franssen³, Casper H. J. van Eijck³, Eric P. Krenning¹, Dik J. Kwekkeboom¹

¹ Department of Radiology & Nuclear Medicine,

² Department of Internal Medicine,

³ Department of Surgery, Erasmus MC, University Medical Center, Rotterdam, The Netherlands

ABSTRACT

In peptide receptor radionuclide therapy (PRRT), the bone marrow (BM) is one of the dose-limiting organs. The accepted dose limit for BM is 2 Gy, adopted from ^{131}I treatment. We investigated the incidence and duration of hematological toxicity and its risk factors in patients treated with PRRT with $^{177}\text{Lu-DOTA}^0\text{-Tyr}^3\text{-octreotate}$ ($^{177}\text{Lu-DOTATATE}$). Also, absorbed BM dose estimates were evaluated and compared with the accepted 2 Gy dose limit.

Methods:

The incidence and duration of grade 3 or 4 hematological toxicity (according to CTCAE v3.0) and risk factors were analyzed. Mean BM dose per unit (Gigabecquerels) of administered radioactivity was calculated and the correlations between doses to the BM and hematological risk factors were determined.

Results:

Hematological toxicity (grade 3/4) occurred in 34 (11 %) of 320 patients. In 15 of the 34 patients, this lasted more than 6 months or blood transfusions were required. Risk factors significantly associated with hematological toxicity were: poor renal function, white blood cell (WBC) count $<4.0 \times 10^9/\text{l}$, age over 70 years, extensive tumor mass and high tumor uptake on the OctreoScan. Previous chemotherapy was not associated. The mean BM dose per administered activity in 23 evaluable patients was 67 ± 7 mGy/GBq, resulting in a mean BM dose of 2 Gy in patients who received four cycles of 7.4 GBq $^{177}\text{Lu-DOTATATE}$. Significant correlations between (cumulative) BM dose and platelet and WBC counts were found in a selected group of patients.

Conclusion:

The incidence of subacute hematological toxicity after PRRT with $^{177}\text{Lu-DOTATATE}$ is acceptable (11 %). Patients with impaired renal function, low WBC count, extensive tumor mass, high tumor uptake on the OctreoScan and/or advanced age are more likely to develop grade 3/4 hematological toxicity. The BM dose limit of 2 Gy, adopted from ^{131}I , seems not to be valid for PRRT with $^{177}\text{Lu-DOTATATE}$.

Keywords:

PRRT, $^{177}\text{Lu-DOTATATE}$, Bone marrow, Toxicity, Dosimetry

INTRODUCTION

In the past two decades, peptide receptor radionuclide therapy (PRRT) with radiolabelled somatostatin analogues has been used successfully in patients with somatostatin receptor-positive tumors. One of the most frequently used radiopharmaceuticals is ¹⁷⁷Lu-DOTA⁰-Tyr³-octreotate (¹⁷⁷Lu- DOTATATE). Patients with neuroendocrine tumors treated with ¹⁷⁷Lu-DOTATATE have a radiological response rate of 15 – 35 % [1–5]. Generally, PRRT is well tolerated, but the kidneys and bone marrow (BM) are usually the dose-limiting organs.

BM toxicity results from irradiation of and damage to hematopoietic tissue. Grade 3 or 4 hematological toxicity develops in about 5 – 10 % of patients [6–11]. The nadir normally occurs 4 – 6 weeks after each treatment, followed by a recovery phase. The generally accepted threshold dose for radiation-induced BM suppression is 2 Gy, adopted from ¹³¹I therapy studies [12, 13]. However, up to now, no data have been published that confirm or reject this BM dose limit for ¹⁷⁷Lu-DOTATATE.

The aim of this study was to analyze short-term hematological toxicity after PRRT with ¹⁷⁷Lu-DOTATATE. Risk factors analyzed included renal function, chemotherapy, baseline cytopenia, tumor mass and patient age. In addition, the individual and mean BM doses were calculated in a subgroup of patients.

MATERIALS AND METHODS

Patients

The study included 320 Dutch patients who were treated from January 2000 to December 2007. Inclusion criteria were: patients with neuroendocrine tumor and baseline tumor uptake on [¹¹¹In-DTPA⁰] octreotide scintigraphy (OctreoScan[®]; Mallinckrodt, Petten, The Netherlands) with accumulation in the tumor at least as high as in normal liver tissue; no prior treatment with PRRT; baseline serum hemoglobin (Hb) ≥6 mmol/l; white blood cell (WBC) count ≥2×10⁹/l; platelet (PLT) count ≥75×10⁹/l; serum creatinine ≤150 μmol/l or creatinine clearance ≥40 ml/min and Karnofsky performance status ≥50. Only Dutch patients were selected, because loss to follow-up is limited in these patients.

This study was part of the ongoing prospective study in patients with neuroendocrine tumors treated with ¹⁷⁷Lu-octreotate at the Department of Nuclear Medicine, Erasmus University Medical Center Rotterdam. The hospital's medical ethics committee approved the study. All patients gave written informed consent for participation in the study.

Treatment

[DOTA⁰,Tyr³] octreotate was obtained from BioSynthema (St. Louis, MO). ¹⁷⁷LuCl₃ was supplied by IDB-Holland (Baarle-Nassau, The Netherlands) and ¹⁷⁷Lu-DOTATATE was prepared locally [14].

Granisetron 3 mg or ondansetron 8 mg was injected intravenously 30 min before infusion of ¹⁷⁷Lu-DOTATATE. Infusion of amino acids (2.5 % arginine and 2.5 % lysine, 1 l) was started 30 min before administration of the radiopharmaceutical and lasted for 4 h. The radiopharmaceutical was coadministered for 30 min using a second pump system. Cycle dosages of 1.85 GBq (50 mCi) were given in 4 patients, 3.7 GBq (100 mCi) in 13 patients, 5.6 GBq (150 mCi) in 14 patients, and 7.4 GBq (200 mCi) in the remaining patients, injected over 30 min. The interval between treatments was 6 – 16 weeks. The intended cumulative dose was 29.6 GBq (800 mCi). Median cumulative activity was 29.6 GBq, range 7.4 – 29.6 GBq. However, the dose was lowered if the calculated kidney dose was higher than 23 Gy. Other reasons for dose reduction or cessation of further therapy were recurrent grade 3 or 4 hematological toxicity and persistent low blood counts.

Dosimetry

Biodistribution and dosimetry studies were performed in three subgroups of patients. The data on estimated BM doses have been published previously [14–16]. Only patients meeting the inclusion criteria, as stated above, and with complete datasets for dosimetry were included in the present analysis. The BM dose (D_{rm}) is derived from three sources: (1) from the blood circulating through the marrow cavities (rm), (2) from large organs and tumors with high radioactivity uptake (h), and (3) from the general distribution of radioactivity throughout the remaining whole body (rb):

$$D_{rm} = \tilde{A}_{rm}DF(rm \leftarrow rm) + \tilde{A}_hDF(rm \leftarrow h) + \tilde{A}_{rb}DF(rm \leftarrow rb) \quad (2.13)$$

where \tilde{A} is the cumulative activity and DF are the dose factors for red marrow to red marrow, large organs to red marrow, and remainder of the body to red marrow. The contribution to the BM dose from radioactivity distribution within the remainder was calculated (and corrected) according to the method of Wessels et al. [17].

Calculated dose contributions were based on planar scans (at 24, 96 and 168 h after injection), and radioactivity measured in urine (at 1, 6, 24, 48 h after injection) and blood samples (at 0, 10, 30, 60, 90, 120, 360 and 1,440 min after injection). A pharmacokinetics (PK) compartment model was used to describe the biodistribution of radioactivity in organs over time. Organs with physiological uptake (kidneys and abdomen) were added to the central (blood) compartment (Figure 1). A single compartment linked

to the kidney was able to model the urine data. An additional remainder-of-the-body compartment was used to fit the data. Flow in both directions between compartments was modeled by kinetic transfer components, $k(i,j)$. The PK compartment model was numerically solved using SAAMII software (Simulation Analysis and Modeling; SAAM Institute, Seattle, WA). BM dose values were computed using the Olinda/EXM software package (Vanderbilt University) and using dose factors for ^{177}Lu [18].

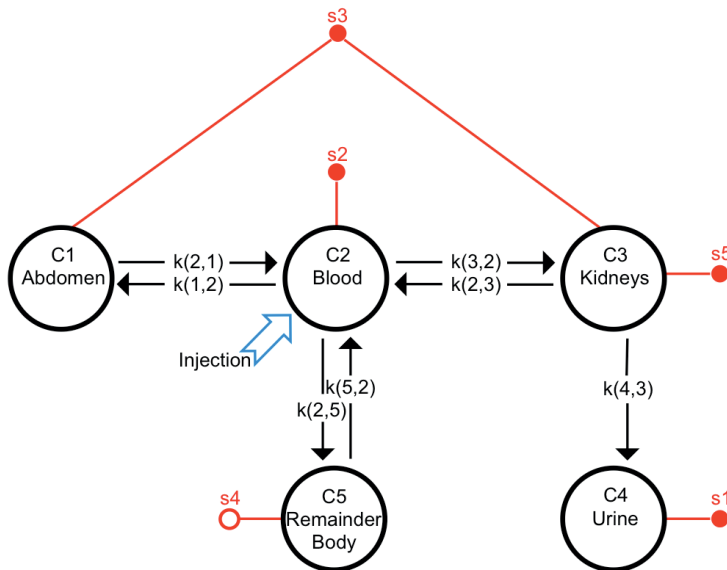


Figure 1 – Generalized compartment model for the biodistribution of ^{177}Lu -DOTATATE in humans. Compartments (C1 to C5) represent different organs. Flow in both directions between compartments is represented by kinetic transfer components, $k(i,j)$. The shaded grey circles represent input (radioactivity) data and the open grey circle represents modeled output. Injection is a simulated bolus of ^{177}Lu -DOTATATE in the blood compartment.

Toxicity assessment

Hematology, and liver and renal function tests were performed during the 6 weeks before the first therapy, 4 and 6 weeks after each therapy, and at follow-up visits. Hematological toxicity was assessed according to Common Terminology Criteria for Adverse Events (CTCAE v3.0) [19]. This version of CTCAE was used because of well-defined criteria for thrombocytopenia, leucocytopenia and anemia. Hematological toxicity was modeled for toxicity grade 3/4 in PLT count, WBC count, Hb and a combination of all three. The duration of grade 3/4 hematological toxicity was defined as the time from the last therapy until recovery to toxicity grade 2 or lower.

Statistical analysis and parameters

SPSS software (SPSS 19; IBM, New York, NY) was used for statistical analysis. Distributions were examined for normality using the Kolmogorov-Smirnov test. Correlations between distributions were evaluated using the χ^2 test, t-test and analysis of variance. Spearman's rank correlation coefficient was used for correlation analysis. Regression analysis was performed with the binary logistic model. Conditional step- forward and step-backward methods were used with the following parameters: classification cut-off 0.5, maximum iterations 20, probability for entry 0.05 and removal 0.20. P values <0.05 (for both step-forward and step-backward) were considered significant. The following discrete baseline variables were included in the analysis: gender, age over 70 years, presence of bone metastasis, prior chemotherapy, prior external beam radiotherapy, uptake on the OctreoScan, tumor load, chromogranin A >2,000 $\mu\text{g/l}$, splenectomy, baseline PLT count <150 $\times 10^9/\text{l}$ and baseline WBC count <4.0 $\times 10^9/\text{l}$. The creatinine clearance was estimated with the Cockcroft-Gault formula and evaluated as a continuous variable. Similar regression analyses were performed setting thresholds for decreases in PLT count, WBC count and Hb of 15 % and 25 % after the first therapy. Univariate analysis was performed in a subgroup of patients with transient and persistent grade 3/4 hematological toxicity. In the dosimetric subgroups, the correlations between the percentage reductions in blood cells (Hb, PLT count, WBC count) after the first therapy and dose to the BM were determined using Spearman's rank correlation coefficients (r_s). The median and mean doses to the BM per unit (gigabecquerels) of administered radioactivity were calculated for each subgroup separately and for all three subgroups combined.

RESULTS

In total, 324 patients were evaluated. The patient characteristics are summarized in Table 1. Four patients were excluded because of unrelated hematological toxicity (internal bleeding in three and iron-deficiency anemia in one).

Toxicity

Severe subacute hematological toxicity (grade 3/4) occurred 4 to 8 weeks after administration in 34 (11 %) of the 320 patients, with thrombocytopenia in 25 (8 %), leucocytopenia in 17 (5 %), anemia in 10 (3 %) and pancytopenia (1 %) (Figure 2).

Two patients were excluded from the analyses for toxicity duration. One patient (with grade 4 thrombocytopenia) died 6 weeks after last the treatment due to bowel obstruction, and one patient (with grade 3 thrombocytopenia and grade 3 anemia) died 9 weeks after last the treatment due to progressive disease. Of 30 patients, 15 (50 %) had grade 3/4 hematological toxicity lasting more than 6 months or required blood

transfusion. The duration of hematological toxicity in these patients is presented in Figure 3.

Table 1 - Baseline characteristics of 320 Dutch patients

Characteristic	Number of patients (%)
Male	164 (51)
Age ≥70 years	62 (19)
Karnofsky performance status ≤70	46 (14)
Elevated chromogranin A	237 (74)
Bone metastasis	72 (23)
Splenectomy	12 (4)
WBC count <4.0 × 10 ⁹ /l at baseline PRRT	16 (5)
Previous therapy	
Chemotherapy	38 (12)
Radiotherapy (external)	32 (10)
Tumor type	
Neuroendocrine	278 (87)
Other	42 (13)
Tumor uptake on baseline OctreoScan	
Equal to or more than normal liver	248 (77)
Higher than kidneys	72 (23)
Tumor mass on baseline OctreoScan	
Equal to or more than normal liver	264 (82)
Higher than kidneys	56 (18)
Cumulative activity (GBq)	
≤22.2	103 (32)
≤29.6	215 (67)
Kidney function, mean (range) creatinine clearance	
in milliliters per minute, Cockcroft-Gault	99 (35 – 246)

Baseline parameters that were significantly associated with grade 3/4 hematological toxicity were: decreased renal function, WBC <4.0×10⁹/l, age >70 years, extensive tumor mass, and tumor uptake on the OctreoScan more than uptake in the kidneys (Table 2). No significant association was found for previous chemotherapy.

Of 30 patients with persistent (more than 6 months) hematological toxicity or who required blood transfusions, 15 had significantly more tumor mass on the baseline OctreoScan than patients with transient (6 months or less) grade 3/4 hematological toxicity. No significant difference in other baseline variables was found between these

two sub- groups (data not shown). In patients with decrease in Hb of more than 15 % after the first therapy, previous radiotherapy was an additional significant factor in the logistic regression analysis ($p = 0.005$ and $p = 0.001$ for step-forward and step-backward methods, respectively). In patients with a decrease in Hb, PLT count and/or WBC count of more than 25 % after the first therapy, decreased renal function at baseline was the only significant variable ($p < 0.05$).

Table 2 - Baseline clinical parameters associated with grade 3/4 hematological toxicity in 34 of 320 patients treated with a median cumulative dose of 29.6 GBq ^{177}Lu -DOTATATE from logistic regression analysis with the stepwise method (step-forward and step-backward).

Variable	Step-forward		Step-backward	
	Coefficient ^b	p value	Coefficient	p value
Any toxicity (Hb/PLT/WBC)				
Creatinine clearance (Cockcroft-Gault) ^a	-0.160	0.028	-0.150	0.044
Bone metastasis	1.055	0.017	0.912	0.056
WBC count $< 4.0 \times 10^9/\text{l}$ at baseline ^a	1.828	0.005	1.741	0.011
Tumor uptake on Octreoscan $>$ kidney uptake	0.867	0.051	1.055	0.023
Previous radiotherapy	Not in predictive equation		1.225	0.074
Previous chemotherapy	Not in predictive equation		1.171	0.161
Hemoglobin				
Age > 70 years ^a	1.698	0.045	1.860	0.039
Extensive tumor mass ^a	2.551	0.002	2.570	0.003
Previous radiotherapy	Not in predictive equation		2.165	0.036
Platelets				
Creatinine clearance (Cockcroft-Gault) ^a	-0.022	0.01	-0.025	0.008
Bone metastasis	1.268	0.009		
WBC count $< 4.0 \times 10^9/\text{l}$ at baseline	1.731	0.016	1.565	0.196
Extensive tumor mass	Not in predictive equation		1.174	0.024
Previous radiotherapy	Not in predictive equation		1.392	0.055
Previous chemotherapy	Not in predictive equation		-1.604	0.144
White blood cells				
Age > 70 years	Not in predictive equation		1.161	0.062
WBC count $< 4.0 \times 10^9/\text{l}$ at baseline ^a	2.436	0.001	2.531	0.000
Tumor uptake on Octreoscan $>$ kidney uptake ^a	1.321	0.022	1.549	0.010
Previous radiotherapy	1.363	0.068	Not in predictive equation	

^a Variable statistically significant ($p < 0.05$) in multivariate analyses

^b Logistic coefficient in predictive equation

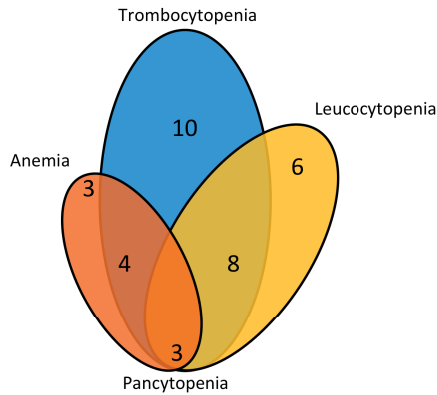


Figure 2 - Venn diagram of hematological toxicity (grade 3/4) in 34 out of 320 patients treated with a median cumulative dose of 29.6 GBq ¹⁷⁷Lu- DOTATATE.

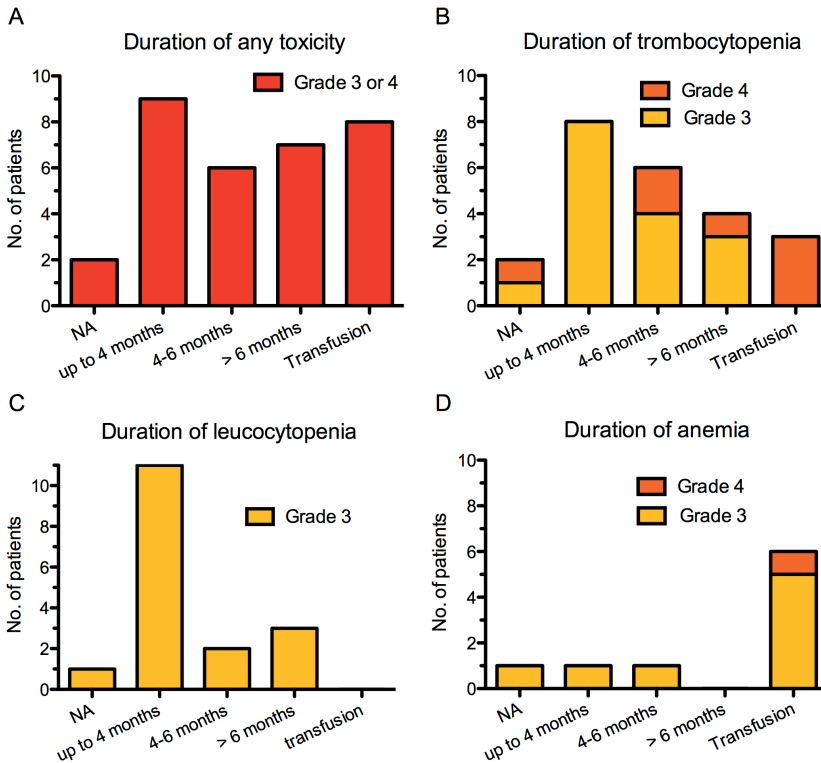


Figure 3 – Duration of subacute hematological toxicity (grade 3/4) in 32 of 320 patients treated with a median cumulative dose of 29.6 GBq ¹⁷⁷Lu-DOTATATE: a any toxicity in 32 patients, b thrombocytopenia in 23 patients, c leucocytopenia in 17 patients, and d anemia in 9 patients (NA results not available during follow-up, Transfusion patients who received blood cell transfusion after grade 3/4 hematological toxicity. Two patients were excluded (see text).

Dosimetry

The dosimetry analysis included 32 patients split into three groups with different cycle doses (1.85, 3.7 and 7.3 GBq ^{177}Lu -DOTATATE). Of the 32 patients, 25 patients were treated according protocol; in two patients no complete dosimetric data were available. The BM dose after the first therapy was determined in 25 patients: 4 patients in group 1 (cycle dose 1.85 GBq), 7 patients in group 2 (cycle dose 3.7 GBq) and 14 patients in group 3 (cycle dose 7.3 GBq). The cumulative dose was 14.8 GBq in 1 patient, 22.2 GBq in 9 patients and 29.6 GBq in 15 patients. The median dose (and range) to the BM per unit of administered radioactivity in patients in group 1 and group 2 was 69 mGy/GBq (54 – 73 mGy/GBq) and 75 mGy/GBq (35 – 139 mGy/GBq), respectively. In group 3 the median dose (and range) was 51 mGy/GBq (24 – 116 mGy/GBq) excluding one outlier of 331 mGy/GBq. In this patient the urinary excretion data could not be fitted correctly in the compartment model. This resulted in a long residence time of activity in the total body and in an exceptionally high BM dose, leading to the exclusion of this patient from further analysis (Supplementary Data). Despite a high calculated BM dose, this patient did not develop grade 3 or 4 hematological toxicity.

Data from groups 1, 2 and 3 combined were normally distributed (Kolmogorov-Smirnov test) allowing calculation of the mean BM dose. The mean BM dose (excluding one outlier) per unit of administered activity in the 24 evaluable patients was 0.067 ± 0.007 mGy/MBq. At an activity administration schedule of 4×7.4 GBq (which most patients received) this would lead to a BM dose of 2.0 ± 0.2 mGy. Three (13 %) of 23 patients developed grade 3/4 hematological toxicity. No significant difference in BM dose was observed between these 3 patients and the other 20. Significant Spearman's rank correlation coefficients and P values (one-tailed) were found in group 3 between (cumulative) BM dose and PLT count after the first and last treatments ($r_s = -0.51$ with $P < 0.05$ and $r_s = -0.59$ with $P = 0.02$, respectively) and WBC count ($r_s = -0.70$ with $P = 0.01$ and $r_s = -0.51$ with $P < 0.05$, respectively; Figure 4). No significant correlation between (cumulative) BM dose and hemoglobin was found in group 3, and no significant correlations were found between (cumulative) BM dose and blood cells in group 1 and group 2.

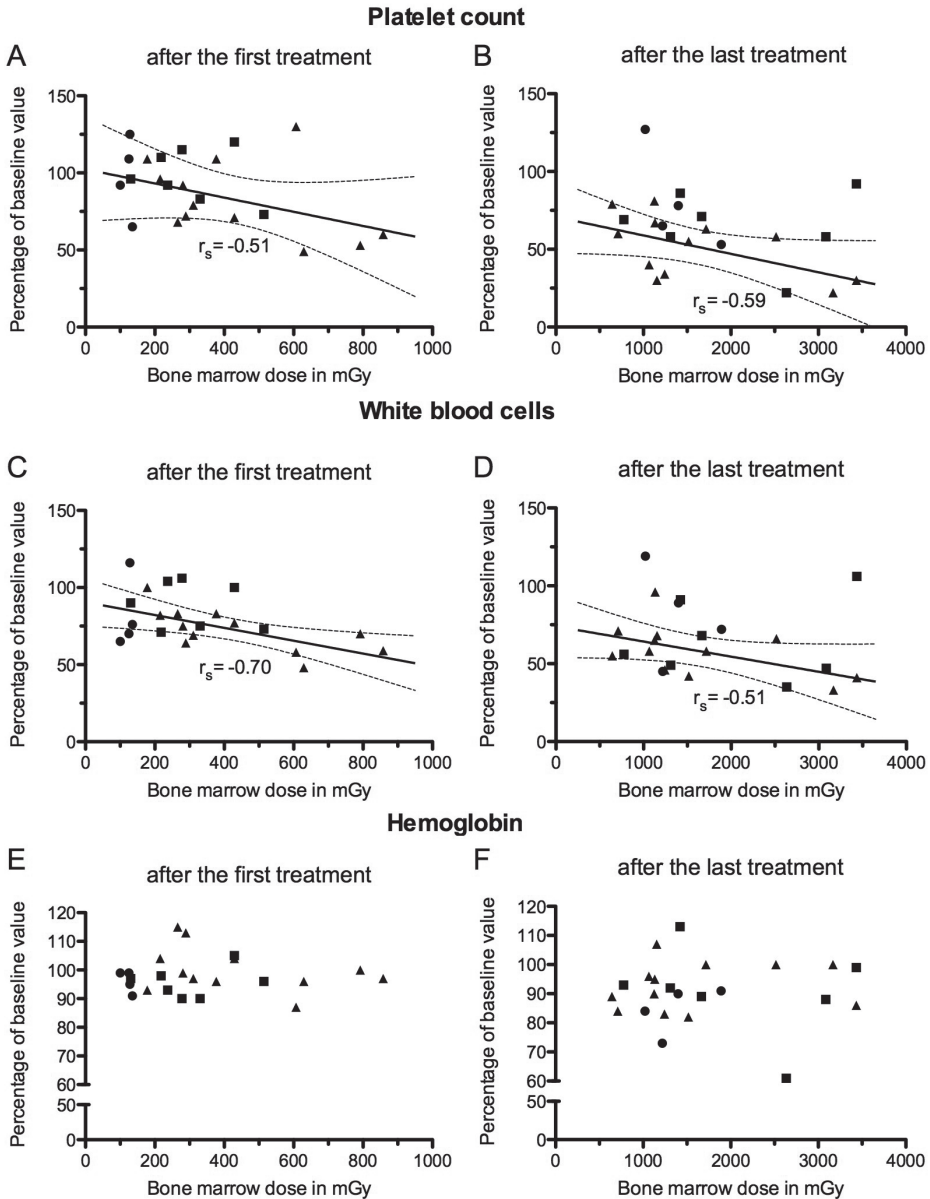


Figure 4 - Platelet counts (a,b), white blood cell counts (c, d) and hemoglobin (e, f) expressed as percentages of the baseline values in relation to bone marrow dose in 23 patients after the first and last treatments with ^{177}Lu - DOTATATE (● circles group-1, 1.85 GBq, n=4; ■ squares group 2, 3.70 GBq, n=7; ▲ triangles group 3, 7.40 GBq, n=12). Solid lines are linear regression with 95 % confidence intervals (dotted lines). Significant Spearman's rank correlation coefficients with (one-tailed) P values in group 3: a $r_s = -0.51$ with $P < 0.05$, b $r_s = -0.59$ with $P = 0.02$, c $r_s = -0.70$ with $P = 0.01$, d $r_s = -0.51$ with $P < 0.05$.

DISCUSSION

Subacute hematological grade 3/4 toxicity was observed in 34 (11 %) of 320 patients receiving ^{177}Lu -DOTATATE. In half of these patients, toxicity persisted for more than 6 months or blood transfusions were required. This is in accordance with data from other groups [5–10]. Long-term hematological toxicities, such as myelodysplastic syndrome (MDS) and acute leukemia (AL), have been found in patients receiving PRRT with ^{177}Lu -DOTATATE [6, 11]. Also in our patient group, MDS and AL were observed, but since these events have a rare complex stochastic character, they will be reported in a separate study. In a recent study, long-term side effects of PRRT with ^{90}Y -octreotide and/or ^{177}Lu -octreotate were investigated [6]. The authors found more hematological toxicity after PRRT in patients with baseline nephrotoxicity (transient or persistent elevation in creatinine). The prolonged circulation time of ^{177}Lu -DOTATATE in patients with a poor renal function is probably the most important factor that explains the increased toxicity to the BM, as shown by Svensson et al. [20]. Also anemia is common in these patients due to a reduction in renal erythropoietin production. In our study, poor renal function was also found to be a predictor of hematological toxicity. We also found that a low baseline WBC count is a predictor of grade 3/4 hematological toxicity. This is in line with the findings of a recent study showing that baseline cytopenia is a predictor of hematological toxicity after PRRT [9].

From a dosimetric point of view, it has been theorized that patients with a large tumor burden and high receptor density have lower amounts of circulating activity [21]. Therefore the radiation to normal tissues could be less than in patients with a low tumor burden. However, in our study, patients with more tumor mass at baseline were significantly more likely to have grade 3/4 hematological toxicity. Furthermore, high tumor burden was more frequently found in patients with persistent grade 3/4 hematological or who required blood transfusion. This suggests that tumor burden plays a role in the development and duration of hematological toxicity, in contrast to the recently described tumor sink effect [22]. That study showed that internalization of ^{68}Ga -DOTATATE in the tumor leads to a significant decrease in uptake in healthy tissue, the so-called tumor sink effect [22]. The authors extrapolated their results and speculated on a similar effect for PRRT. However, the main contributing factor for radiation dose to an organ (i.e. the BM) from PRRT is the exposure to radiation over time and the organ dose cannot be based on a distribution with only one time point. In our limited subgroup of patients in whom biodistribution and dosimetry data were available, we were not able to demonstrate the tumor sink effect.

Past chemotherapy was not a clear risk factor in our analyses. This finding can be explained by the limited number of patients who received chemotherapy in our series (38 of 320 patients, 12 %). In other studies more than 25 % of patients have had a history

of chemotherapy [6, 8, 9]. In particular, chemotherapy regimens with alkylating agents (e.g. cisplatin, carboplatin, oxaliplatin) or topoisomerase II inhibitors (e.g. etoposide) can damage the DNA of hematopoietic cells [23]. A small number (12 %) of patients in our study had received this type of chemotherapy in the past, therefore limiting the statistical power of this (possible) risk factor.

A potential protective effect of splenectomy on the development of hematological toxicity in patients receiving ¹⁷⁷Lu-DOTATATE has recently been reported [9]. The spleen is a major reservoir of blood cells and uptake of radioactivity is mainly caused by the presence of somatostatin receptors on lymphocytes [14, 24]. Blood cells circulating throughout the spleen may be damaged leading to a reduction in peripheral blood cell counts. However, in another clinical study with ¹⁷⁷Lu-DOTATATE/DOTATOC, no correlation was found between dose to the spleen and hematological toxicity during PRRT [25]. In our study, none of the 12 patients who had had a splenectomy developed grade 3/4 hematological toxicity. This supports the idea that splenectomy has a protective effect in patients receiving PRRT, but statistical analysis could not be performed due to the limited number of patients with splenectomy.

PRRT using ¹⁷⁷Lu-DOTATATE shows similarities to ¹³¹I treatment, because of the comparable half-life (6.7 and 8.0 days, respectively) and similar energies of the emitted β radiation (with average energies of 133 and 182 keV, respectively). Therefore in 2000, we accepted a maximum BM dose for PRRT with ¹⁷⁷Lu-DOTATATE, which was adopted from clinical studies with ¹³¹I treatments. The upper BM dose limit was set to 2 Gy, based on early work in thyroid cancer patients treated with ¹³¹I [12]. In that study, 122 doses of ¹³¹I were administered to 59 patients with metastasized thyroid cancer. In 14 administrations of ¹³¹I, serious radiation complications were observed (Table 3, original table). The authors stated that serious radiation complications per treatment cycle were more frequent when the total dose to the blood exceeded 200 rad (2 Gy) with a significance of $P = 0.03$ (Table 3). However, only 8 of 14 serious radiation complications were related to the BM; the other complications were pneumonitis or vomiting. When we repeated the analysis, taking into account only serious BM complications (Table 3, modified table), no significantly higher frequency of hematological toxicity for BM radiation doses more than 2 Gy could be demonstrated (Fisher's exact test, $P = 0.68$). Also, all eight patients with radiation complications (related to the BM) had metastatic disease to the bone. Bone metastases are a source of radiation after PRRT and could contribute to an increase in BM dose. However, in our multivariate analysis, the presence of bone metastases was not a risk factor for developing grade 3/4 hematological toxicity.

Another comment on the study by Benua et al. is that the radiation complications per unit administered dose were analyzed and the cumulative BM dose per patient was not considered. This resulted in a double count of radiation complications in one patient

(after the first and second dose of ^{131}I). In our study, hematological toxicity was counted only once per patient since the chance of recurrent hematological toxicity in one patient is relatively high. We also analyzed the cumulative BM dose instead of complications per administration, considering that multiple sequential treatments reduce the BM reserve. In a more recent article, the BM limit was set to 3 Gy for ^{131}I treatment, based on 104 treatments in 83 thyroid cancer patients [26]. No permanent BM suppression was observed, but two patients required PLT and red blood cell transfusion because of pancytopenia.

Table 3 - Complications in relation to total BM radiation dose reported by Benua et al. [12], and with new modifications. Data were derived from patients treated with radioiodine ^{131}I treatment.

Blood total radiation (Gy)	No. of doses	Original table ^a			Modified table ^b		
		Radiation complications			Radiation complications		
		Severe	Fatal	Total in percent	Severe	Fatal	Total in percent
0–0.99	5	0	0	0	0	0	0
1.00–1.99 ^c	24	1	0	4	1	0	4
2.00–2.99	33	5	1	18	3	1	12
3.00–3.99	7	1	1	29	1	0	14
4.00–4.99	9	0	2	22	0	1	11
Over5.00	7	2	0	29	1	0	14
Unknown	37	1	0	3	0	0	0
Total	122	10	4	7	6	2	7

^a Original table of Benua et al. [12]

^b Modified table with only serious bone marrow radiation complications

^c Significantly more frequent complications with total dose >200 rad are stated in the original table, but are not significant in the modified table

In the past decade, several studies with BM dose estimates using ^{177}Lu -DOTATATE have been reported (Table 4). Variations in the reported BM dose estimates can partly be attributed to differences in accuracy of dosimetric methods [27]. In a recent Swedish study, 200 patients who were treated with 7.4 GBq ^{177}Lu -DOTATATE were analysed and BM doses were calculated based on blood-based and organ-based analysis of the whole-body images. The authors calculated a maximum BM dose of 0.4 Gy per cycle of 7.4 GBq, which would result in a cumulative BM dose of 1.6 Gy for four cycles. Our data showed an estimated mean BM dose of 2.0 Gy (SD 0.2 Gy) in 184 out of 320 patients who received four cycles of 7.4 GBq ^{177}Lu -DOTATATE. Therefore, half of these patients (92 of 184) received a BM dose of more than 2 Gy. If the true maximum tolerated dose to the BM were 2 Gy, these 92 patients would theoretically be more prone to develop

hematological toxicity. However, we found hematological toxicity in only 34 of the 320 patients. This supports the idea that a higher BM dose limit for PRRT with ¹⁷⁷Lu-DOTATATE is appropriate. Another argument for a different BM dose maximum is the success of retreatment with extra cycles of PRRT without serious hematological side effects [28]. In our analysis of this type of retreatment, in which selected patients received a cumulative BM dose of approximately 3 Gy, only 5 (16 %) of 32 patients developed grade 3/4 hematological toxicity after two additional cycles of ¹⁷⁷Lu-DOTATATE. In another study reversible hepatotoxicity (grade 3/4) was found in 7 (21.2 %) of 33 patients who underwent salvage PRRT [29]. In our ongoing study in Erasmus MC, we have treated a selected group of patients with multiple additional cycles of ¹⁷⁷Lu-DOTATATE with cumulative doses up to 59.2 GBq resulting in an estimated mean BM dose of more than 3 Gy with limited hematological toxicity (unpublished data).

Table 4 - Overview of reported data on BM dosimetry for PRRT with ¹⁷⁷Lu-DOTATATE

Reference	Number of patients	Dosimetric method	Administered activity (GBq)	Amino acids	BM dose	
					Per unit administered activity (Gy/GBq)	For four cycles of 7.4 GBq (Gy)
14	5	Planar	1.85	Lys/Arg	0.070 ± 0.009	2.1
36	69	Planar	3–7	Lys/Arg	0.050 ± 0.020	1.5
16	13	Planar	7.47	Lys/Arg	0.01 – 0.13	0.30 – 3.85
4	16	SPECT/CT	7.4	Vamin 14	0.070 ± 0.020	2.1
2	12	Not reported	3.7 – 7.4	Lys	0.002 – 0.060	0.6 – 1.8
37	200	SPECT/CT	7.4	Vamin 14	0.006 – 0.050	0.2 – 1.5
This study	25a	Planar	1.85 – 7.3	Lys/Arg	0.067 ± 0.007	2

Lys/Arg lysine 2.5%/arginine 2.5 %, Lys lysine 2.5 %

^a Of 320 patients

Several groups have investigated the role of BM dosimetry in radionuclide treatments for predicting hematological toxicity. A weak negative correlation ($r_p = -0.47$) between neutrophils at nadir and measured whole-body absorbed dose was found in 20 patients treated with ¹³¹I-MIBG [30]. In a PRRT study with ⁹⁰Y-DOTATOC, a correlation ($R=0.58$) was found between BM absorbed dose and PLT count reduction at nadir [31, 32]. BM dose was calculated in 12 patients based on plasma samples, assuming that the activity concentration in the BM was equal to that in the plasma. ⁸⁶Y-DOTATOC PET was performed after therapy and showed uptake in the vertebrae. Taking the radioactivity in the spine into the dosimetric calculations, a better correlation ($R=0.82$) was found between BM absorbed dose and PLT count reduction at nadir. However, 24 patients did

not demonstrate sufficient uptake of ^{86}Y -DOTATOC in the spine to provide usable BM dose measurements. In our study, we found similar correlation coefficients between the relative decrease in blood cells and (cumulative) radiation dose to the BM. We found no correlation between BM dose and Hb, which can be explained by minimal effects on circulating erythrocytes after 2 Gy of irradiation [33]. These weak correlations between decreases in blood count and BM dose indicate that current dosimetry cannot fully predict hematological toxicity. Additional clinical factors have to be taken into account to predict hematological toxicity in PRRT.

Further research should focus on reporting BM dose in patients receiving PRRT with ^{177}Lu -DOTATATE. BM dose limits should be explored at the population level with clinical toxicity grading (e.g. CTCAE) as outcome. However, current BM dosimetry is imprecise and varies due to differences in method of BM dose calculation [34]. Also the absorbed BM dose does not reflect the damage done to the hematopoietic stem cell department. If BM dosimetry can reflect the actual dose to hematopoietic stem cells, it will have a more prominent place in clinical practice during PRRT. In vivo markers might also be an option for assessment of BM status after irradiation with PRRT. In a recent article, γ -H2AX foci in lymphocytes were successfully used for monitoring ionizing radiation-induced DNA double-strand breaks in patients treated with ^{177}Lu -DOTATATE [35]. However, the response of γ -H2AX foci varied significantly between patients over time, making it less suitable for individual monitoring. In future, BM radiation dose could provide information for decision-making in a clinical setting, but at present BM dosimetry plays a minor role in clinical practice. Clinical parameters and blood cell count recovery are currently the most important criteria for individual PRRT planning.

CONCLUSION

The prevalence of subacute hematological toxicity (grade 3 or 4) after PRRT with ^{177}Lu -DOTATATE is low (11 %). Our dosimetric calculations of the absorbed BM dose support the idea that a BM dose limit of more than 2 Gy seems appropriate for PRRT with ^{177}Lu -DOTATATE. A correlation was found between BM dose and decreases in blood counts, but clinical risk factors are currently the most important parameters for prediction of clinical toxicity. Patients with impaired renal function, low WBC count, extensive tumor mass, high tumor uptake on the OctreoScan and/or those of advanced age are more likely to develop grade 3 or 4 hematological toxicity. Our data support the idea that a higher BM dose limit of 2 Gy is appropriate for PRRT with ^{177}Lu -DOTATATE.

SUPPLEMENTAL DATA

Methods

Dosimetry

The method used for calculating the bone marrow (BM) radiation dose takes into account the radiation from β -rays of ^{177}Lu -DOTATATE in the blood circulating through the trabecular bone, and from penetrating γ -rays from radioactivity dispersed throughout the remainder of the body. The absorbed dose (D) to red marrow (rm) can be estimated using the MIRD schema. Contributions to the BM dose are from localized in the marrow tissues (self-dose) and in the remainder tissues (rm) of the body (cross-dose):

$$D_{rm} = D_{rm}^{Self} + D_{rm}^{Cross} \quad (2.14)$$

$$D_{rm} = \tilde{A}_{rm}S(rm \leftarrow rm) + (\tilde{A}_{WB} - \tilde{A}_{rm})S(rm \leftarrow rb) \quad (2.15)$$

where \tilde{A} is the cumulated activity and S are the S factor for red marrow to red marrow and the remainder of the body to red marrow.

Our BM dose (D_{rm}) is derived from three source contributions: (1) from the blood circulating through the marrow cavities (rm), (2) from large organs and tumors with high radioactivity uptake (h) and (3) from the general distribution of radioactivity throughout the remaining whole body (rb):

$$D_{rm} = \tilde{A}_{rm}DF(rm \leftarrow rm) + \sum_h \tilde{A}_h DF(rm \leftarrow h) + \tilde{A}_{rb}DF(rm \leftarrow rb) \quad (2.16)$$

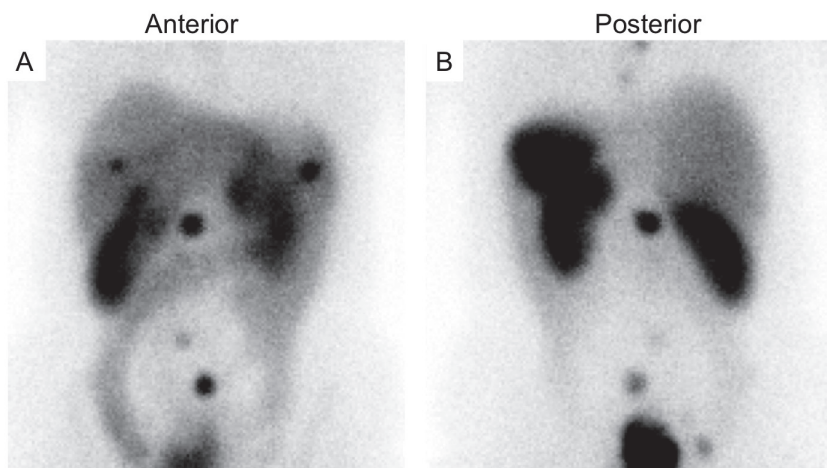
where \tilde{A} is the cumulated activity and DF are the dose factors for red marrow to red marrow, large organs to red marrow and remainder of the body to red marrow. Contribution to the bone marrow dose from radioactivity distribution within the remainder were calculated according to the method by Wessels et al. [17]. Radioactivity in the bone marrow first follows the plasma perfusion through the marrow space and at later times will be according to the whole body distribution. Both contributions have been taken into account in accordance with the bone marrow dosimetry performed by Forrer et al. [16], which data are included in the present data set.

Results

Incomplete dosimetric DATA

*Incomplete 1, Patient (Po****)*

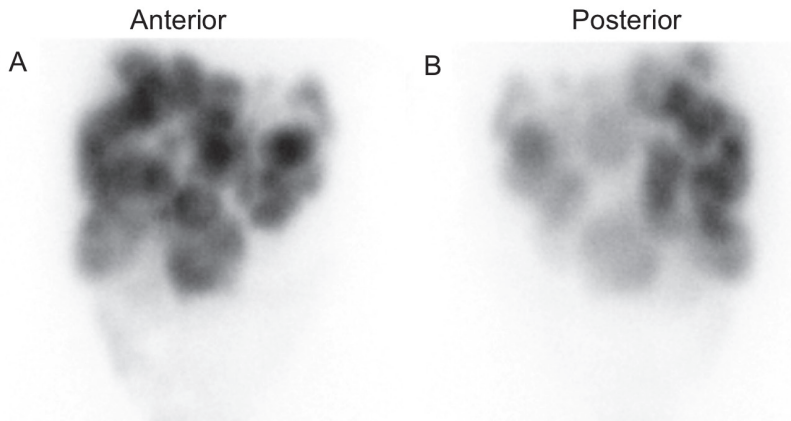
In this patient no data for urinary clearance was available, therefore it was not possible to perform bone marrow dose calculation using the compartment model.



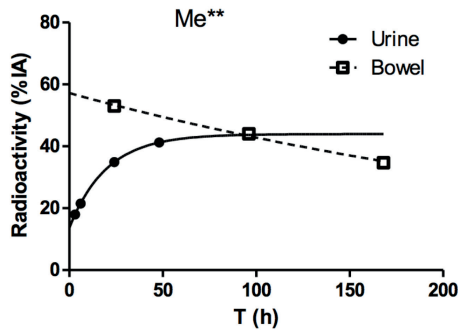
Supplemental figure 1 - Anterior (A) and posterior (B) planar scans, 24 hr after the 1st therapy of patient Po****.

*Incomplete 2, Patient (Me****)*

In this patient no blood radioactivity data were available. Consequently no compartment modeling was possible and numerical fitting was performed to obtain the cumulated activity in the bowel and the remainder of the body. The uptake in the bowel was exceptionally high, leading to a residence time of 79 h. As only 41% of the activity was cumulatively excreted in the urine at 48 h this lead to a total body residence time of 135 h. Using the dose conversion factor $DF (BM\text{-}remainder) = 2.67 \text{ E-}7 \text{ mGy/MBq.s}$ from Olinda [18], this would lead to a bone marrow dose of 0.13 mGy/MBq.



Supplemental figure 2 - Anterior (A) and posterior (B) planar scans, 24 hr after the 1st therapy of patient Me****.

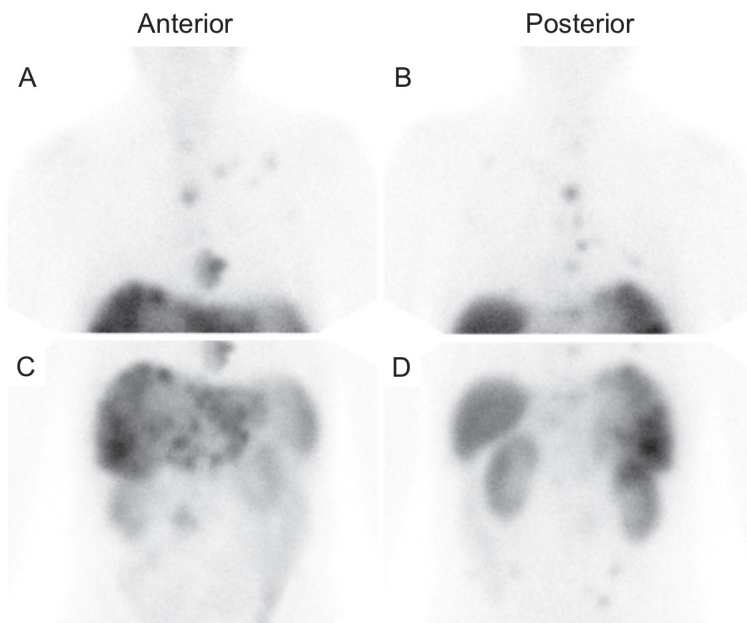


Supplemental figure 3 - Time-activity curves for urinary clearance and total bowel uptake of ^{177}Lu -Dotatate in patient Me****. Only 44% (95%CI: 42-45%) of the radioactivity is measured in the cumulative urinary clearance and it shows a half-life of 14 h (12-16 h). The 57% (43-71%) uptake in the bowel clears with 239 h (127 – 2183 h) half-life.

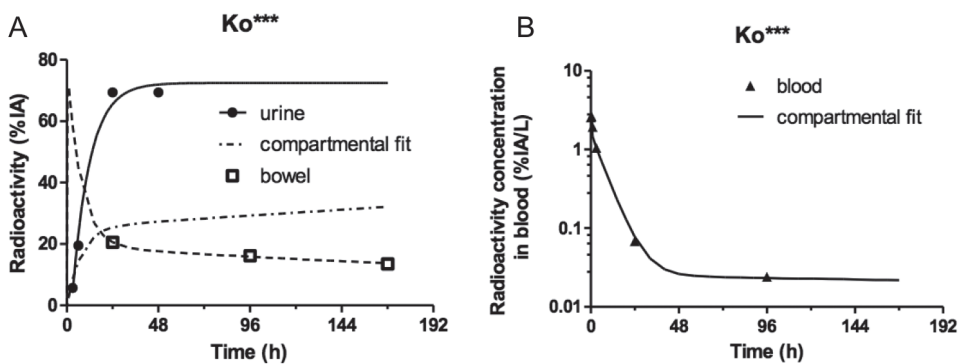
Outliers

Outlier, Patient (Ko****)

The compartmental model failed to fit the urinary excretion data of patient Ko*** correctly. The clearance from the bowel was slow with final clearance half-life of 290 h, leading to a residence time of 33 h. The total body residence time is 72 h, based on the numerical fit, this leads to a bone marrow dose of 69 $\mu\text{Gy}/\text{MBq}$. This value is 5σ above the mean value of $14 \pm 10 \mu\text{Gy}/\text{MBq}$. In this case the blood time-activity curve determines the bone marrow residence time to be 1.0 h and the contribution to the bone marrow dose from the remainder needs to be corrected according to the method by Wessels et al. [17]. This leads to a corrected bone marrow dose by the remainder of 3.1 $\mu\text{Gy}/\text{MBq}$, which is still 5σ above the corrected mean value of $0.67 \pm 0.46 \mu\text{Gy}/\text{MBq}$.



Supplemental figure 4 - Anterior (A) and posterior (B) planar scans, 24 hr after the 1st therapy of patient Kon****-2.



Supplemental figure 5 - Time-activity curves for urine, bowel and blood activity in patient Ko***. The curves through the data are the result of the compartmental fitting, except for through the urine data, where a single-exponential build-up curve was fitted numerically instead.

REFERENCES

1. Kwekkeboom DJ, Teunissen JJ, Bakker WH, Kooij PP, de Herder WW, Feelders RA, et al. Radiolabeled somatostatin analog [¹⁷⁷Lu-DOTA₀, Tyr₃] octreotate in patients with endocrine gastroenteropancreatic tumors. *J Clin Oncol.* 2005;23(12): 2754–62.
2. Bodei L, Cremonesi M, Grana CM, Fazio N, Iodice S, Baio SM, et al. Peptide receptor radionuclide therapy with ¹⁷⁷Lu- DOTATATE: the IEO phase I-II study. *Eur J Nucl Med Mol Imaging.* 2011;38(12):2125–35.
3. Swärd C, Bernhardt P, Ahlman H, Wängberg B, Forssell-Aronsson E, Larsson M, et al. [¹⁷⁷Lu-DOTA 0-Tyr 3]-octreotate treatment in patients with disseminated gastroenteropancreatic neuroendocrine tumors: the value of measuring absorbed dose to the kidney. *World J Surg.* 2010;34(6):1368–72.
4. Garkavij M, Nickel M, Sjögren-Gleisner K, Ljungberg M, Ohlsson T, Wingårdh K, et al. ¹⁷⁷Lu-[DOTA₀, Tyr₃] octreotate therapy in patients with disseminated neuroendocrine tumors: analysis of dosimetry with impact on future therapeutic strategy. *Cancer.* 2010;116(4 Suppl):1084–92.
5. Paganelli G, Sansovini M, Ambrosetti A, Severi S, Monti M, Scarpi E, et al. ¹⁷⁷Lu-Dota-octreotate radionuclide therapy of advanced gastrointestinal neuroendocrine tumors: results from a phase II study. *Eur J Nucl Med Mol Imaging.* 2014;41(10):1845–51.
6. Bodei L, Kidd M, Paganelli G, Grana CM, Drozdov I, Cremonesi M, et al. Long-term tolerability of PRRT in 807 patients with neuroendocrine tumours: the value and limitations of clinical factors. *Eur J Nucl Med Mol Imaging.* 2015;42(1):5–19.
7. Pfeifer AK, Gregersen T, Grønbaek H, Hansen CP, Müller-Brand J, Herskind Bruun K, et al. Peptide receptor radionuclide therapy with Y-DOTATOC and (¹⁷⁷Lu-DOTATOC in advanced neuroendocrine tumors: results from a Danish cohort treated in Switzerland. *Neuroendocrinology.* 2011;93(3):189–96.
8. Delpassand ES, Samarghandi A, Zamanian S, Wolin EM, Hamiditabar M, Espenan GD, et al. Peptide receptor radionuclide therapy with ¹⁷⁷Lu-DOTATATE for patients with somatostatin receptor-expressing neuroendocrine tumors: the first US phase 2 experience. *Pancreas.* 2014;43(4):518–25.
9. Sabet A, Ezziddin K, Pape UF, Ahmadzadehfar H, Mayer K, Pöppel T, et al. Long-term hematotoxicity after peptide receptor radionuclide therapy with ¹⁷⁷Lu-octreotate. *J Nucl Med.* 2013;54(11):1857–61.
10. Gupta SK, Singla S, Bal C. Renal and hematological toxicity in patients of neuroendocrine tumors after peptide receptor radionuclide therapy with ¹⁷⁷Lu-DOTATATE. *Cancer Biother Radiopharm.* 2012;27(9):593–9.
11. Kwekkeboom DJ, de Herder WW, Kam BL, van Eijck CH, van Essen M, Kooij PP, et al. Treatment with the radiolabeled somatostatin analog [¹⁷⁷Lu-DOTA₀, Tyr₃] octreotate: toxicity, efficacy, and survival. *J Clin Oncol.* 2008;26(13):2124–30.
12. Benua RS, Cicale NR, Sonenberg M, Rawson RW. The relation of radioiodine dosimetry to results and complications in the treatment of metastatic thyroid cancer. *Am J Roentgenol Radium Ther Nucl Med.* 1962;87:171–82.
13. Lassmann M, Hänscheid H, Chiesa C, Hindorf C, Flux G, Luster M; EANM Dosimetry Committee. EANM Dosimetry Committee series on standard operational procedures for pre-therapeutic dosimetry I: blood and bone marrow dosimetry in differentiated thyroid cancer therapy. *Eur J Nucl Med Mol Imaging.* 2008;35(7): 1405–12.
14. Kwekkeboom DJ, Bakker WH, Kooij PP, Konijnenberg MW, Srinivasan A, Erion JL, et al. [¹⁷⁷Lu-DOTA₀Tyr₃] octreotate: comparison with [¹¹¹In-DTPA₀]octreotide in patients. *Eur J Nucl Med.* 2001;28(9):1319–25.
15. Esser JP, Krenning EP, Teunissen JJ, Kooij PP, van Gameren AL, Bakker WH, et al. Comparison of [¹⁷⁷Lu-DOTA(0), Tyr(3)]octreotate and [¹⁷⁷Lu-DOTA(0), Tyr(3)]octreotide: which peptide is preferable for PRRT? *Eur J Nucl Med Mol Imaging.* 2006;33(11):1346–51.

16. Forrer F, Krenning EP, Kooij PP, Bernard BF, Konijnenberg M, Bakker WH, et al. Bone marrow dosimetry in peptide receptor radionuclide therapy with [177Lu-DOTA(0), Tyr(3)] octreotate. *Eur J Nucl Med Mol Imaging*. 2009;36(7): 1138–46.
17. Wessels BW, Bolch WE, Bouchet LG, Breitz HB, Denardo GL, Meredith RF, et al. Bone marrow dosimetry using blood-based models for radiolabeled antibody therapy: a multiinstitutional comparison. *J Nucl Med*. 2004;45(10):1725–33.
18. Stabin MG, Sparks RB, Crowe E. OLINDA/EXM: the second-generation personal computer software for internal dose assessment in nuclear medicine. *J Nucl Med*. 2005;46(6):1023–7.
19. Cancer Therapy Evaluation Program. Common terminology criteria for adverse events v3.0 (CTCAE). Bethesda, MD: Division of Cancer Treatment and Diagnosis, National Cancer Institute; 2006. http://ctep.cancer.gov/protocolDevelopment/electronic_applications/docs/ctcaev3.pdf.
20. Svensson J, Berg G, Wängberg B, Larsson M, Forssell-Aronsson E, Bernhardt P. Renal function affects absorbed dose to the kidneys and haematological toxicity during (177) Lu-DOTATATE treatment. *Eur J Nucl Med Mol Imaging*. 2015;42(6):947–55.
21. Sandström M, Garske U, Granberg D, Sundin A, Lundqvist H. Individualized dosimetry in patients undergoing therapy with (177) Lu-DOTA-D-Phe(1)-Tyr(3)-octreotate. *Eur J Nucl Med Mol Imaging*. 2010;37(2):212–25.
22. Beaugregard JM, Hofman MS, Kong G, Hicks RJ. The tumour sink effect on the biodistribution of 68Ga-DOTA-octreotate: implications for peptide receptor radionuclide therapy. *Eur J Nucl Med Mol Imaging*. 2012;39(1):50–6.
23. Corey SJ, Minden MD, Barber DL, Kantarjian H, Wang JC, Schimmer AD. Myelodysplastic syndromes: the complexity of stem-cell diseases. *Nat Rev Cancer*. 2007;7(2):118–29.
24. Sreedharan SP, Kodama KT, Peterson KE, Goetzi EJ. Distinct subsets of somatostatin receptors on cultured human lymphocytes. *J Biol Chem*. 1989;264(2):949–52.
25. Kulkarni HR, Prasad V, Schuchardt C, Baum RP. Is there a correlation between peptide receptor radionuclide therapy-associated hematological toxicity and spleen dose? *Recent Results Cancer Res*. 2013;194:561–6.
26. Dorn R, Kopp J, Vogt H, Heidenreich P, Carroll RG, Gulec SA. Dosimetry-guided radioactive iodine treatment in patients with metastatic differentiated thyroid cancer: largest safe dose using a risk-adapted approach. *J Nucl Med*. 2003;44(3):451–6.
27. Flux G, Bardies M, Monsieurs M, Savolainen S, Strands SE, Lassmann M; EANM Dosimetry Committee. The impact of PET and SPECT on dosimetry for targeted radionuclide therapy. *Z Med Phys*. 2006;16(1):47–59.
28. Van Essen M, Krenning EP, Kam BL, de Herder WW, Feelders RA, Salvage therapy with (177) Lu-octreotate in patients with bronchial and gastroenteropancreatic neuroendocrine tumors. *J Nucl Med*. 2010;51(3):383–90.
29. Sabet A, Haslerud T, Pape UF, Sabet A, Ahmadzadehfar H, Grünwald F, et al. Outcome and toxicity of salvage therapy with 177Lu-octreotate in patients with metastatic gastroenteropancreatic neuroendocrine tumours. *Eur J Nucl Med Mol Imaging*. 2014;41(2):205–10.
30. Buckley SE, Chittenden SJ, Saran FH, Meller ST, Flux GD. Whole-body dosimetry for individualized treatment planning of 131I-MIBG radionuclide therapy for neuroblastoma. *J Nucl Med*. 2009;50(9):1518–24.
31. Walrand S, Barone R, Pauwels S, Jamar F. Experimental facts supporting a red marrow uptake due to radiometal transchelation in 90Y-DOTATOC therapy and relationship to the decrease of platelet counts. *Eur J Nucl Med Mol Imaging*. 2011;38(7):1270–80.

- 32.** Pauwels S, Barone R, Walrand S, Borson-Chazot F, Valkema R, Kvols LK, et al. Practical dosimetry of peptide receptor radionuclide therapy with (90)Y-labeled somatostatin analogs. *J Nucl Med.* 2005;46 Suppl 1:92S–8.
- 33.** IAEA. Manual on radiation haematology. Technical Reports Series No. 123. Vienna: International Atomic Energy Agency; 1971. 34. Ferrer L, Kraeber-Bodéré F, Bodet-Milin C, Rousseau C, Le Gouill
- 34.** S, Wegener WA, et al. Three methods assessing red marrow dosimetry in lymphoma patients treated with radioimmunotherapy. *Cancer.* 2010;116(4):1093–100.
- 35.** Denoyer D, Lobachevsky P, Jackson P, Thompson M, Martin OA, Hicks RJ. Analysis of ¹⁷⁷Lu-DOTA-octreotate therapy-induced DNA damage in peripheral blood lymphocytes of patients with neuroendocrine tumors. *J Nucl Med.* 2015;56(4):505–11.
- 36.** Wehrmann C, Senftleben S, Zachert C, Müller D, Baum RP. Results of individual patient dosimetry in peptide receptor radionuclide therapy with ¹⁷⁷Lu DOTA-TATE and ¹⁷⁷Lu DOTA-NOC.
- 37.** *Cancer Biother Radiopharm.* 2007;22(3):406–16. 37. Sandström M, Garske-Román U, Granberg D, Johansson S, Widström C, Eriksson B, et al. Individualized dosimetry of kidney and bone marrow in patients undergoing ¹⁷⁷Lu-DOTA-octreotate treatment. *J Nucl Med.* 2013;54(1):33–41.

2.3

THERAPY-RELATED MALIGNANCIES AFTER PRRT WITH ¹⁷⁷LU-DOTATATE: INCIDENCE, COURSE & PREDICTING FACTORS

Hendrik Bergsma¹, Kirsten van Lom², Mark HGP Raaijmakers², Mark Konijnenberg¹, Boen L.R. Kam¹,
Jaap J.M. Teunissen¹, Wouter W. de Herder³, Eric P. Krenning¹, Dik J. Kwekkeboom¹

¹ Department of Radiology & Nuclear Medicine,

² Department of Hematology

³ Department of Internal Medicine, Erasmus MC, University Medical Center, Rotterdam, The Netherlands

ABSTRACT

Peptide Receptor Radionuclide Therapy (PRRT) may induce long-term toxicity to the bone marrow (BM). The aim of this study was to analyze persistent dysfunction of the hematopoietic system after PRRT with ^{177}Lu -DOTATATE in patients with gastroenteropancreatic neuroendocrine tumors (GEP-NETs).

Methods:

The incidence and course of persistent hematological dysfunction (PHD) was analyzed in 274 (=GEP-NET) out of 367 patients with somatostatin receptor-positive tumors. PHD was defined as diagnosis of Myelodysplastic Syndrome (MDS), Acute Myeloid Leukemia (AML), Myeloproliferative Neoplasms (MPN), Myelodysplastic/Myeloproliferative neoplasms (MDS/MPN) or otherwise unexplained cytopenia (for more than 6 months). Using data from the Dutch cancer registry, the expected number of hematopoietic neoplasms (MDS, AML, MPN, MDS/MPN) was calculated and adjusted for sex, age and follow-up period.

Assessment of risk factors was performed in 274 GEP-NET patients with the following risk factors: gender, age over 70 years, bone metastasis, prior chemotherapy, prior external beam radiotherapy, uptake on the OctreoScan®, tumor load, grade 3-4 hematological toxicity during treatment, estimated absorbed BM dose, elevated plasma chromogranin A, baseline blood counts and renal function.

Results:

We identified 11 (3.7%) out of 274 GEP-NET patients with PHD following treatment with ^{177}Lu -DOTATATE: 8 (2.9%) patients developed a hematopoietic neoplasm (4 MDS, 1 AML, 1 MPN, 2 MDS/MPN) and 3 (1.1%) patients developed BM failure characterized by cytopenia and BM aplasia. The median latency period at diagnosis (or first suspicion of a hematological malignancy) for 11 patients was 41 (range 15 - 84) months. The expected number of hematopoietic neoplasms for our 274 GEP-NET patients was 3.0 resulting in a relative risk of 2.7 (CI 0.7 – 10.0).

No risk factors for PHD could be identified for the GEP-NET patients, including bone metastasis and estimated BM dose. Seven patients with PHD developed anemia in combination with a rise in mean corpuscular volume.

Conclusion:

The prevalence of persistent hematological dysfunction after PRRT with ^{177}Lu -DOTATATE is 3.7% in our specific patient population. The median time when PHD can develop is 41 months after the first PRRT cycle. The RR for developing a hematopoietic neoplasm is 2.7. No risk factors were identified for developing PHD in GEP-NET patients.

Keywords:

PRRT, ^{177}Lu -DOTATATE, Bone marrow, Toxicity, MDS, Leukemia, Neuroendocrine tumor, NET

INTRODUCTION

Peptide receptor radionuclide therapy (PRRT) has been in use for twenty-five years as second-line therapy in patients with inoperable (metastatic) gastroenteropancreatic neuroendocrine tumors (GEP-NETs). Indium-111 radiolabeled somatostatin analogs were used in early studies (1,2). Besides encouraging results with regard to symptom relief, the reported number of objective responses was low. Myelodysplastic syndrome (MDS) or leukemia was reported in half of the NET patients who received a very high dosage (>100 GBq) of [¹¹¹In-DTPA⁰]Octreotide. PRRT with ¹⁷⁷Lu-DOTA⁰-Tyr³-octreotate (¹⁷⁷Lu-DOTATATE) results in a better radiological response rate of 15 – 35% (3-6). In general, side effects are mild, although serious hematological toxicity has been reported, making the bone marrow (BM) the main dose-limiting organ. In 11% of the patients, (sub)acute grade 3-4 hematological toxicity is observed after PRRT with ¹⁷⁷Lu-DOTATATE (7). Also long-term hematological toxicity like acute myeloid leukemia (AML) and MDS were reported in 1-2% of the patients treated with ¹⁷⁷Lu and/or ⁹⁰Y based PRRT (8-11). Up to now, no in depth report of therapy related long-term hematological toxicity in patients treated with ¹⁷⁷Lu-DOTATATE has been published.

The aim of this study was to analyze long-term persistent hematological dysfunction (PHD) after PRRT with ¹⁷⁷Lu-DOTATATE in GEP-NET patients. Incidence, clinical course and predicting factors were evaluated in a large group of GEP-NET patients.

MATERIALS AND METHODS

Patients

In this study, Dutch patients were analyzed who were treated from January 2000 to December 2007. Follow-up data were used up to December 2012 since we expected therapy related malignancies within 5 years after therapy and because of changes in our follow-up protocol after December 2012. Only Dutch patients were selected, because loss to follow-up was limited in these patients. Only GEP-NETs were selected in our analysis, since ¹⁷⁷Lu-DOTATATE is indicated for this group of patients.

Inclusion criteria were: patients with somatostatin receptor-positive tumors and baseline tumor uptake on somatostatin receptor scintigraphy with [¹¹¹In-DTPA⁰] octreotide (OctreoScan[®]; Mallinckrodt, Petten, The Netherlands) with accumulation in the tumor at least as high as in normal liver tissue; no prior treatment with a radionuclide therapy; baseline serum hemoglobin ≥ 6 mmol/l; white blood cell count $\geq 2 \times 10^9$ /l; platelet count $\geq 75 \times 10^9$ /l; serum creatinine ≤ 150 μ mol/l or creatinine clearance ≥ 40 ml/min and Karnofsky performance status ≥ 50 .

The intensity of tumor uptake and the extent of tumor burden were scored according to simple scaling systems (3).

This study was part of the ongoing prospectively designed study in patients with neuroendocrine tumors treated with ^{177}Lu -DOTATATE at the Department of Radiology and Nuclear Medicine, Erasmus University Medical Center Rotterdam. The hospital's medical ethics committee approved the study. All patients gave written informed consent for participation in the study.

Treatment

[DOTA⁰,Tyr³]octreotate was obtained from BioSynthema (St. Louis, MO). $^{177}\text{LuCl}_3$ was supplied by IDB-Holland (Baarle-Nassau, The Netherlands) and ^{177}Lu -DOTATATE was prepared locally (12).

Granisetron 3 mg, or ondansetron 8 mg was injected intravenously 30 min before infusion of ^{177}Lu -DOTATATE. Infusion of amino acids (2.5 % arginine and 2.5 % lysine, 1 l) was started 30 min before administration of the radiopharmaceutical and lasted for 4 h. The radiopharmaceutical was coadministered for 30 min using a second pump system. Cycle dosage(s) of 1.85 GBq (50 mCi) was given in 1 patients, 3.7 GBq (100 mCi) in 13 patients, 5.6 GBq (150 mCi) in 12 patients, and 7.4 GBq (200 mCi) in the remaining patients, injected over 30 min. The interval between treatments was 6 – 16 weeks. The intended cumulative dose was 29.6 GBq (800 mCi) ^{177}Lu -DOTATATE. The median number of therapy cycles was 4 (range 1-8) with a median cumulative activity of 29.6 GBq (range, 7.4–59.2 GBq) of ^{177}Lu -DOTATATE. However, the dose was lowered if the calculated kidney dose was higher than 23 Gy. Other reasons for dose reduction or cessation of further therapy were recurrent grade 3 or 4 hematological toxicity and/or persistent low blood counts.

Follow-up & Toxicity Assessment

Hematology, and liver and renal function tests were performed during the 6 weeks before the first therapy, 4 and 6 weeks after each therapy cycle, and at follow-up visits. Subacute hematological toxicity was assessed according to Common Terminology Criteria for Adverse Events v3.0 (13). This version was used because of well-defined grades (1 to 5) for adverse events in platelets, leucocytes and hemoglobin.

Patient with PHD were defined as having one or more characteristics: MDS, AML, myeloproliferative disorders (MPN), myelodysplastic/myeloproliferative neoplasms (MDS/MPN) according to the revised WHO 2008 diagnostic criteria (14) or unexplained hematological toxicity grade 3-4 (> 6 months) in hemoglobin, platelets and/or white blood cells (with/without requirement of multiple blood transfusions).

Latency period was defined as the time from the 1st treatment with ¹⁷⁷Lu-DOTATATE to the date of diagnosis. If no diagnosis was made, the date of the first BM biopsy or aspiration was used. In case of no available BM biopsy/aspiration, the date of diagnosis was replaced by the date when hematological malignancy was suspected in the patient's medical file.

The estimated absorbed BM dose was calculated based on a group-averaged estimated BM dose in 23 patients (7). Therefore, this mean BM dose per administered activity of 0.067 ± 0.007 mGy/MBq (7) was multiplied by the individual cumulative injected activity of ¹⁷⁷Lu-DOTATATE.

The Netherlands Cancer Registry

The expected number of patients with hematopoietic neoplasms was calculated using data of Dutch cancer figures (www.cijfersoverkanker.nl). This database contains the statistics on cancer in the Netherlands that are registered in the Netherlands Cancer Registry, which is managed by the Netherlands Comprehensive Cancer Organization. Data on incidence, prevalence, survival, mortality and risk are available on this website. Users can make their own graphs and tables on cancer incidence according to localization, region, sex and age. Data are available from 1989 to 2016.

The incidence (number of cancers per 100,000 persons a year) of hematopoietic neoplasms was used for four categories; MDS, AML, MPN and MDS/MPN.

Data were categorized by sex and age (in 5-year cohorts). Average incidence rates (per 100,000 residents) between 2001-2011 of the four categories were calculated. Expected cases per category were compiled, based on the number of patients and years of follow-up in our study. Expected numbers were adjusted for sex, age and duration of follow-up period.

Statistics

The SPSS software (SPSS 19; IBM, New York, N.Y., USA) was used for statistical analysis. Distributions were examined for normality using the Kolmogorov-Smirnov and Shapiro-Wilk test. Correlations between distributions were evaluated using the Chi-squared and unpaired-t test.

PHD was analyzed as a discrete variable. The following baseline variables were included in the analysis: gender, age over 70 years, presence of bone metastases, prior chemotherapy, prior external beam radiotherapy, uptake on the OctreoScan®, tumor load, grade 3-4 hematological toxicity during treatment and plasma chromogranin A >2,000 µg/l (ref < 100 µg/l). Continuous variables included in the analysis were: baseline hemoglobin, baseline platelet count, baseline white blood cell count and estimated absorbed BM dose. The creatinine clearance was estimated with the Cockcroft-Gault formula and evaluated as a continuous variable.

RESULTS

In total 367 patients with somatostatin receptor-positive tumors were treated of whom 274 with GEP-NETs, 34 NETs with unknown primary/other location and 59 with other tumors. In the group of GEP-NET patients, 22 out of 274 patients did not meet the inclusion criteria for various reasons e.g. low tumor uptake, concomitant radiotherapy. The median follow-up time of the 274 GEP-NET patients was 29 (range, 0 - 142) months. Twenty-six (10%) out of 274 GEP-NET patients had been treated with cytotoxic chemotherapy in the past and/or 18 out of 274 patients with external beam radiation therapy. Full patient characteristics are summarized in table 1.

Long-term Hematological Toxicity

We identified 11 patients (6 females and 5 males) with PHD out of 274 GEP-NET patients following treatment with ^{177}Lu -DOTATATE (3.7%). Eight patients developed a hematopoietic malignancy (4 MDS, 1 AML, 1 MPN, 2 MDS/MPN) and 3 patients developed BM failure characterized by cytopenia and BM aplasia (table 2). Two patients were excluded since they did not have GEP-NETs (see inclusion criteria); one patient with thyroid carcinoma died two weeks after a BM biopsy demonstrating BM hypoplasia. Another patient with a NET (unknown primary) developed BM failure most likely due to significantly decreased kidney function (GFR < 50 ml/min). Characteristics of the 11 GEP-NET patients with persistent dysfunction of the hematopoietic system are shown in table 3.

The median latency period from initiation of PRRT to the diagnosis of hematopoietic disease in 11 out of 274 GEP-NET patients was 41 (range 15-84) months (Figure 1).

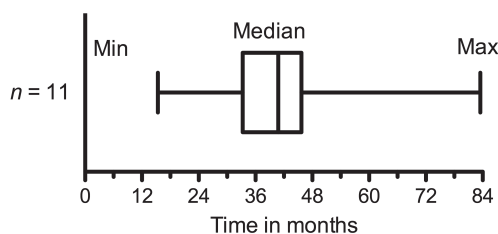


Figure 1 – Median latency time in 11 patients with persistent hematological dysfunction. Whisker boxplot of latency time (period between first treatment and date of diagnosis) in 11 out of 274 GEP-NET patients with persistent hematological dysfunction (PHD) after peptide receptor radiotherapy (PRRT) with ^{177}Lu -DOTATATE. Whiskers represent minimum (15 months) and maximum (84 months) latency time. The width of the box shows the interquartile range and the vertical line in the box is the median (41 months) latency time.

Table 1 - Baseline characteristics of 274 Gastroenteropancreatic Neuroendocrine Tumors (GEP-NETs).

Patient characteristics	Number of patients (%)	
	Yes	No
Male	139 (51)	135 (49)
Age ≥ 70	52 (19)	222 (81)
KPS ≤ 70	38 (14)	236 (86)
Elevated Chromogranin A	72 (26)	202 (74)
Bone metastases	59 (22)	215 (78)
Patients who met inclusion criteria	252 (92)	22 (8)
<i>Previous therapy</i>		
- Chemotherapy	26 (10)	248 (90)
- Radiotherapy (external)	18 (7)	256 (93)
<i>NET Location</i>		
- Gastrointestinal	172 (63)	
- Pancreas	86 (31)	
- Bronchus	16 (6)	
<i>Tumor uptake on baseline Octreoscan</i>		
- Less to normal liver	8 (3)	
- Equal or more to normal liver	203 (74)	
- Higher than kidneys	63 (23)	
<i>Tumor mass on baseline OctreoScan</i>		
- Limited and Moderate	223 (81)	
- Extensive	51 (19)	
<i>Cumulative administered activity (¹⁷⁷Lu-DOTATATE)</i>		
- up to 22.2 GBq	73 (27)	
- 22.3 to 29.6 GBq	122 (44)	
- 29.7 Gbq to 44.4 GBq	71 (26)	
- 44.5 to 59.2 GBq	8 (3)	
<i>Age range at first treatment</i>		
15-29	1 (0.5)	
30-44	31 (11.5)	
45-59	109 (40)	
60-74	110 (40)	
75-89	23 (8)	

In 5 out of 11 patients, PRRT was interrupted and the planned cumulative activity of 29.6 GBq ^{177}Lu -DOTATATE was not administered. The median cumulative estimated BM dose in 263 patients without PHD was 2.0 Gy (range, 0.2 - 4.0 Gy). In the group of GEP-NET patients with PHD (n=11), the median BM dose was 1.8 Gy (range, 1.0 -2.0 Gy) (Figure 2). Seven out of 11 patients received a BM dose of less than 2.0 Gy.

Table 2 – Classification of 11 out of 274 Gastroenteropancreatic neuroendocrine tumors (GEP-NETs) patients with persistent hematological dysfunction (PHD) after peptide receptor radiotherapy (PRRT) with ^{177}Lu -DOTATATE. Eight patients were classified according to the World Health Organization (WHO) (14). Three patients were classified as bone marrow failure with specific characteristics.

Classification	Number of patients
Hematopoietic Neoplasms according to WHO	
<i>Myelodysplastic syndrome (MDS)</i>	
- RAEB-II	1
- RARS	1
- Other	2
<i>Acute myeloid leukemia and related neoplasms (AML)</i>	
- Acute myeloid leukemia with recurrent genetic abnormalities	1
<i>Myeloproliferative Neoplasms (MPN)</i>	
- Myelofibrosis	1
<i>Myelodysplastic/myeloproliferative neoplasms (MDS/MPN)</i>	
- Chronic Myeloid Leukemia (CML)	1
- Chronic myelomonocytic Leukemia (CMML)	1
Bone marrow failure characterized by (not WHO)	
- BM hypoplasia	1
- BM aplasia	1
- Pancytopenia	1

A total of 274 (139 male and 135 female) GEP-NET patients were analyzed for calculating the expected number of patients with hematopoietic neoplasms. The cumulative follow-up was 1113 person years, resulting in an expected number of MDS, AML, MPN and MDS/MPN cases of 1.10, 1.27, 0.48 and 0.19 respectively, with a total number of 3.0 patients based on Netherlands Comprehensive Cancer Organization data (Figure 3).

The RR is the chance that a hematopoietic neoplasms occurs when exposed (8/274) to PRRT, divided by the chance that hematopoietic neoplasms occur when non-exposed (3/274). This results in an RR of 2.7 (95% CI 0.7 – 10.0) meaning that patients treated with PRRT have more than three times higher risk of developing hematopoietic neoplasms than patients not treated with PRRT.

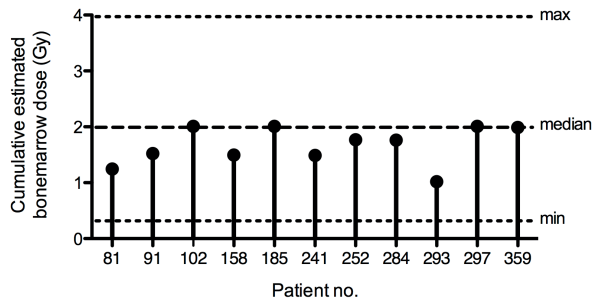


Figure 2 – Estimated bonemarrow dose in 11 GEP-NET patients with persistent hematological dysfunction. Spikeplot of cumulative estimated bonemarrow (BM) dose in 11 GEP-NET patients with persistent hematological dysfunction (PHD) after peptide receptor radiotherapy (PRRT) with ¹⁷⁷Lu-DOTATATE.

Note the median (and range) estimated BM dose (dashed lines) in 263 NET patients without PHD.

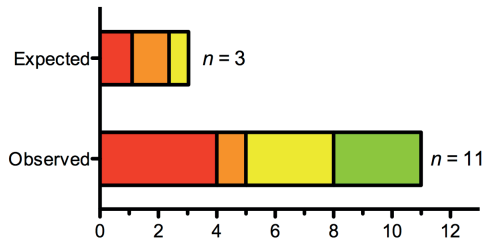


Figure 3 – Expected number of patients (3) with hematopoietic neoplasms and type, based on data from The Netherlands Cancer Registry. Observed number of patients (11 out of 274 GEP-NET patients) with persistent hematological dysfunction (PHD) after peptide receptor radiotherapy (PRRT) with ¹⁷⁷Lu-DOTATATE including 8 patients with hematopoietic neoplasms and 3 with bonemarrow failure.

■ Myelodysplastic Syndrome (MDS), ■ Acute Myeloid Leukemia (AML), ■ Myeloproliferative Neoplasms (MPN) + Myelodysplastic/Myeloproliferative neoplasms (MDS/MPN) and ■ Bone Marrow failure.

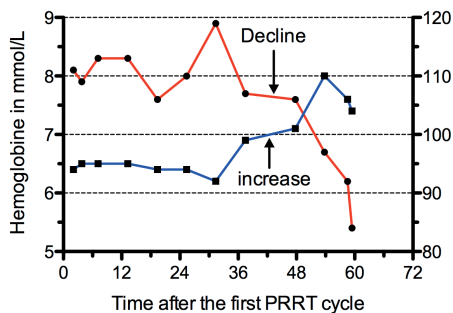


Figure 4 – Course of hemoglobin (Hb) and mean corpuscular volume (MCV) in patient no. 185 diagnosed with myelodysplastic syndrome (MDS)/Myeloproliferative disease (MPN) after peptide receptor radiotherapy (PRRT) with ¹⁷⁷Lu-octreotate. Time zero is the date of the last PRRT cycle. A decline in Hb (upper red arrow) was followed by an increase in MCV (lower red arrow).

Table 3 – Characteristics of 11 out of 274 Gastroenteropancreatic neuroendocrine tumors (GEP-NETs) patients with persistent hematological dysfunction (PHD) after peptide receptor radiotherapy (PRRT) with ¹⁷⁷Lu-DOTATATE (¹⁷⁷Lu).

Patient no.	sex	Age	Diagnosis		Previous therapy	Administered Activity (GBq)	PRRT Interrupted	Protocol	Bone marrow		Latency period (months)
			Diagnosis	Age					Cytopenia	Diagnosis	
359	f	70	NET	70	Octreotide	30.0	No	On	Hb	MDS, RARS	42.4
297	f	60	NET	60	Octreotide	18.6	Yes, maximum kidney dose	On	Hb, PLT, WBC	Hypoplasia	36.3
293	m	61	PNET	61	chemo-embolisation	29.3	No	On	Hb, PLT	CML	42.3
284	m	57	PNET	57	-	29.7	No	On	Hb	MDS, RAEB-II	33.3
252	f	64	NET	64	Octreotide	30.0	No	On	Hb, WBC	Pancytopenia	45.7
241	f	41	PNET	41	-	26.3	Yes, hematological toxicity	On	Hb, PLT, WBC	Aplasia	34.3
185	m	74	PNET	74	-	26.4	No	On	Hb, PLT	MDS/MPN: CMML-1	63.6
158	m	62	NET	62	Octreotide	22.2	Yes, maximum kidney dose	Off	Hb, PLT, WBC	MDS, RAEB-II	15.4
102	m	68	NET	68	-	30.0	no	On	Hb, PLT, WBC	MDS, Hypocellular	20.2
91	f	59	NET	59	Octreotide, local EBRT	22.7	Yes, maximum kidney dose	On	Hb, PLT, WBC	AML	83.5
81	f	58	NET	58	Octreotide	22.3	Yes, maximum kidney dose	On	Hb, PLT, WBC	Myelofibrosis/MPN	40.8

Neuroendocrine tumor (NET), Neuroendocrine tumor of the pancreas (PNET), cold Octreotide (Octreotide), External beam radiotherapy (EBRT), Hemoglobin (Hb), Platelets (PLT), White Blood Cells (WBC), Myelodysplastic syndrome (MDS), Refractory anaemia with ringed sideroblasts (RARS), Chronic myeloid leukemia (CML), Refractory Anaemia with Excess Blasts type II (RAEB-II), Myelodysplastic/Myeloproliferative neoplasms (MDS/MPN), chronic myelomonocytic leukemia (CMML), Acute Myeloid Leukemia (AML), Myeloproliferative neoplasms (MPN).

Table 4 – Results of analysis in 367 patients with somatostatin positive tumors after peptide receptor radiotherapy (PRRT) with ¹⁷⁷Lu-DOTATATE (¹⁷⁷Lu). Persistent hematological dysfunction (PHD), Gastroenteropancreatic Neuroendocrine tumors (GEP-NETs), Bonemarrow (BM), Not calculated (NC) because of low statistical power.

Characteristic	All patients	Lung + GEP-NET	Non GEP-NETs*
Total number of patients	367	274	93
PHD patients	13	11	2
Prevalence	3.5%	3.7%	2.2%
Median latency period (and range) in months	36 (5 - 84)	41 (15 – 84)	5.8 (5 – 7)
Median FU time (and range) in months	24 (0 - 143)	29 (0 - 142)	12 (0 – 116)
Cumulative median BM dose (and range) in Gy:			
without PHD	2.0 (0.2 - 4.0)	2.0 (0.2 - 4.0)	1.5 (0.2 – 3.9)
with PHD	1.5 (1.0 - 2.0)	1.76 (1.0 – 2.0)	1.2 (1.0 – 1.5)
Expected number of MDS/leukemia	4.4	3.0	<1
Follow-up in years	1309	1113	-
Relative Risk (RR) and 95% Confidence Interval	1.9 (1.0 - 3.6)	2.7 (0.7 – 10.0)	-
Significant Risk factors	- Baseline WBC was significantly lower (p=0.01) in the 13 NET patients with PHD. - Subacute hematological toxicity grade 3-4 during PRRT was marginally significantly (p=0.053) different in patients with PHD.	None	NC
Remark	- Including a non GEP-NET patient* treated with ¹³¹ I, resulting in BM failure, 5 months after the first PRRT cycle.		

* Patients with non GEP-NET, e.g. NET unknown primary, thyroid carcinoma, paraganglioma.

Risk Factors and Course

Risk factor assessment was performed in 274 GEP-NET patients, including 11 GEP-NET patients with PHD. The presence of bone metastases or prior chemotherapy was not more prevalent in NET patients with PHD as compared to those without PHD. For the other defined risk factors (gender, age over 70 years, prior external beam radiotherapy, uptake on the OctreoScan®, tumor load, grade 3-4 hematological toxicity during treatment, estimated absorbed BM dose, elevated plasma chromogranin A, baseline

blood counts and renal function), no significant differences were found between GEP-NET patients with and patients without PHD.

Seven patients with PHD had anemia in combination with an elevated mean corpuscular volume, for example patient no. 185 (Figure 4).

Incidence of PHD, expected number of hematopoietic neoplasms and risk assessment was also performed in all 367 patients with somatostatin receptor-positive tumors, see table 4.

DISCUSSION

MDS covers a heterogeneous group of myeloid malignancies and occurs in 2-4 individuals per 10^5 persons per year in the Dutch population (15). AML and related precursor neoplasms occur in 3-4 individuals per 10^5 persons per year in the European population (16). The incidence of myeloid neoplasms and leukemia are strongly determined by age and sex. Also exposure to radiation increases the frequency of hematological malignancies (17).

The total observed incidence of hematopoietic neoplasms after PRRT is a summation of *de novo* incidence (e.g. without exposure to radiation) and therapy-related (with radiation exposure) incidence. The total number of patients with PHD after PRRT is significantly higher than we would expect, based on the expected number of (*de novo*) hematopoietic neoplasms. Our incidence of PRRT related PHD is 3.7%, however this percentage is patient-group dependent since sex, age and previous (chemotherapeutic) treatments influence the incidence of hematopoietic neoplasms. In a large retrospective analysis of a ^{90}Y -DOTATOC phase II trial, only 2 (<1%) out of 1109 patients developed myeloproliferative diseases (10). Considering the number of patients and mean follow-up of 23 months in this study, one would expect an incidence of more than 2 *de novo* hematopoietic neoplasms alone. Therefore the reported number of myeloproliferative events after PRRT in this study does not seem accurate. Bodei *et al.* found in a large retrospective study of 807 NET patients treated with ^{177}Lu and/or ^{90}Y -labelled somatostatin analogs, an incidence of MDS and acute leukemia of 3.3% (8). This is in line with our findings. In the same retrospective study of Bodei *et al.* a mean latency time of 45 and 57 months was reported between start of PRRT and the development of MDS or leukemia, respectively (8). Our median latency period was 41 months, which is approximately the same as reported by Bodei *et al.* (8).

PRRT with ^{177}Lu -DOTATATE has significant similarities to therapy with radioiodine (^{131}I), like the physical decay characteristics and the human biodistribution in blood and BM. In patients with thyroid cancer treated with radioiodine (^{131}I), a leukemia

incidence of 0.2 - 0.3% is observed in comparison to the general population (18,19). In a comprehensive meta-analysis the pooled RR for development of leukemia increased 2.5-fold in patients treated with ¹³¹I as compared with thyroid cancer survivors not treated with radioiodine (20,21). In our study, we found a RR in our GEP-NET patients treated with ¹⁷⁷Lu-DOTATATE, which was similar to that in thyroid cancer patients treated with ¹³¹I. However, the number of *de novo* (=expected) MDS and leukemia cases is age dependent. Therefore, the incidence can vary between studies in patient populations with a different age distribution. Also in the radio immunotherapy, myelosuppression is the primary toxicity and raised concerns about the risk of treatment-related MDS or acute leukemia. In the database of the radioiodine (¹³¹I) labeled monoclonal antibody (Bexxar), 35 (3.5%) out of 995 non-Hodgkin lymphoma patients developed MDS or acute leukemia (22). Whereas, clinical studies with the yttrium-90 or indium-111 labeled monoclonal antibody (Zevalin), reported an incidence of 2.3% and the malignancies were diagnosed 23 months after radioimmunotherapy (23).

In our study, we did not find a difference in cumulative estimated BM dose between patients with or without PHD. This is in line with BM dose calculation of Bodei and colleagues (8), for a comparison see Figure 5. However, about half of our patients with PHD, did not receive the intended cumulative administered activity of 29 GBq ¹⁷⁷Lu-DOTATATE. These patients were also excluded for salvage therapy with ¹⁷⁷Lu-DOTATATE, therefore creating a bias in our results. Despite this selection bias, about 30% of our patients received a cumulative injected dose of > 30 GBq with an estimated BM dose of more than 2 Gy. However, none of these patients developed PHD. Therefore, the cumulative administered activity of ¹⁷⁷Lu-DOTATATE and estimated BM dose is currently not a dominant factor for predicting PHD after PRRT with ¹⁷⁷Lu-DOTATATE using our treatment regimen.

In general, signs and symptoms in patients with MDS are non-specific. Many patients are asymptomatic at diagnosis and only come to the physician's attention based upon abnormalities found on routine blood counts (e.g., anemia, neutropenia, and thrombocytopenia) (24). First, common causes of anemia have to be excluded, like nutrient deficiencies (iron, folate, and vitamin B12) and anemia secondary to renal failure (25). In our patient group, the red blood cells are the most frequently affected cell line followed by a reduction in platelets and/or white blood cells. In more than half of our patients, we observed a decrease in Hb combined with a rise in mean corpuscular volume. The decrease in red blood cells reflects the imbalance between their production and survival, whereas the increased mean corpuscular volume represents an increase in size resulting from an abnormal blood cell production.

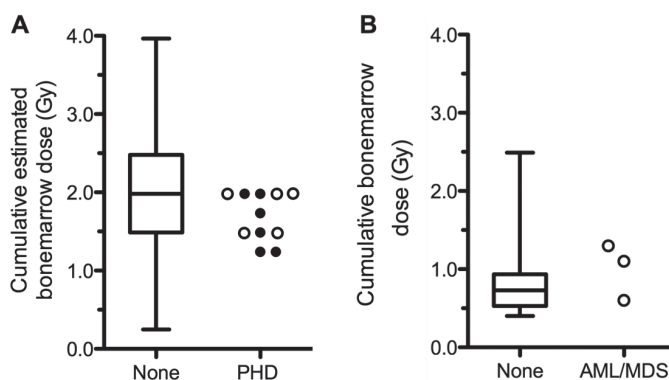


Figure 5 – Comparison of hematological malignancies and cumulative dose to the bonemarrow. A. Whisker and scatter plot of cumulative estimated bone marrow dose in 11 patients (including 5 AML/MDS patients **○**) with persistent hematological dysfunction (PHD) and 263 patients without PHD. B. Whisker and scatter plot of bonemarrow dose in 3 patients with AML/MDS (**○**) and 28 patients without AML/MDS. Data of dosimetry analysis in a subgroup of 807 patients adopted from bodei *et al.* (8). Whiskers represent minimum and maximum (estimated) bone marrow dose in Gy. The height of the box shows the interquartile range and the horizontal line in the box is the median (estimated) bone marrow dose in Gy.

In another paper, we have identified several risk factors for (sub)acute hematological toxicity following PRRT with ^{177}Lu -DOTATATE, like: impaired renal function, low white blood cells, extensive tumormass, high tumoruptake on the OctreoScan[®] and/or advanced age (7). As for long-term hematological toxicity, Bodei *et al.* reported the following risk factors associated with MDS and leukemia after PRRT with ^{177}Lu -DOTATATE (8): previous chemotherapy, tumor invasion of the BM, platelet toxicity grade and other previous myelotoxic therapies. In our study, we could not identify any risk factors for GEP-NET patients who develop PHD after PRRT with ^{177}Lu -DOTATATE. However, analysis in all 367 patients with somatostatin receptor positive tumors positive demonstrated a significantly lower white blood cells in patients with PHD (table 4). Also a trend was observed, where subacute hematological toxicity (grade 3-4) during PRRT was more frequent in patients with PHD in comparison to patients without PHD.

In a recent study, a high incidence (20%) of MDS/AML after chemotherapy and PRRT with ^{177}Lu -DOTATATE was reported in a small group of metastatic GEP-NET patients (26). A critical response was written about the limited (biased) group of patients in this study (27). The high dose of alkylating chemotherapy was the main contributing factor for development of MDS/AML in these patients. In our study, the number of patients treated with chemo(embolization)therapy prior to PRRT is low. Therefore, the statistical power of this (possible) risk factor is limited in our study.

CONCLUSION

The prevalence of therapy-related persistent hematological dysfunction after PRRT with ¹⁷⁷Lu-DOTATATE in GEP-NET patients was 3.7% implying a RR of 2.7. The median latency time to disease development was 41 months.

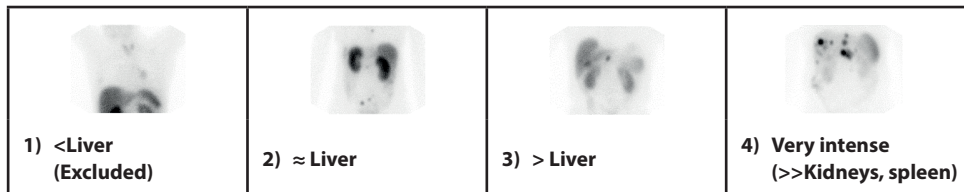
In the group of GEP-NET patients, no risk factors could be identified for the development of therapy-related persistent hematological malignancies. Anemia combined with a rise in MCV occurred in half of the patients with therapy-related hematological malignancies after PRRT with ¹⁷⁷Lu-DOTATATE.

SUPPLEMENTAL DATA

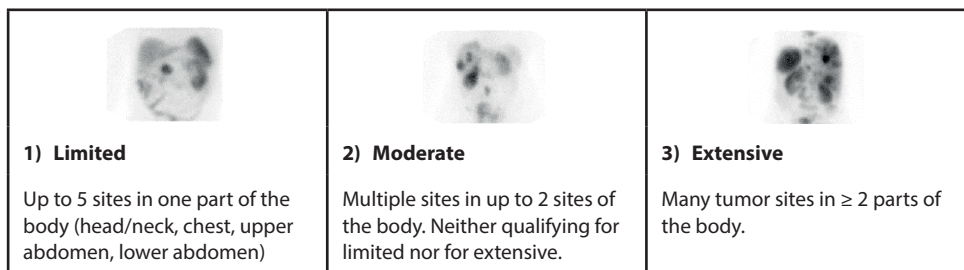
Materials and Methods

Uptake and Extent Scale

The intensity of tumor uptake on OctreoScan® and the extent of tumor burden is to be scored according to simple scaling systems, see Supplemental figures 1 and 2.



Supplemental figure 1 - Tumor uptake scaling system; 1. Uptake less than the liver (excluded) 2. Uptake equal to the liver 3. Uptake more than the liver 4. Uptake more than kidneys and/or spleen.



Supplemental figure 2 - Tumormass on OctreoScan; 1. Limited tumor mass is up to 5 sites in one part of the body (head/neck, chest, upper abdomen, lower abdomen) 2. Moderate tumor mass is multiple sites in up to 2 sites of the body, neither qualifying for limited nor for extensive 3. Extensive tumor mass is many tumor sites in ≥ 2 parts of the body. Usually a combination of extensive liver and lymph node involvement or diffuse skeletal metastases. Diffuse liver metastasis with limited abdominal involvement does not qualify.

Method - The Netherlands Cancer Registry

The expected number of patients with dysfunction of the hematopoietic system was calculated using the website of Dutch cancer figures (www.cijfersoverkanker.nl).

The incidence (number of cancers per 100,000 persons a year) was used for four categories with the following selection criteria:

1. Myelodysplastic Syndrome (MDS) – the selected tumor group was “MDS and Myelodysplastic/myeloproliferative disorders” with subgroup “Myelodysplastic Syndrome”.
2. Acute myeloid leukaemia (AML) – the selected tumor group was “Acute Myeloid Leukaemia” including all subgroups.
3. Myeloproliferative disorders (MPN) - the selected tumor group was “Myeloproliferative disorders” with subgroup “Myeloproliferative neoplasm, other”.
4. Myelodysplastic/myeloproliferative neoplasms (MDS/MPN) - the selected tumor group was “MDS and Myelodysplastic/myeloproliferative disorders” with subgroup “Myelodysplastic/Myeloproliferative disorders” plus tumor group “Myeloproliferative disorders” with subgroup “Chronic Myeloid Leukaemia”.

Incidence data extracted from the website, sorted by 5-years age category and sex can be found in supplemental table 1 - 10. Expected numbers were adjusted for sex, age and duration of follow-up period.

Patient age, sex and follow-up characteristics in all 367 and 274 Gastroenteropancreatic Neuroendocrine tumors (GEP-NETs) patients with expected number of expected number of hematopoietic neoplasms can be found in supplemental table 11 - 14.

Method – Relative Risk

The Relative risk (RR), its standard error and 95% confidence interval are calculated according to Altman (28).

The relative risk or risk ratio is given by

$$RR = \frac{a/(a+b)}{c/(c+d)} \quad (2.17)$$

where a is the number of exposed patients with a positive (bad) outcome, b is the number of exposed patients with a negative (good) outcome, c is the number of non-exposed patients with a positive (bad) outcome and d is the number of non-exposed patients with a negative (good) outcome.

$$SE\{\ln(RR)\} = \sqrt{\frac{1}{a} + \frac{1}{c} - \frac{1}{a+b} - \frac{1}{c+d}} \quad (2.18)$$

with a 95% confidence interval of

$$95\%CI = \exp(\ln(RR) - 1.96 \cdot SE\{\ln(RR)\}) \text{ to } \exp(\ln(RR) + 1.96 \cdot SE\{\ln(RR)\}) \quad (2.19)$$

Where zeros cause problems with computation of the relative risk or its standard error, 0.5 is added to all cells (a,b,c,d) (29,30).

Results

In total 367 patients were treated of whom 324 patients met the inclusion criteria. Forty-three patients were off-protocol for various reasons (see Supplemental table 15). The tumor type of 93 non GEP-NET patients can be found in Supplemental table 16. Patient characteristics of all 13 patients with persistent hematological dysfunction (PHD) can be found in Supplemental table 17. Calculations of the relative risk can be found in Supplemental table 18.

Supplemental Table 1 – Incidence of Myeloproliferative Neoplasms (MPN) in males per age category from 2001–2011 in The Netherlands, obtained from the Netherlands Cancer Registry (www.cijfersoverkanker.nl).

Cat	Age	Incidence Myeloproliferative Neoplasms (MPN) (excluding CML) per year										Average Incidence MPN (excluding CML)				
		2001	2002	2003	2004	2005	2006	2007	2008	2009	2010		2011			
1	0-4	0	0	0	0	0	0	0	0	0	0	0	0	0	0	0.0
2	5-9	0	0	0	0	0	0	0	0	0	0	0	0	0	0	0.0
3	10-14	0	0	0	0	0	0	0	0	0	0	0	0	0	0	0.0
4	15-19	0	0	0	0	0	0	0	0	0	0	0	0	0	0	0.0
5	20-24	0	0	0	0	0	0	0	0	0	0	0	0	0.19	0	0.0
6	25-29	0	0	0	0	0	0	0	0	0	0	0	0.2	0	0	0.0
7	30-34	0	0	0	0.16	0	0	0	0	0	0	0	0	0	0.6	0.1
8	35-39	0	0.15	0	0.15	0	0	0.32	0.17	0.17	0.17	0	0.31	0	0.1	0.1
9	40-44	0.16	0	0	0.46	0	0.3	0.15	0	0.31	0	0.46	0.31	0	0.46	0.2
10	45-49	0	0	0	0.17	0.33	0.16	0.16	0.16	0.35	0	0.51	1.17	0.5	0.5	0.5
11	50-54	0	0.35	0.35	0.71	1.07	0.35	0.35	0.35	0.9	0.9	0.55	2.02	0.73	0.73	1.1
12	55-59	0	1.38	1.67	1.44	1.05	1.75	1.75	1.66	1.66	1.66	1.96	1.7	1.65	1.47	1.3
13	60-64	0.81	0.79	0.76	0.49	1.2	1.58	1.66	2.28	2.28	2.28	2.21	4.26	2.58	2.67	2.4
14	65-69	1.95	2.25	2.53	0.92	2.4	2.04	2.61	4.77	4.77	4.77	3.94	4.52	3.03	4.57	3.1
15	70-74	2.4	0.39	3.48	2.29	1.89	2.61	5.05	5.4	5.4	5.4	3.36	3.75	5.98	4.06	4.1
16	75-79	3.85	4.91	2.7	3.19	2.59	4.93	3.22	3.22	3.22	3.22	1.57	4.57	4.4	5.64	3.8
17	80-84	4.93	3.76	1.79	2.57	4.18	4.93	0	0	0	0	0	4.73	1.52	5.86	2.3
18	85-89	2.24	0	4.42	4.38	2.07	0	0	0	0	0	0	0	5.64	0	1.1
19	90-94	0	0	0	0	6.86	0	0	0	0	0	0	0	0	0	0.0
20	95-99	0	0	0	0	0	0	0	0	0	0	0	0	0	0	0.0
Total	0-99															1.0

Supplemental Table 2 – Incidence of Chronic Myeloid Leukemia (CML) in males per age category from 2001-2011 in The Netherlands, obtained from the Netherlands Cancer Registry (www.cijfersoverkanker.nl).

Male Cat	Age	Incidence Chronic Myeloid Leukemia (CML) per year										Average Incidence CML				
		2001	2002	2003	2004	2005	2006	2007	2008	2009	2010		2011			
1	0-4	0	0	0.19	0.19	0	0	0	0	0	0	0	0	0	0	0.0
2	5-9	0.2	0.2	0	0.2	0	0.2	0	0	0.19	0.19	0	0	0.19	0	0.1
3	10-14	0.4	0	0.39	0	0.19	0.39	0.2	0	0.2	0.39	0.19	0	0.2	0	0.2
4	15-19	0	0.21	0.61	0	0.2	0	0.39	0.39	0.19	0	0	0	0	0	0.2
5	20-24	0	0.41	0.41	0.2	0.2	0	1.02	0.6	0.79	0.39	0.19	0.19	0.19	0.19	0.4
6	25-29	0.18	0.57	1.36	0.6	0	1.01	0.2	0.8	0.8	0.2	0.2	0.2	0.2	0.2	0.6
7	30-34	0.6	0	0.93	0.81	0.17	1.46	0.38	0.59	0.6	1.59	0.2	0.2	0.2	0.2	0.7
8	35-39	0.59	0.44	1.04	0.45	0.75	0.15	1.24	0.63	0.66	1.22	1.46	1.46	1.46	1.46	0.8
9	40-44	0.79	1.72	0.46	1.21	0.45	0.6	1.06	1.37	0.61	1.07	1.38	1.38	1.38	1.38	1.0
10	45-49	0.52	0.68	1.85	0.5	1.15	0.81	1.91	1.1	1.55	1.23	0.61	0.61	0.61	0.61	1.1
11	50-54	0.51	1.74	0.88	1.07	1.07	1.23	1.22	0.87	0.85	0.5	1.98	1.98	1.98	1.98	1.1
12	55-59	1.29	2.36	1.3	0.54	1.92	0.88	1.44	1.46	0.92	1.28	2	2	2	2	1.4
13	60-64	2.42	1.05	1.53	0.74	0.96	1.81	2.08	1.17	1.32	2.2	1.65	1.65	1.65	1.65	1.5
14	65-69	2.92	1.61	0.32	4	2.1	2.34	2.56	2.21	1.06	2.58	1.94	1.94	1.94	1.94	2.1
15	70-74	1.2	3.14	1.55	2.67	1.51	1.49	2.57	2.51	2.09	4.71	2.29	2.29	2.29	2.29	2.3
16	75-79	6.6	6	7.57	2.66	4.15	5.05	5.4	4.79	1.88	2.76	3.61	3.61	3.61	3.61	4.6
17	80-84	4.93	5.63	3.58	5.99	5.85	4.93	6.43	1.57	6.09	2.2	4.23	4.23	4.23	4.23	4.7
18	85-89	0	6.65	4.42	4.38	2.07	3.82	0	1.67	4.73	0	0	0	0	0	2.5
19	90-94	15.83	7.68	0	14.22	0	0	0	0	6.15	0	5.03	5.03	5.03	5.03	4.4
20	95-99	42.46	0	0	0	0	0	37.64	0	0	0	0	0	0	0	7.3
Total	0-99															1.9

Supplemental Table 3 – Incidence of Myelodysplastic/myeloproliferative neoplasms (MDS/MPN) in males per age category from 2001–2011 in The Netherlands, obtained from the Netherlands Cancer Registry (www.cijfersoverkanker.nl).

Male Cat	Age	Incidence Myelodysplastic/myeloproliferative neoplasms (MDS/MPN) per year										Average Incidence MDS/MPN	
		2001	2002	2003	2004	2005	2006	2007	2008	2009	2010		2011
1	0-4	0	0.19	0.38	0	0.39	0.2	0.82	0.62	0.63	0.21	0.21	0.3
2	5-9	0	0	0	0	0	0	0	0	0	0	0	0.0
3	10-14	0	0	0	0	0	0	0	0	0	0	0	0.0
4	15-19	0	0	0	0	0	0	0	0	0	0.19	0	0.0
5	20-24	0	0	0	0	0	0.2	0	0	0	0	0	0.0
6	25-29	0	0	0	0	0	0	0	0	0	0	0	0.0
7	30-34	0.15	0	0	0	0.34	0	0	0	0.2	0	0	0.1
8	35-39	0	0	0	0.15	0	0	0	0	0	0	0	0.0
9	40-44	0	0	0	0.15	0	0.15	0	0	0	0	0	0.0
10	45-49	0	0.17	0.51	0	0.16	0	0.32	0	0	0.15	0.15	0.1
11	50-54	0.34	0.17	0.35	0.53	0.36	0	0	0.17	0	0	0	0.2
12	55-59	0.21	0.59	0.56	0.9	0.7	0.35	0.36	0.73	0.55	0.92	0.73	0.6
13	60-64	0.54	1.05	1.27	2.22	1.2	0.68	1.04	2.15	1.13	1.1	1.1	1.2
14	65-69	2.27	2.57	2.84	2.16	3.3	3.21	1.42	3.31	3.99	3.36	2.43	2.8
15	70-74	3.2	3.93	3.48	4.2	4.91	2.98	5.13	5.74	7.3	4.04	4.9	4.5
16	75-79	3.3	4.91	4.33	5.85	6.22	10.6	8.84	6.71	5.63	7.36	5.86	6.3
17	80-84	6.9	8.45	5.37	7.7	5.01	8.22	4.82	5.49	10.66	13.19	9.87	7.8
18	85-89	6.72	4.43	0	10.95	0	5.73	7.15	10.03	11.04	7.58	11.72	6.9
19	90-94	0	0	0	0	0	0	0	0	12.3	5.64	10.07	2.5
20	95-99	0	0	0	0	0	0	0	0	0	0	0	0.0
Total	0-99												1.7

Supplemental Table 4 – Incidence of Myelodysplastic syndrome (MDS) in males per age category from 2001-2011 in The Netherlands, obtained from the Netherlands Cancer Registry (www.cijferoverkanker.nl).

Male Cat	Age	Incidence Myelodysplastic syndrome (MDS) per year										Average Incidence MDS		
		2001	2002	2003	2004	2005	2006	2007	2008	2009	2010		2011	
1	0-4	0	0.38	0.38	0	0.2	0	0.41	0.42	0	0	0	0	0.2
2	5-9	0.2	0	0	0.4	0	0	0	0.39	0	0.2	0.2	0.4	0.1
3	10-14	0	0	0.58	0.97	0	0.2	0	0	0	0	0	0.58	0.2
4	15-19	0	0	0	1	0.2	0.2	0.39	0.39	0	0.39	0	0.19	0.3
5	20-24	0	0	0	0.2	0	0	0.2	0.2	0.2	0	0	0	0.1
6	25-29	0	0.19	0.39	0.4	0.2	0	0.4	0	0.4	0.2	0.2	0.2	0.2
7	30-34	0.15	0.15	0.31	0.16	0.34	0.18	0.19	0	0	0.2	0.2	0.2	0.2
8	35-39	0.15	0.3	0.15	0.15	0.6	0.15	0	0.16	0.33	0.52	0.37	0.3	0.3
9	40-44	0	0.31	0.46	0.15	0.15	0.45	0.6	0.46	0.92	0.61	0.31	0.4	0.4
10	45-49	1.03	0.68	0.84	0.83	0.98	0.49	0.8	0.79	0.77	1.07	0.76	0.8	0.8
11	50-54	1.35	1.91	3.35	1.42	1.6	2.29	2.1	2.77	2.22	0.84	1.32	1.9	1.9
12	55-59	1.29	2.76	2.98	3.24	1.75	2.81	3.6	2.93	3.86	3.3	2.54	2.8	2.8
13	60-64	5.1	4.99	3.82	5.42	6.47	5.88	5.81	7.64	6.8	8.07	4.96	5.9	5.9
14	65-69	10.71	12.53	13.59	12.01	11.09	11.39	13.11	14.91	14.91	14.99	15.3	13.1	13.1
15	70-74	19.59	23.17	27.07	19.86	21.51	18.62	25.67	30.83	25.73	25.91	22.85	23.7	23.7
16	75-79	34.12	32.75	31.37	41.5	42.53	37.86	45.69	41.7	49.75	39.58	42.38	39.9	39.9
17	80-84	33.49	50.71	62.62	53.03	54.3	56.7	54.67	72.97	62.43	63.04	51.45	55.9	55.9
18	85-89	51.54	68.69	66.36	70.08	47.55	61.14	71.46	61.84	64.66	72.79	54.22	62.8	62.8
19	90-94	39.57	46.1	51.95	85.35	75.5	53.8	65.34	44.55	67.65	39.48	75.52	58.6	58.6
20	95-99	84.93	0	42.4	41.72	40.63	39.39	0	71.29	33.08	31.38	60.79	40.5	40.5
Total	0-99													15.4

Supplemental Table 5 – Incidence of Acute myeloid Leukemia (AML) in males per age category from 2001–2011 in The Netherlands, obtained from the Netherlands Cancer Registry (www.cijfersoverkanker.nl).

Male Cat	Age	Incidence Acute myeloid Leukemia (AML) per year										Average Incidence AML	
		2001	2002	2003	2004	2005	2006	2007	2008	2009	2010		2011
1	0-4	1.75	1.54	1.15	1.15	1.76	1.2	1.23	1.67	1.05	1.27	1.06	1.3
2	5-9	0.2	0.59	0.6	0.4	0.59	0.39	0.19	0.97	0.58	0.59	0.4	0.5
3	10-14	0.99	1.57	1.36	0.58	0.97	0.79	0.99	0.4	0.6	0.59	0.39	0.8
4	15-19	0.83	1.03	1.41	0.6	0.99	0.59	0.59	0.39	0.58	0.39	0.58	0.7
5	20-24	0.2	0.41	1.22	0.82	0.2	0.61	1.22	0.2	0.39	1.16	1.14	0.7
6	25-29	1.09	1.32	1.75	0.8	1.21	1.01	0.61	1.41	0.8	1.59	0.99	1.1
7	30-34	1.49	1.06	0.78	0.65	1.2	0.91	0.76	1.57	1.39	1	0.99	1.1
8	35-39	1.18	1.33	1.34	1.2	1.5	1.06	0.62	0.79	0.99	2.26	1.46	1.2
9	40-44	1.27	1.4	1.69	1.52	1.2	1.65	1.06	0.91	2.44	1.22	1.54	1.4
10	45-49	2.41	3.91	2.7	2.99	1.48	2.59	2.55	2.99	2.01	2.3	2.44	2.6
11	50-54	4.06	4.17	3.35	4.44	2.84	2.29	3.15	4.15	2.73	3.36	3.14	3.4
12	55-59	5.36	5.32	6.7	5.03	5.42	5.44	6.12	4.94	6.61	6.41	4.72	5.6
13	60-64	6.99	7.35	9.69	7.39	8.39	8.14	5.6	7.44	8.88	8.25	10.28	8.0
14	65-69	15.25	13.17	13.27	13.86	9.89	14.02	13.11	10.49	11.98	11.63	12.14	12.6
15	70-74	15.19	22.38	17.4	17.57	18.12	15.64	16.5	20.08	15.99	14.8	19.91	17.6
16	75-79	31.92	23.47	20.01	16.49	27.49	22.72	23.09	27.32	22.53	18.87	29.3	23.9
17	80-84	32.51	19.72	27.73	33.36	29.24	17.26	28.94	29.03	34.26	31.52	28.9	28.4
18	85-89	29.13	24.37	19.91	32.85	14.47	26.75	17.86	16.71	20.5	18.2	27.84	22.6
19	90-94	15.83	23.05	29.69	35.56	13.73	20.18	19.6	6.36	43.05	22.56	15.1	22.2
20	95-99	42.46	42.46	0	0	81.27	39.39	0	0	33.08	0	0	21.7
Total	0-99												8.9

Supplemental Table 6 – Incidence of Myeloproliferative Neoplasms (MPN) in females per age category from 2001-2011 in The Netherlands, obtained from the Netherlands Cancer Registry (www.cijfersoverkanker.nl).

Female Cat	Age	Incidence Myeloproliferative Neoplasms (MPN) (excluding CML) per year										Average Incidence MPN (excluding CML)					
		2001	2002	2003	2004	2005	2006	2007	2008	2009	2010		2011				
1	0-4	0	0	0	0	0	0	0	0	0	0	0	0	0	0	0	0.0
2	5-9	0	0	0	0	0	0	0	0	0	0	0	0	0	0	0	0.0
3	10-14	0	0	0	0	0	0	0	0	0	0	0	0	0	0	0	0.0
4	15-19	0	0	0	0	0	0	0	0	0	0	0	0	0	0	0	0.0
5	20-24	0	0	0	0	0	0	0.21	0	0	0	0	0	0	0	0.19	0.0
6	25-29	0	0	0	0	0	0	0	0	0	0	0	0	0	0	0	0.0
7	30-34	0.31	0.16	0.16	0	0.17	0	0	0	0.2	0	0	0	0	0	0	0.1
8	35-39	0	0	0.15	0	0.15	0	0	0	0.17	0	0	0.16	0	0.18	0	0.1
9	40-44	0	0.16	0	0	0.31	0	0	0	0.16	0	0	0.16	0	0.16	0	0.1
10	45-49	0.18	0.17	0	0.17	0.17	0	0	0	0.32	0	0	0.16	0	0.16	0	0.1
11	50-54	0.35	0	0.18	0.18	0	0.18	0	0.18	0	0.17	0.17	0.17	0.17	0.17	0.17	0.1
12	55-59	0.44	0.81	0.57	0.55	0.18	0.36	0.18	0.36	0.18	0.18	0.19	0.56	0.18	0.73	0.4	0.4
13	60-64	0.27	0.26	0.51	0.25	0.72	0.23	0.63	0.23	0.72	0.63	0.79	0.76	1.29	0.55	0.6	0.6
14	65-69	1.18	1.78	0.88	1.45	1.7	2.23	1.37	1.34	1.7	2.23	1.37	1.34	1.55	0.76	0.48	1.3
15	70-74	0.32	0.96	0.64	1.91	1.28	2.55	3.18	2.52	1.28	2.55	3.18	2.52	2.78	2.42	2.96	2.0
16	75-79	1.46	1.47	1.85	0.37	1.84	1.1	2.53	1.8	1.1	2.53	1.8	3.58	2.5	1.78	1.8	1.8
17	80-84	1.55	0	1.45	3.75	0.92	0.93	4.16	1.85	0.92	0.93	4.16	1.85	2.76	1.82	3.14	2.0
18	85-89	1.75	0	0	0.88	0.85	3.23	1.54	0.74	0.85	3.23	1.54	0.74	0	2.08	1.37	1.1
19	90-94	2.21	0	0	2.08	0	0	0	0	0	0	0	0	0	0	1.68	0.5
20	95-99	0	0	0	0	0	0	0	0	0	0	0	0	0	0	0	0.0
Total	0-99																0.5

Supplemental Table 7 – Incidence of Chronic Myeloid Leukemia (CML) in females per age category from 2001-2011 in The Netherlands, obtained from the Netherlands Cancer Registry (www.cijfersoverkanker.nl).

Female Cat	Age	Incidence Chronic Myeloid Leukemia (CML) per year										Average Incidence CML			
		2001	2002	2003	2004	2005	2006	2007	2008	2009	2010		2011		
1	0-4	0.2	0	0	0	0	0	0	0	0	0	0	0	0	0.0
2	5-9	0.21	0	0	0	0	0	0.2	0	0	0	0	0	0	0.0
3	10-14	0	0	0	0	0	0	0	0	0.21	0	0.21	0	0.21	0.1
4	15-19	0	0	0	0	0.21	0	0	0.2	0.2	0.2	0	0.2	0	0.1
5	20-24	0.21	0.21	0.21	0	0.42	0	0	0	0	0.4	0.2	0	0.2	0.2
6	25-29	0.37	0.77	0.39	0.2	0	0	0.61	0.41	0.2	0.2	0.2	0.4	0.3	0.3
7	30-34	0.15	0.31	0.48	0.33	0.35	0	0.76	0.59	1	0	0	0.6	0.4	0.4
8	35-39	0.61	0.77	0.62	0.31	0.46	0.47	1.1	1.44	0.66	0.52	0.52	0.91	0.7	0.7
9	40-44	0.98	0.96	0.16	0.47	0.77	0.77	0.47	0.47	0.78	0.94	0.94	0.62	0.7	0.7
10	45-49	1.41	1.04	0.86	1.01	1.33	0.99	1.46	0.64	0.63	0.94	0.94	0.47	1.0	1.0
11	50-54	0.87	1.43	0.18	1.45	1.08	1.25	1.59	2.1	0.34	0.68	1.17	1.17	1.1	1.1
12	55-59	0.44	0.2	1.53	2.21	1.97	1.07	1.65	1.11	1.3	0.92	2.19	2.19	1.3	1.3
13	60-64	0.53	2.09	1.02	1.49	2.41	1.37	1.05	1.18	1.52	0.37	2.03	2.03	1.4	1.4
14	65-69	1.78	3.55	1.47	2.31	1.42	1.95	0.82	0.8	2.07	1.26	1.66	1.66	1.7	1.7
15	70-74	2.89	2.55	2.55	1.59	1.28	2.55	2.23	0.63	2.47	1.21	2.08	2.08	2.0	2.0
16	75-79	2.92	1.47	3.7	2.22	4.06	2.56	1.81	2.51	1.43	3.21	1.78	1.78	2.5	2.5
17	80-84	3.63	4.51	2.42	2.81	2.31	3.24	3.7	2.31	2.3	0.91	0.9	0.9	2.6	2.6
18	85-89	3.5	1.74	3.51	5.28	4.26	2.42	1.54	4.43	1.42	2.77	1.37	1.37	2.9	2.9
19	90-94	2.21	6.55	0	2.08	4.06	0	1.95	0	0	0	1.68	1.68	1.7	1.7
20	95-99	0	0	0	8.6	0	0	7.69	0	0	0	0	0	1.5	1.5
Total	0-99														1.1

Supplemental Table 8 – Incidence of Myelodysplastic/Myeloproliferative Neoplasms (MDS/MPN) in females per age category from 2001-2011 in The Netherlands, obtained from the Netherlands Cancer Registry (www.cijfersoverkanker.nl).

Female Cat	Age	Incidence Myelodysplastic/myeloproliferative neoplasms (MDS/MPN) per year										Average Incidence MDS/MPN	
		2001	2002	2003	2004	2005	2006	2007	2008	2009	2010		2011
1	0-4	0	0	0.2	0.2	0.2	0.21	0.21	0.44	0	0.22	0.22	0.2
2	5-9	0	0	0	0	0	0	0	0	0	0	0	0.0
3	10-14	0	0	0	0	0.2	0	0.21	0	0	0	0	0.0
4	15-19	0	0	0	0	0	0	0	0	0	0	0	0.0
5	20-24	0.21	0	0	0	0	0.21	0	0	0	0	0	0.0
6	25-29	0	0	0	0	0	0.2	0	0	0	0	0.2	0.0
7	30-34	0	0	0	0	0	0	0	0	0	0	0	0.0
8	35-39	0	0	0	0.15	0	0	0	0.16	0	0	0	0.0
9	40-44	0.16	0	0	0	0	0	0.16	0.31	0	0.16	0	0.1
10	45-49	0	0	0	0	0	0.49	0	0.16	0	0.16	0	0.1
11	50-54	0.35	0	0.36	0.18	0	0	0.18	0.52	0.69	0.34	0.17	0.3
12	55-59	0.22	0	0.19	0.18	0.36	0.18	1.1	0.19	0.37	0.37	0.18	0.3
13	60-64	0.53	0.78	0.26	0.5	0.72	0.68	0.84	0.39	0.38	0.37	0.37	0.5
14	65-69	0.89	1.48	1.47	1.45	1.98	0.83	0.27	1.07	1.55	1.26	1.66	1.3
15	70-74	0.32	0.64	1.91	2.55	2.87	2.23	2.23	0.95	3.09	2.12	2.96	2.0
16	75-79	2.56	1.1	2.59	2.22	1.48	3.29	3.62	3.23	1.07	3.57	2.85	2.5
17	80-84	2.07	2.51	2.91	3.28	2.31	3.24	3.24	6.01	2.76	4.55	4.04	3.4
18	85-89	3.5	1.74	1.75	1.76	5.11	6.46	2.32	4.43	4.95	3.46	2.06	3.4
19	90-94	0	2.18	0	0	2.03	3.99	0	0	0	3.62	0	1.1
20	95-99	0	0	0	0	0	0	7.69	7.32	0	0	0	1.4
Total	0-99												0.8

Supplemental Table 9 – Incidence of Myelodysplastic syndrome (MDS) in females per age category from 2001-2011 in The Netherlands, obtained from the Netherlands Cancer Registry (www.cijfersoverkanker.nl).

Female Cat	Age	Incidence Myelodysplastic syndrome (MDS) per year										Average Incidence MDS		
		2001	2002	2003	2004	2005	2006	2007	2008	2009	2010		2011	
1	0-4	0.2	0.2	0	0	0.2	0.21	0	0	0	0	0	0.22	0.1
2	5-9	0	0.41	0	0	0.21	0	0	0.41	0.2	0.21	0	0	0.1
3	10-14	0	0	0	0	0	0.21	0.42	0.21	0	0.21	0	0	0.1
4	15-19	0	0.43	0	0	0	0.21	0	0.61	0.2	0.2	0.2	0.2	0.2
5	20-24	0.42	0	0.62	0	0	0.21	0.21	0	0.2	0.2	0.2	0.19	0.2
6	25-29	0.37	0.38	0.39	0.2	0.2	0.4	0.2	0	0.4	0.2	0	0	0.2
7	30-34	0	0.31	0.32	0.33	0.17	0.18	0.19	0	0	0	0	0	0.1
8	35-39	0.61	0.15	0.46	0.15	0.31	0.16	0.16	0.32	0.5	0.35	0.18	0.18	0.3
9	40-44	0.49	0.64	0.47	0.62	0.62	0.31	0.62	0.47	0.62	0.78	0.31	0.31	0.5
10	45-49	0.53	1.04	0.69	0.51	0.33	0.33	0.65	0.96	0.79	1.4	1.09	1.09	0.8
11	50-54	1.22	1.25	1.09	0.73	0.72	1.07	1.06	1.05	1.03	1.18	1	1	1.0
12	55-59	1.76	2.23	1.91	1.47	3.4	2.5	1.83	2.04	2.05	1.85	2.56	2.56	2.1
13	60-64	3.45	2.35	4.34	3.47	3.86	5.01	6.07	4.14	3.8	3.88	2.77	2.77	3.9
14	65-69	4.74	9.18	8.23	7.23	4.53	8.07	8.48	5.87	7.25	6.81	8.56	8.56	7.2
15	70-74	10.29	13.73	10.19	13.38	8.93	11.48	11.45	13.86	10.51	15.11	12.75	12.75	12.0
16	75-79	16.8	12.13	24.03	15.93	20.29	12.79	18.09	17.6	28.26	22.12	22.41	22.41	19.1
17	80-84	18.14	21.57	25.68	19.21	25.89	29.62	33.77	24.49	30.84	25.04	23.34	23.34	25.2
18	85-89	24.52	20.93	29.82	24.62	34.9	30.7	29.34	24.35	26.18	28.37	26.07	26.07	27.3
19	90-94	17.69	17.47	17.12	16.64	22.33	21.94	15.64	32.75	15.19	25.31	16.84	16.84	19.9
20	95-99	0	9.12	17.82	8.6	8.24	0	15.38	0	6.95	6.65	19.26	19.26	8.4
Total	0-99													6.4

Supplemental Table 10 – Incidence of Acute Myeloid Leukemia (AML) in females per age category from 2001–2011 in The Netherlands, obtained from the Netherlands Cancer Registry (www.cijfersoverkanker.nl).

Cat	Age	Incidence Acute myeloid Leukemia (AML) per year										Average Incidence AML	
		2001	2002	2003	2004	2005	2006	2007	2008	2009	2010		2011
1	0-4	1.02	1.21	1	1.41	1.64	1.26	1.07	1.09	0.88	0.44	1.33	1.1
2	5-9	0.21	0.41	0	0.62	0.21	0.41	0.2	0.2	0.41	0.21	0.21	0.3
3	10-14	0.41	0.82	0.61	0.61	0.41	0.41	0.42	0.84	0.42	0	0.41	0.5
4	15-19	0.22	0.86	0	0	2.28	1.23	1.23	0.41	0.4	1.01	0.61	0.8
5	20-24	1.26	1.04	0.62	1.04	0.42	0.42	1.67	0.61	0.4	1.18	0.78	0.9
6	25-29	0.74	0.96	1.58	0.6	1.62	1.01	0.81	1.42	2.02	0.6	1	1.1
7	30-34	1.24	1.09	1.11	1.15	0.35	1.83	0.76	1.38	1.99	1.2	0.99	1.2
8	35-39	1.69	1.38	1.54	1.86	1.24	2.17	2.04	1.76	1	2.09	2	1.7
9	40-44	2.11	1.6	1.58	3.12	3.4	2.16	1.86	1.87	2.19	1.71	1.56	2.1
10	45-49	2.11	3.48	1.72	3.72	2.33	2.46	2.91	2.24	2.36	2.65	3.27	2.7
11	50-54	3.49	1.97	2.17	2.54	1.63	4.83	2.3	3.15	2.92	3.39	2.5	2.8
12	55-59	3.53	5.67	5.34	4.97	3.93	4.83	4.77	4.46	4.28	4.99	3.29	4.6
13	60-64	3.99	6.27	7.65	4.95	6.52	3.65	3.35	5.72	5.9	4.43	4.61	5.2
14	65-69	4.15	6.52	9.41	10.41	5.95	8.35	6.57	7.48	8.8	9.33	9.75	7.9
15	70-74	9.97	12.45	10.5	12.42	9.56	8.61	7	9.45	9.89	14.81	10.97	10.5
16	75-79	9.86	13.24	15.9	13.34	12.17	14.26	13.39	13.65	16.81	14.98	13.87	13.8
17	80-84	12.96	16.55	16.48	18.27	12.48	17.58	15.27	15.25	13.35	18.21	19.75	16.0
18	85-89	10.51	11.34	14.04	14.07	14.47	10.5	15.44	20.66	21.94	13.15	19.21	15.0
19	90-94	8.84	6.55	4.28	16.64	10.15	15.96	9.77	9.63	9.5	9.04	10.1	10.0
20	95-99	9.4	0	8.91	0	8.24	0	7.69	0	0	0	0	3.1
Total	0-99												5.1

Supplemental Table 11 – Patient age, sex and follow-up characteristics in 367 patients. Age category (Age-Cat), Follow-up (FU)

Age-Cat	Age	Total no.	Male	Female	FU in yrs.	FU-Male	FU-Female
1	0-4	0	0	0	0.0	0.0	0.0
2	5-9	0	0	0	0.0	0.0	0.0
3	10-14	0	0	0	0.0	0.0	0.0
4	15-19	0	0	0	0.0	0.0	0.0
5	20-24	0	0	0	0.0	0.0	0.0
6	25-29	0	0	0	0.0	0.0	0.0
7	30-34	14	7	7	20.6	7.1	13.4
8	35-39	12	2	10	28.2	7.0	21.3
9	40-44	29	14	15	53.9	15.3	38.5
10	45-49	38	20	18	228.2	59.9	168.3
11	50-54	44	23	21	135.8	68.0	67.8
12	55-59	66	33	33	173.6	85.3	88.3
13	60-64	62	34	28	317.7	108.3	209.4
14	65-69	34	14	20	145.2	73.5	71.7
15	70-74	39	19	20	104.2	51.2	53.0
16	75-79	22	13	9	73.5	42.9	30.6
17	80-84	6	4	2	20.9	11.9	9.0
18	85-89	1	0	1	7.0	4.3	2.7
19	90-94	0	0	0	0.0	0.0	0.0
20	95-99	0	0	0	0.0	0.0	0.0
Total	0-99	367	183	184	1308.8	534.7	774.1

Supplemental Table 12 - Expected number of hematological malignancies in 367 patients; Myeloproliferative Neoplasms (MPN), Chronic Myeloid Leukemia (CML), Myelodysplastic/Myeloproliferative neoplasms (MDS/MPN), Myelodysplastic Syndrome (MDS) and Acute Myeloid Leukemia (AML).

Age-Cat	Age	MPN (without CML)	CML	MDS/MPN	MDS	AML
1	0-4	0.000	0.000	0.000	0.000	0.000
2	5-9	0.000	0.000	0.000	0.000	0.000
3	10-14	0.000	0.000	0.000	0.000	0.000
4	15-19	0.000	0.000	0.000	0.000	0.000
5	20-24	0.000	0.000	0.000	0.000	0.000
6	25-29	0.000	0.000	0.000	0.000	0.000
7	30-34	0.000	0.001	0.000	0.000	0.002
8	35-39	0.000	0.002	0.000	0.000	0.004
9	40-44	0.001	0.006	0.000	0.002	0.015
10	45-49	0.005	0.043	0.004	0.042	0.111
11	50-54	0.010	0.033	0.006	0.035	0.094
12	55-59	0.044	0.078	0.026	0.146	0.291
13	60-64	0.080	0.137	0.076	0.345	0.600
14	65-69	0.044	0.047	0.047	0.280	0.243
15	70-74	0.051	0.044	0.065	0.358	0.283
16	75-79	0.028	0.033	0.042	0.298	0.171
17	80-84	0.002	0.003	0.004	0.029	0.016
18	85-89	0.000	0.000	0.000	0.001	0.000
19	90-94	0.000	0.000	0.000	0.000	0.000
20	95-99	0.000	0.000	0.000	0.000	0.000
Total	0-99	0.265	0.425	0.271	1.536	1.831

Supplemental Table 13 – Patient age, sex and follow-up characteristics in 274 Gastroenteropancreatic Neuroendocrine tumors (GEP-NETs) patients.

Age-Cat	Age	Total no.	Male	Female	FU in yrs	FUMale	FUFemale
1	0-4	0	0	0	0.0	0.0	0.0
2	5-9	0	0	0	0.0	0.0	0.0
3	10-14	0	0	0	0.0	0.0	0.0
4	15-19	0	0	0	0.0	0.0	0.0
5	20-24	0	0	0	0.0	0.0	0.0
6	25-29	0	0	0	0.0	0.0	0.0
7	30-34	6	3	3	9.4	5.8	3.6
8	35-39	7	1	6	23.1	6.3	16.8
9	40-44	19	10	9	38.3	9.7	28.6
10	45-49	26	13	13	203.2	45.7	157.5
11	50-54	36	19	17	108.2	49.4	58.8
12	55-59	47	23	24	144.6	75.5	69.1
13	60-64	53	29	24	298.0	94.8	203.2
14	65-69	28	12	16	125.9	63.6	62.4
15	70-74	29	15	14	87.8	46.9	40.9
16	75-79	18	11	7	54.1	36.5	17.6
17	80-84	5	3	2	16.2	9.5	6.8
18	85-89	0	0	0	4.3	3.8	0.5
19	90-94	0	0	0	0.0	0.0	0.0
20	95-99	0	0	0	0.0	0.0	0.0
Total	0-99	274	139	135	1113.2	447.3	665.8

Supplemental Table 14 – Expected number of hematological malignancies in 274 patients; Myeloproliferative Neoplasms (MPN), Chronic Myeloid Leukemia (CML), Myelodysplastic/Myeloproliferative neoplasms (MDS/MPN), Myelodysplastic Syndrome (MDS) and Acute Myeloid Leukemia (AML).

Age-Cat	Age	MPN (without CML)	CML	MDS/MPN	MDS	AML
1	0-4	0.000	0.000	0.000	0.000	0.000
2	5-9	0.000	0.000	0.000	0.000	0.000
3	10-14	0.000	0.000	0.000	0.000	0.000
4	15-19	0.000	0.000	0.000	0.000	0.000
5	20-24	0.000	0.000	0.000	0.000	0.000
6	25-29	0.000	0.000	0.000	0.000	0.000
7	30-34	0.000	0.000	0.000	0.000	0.000
8	35-39	0.000	0.001	0.000	0.000	0.002
9	40-44	0.000	0.003	0.000	0.002	0.007
10	45-49	0.003	0.027	0.002	0.020	0.070
11	50-54	0.006	0.021	0.004	0.028	0.060
12	55-59	0.026	0.046	0.015	0.085	0.173
13	60-64	0.063	0.109	0.060	0.354	0.474
14	65-69	0.031	0.034	0.034	0.172	0.175
15	70-74	0.033	0.028	0.043	0.235	0.184
16	75-79	0.019	0.022	0.028	0.184	0.113
17	80-84	0.001	0.002	0.003	0.019	0.010
18	85-89	0.000	0.000	0.000	0.000	0.000
19	90-94	0.000	0.000	0.000	0.000	0.000
20	95-99	0.000	0.000	0.000	0.000	0.000
Total	0-99	0.183	0.292	0.190	1.100	1.268

Supplemental Table 15 - 43 out of 367 off-protocol with reason:

Reason	Number of patients
Low uptake (on first post therapy scan)	14
Concomitant Radiotherapy	6
Diagnostic	4
Previous ¹¹¹ In-PRRT	3
Low Karnofsky score	3
Poor renal function	3
Low baseline Hb, platelets or WBC	3
Previous ⁹⁰ Y-PRRT	2
No pathology available	2
Hb transfusion prior to PRRT	1
Previous ¹³¹ I-therapy	1
Patient was not able to give fully consent	1
Totaal	43

Supplemental Table 16 - 93 out of 367 patients with Non GEP-NETs:

Type of tumor	Number of patients
NET - thorax/chest	2
NET - unknown primary	28
NET - other locations	4
Tyroid carcinoma	19
Paraganglioma	14
Feochromocytoma	2
Meningioma	4
Hurthecell carcinoma	6
SCLC	1
Grawitz pancreas	1
Mamma carcinoma	3
Erdheim chester	1
HCC	2
Prostaat carcinoma	1
Esthesioneuroblastoom	1
Melanoma	2
Meduloblastoma	1
Rectum carcinoma	1
Totaal	93

Supplemental Table 17 – Characteristics of 13 patients with persistent hematological dysfunction (PHD) after peptide receptor radiotherapy (PRRT) with ¹⁷⁷Lu-DOTATATE (¹⁷⁷Lu). Neuroendocrine tumor (NET), Neuroendocrine tumor of the pancreas (PNET), Radioactive iodine I-131 therapy (¹³¹I), cold Octreotide (Octreotide), External beam radiotherapy (EBRT), Hemoglobin (Hb), Platelets (PLT), White Blood Cells (WBC).

Patient no.	sex	Age	Diagnosis	Previous therapy	Administered Activity (GBq)	PRRT interrupted	Reason	Blood work				Latency Period in months		
								Cytopenia	1. Aspirate	2. Flow	3. Cytogenetics		4. Biopsy	Diagnosis
359	f	70	NET	Octreotide	30.0	no	-	Hb	yes	no	no	yes	MDS, RARS	33.3
297	f	60	NET	Octreotide	18.6	yes	Maximum kidney dose	Hb, PLT, WBC	yes	no	no	yes	Hypoplasia	45.7
293	m	61	PNET	chemo-embolisation	29.3	no	-	Hb, PLT	yes	yes	46,XY, t(9;22)	yes	CML	5.1
284	m	57	PNET	-	29.7	no	-	Hb	yes	no	-5,-7,del(12p), +mar	yes	MDS, RAEB-II	34.3
252	f	64	NET	Octreotide	30.0	no	-	Hb, WBC	no	no	no	no	Pancytopenia	63.6
241	f	41	PNET	-	26.3	yes	Hematological toxicity	Hb, PLT, WBC	yes	no	no	yes	Aplasia	15.4
185	m	74	PNET	-	26.4	no	-	Hb, PLT	yes	yes	45,XY,-7 [20]	yes	MDS/MPN: CMML-1	42.4
158	m	62	NET	Octreotide	22.2	yes	Maximum kidney dose	Hb, PLT, WBC	yes	yes	no	yes	MDS, RAEB-II	6.4
105	v	67	NET	-	22.3	yes	Hematological toxicity	WBC	yes	no	no	yes	Hypoplasia	42.3
102	m	68	NET	-	30.0	no	-	Hb, PLT, WBC	yes	yes	no	yes	MDS, Hypocellular	20.2
91	f	59	NET	Octreotide, local EBRT	22.7	yes	Maximum kidney dose	Hb, PLT, WBC	yes	yes	46,XX	yes	AML	83.5
81	f	58	NET	Octreotide	22.3	yes	Maximum kidney dose	Hb, PLT, WBC	yes	no	no, JAK2 neg	yes	Myelofibrosis/MPN	36.3
45	f	58	Thyroid cancer	Radioactive iodine therapy	16.7 (¹³¹ I) & 15.2 (¹⁷⁷ Lu)	no	-	Hb, PLT	yes	no	no	yes	Hypoplasia	40.8

Supplemental Table 18 – Calculations for the relative risk (RR) in all 367 patients and 274 Neuroendocrine gastroenteropancreatic tumors (GEP-NETs).

	All 367 patients	274 GEP-NET patients
Exposed group		
Number with positive (bad) outcome (a):	8	8
Number with negative (good) outcome (b):	359	266
Control group		
Number with positive (bad) outcome (c):	4.4	3
Number with negative (good) outcome (d):	362.6	271
Relative Risk	1.82	2.67
95% Confidence Interval	1.26 to 2.62	0.72 to 9.95
Z statistic	3.22	1.46
Significance level	P = 0.0013	P = 0.1442
NNT (Harm)	101.81	54.800
95% Confidence Interval	254.25 (Harm) to 63.65 (Harm)	23.99 (Harm) to ∞ to 192.77 (Harm)

REFERENCES

1. Krenning EP, Kooij PP, Bakker WH, et al. Radiotherapy with a radiolabeled somatostatin analogue, [¹¹¹In-DTPA-D-Phe¹]-octreotide. A case history. *Ann N Y Acad Sci.* 1994;733:496-506.
2. Valkema R, De Jong M, Bakker WH, et al. Phase I study of peptide receptor radionuclide therapy with [¹¹¹In-DTPA]octreotide: the Rotterdam experience. *Semin Nucl Med.* 2002;32:110-122.
3. Kwekkeboom DJ, Teunissen JJ, Bakker WH, et al. Radiolabeled somatostatin analog [¹⁷⁷Lu-DOTA₀Tyr₃]octreotate in patients with endocrine gastroenteropancreatic tumors. *J Clin Oncol.* 2005;23:2754-2762.
4. Bodei L, Cremonesi M, Grana CM, et al. Peptide receptor radionuclide therapy with (1)(7)(7)Lu-DOTATATE: the IEO phase I-II study. *Eur J Nucl Med Mol Imaging.* 2011;38:2125-2135.
5. Paganelli G, Sansovini M, Ambrosetti A, et al. ¹⁷⁷ Lu-Dota-octreotate radionuclide therapy of advanced gastrointestinal neuroendocrine tumors: results from a phase II study. *Eur J Nucl Med Mol Imaging.* 2014;41:1845-1851.
6. Strosberg J, El-Haddad G, Wolin E, et al. Phase 3 Trial of ¹⁷⁷Lu-Dotatate for Midgut Neuroendocrine Tumors. *N Engl J Med.* 2017;376:125-135.
7. Bergsma H, Konijnenberg MW, Kam BL, et al. Subacute haematotoxicity after PRRT with (¹⁷⁷)Lu-DOTA-octreotate: prognostic factors, incidence and course. *Eur J Nucl Med Mol Imaging.* 2016;43:453-463.
8. Bodei L, Kidd M, Paganelli G, et al. Long-term tolerability of PRRT in 807 patients with neuroendocrine tumours: the value and limitations of clinical factors. *Eur J Nucl Med Mol Imaging.* 2015;42:5-19.
9. Kwekkeboom DJ, de Herder WW, Kam BL, et al. Treatment with the radiolabeled somatostatin analog [¹⁷⁷ Lu-DOTA 0,Tyr₃]octreotate: toxicity, efficacy, and survival. *J Clin Oncol.* 2008;26:2124-2130.
10. Imhof A, Brunner P, Marincek N, et al. Response, survival, and long-term toxicity after therapy with the radiolabeled somatostatin analogue [⁹⁰Y-DOTA]-TOC in metastasized neuroendocrine cancers. *J Clin Oncol.* 2011;29:2416-2423.
11. Pfeifer AK, Gregersen T, Gronbaek H, et al. Peptide receptor radionuclide therapy with Y-DOTATOC and (¹⁷⁷)Lu-DOTATOC in advanced neuroendocrine tumors: results from a Danish cohort treated in Switzerland. *Neuroendocrinology.* 2011;93:189-196.
12. Kwekkeboom DJ, Bakker WH, Kooij PP, et al. [¹⁷⁷Lu-DOTAOTyr₃]octreotate: comparison with [¹¹¹In-DTPA]octreotide in patients. *Eur J Nucl Med.* 2001;28:1319-1325.
13. Common Terminology Criteria for Adverse Events (CTCAE) v3.0. 9 August 2006; http://ctep.cancer.gov/protocolDevelopment/electronic_applications/docs/ctcae3.pdf.
14. Arber DA, Orazi A, Hasserjian R, et al. The 2016 revision to the World Health Organization classification of myeloid neoplasms and acute leukemia. *Blood.* 2016;127:2391-2405.
15. Dinmohamed AG, Visser O, van Norden Y, et al. Trends in incidence, initial treatment and survival of myelodysplastic syndromes: a population-based study of 5144 patients diagnosed in the Netherlands from 2001 to 2010. *Eur J Cancer.* 2014;50:1004-1012.
16. Visser O, Trama A, Maynadie M, et al. Incidence, survival and prevalence of myeloid malignancies in Europe. *Eur J Cancer.* 2012;48:3257-3266.
17. Folley JH, Borges W, Yamawaki T. Incidence of leukemia in survivors of the atomic bomb in Hiroshima and Nagasaki, Japan. *Am J Med.* 1952;13:311-321.
18. Rubino C, de Vathaire F, Dottorini ME, et al. Second primary malignancies in thyroid cancer patients. *Br J Cancer.* 2003;89:1638-1644.

19. Brown AP, Chen J, Hitchcock YJ, Szabo A, Shrieve DC, Tward JD. The risk of second primary malignancies up to three decades after the treatment of differentiated thyroid cancer. *J Clin Endocrinol Metab.* 2008;93:504-515.
20. Sawka AM, Thabane L, Parlea L, et al. Second primary malignancy risk after radioactive iodine treatment for thyroid cancer: a systematic review and meta-analysis. *Thyroid.* 2009;19:451-457.
21. Subramanian S, Goldstein DP, Parlea L, et al. Second primary malignancy risk in thyroid cancer survivors: a systematic review and meta-analysis. *Thyroid.* 2007;17:1277-1288.
22. Bennett JM, Kaminski MS, Leonard JP, et al. Assessment of treatment-related myelodysplastic syndromes and acute myeloid leukemia in patients with non-Hodgkin lymphoma treated with tositumomab and iodine I131 tositumomab. *Blood.* 2005;105:4576-4582.
23. Czuczman MS, Emmanouilides C, Darif M, et al. Treatment-related myelodysplastic syndrome and acute myelogenous leukemia in patients treated with ibritumomab tiuxetan radioimmunotherapy. *J Clin Oncol.* 2007;25:4285-4292.
24. Garcia-Manero G. Myelodysplastic syndromes: 2015 Update on diagnosis, risk-stratification and management. *Am J Hematol.* 2015;90:831-841.
25. Pang WW, Schrier SL. Anemia in the elderly. *Curr Opin Hematol.* 2012;19:133-140.
26. Brieau B, Hentic O, Lebtahi R, et al. High risk of myelodysplastic syndrome and acute myeloid leukemia after 177Lu-octreotate PRRT in NET patients heavily pretreated with alkylating chemotherapy. *Endocr Relat Cancer.* 2016;23:L17-23.
27. Bodei L, Modlin I, Luster M, et al. Myeloid neoplasms after alkylating chemotherapy and PRRT: myth and reality. *Endocr Relat Cancer.* 2016.
28. Altman D. Practical Statistics for Medical Research Chapman & Hall London Google Scholar. 1991.
29. Pagano M, Gauvreau K. Comparison of two means. *Principles of Biostatistics, edited by Pagano M and Gauvreau K Belmont, CA: Duxbury Thompson Learning.* 2000.
30. Deeks JJ, Higgins JP. Statistical algorithms in review manager 5. *Statistical Methods Group of The Cochrane Collaboration.* 2010:1-11.

2.4

SPLEEN VOLUME DECREASE AFTER PRRT: CLINICAL AND DOSIMETRIC CORRELATION

Wouter A. van der Zwan¹, Mark W. Konijnenberg¹, Jifke F. Veenland¹, Eric P. Krenning¹, Saima Khan¹, Hendrik Bergsma¹, Dik J. Kwekkeboom¹

¹ Department of Radiology & Nuclear Medicine, Erasmus MC, University Medical Center, Rotterdam, The Netherlands

Submitted

ABSTRACT

The spleen is the only lymphoid tissue directly interposed in the blood circulation and receives a high-absorbed dose during treatment with PRRT. However, little is known about the clinical consequences. The aim of this study was to examine the correlation between the cumulative radiation dose to the spleen, changes in spleen volume and peripheral blood counts after multiple cycles of PRRT.

Methods:

Data of spleen volume, spleen dosimetry and leucocyte count (total and differential) were collected at baseline, 3 months and 12 months after completion of initial treatment cycles and within 3 months after re-treatment. Only patients who received a cumulative dose of 30 GBq and an extra dose for retreatment of 15 GBq were included in the analysis. Patient medical files were reviewed for the occurrence and type of documented infections.

Results:

Significant smaller splenic volumes were measured ($p < 0.001$, $r = -0.55$) 12 months after initial treatment with ^{177}Lu -Octreotate, compared to baseline. An increasing decline in volume was observed after re-treatment when compared to 12 months follow-up ($p < 0.001$, $r = -0.43$). An overall decline of 55% in volume was observed. The median absorbed dose to the spleen was 52 Gy (23-110 Gy), no minimum threshold for spleen volume reduction was found. A decline in White Blood Count (WBC), total and differential, was observed in all patients after treatment. Lymphocyte count was only decreased after re-treatment in comparison to the blood counts after 12 months, ($p < 0.001$, $r = -0.81$).

No correlation was found between the absorbed spleen dose and decrease in WBC count or lymphocyte count. There was also no association between spleen volume and difference in lymphocyte count at 12 months follow-up and at 3 months after re-treatment. Evaluation of the medical files demonstrated no infection of patients caused by a pneumococcal, meningococcal and/or Haemophilus influenzae type b based bacteria.

Conclusion:

Administration of multiple cycles of PRRT reduces spleen volume and lymphocyte count. Reduction in spleen volume combined with a decrease in lymphocyte count does not have clinical consequences. No increased risk of infection, based on encapsulated bacteria, was found.

Key words:

PRRT, ^{177}Lu -Octreotate, Spleen, Dosimetry, Volume, toxicity

INTRODUCTION

Peptide receptor radionuclide therapy (PRRT) with radiolabelled somatostatin analogues is increasingly being used in patients with metastasized and/or inoperable neuroendocrine tumors. Since the introduction of PRRT in the late nineties, an increase in clinical experience has supported the growth in knowledge regarding the (side) effects of PRRT.

After PRRT with ^{177}Lu -octreotate, physiological accumulation of the radiopeptide can be found in the liver, kidneys, spleen and occasionally in the pituitary gland. Uptake of the radioligand can also be seen in neuroendocrine tumours because of their rich expression of the somatostatin receptor (sst), particular subtype 2 (1,2). Dosimetric analysis also indicates high-absorbed doses to the spleen and kidneys (1,3). The absorbed doses to the spleen are in the range of dose limits, generating deterministic radiation effects. However, clinically observed radiation-induced toxicities are low.

Coinfusion of amino acids during PRRT lowers the absorbed dose to the kidneys and reduces renal toxicity (4,5). Accumulation of the radioligand in the pituitary gland can induce transient inhibitory effects on spermatogenesis in male patients and can lead to a decrease of gonadotropin levels in post-menopausal females (6). However, little is known about the clinical consequence of a high-absorbed dose to the spleen.

The spleen is the only lymphoid tissue directly interposed in the blood circulation and fulfills an important immunological, moreover it acts as reservoir for platelets, red and white blood cells (7). Up to now, the bone marrow is considered as one of the main dose limiting organs for PRRT. Interestingly, Svensson et al. recently found a correlation between total absorbed spleen dose and decrease in hemoglobin, but such a correlation was not observed for spleen dose and white blood cell and/or platelet count (8). These findings contradict the results of an earlier study done by Kulkarni et al., they found no relation between hematological toxicity and absorbed spleen dose after PRRT with ^{177}Lu -DOTATATE or ^{177}Lu -DOTATOC (9).

The combination of radiation exposure to the bone marrow and the spleen after PRRT may lead to a different hematological response compared to irradiation of only the bone marrow, like in radioiodine (^{131}I) therapy in patients with thyroid cancer.

The aim of this study was to explore the correlation between cumulative mean absorbed spleen dose, the changes in spleen volume and change in peripheral blood counts after multiple cycles of PRRT. Since the spleen has an important immunological role, changes in leucocyte count and vulnerability to infectious disease were also taken into account.

MATERIALS AND METHODS

Patients

The study included Dutch patients who were treated from January 2000 to October 2010. Only patients who completed initial treatment followed by re-treatment after renewed progressive disease were selected.

Inclusion criteria were: patients with neuroendocrine tumor and baseline tumor uptake on [¹¹¹In-DTPA⁰] octreotide scintigraphy (OctreoScan®; Mallinckrodt, Petten, The Netherlands) with accumulation in the tumor at least as high as in normal liver tissue; no prior treatment with PRRT; baseline serum hemoglobin (Hb) ≥ 6 mmol/l; white blood cell (WBC) count $\geq 2 \times 10^9$ /l; platelet (PLT) count $\geq 75 \times 10^9$ /l; serum creatinine ≤ 150 μ mol/l or creatinine clearance ≥ 40 ml/min and Karnofsky performance status ≥ 50 . Only Dutch patients were selected, because loss to follow-up is limited in these patients.

This study was part of the ongoing prospective study in patients with neuroendocrine tumors treated with ¹⁷⁷Lu-octreotate at the Department of Nuclear Medicine, Erasmus University Medical Center Rotterdam. The hospital's medical ethics committee approved the study. All patients gave written informed consent for participation in the study.

Treatment

[DOTA⁰,Tyr³] octreotate was obtained from BioSynthema (St. Louis, MO). ¹⁷⁷LuCl₃ was supplied by IDB-Holland (Baarle-Nassau, The Netherlands) and ¹⁷⁷Lu-octreotate was prepared locally (1). Granisetron 3 mg or ondansetron 8 mg was injected intravenously 30 min before infusion of ¹⁷⁷Lu-octreotate. Infusion of amino acids (2.5 % arginine and 2.5 % lysine, 1 l) was started 30 min before administration of the radiopharmaceutical and lasted for 4 h. The radiopharmaceutical was coadministered for 30 min using a second pump system. The intended cumulative dose for the initial treatment was 30.0 GBq, given in 4 cycles. Two additional cycles of 7.4 GBq (=re-treatment) were given after renewed progressive disease.

Data acquisition & statistical analysis

Data on spleen volume, spleen dosimetry and leucocyte count (total and differential) collected at baseline, 3 months and 12 months after completing the initial treatment cycles and within 3 months after finishing re-treatment was analyzed. Spleen volume was based on diagnostic CT-scans and volume was calculated using MeVisLab software (version 2.4, MeVis Medical Solutions AG, Bremen, Germany). An MD reviewed patient medical files for the occurrence and type of documented infections.

A nonparametric test for dependent samples was used to assess changes in spleen volume and leucocyte count; p-values ≤ 0.05 were considered significantly different. Correlations between mean absorbed dose to spleen, spleen volume and leucocyte count were tested using binary logistic regression and linear regression tests (SPSS version 20; Inc., Chicago, IL).

Dosimetry

Dosimetric calculations were performed according to the MIRD scheme (10). The mean absorbed dose ($D(r_T, T_D)$), to target tissue (r_T) can be calculated over a dose-integration period (T_D) from a uniformly distributed compound within a source tissue (r_S):

$$D(r_T, T_D) = \sum_{r_S} \tilde{A}(r_S, T_D) S(r_T \leftarrow r_S) \quad (2.20)$$

<=>

$$D(r_T, T_D) = \tilde{A}_1 \cdot S_{(k \leftarrow h_1)} + \tilde{A}_2 \cdot S_{(k \leftarrow h_2)} + \tilde{A}_3 \cdot S_{(k \leftarrow h_3)} + \dots + \tilde{A}_n \cdot S_{(k \leftarrow h_n)} \quad (2.21)$$

where $\tilde{A}(r_S, T_D)$ is the time-integrated activity (no. of nuclear transformations) in r_S over T_D and $S(r_T \leftarrow r_S)$ is the absorbed dose rate in r_T per nuclear transformation in r_S . Highest physiological uptake of the radiopeptide was observed in the kidneys and spleen. Therefore

$$D_{spl} = \tilde{A}_{spl} DF(spl \leftarrow spl) + \tilde{A}_{kidneys} DF(spl \leftarrow kidneys) \quad (2.22)$$

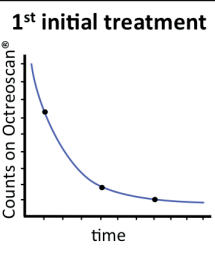
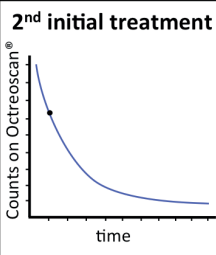
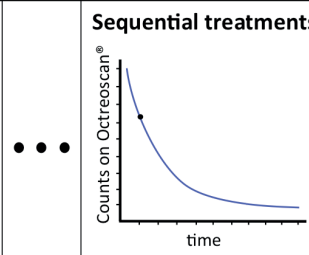
where D_{spl} is the radiation dose to the spleen (spl), \tilde{A} is the cumulative activity and DF are the dose factors for the specific organs. Since contribution of cross-dose from gamma radiation of the surrounding organs to the absorbed spleen dose is limited (11), we can further reduce equation (2.23) to

$$D_{spl} = \tilde{A}_{spl} DF(spl \leftarrow spl) \quad (2.23)$$

After the first therapy cycle of initial treatment, planar whole body scans were performed at 24, 96 and 168 hours after the administration of the radiopharmaceutical. A monoexponential curve was fitted through the spleen conjugate-view background corrected time-activity data (Excel, Microsoft). Time-integrated activity coefficients (TIAC) in the spleen and other organs with physiological uptake were acquired by integration of the exponential curve folded with the ^{177}Lu decay curve (with half-life $T_{1/2} = 6.647$ d).

After the second and sequential therapy cycles, planar whole body scans were performed at 24 hours after the administration of the radiopharmaceutical. Splenic dose calculations for second and sequential therapy cycles were calculated by normalization of the monoexponential function (calculated after the first initial treatment) and the amount of radioactivity measured at the whole body scan (table 1). The resulting organ TIACS were used as input for the Olinda/EXM dosimetry software with correction for the actual spleen mass, by modifying the standard spleen masses (female: 150g, male: 183g) with the measured spleen mass taking a density of 1 g/cm³.

Table 1 - Methods of splenic dose calculations after different therapy cycles with ¹⁷⁷Lu-Octreotate.

	1st initial treatment	2nd initial treatment	• • •	Sequential treatments
				
Time-activity curve based on:	3 timepoints with monoexponential fit	1 timepoint and normalization		1 timepoint and normalization
Kidney volume based on:	Baseline CT-scan	Baseline CT-scan		Current CT-scan

RESULTS

A total of 35 of 67 patients completed the full treatments and had complete follow-up at the required time points. Thirty-five patients were analyzed, see table 2 for the patient and treatment characteristics. Overall, patients received a total of 6 PRRT cycles, with a minimum of 5 and maximum 7 therapy cycles. Median follow-up was 37.7 (range 21.4 - 68.5) months.

Complete dosimetric data was available in 27 patients. The median absorbed dose to the spleen was 52 Gy (23-110 Gy). No minimal threshold for the induction of a spleen volume reduction was found.

Median splenic volumes at baseline and during follow-up are summarized in table 3. Significant smaller splenic volumes (Wilcoxon signed rank test; $p < 0.01$, $r = -0.58$) were measured at 12 months follow-up after initial treatment in comparison to baseline measurements. Also, significant changes (Wilcoxon signed rank test; $p < 0.01$, $r = -0.55$) were observed after re-treatment with ¹⁷⁷Lu-Octreotate in comparison to baseline measurements. Likewise, splenic volumes after 12 months follow-up and after re-

treatment were significantly different (Wilcoxon signed rank test; $p < 0.01$, $r = -0.43$). Figure 1 shows the absolute change in volume per individual patient. In two cases the spleen increased in size between 12 months follow-up and retreatment. However, in both patients a volume reduction was observed at the 12 months follow-up CT-scan. An example of spleen volume loss on CT-scan in two patients is displayed in figure 2.

Table 2 - Characteristics of 35 (16 male and 19 female) Dutch patients with complete data of initial- and retreatment.

Characteristic	Value (and range)
<i>Initial Treatment</i>	
- Age at initial treatment (years)	57 (39-72)
- Cumulative activity initial treatment (GBq)	29.9 (22.4 - 30.5)
Interval initial treatment to re-treatment (months)	30.5 (10.5 -59.5)
<i>Retreatment</i>	
- Age at re-treatment in (years)	60 (41 -76)
- Cumulative activity re-treatment (GBq)	44.9 (36.3 - 46.4)
- Cumulative absorbed dose to the spleen (Gy)	52 (23 - 110)

Table 3 - Median splenic volume at different times during initial- and re-treatment.

Measured at	Median (and range) volume in ml
<i>Initial treatment</i>	
- Baseline	219 (44 – 508)
- 3 months follow-up	173 (37 – 471)
- 12 months follow-up	152 (31 – 410)
<i>Retreatment</i>	
- ≤ 3 months follow-up	122 (20 – 386)

A persistent decrease in WBC (total and differential) occurred in all patients. However, only lymphocyte count was persistently decreased after re-treatment in comparison to 12 months counts, Wilcoxon signed rank test; $p < 0.00$, $r = -0.81$ (table 4). Other blood counts did not show a significant change. No correlation was found between absorbed spleen dose and decrease in WBC count ($p = 0.18$) or lymphocyte count ($p = 0.46$). Also spleen volume and lymphocyte count alterations were not significantly correlated at 12 months follow-up ($p = 0.58$) and at 3 months after re-treatment ($p = 0.33$).

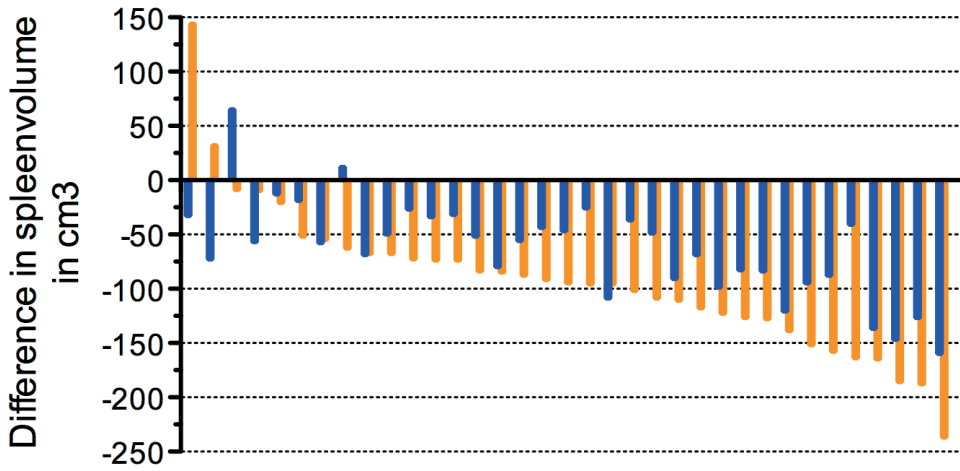


Figure 1 - Absolute change in splenic volume (in cm³) measured in 35 patients treated with ¹⁷⁷Lu-Octreotate. Baseline spleen volumes were compared to spleen volumes at 12 months follow-up after initial treatment (■ blue bars) and 6 weeks or 3 months follow-up after re-treatment with PRRT (■ orange bars).

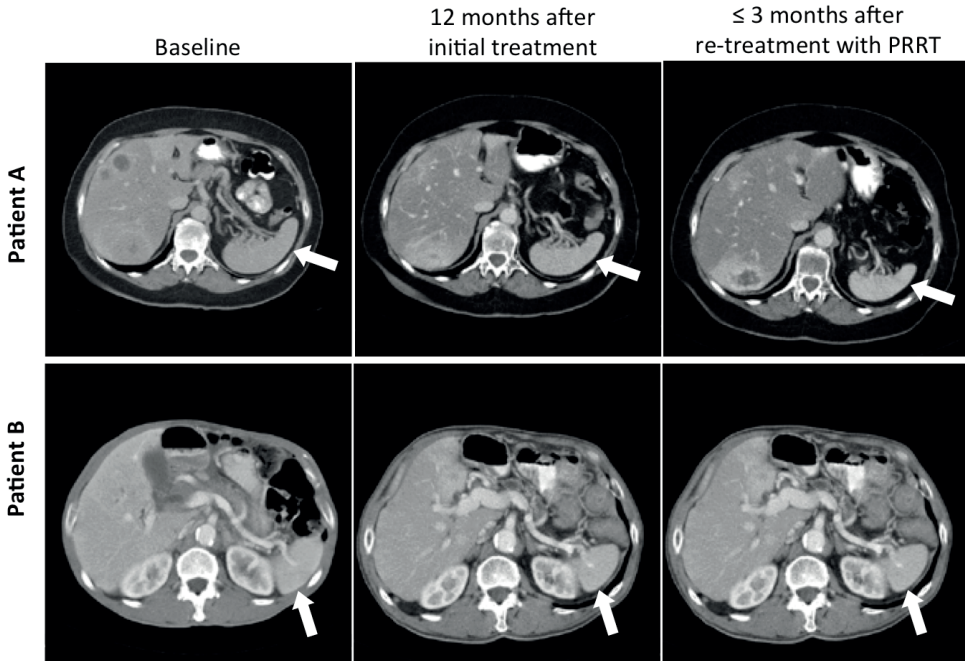


Figure 2 - Images of CT-scans in two patients (A & B) at baseline, 12 months after initial treatment and ≤ 3 months after re-treatment with ¹⁷⁷Lu-Octreotate. The spleen (white arrow) appears smaller on CT-scan after multiple cycles of PRRT.

Table 4 - Overview of absolute Blood Counts (and ranges) in 35 patients treated with ¹⁷⁷Lu-Octreotate. Comparison of 3, 12 months follow-up (FU) to baseline blood counts and 3 months after re-treatment to 12 months FU blood counts.

Measured at	Leucocytes	Basophils	Eosinophils	Neutrophils	Lymphocytes	Monocytes
<i>Initial treatment</i>						
Baseline	6.10 (5.20, 7.60)	0.04 (0.00, 0.07)	0.12 (0.08, 0.22)	4.12 (2.29, 5.25)	1.54 (1.13, 1.98)	0.49 (0.36, 0.63)
3 Months FU	3.50 (2.80, 4.30)	0.00 (0.00, 0.03)	0.09 (0.05, 0.17)	2.33 (1.76, 2.88)	0.66 (0.47, 0.85)	0.36 (0.28, 0.46)
12 Months FU	4.40 (3.60, 5.60)*	0.00 (0.00, 0.04)*	0.11 (0.04, 0.14)*	2.81 (2.29, 3.64)*	0.92 (0.70, 1.31)*	0.42 (0.30, 0.52)*
<i>Retreatment</i>						
3 Months FU	4.20 (3.10, 5.20)	0.00 (0.00, 0.04)	0.10 (0.06, 0.18)	2.74 (2.08, 3.55)	0.76 (0.47, 0.91)**	0.43 (0.34, 0.50)

Significant differences are indicated by an * and an ** respectively.

Evaluation of the medical files showed no diagnosis of patients with an infection caused by a pneumococcal, meningococcal and/or Haemophilus influenzae type b based bacteria (Table 5).

Table 5 - Reported infections in 35 patients during/after PRRT with ¹⁷⁷Lu-Octreotate.

	n=
Common Cold	9
Herpes Zoster	1
Influenza	7
Sinusitis	2
Urinary Tract Infection	4

DISCUSSION

The first objective of this study was to explore correlations between cumulative mean absorbed dose to the spleen and changes in spleen volume or peripheral blood counts after multiple cycles of PRRT. The second objective was an exploration of the clinical consequences regarding the change in splenic volume.

In the 1930s and 1940s, the radiocontrast agent Thorotrast, containing the radioactive compound thorium dioxide (ThO₂), was used in medical radiography. Thorium is retained in the body and emits harmful α-radiation and can induce alterations in splenic volume. The compound lost its clinical application due to a high lifetime risk of developing hemangioendothelioma and/or cholangiocarcinomas originating in the

liver (12,13). Our study demonstrates that multiple administrations with PRRT, based on β -emitting radionuclide ^{177}Lu -Lutetium-Octreotate, will result in significant spleen volume reduction. No significant dose-dependent relationship between the mean absorbed dose to the spleen and volume decline was found. Svensson et al. recently published a similar observation of spleen volume decline after treatment with ^{177}Lu -Octreotate (8). However, two patients in our study had a spleen volume increase after retreatment, although a decrease in volume was seen at the 12 months follow-up CT-scan after the initial cycles with PRRT. Both patients suffered from an increase in ascites at the start of retreatment; therefore it is likely that the increase in spleen volume was due to portal hypertension caused by progressive disease.

The decrease in spleen volume can be explained by fibrotic changes in the splenic tissue, a hypothesis that is in line with earlier studies (14,15). In one of the two studies, histological analyses of surgical pancreas NET specimens after neoadjuvant PRRT was performed, in the other study a hyalinization of tumor tissue was observed in patients who underwent external radiotherapy for Hodgkin's disease.

Currently, little is known about the clinical impact of changes in spleen volume after PRRT. Normally, the spleen has a role of eliminating pitted erythrocytes, damaged or aged blood cells and fulfills an important immunological role in the production of antibodies and filtering out blood borne pathogens (7). Several medical conditions can induce splenic atrophy and compromise the splenic function as an immunological barrier against encapsulated bacteria. Splenic atrophy puts patients at risk of developing an Overwhelming Post-Splenectomy Infection (OPSI) (16-18). OPSI is a serious disease that can present as sepsis, meningitis or pneumonia and has high mortality rates within the first 24 hours (19). Evidence suggests that hyposplenic state can be iatrogenically induced after external beam radiotherapy. Analysis of a historic cohort of patients who underwent postoperative chemoradiotherapy for gastric cancer demonstrated a radiation-induced reduction of spleen volume. Moreover, an incidence and mortality rate of pneumonia and sepsis was observed, comparable to that in patients with a hyposplenic and/or post-splenic state (20).

Our study demonstrates a persistent decrease in complete lymphocyte count after the administration of ^{177}Lu -Octreotate. However, we cannot determine the mechanism of action, whether the observed toxicity is an effect of targeted and prolonged irradiation of the spleen, a known reservoir of white blood cells, or of transient bone marrow irradiation. Radioactive iodine (RAI) does not specifically accumulate in the spleen, therefore irradiation of the bonemarrow and spleen may be different. Studies in

patients with differentiated thyroid cancer who underwent RAI with ^{131}I demonstrated a transient decrease of the total WBC and lymphocyte count after treatment up to 1 year. Lymphocyte subset analyses demonstrated a prolonged B-cell lymphopenia. However, none of the studies reported severe clinical consequences (21-24). These studies support the hypothesis that the decrease in blood cells is mainly caused by irradiation of the bone marrow and in a less extend caused by irradiation of the spleen. Interestingly, patients who underwent splenectomy were protected against hematological toxicity after ^{177}Lu -Octreotate (25).

In our patients, multiple cycles of PRRT with ^{177}Lu -Octreotate induce atrophy of the spleen and a persistent lower complete lymphocyte, compared to baseline measurements. An interesting question is whether patients are prone to develop a hyposplenic state after PRRT.

In the current standard of Centers for Disease Control and Prevention [CDC] 2016, the consensus is to immunize patients with 13-valent pneumococcal conjugate vaccine (PCV13), 23-valent pneumococcal polysaccharide vaccine (PPSV23), Haemophilus influenzae type b (Hib) vaccine and Meningococcal vaccine if patients are at risk of developing an OPSI. The highest incidence of OPSI after splenectomy is observed within 24 months (26). During follow-up of patients in our study with a median of 38 months, no hospitalization was required. Also no infection, based on capsulated bacteria, or OPSI was observed. Therefore it is unlikely that patients develop a hyposplenic state after PRRT with ^{177}Lu -Octreotate.

CONCLUSION

Administration of multiple cycles of PRRT with ^{177}Lu -Octreotate induces splenic volume loss and a decrease in lymphocyte count without clinical consequences. There is no increased risk for developing an infection based on encapsulated bacteria in patients receiving PRRT with ^{177}Lu -Octreotate.

REFERENCES

1. Kwekkeboom DJ, Bakker WH, Kooij PP, et al. [177Lu-DOTAOTyr3]octreotate: comparison with [111In-DTPA]octreotide in patients. *Eur J Nucl Med*. 2001;28:1319-1325.
2. Kwekkeboom D, Kooij P, Bakker W, Mäcke H, Krenning E. Comparison of 111In-DOTA-Tyr3-octreotide and 111In-DTPA-octreotide in the same patients: biodistribution, kinetics, organ and tumor uptake. *Journal of Nuclear Medicine*. Vol 40; 1999:762-767.
3. Bodei L, Cremonesi M, Grana CM, et al. Peptide receptor radionuclide therapy with (1)(7)(7)Lu-DOTATATE: the IEO phase I-II study. *Eur J Nucl Med Mol Imaging*. 2011;38:2125-2135.
4. Bergsma H, Konijnenberg MW, van der Zwan WA, et al. Nephrotoxicity after PRRT with Lu-DOTA-octreotate. *Eur J Nucl Med Mol Imaging*. 2016.
5. Sabet A, Ezziddin K, Pape UF, et al. Accurate assessment of long-term nephrotoxicity after peptide receptor radionuclide therapy with (177)Lu-octreotate. *Eur J Nucl Med Mol Imaging*. 2014;41:505-510.
6. Teunissen JJ, Krenning EP, de Jong FH, et al. Effects of therapy with [177Lu-DOTA 0,Tyr 3] octreotate on endocrine function. *Eur J Nucl Med Mol Imaging*. 2009;36:1758-1766.
7. Mebius RE, Kraal G. Structure and function of the spleen. *Nat Rev Immunol*. 2005;5:606-616.
8. Svensson J, Hagmarker L, Magnander T, Wangberg B, Bernhardt P. Radiation exposure of the spleen during (177)Lu-DOTATATE treatment and its correlation with haematological toxicity and spleen volume. *EJNMMI Phys*. 2016;3:15.
9. Kulkarni HR, Prasad V, Schuchardt C, Baum RP. Is there a correlation between peptide receptor radionuclide therapy-associated hematological toxicity and spleen dose? *Recent Results Cancer Res*. 2013;194:561-566.
10. Sgouros G. Dosimetry of internal emitters. *J Nucl Med*. 2005;46 Suppl 1:185-275.
11. Sandstrom M, Ilan E, Karlberg A, Johansson S, Freedman N, Garske-Roman U. Method dependence, observer variability and kidney volumes in radiation dosimetry of (177)Lu-DOTATATE therapy in patients with neuroendocrine tumours. *EJNMMI Phys*. 2015;2:24.
12. da Horta JS. Late effects of thorotrast on the liver and spleen, and their efferent lymph nodes. *Ann N Y Acad Sci*. 1967;145:676-699.
13. McLoughlin GP, Tothill P, Richmond J, Langlands AO. Splenic atrophy following thorotrast administration. *Br J Radiol*. 1971;44:404.
14. Dailey MO, Coleman CN, Kaplan HS. Radiation-induced splenic atrophy in patients with Hodgkin's disease and non-Hodgkin's lymphomas. *N Engl J Med*. 1980;302:215-217.
15. van Vliet EI, van Eijck CH, de Krijger RR, et al. Neoadjuvant Treatment of Nonfunctioning Pancreatic Neuroendocrine Tumors with [177Lu-DOTA0,Tyr3]Octreotate. *J Nucl Med*. 2015;56:1647-1653.
16. Pearson HA, Spencer RP, Cornelius EA. Functional asplenia in sickle-cell anemia. *N Engl J Med*. 1969;281:923-926.
17. Ferguson A, Hutton MM, Maxwell JD, Murray D. Adult coeliac disease in hyposplenic patients. *Lancet*. 1970;1:163-164.
18. Cuthbert RJ, Iqbal A, Gates A, Toghill PJ, Russell NH. Functional hyposplenism following allogeneic bone marrow transplantation. *J Clin Pathol*. 1995;48:257-259.
19. Hansen K, Singer DB. Asplenic-hyposplenic overwhelming sepsis: postsplenectomy sepsis revisited. *Pediatr Dev Pathol*. 2001;4:105-121.

- 20.** Trip AK, Sikorska K, van Sandick JW, et al. Radiation-induced dose-dependent changes of the spleen following postoperative chemoradiotherapy for gastric cancer. *Radiother Oncol.* 2015;116:239-244.
- 21.** Tofani A, Sciuto R, Cioffi RP, et al. Radioiodine-induced changes in lymphocyte subsets in patients with differentiated thyroid carcinoma. *Eur J Nucl Med.* 1999;26:824-829.
- 22.** Molinaro E, Leboeuf R, Shue B, et al. Mild decreases in white blood cell and platelet counts are present one year after radioactive iodine remnant ablation. *Thyroid.* 2009;19:1035-1041.
- 23.** Prinsen HT, Klein Hesselink EN, Brouwers AH, et al. Bone Marrow Function After (131)I Therapy in Patients With Differentiated Thyroid Carcinoma. *J Clin Endocrinol Metab.* 2015;100:3911-3917.
- 24.** Hu T, Meng Z, Zhang G, et al. Influence of the first radioactive iodine ablation on peripheral complete blood count in patients with differentiated thyroid cancer. *Medicine (Baltimore).* 2016;95:e4451.
- 25.** Sabet A, Ezziddin K, Pape UF, et al. Long-term hematotoxicity after peptide receptor radionuclide therapy with 177Lu-octreotate. *J Nucl Med.* 2013;54:1857-1861.
- 26.** Holdsworth RJ, Irving AD, Cuschieri A. Postsplenectomy sepsis and its mortality rate: actual versus perceived risks. *Br J Surg.* 1991;78:1031-1038.



3

NUCLEAR IMAGING OF PROSTATE & BREAST CANCER

3.1

INTRODUCTION

INTRODUCTION

Prostate cancer (PCa) is the most common cancer in American men and in European males (particularly beyond 70 years of age) (1). About one American man in seven and one European in eight will be diagnosed with PCa during his lifetime. Diagnosis of primary PCa is mainly based on transrectal ultrasound (TRUS) guided biopsies, which has a limited sensitivity after one procedure. Therefore multiple biopsies are required for a reliable outcome. Also, the role of CT, (f)MRI and PET/CT in the diagnosis and staging of PC is not well established because of variations in sensitivity/specificity in different patient groups (2,3).

In women, breast cancer (BC) is the most frequent type of cancer with 1.67 million new cases in the year 2012 (4). In 2015, the number of new cases of BC in men and women were 105 and 17,060, respectively, in the Netherlands (5). Mammography is the most widely used technique of imaging BC, but has several limitations leading to a significant amount of false positive and false negative findings (6). False positive results lead to unnecessary additional tests and anxiety in the patient (7,8), whereas false negative results may cause a delay in diagnosis and treatment (7). When a suspicious lesion is detected by mammography, occasionally additional imaging with ultrasound or MRI is required in a select group of patients (9). Ultrasound and MRI enhance the overall sensitivity, but the specificity is not increased (9).

Targeted nuclear imaging can offer an interesting opportunity to improve the diagnostic imaging yield in prostate- and breast cancer, which could lead to better patient management. The upcoming paragraphs will briefly summarize targeted nuclear imaging in prostate and breast cancer, whereas **Chapter 3.2** will report a novel PET radiotracer [^{68}Ga]SB3 in patients with prostate and breast cancer.

Targeted nuclear imaging and therapy

Targeted nuclear imaging and treatment is based on targeting receptors/proteins, which are overexpressed on cancer cells using radioligands. These radioligands consist of a peptide (which links to the receptor), linker/chelators (for stabilization) and the radionuclide (used for imaging and/or therapy) Figure 1. Several radioligands for imaging (e.g. ^{111}In -pentreotide also known as Octreoscan) and therapy (e.g. ^{177}Lu -DOTATATE) have been successfully developed for targeting the somatostatin receptor (sst). In the clinic, these two radioligands improved imaging and formed new therapeutic options for patients with neuroendocrine tumors (chapter 1.1 & 1.2).

In the past decades, new targets have been identified for prostate and breast cancer (Table 1). Receptor positive tumor can be visualized (and the tumor can possibly be treated) with novel radioligands, following the success of sst in neuroendocrine tumors.

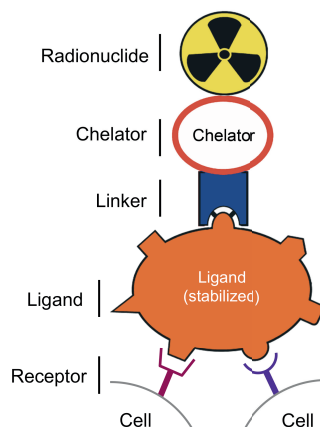


Figure 1 - Structure of somatostatin analogue with binding to the receptor and cell; radionuclide, chelator, linker, ligand and receptor (on the cell membrane).

Table 1 - An overview of malignancies and the target options on the cell membrane. Somatostatin receptor (sst), Prostate Specific Membrane Antigen (PSMA) and gastrin releasing peptide receptor (GRPR).

Malignancy originating from:	Targets options
Neuroendocrine cell	sst
Prostate	PSMA, GRPR
Breast	sst, GRPR
Lung	sst, GRPR

PSMA

Prostate-specific membrane antigen (PSMA) is significantly overexpressed in PCa cells, therefore it is an attractive target in the clinical and diagnostic field. PSMA (also known as folate hydrolase I or glutamate carboxypeptidase II), is a transmembrane 750-amino-acid type II glycoprotein that is primarily expressed in normal human prostate epithelium but is overexpressed in prostate cancer (10), including metastatic disease (11,12). Since almost all prostate cancers express PSMA, it is an attractive target for prostate cancer imaging and therapy. Also, PSMA expression is further increased in poorly differentiated, metastatic, and hormone-refractory carcinomas (13,14). Recently, PSMA ligands with ^{68}Ga , $^{99\text{m}}\text{Tc}$ and radioiodine have been developed, enabling their use for PET or SPECT imaging and therapy. In the past, an ^{111}In -capromab pendetide (ProstaScint) labelled ligand of the intracellular epitope of PSMA was used for imaging of PSMA expression (15). However, ^{111}In -capromab pendetide only binds to the intracellular domain of PSMA which is only accessible in dying, apoptotic or dead tumor cells. ProstaScint has also a low sensitivity because of poor resolution of scintigraphic gamma cameras.

New PSMA-based PET imaging agents have been developed like Glu-NH-CO-NH-Lys-(Ahx)- ^{68}Ga [HBED-CC] (^{68}Ga -PSMA). In more than 1000 patients ^{68}Ga -PSMA have been given for different clinical indications, such as initial assessment and recurrence of disease. ^{68}Ga -PSMA is able to detect a significant uptake in more than 60% of recurrent PCa patients with a PSA level < 1 ng/ml and has a detection rate of $>80\%$ in those with a PSA higher than 2ng/ml (16). However, Afshar-Oromieh *et al* (17) presented some critical notes regarding ^{68}Ga -PSMA: there is no relationship between an increase in PSA level and an increase in tumor detection. Also no correlation was found between Gleason score and uptake on ^{68}Ga -PSMA. However patients with an androgen deprivation therapy at the time of ^{68}Ga -PSMA-ligand PET/CT more frequently showed a positive PET scan compared to patients without such treatment, making ^{68}Ga -PSMA imaging a good candidate for assessment of recurrent disease.

GRPR

The gastrin-releasing peptide receptor (GRPR) is a G protein-coupled receptor with 7 transmembrane spanning domains and is part of the mammalian bombesin receptor family. GRPR's ligand, gastrin releasing peptide (GRP), cascades various biological and pharmacological responses, like smooth muscle contraction in the gastrointestinal tract and urogenital system (18). Expression of the GRPR has been reported in various types of cancer, like prostate, breast and lung cancer (18).

High GRPR expression (85–100 %) has been documented in primary and well-differentiated PC, the expression drops (to 50%) in androgen-refractory bone metastases (19-23). GRPR is also expressed in primary BC (62-74%), whereas all metastases originating from GRPR-positive primaries retain high levels of receptor expression (24-26).

Originally, radiolabeled analogs for targeting of GRPR-positive tumor sites were derived from the bombina bombina frog, containing an active tetradecapeptide, bombesin (27,28). At that time, internalization was considered essential for prolonged lesion retention, which would eventually translate into greater diagnostic sensitivity and therapeutic efficacy. However, this principle has been challenged by accumulating evidence on the superior performance of radiolabeled GRPR antagonists versus their agonist-based counterparts (29,30). For example, the radioantagonist [$^{99\text{m}}\text{Tc}$]DB1 has displayed higher uptake and retention in GRPR-expressing tumors in combination with a much faster background clearance (including the GRPR-rich pancreas) than the radioagonist [$^{99\text{m}}\text{Tc}$]DB4 (29). Another advantage of radioantagonists is their greater inherent biosafety. GRPR agonists (like ^{177}Lu -AMBA) elicit pharmacological effects after receptor binding and are less tolerated by patients (31), whereas GRPR antagonist do not elicit side effects.

In the chapter 3.2, we introduce the [^{99m}Tc]DB1 mimic [^{68}Ga]SB3, whereby the ^{99m}Tc -binding acyclic tetraamine unit has been replaced by the chelator DOTA to allow labeling with the PET radiometal ^{68}Ga . The new PET tracer has been characterized in GRPR-positive cells and animal models using the [^{67}Ga]SB3 surrogate. Furthermore, a first-in-man clinical evaluation of [^{68}Ga]SB3 has been performed in patients with recurrent PC or BC.

REFERENCES

1. Siegel R, Naishadham D, Jemal A. Cancer statistics, 2012. *CA Cancer J Clin.* 2012;62:10-29.
2. Pinto F, Totaro A, Palermo G, et al. Imaging in prostate cancer staging: present role and future perspectives. *Urol Int.* 2012;88:125-136.
3. Hricak H, Choyke PL, Eberhardt SC, Leibel SA, Scardino PT. Imaging prostate cancer: a multidisciplinary perspective. *Radiology.* 2007;243:28-53.
4. Ferlay J, Soerjomataram I, Dikshit R, et al. Cancer incidence and mortality worldwide: sources, methods and major patterns in GLOBOCAN 2012. *Int J Cancer.* 2015;136:E359-386.
5. The Netherlands Cancer Registry - Incidence | Breast cancer - Invasive / Non-invasive / in situ | 2015. Last update 02-02-2017; <http://www.cijfersoverkanker.nl>. Accessed 22 march, 2017.
6. Nelson HD, O'Meara ES, Kerlikowske K, Balch S, Miglioretti D. Factors Associated With Rates of False-Positive and False-Negative Results From Digital Mammography Screening: An Analysis of Registry Data. *Ann Intern Med.* 2016;164:226-235.
7. Brodersen J, Jorgensen KJ, Gotzsche PC. The benefits and harms of screening for cancer with a focus on breast screening. *Pol Arch Med Wewn.* 2010;120:89-94.
8. Lampic C, Thurfjell E, Bergh J, Sjoden PO. Short- and long-term anxiety and depression in women recalled after breast cancer screening. *Eur J Cancer.* 2001;37:463-469.
9. Garcia EM, Storm ES, Atkinson L, Kenny E, Mitchell LS. Current breast imaging modalities, advances, and impact on breast care. *Obstet Gynecol Clin North Am.* 2013;40:429-457.
10. Ghosh A, Heston WD. Tumor target prostate specific membrane antigen (PSMA) and its regulation in prostate cancer. *J Cell Biochem.* 2004;91:528-539.
11. Israeli RS, Powell CT, Fair WR, Heston WD. Molecular cloning of a complementary DNA encoding a prostate-specific membrane antigen. *Cancer Res.* 1993;53:227-230.
12. Horoszewicz JS, Kawinski E, Murphy GP. Monoclonal antibodies to a new antigenic marker in epithelial prostatic cells and serum of prostatic cancer patients. *Anticancer Res.* 1987;7:927-935.
13. Perner S, Hofer MD, Kim R, et al. Prostate-specific membrane antigen expression as a predictor of prostate cancer progression. *Hum Pathol.* 2007;38:696-701.
14. Silver DA, Pellicer I, Fair WR, Heston WD, Cordon-Cardo C. Prostate-specific membrane antigen expression in normal and malignant human tissues. *Clin Cancer Res.* 1997;3:81-85.
15. Kahn D, Austin JC, Maguire RT, Miller SJ, Gerstbrein J, Williams RD. A phase II study of [90Y] yttrium-capromab pentetide in the treatment of men with prostate cancer recurrence following radical prostatectomy. *Cancer Biother Radiopharm.* 1999;14:99-111.
16. Evangelista L, Briganti A, Fanti S, et al. New Clinical Indications for (18)F/(11)C-choline, New Tracers for Positron Emission Tomography and a Promising Hybrid Device for Prostate Cancer Staging: A Systematic Review of the Literature. *Eur Urol.* 2016;70:161-175.
17. Afshar-Oromieh A, Avtzi E, Giesel FL, et al. The diagnostic value of PET/CT imaging with the (68)Ga-labelled PSMA ligand HBED-CC in the diagnosis of recurrent prostate cancer. *Eur J Nucl Med Mol Imaging.* 2015;42:197-209.
18. Jensen RT, Batten JF, Spindel ER, Benya RV. International Union of Pharmacology. LXVIII. Mammalian bombesin receptors: nomenclature, distribution, pharmacology, signaling, and functions in normal and disease states. *Pharmacol Rev.* 2008;60:1-42.

19. Markwalder R, Reubi JC. Gastrin-releasing peptide receptors in the human prostate: relation to neoplastic transformation. *Cancer Res.* 1999;59:1152-1159.
20. Korner M, Waser B, Rehmann R, Reubi JC. Early over-expression of GRP receptors in prostatic carcinogenesis. *Prostate.* 2014;74:217-224.
21. Beer M, Montani M, Gerhardt J, et al. Profiling gastrin-releasing peptide receptor in prostate tissues: clinical implications and molecular correlates. *Prostate.* 2012;72:318-325.
22. Schroeder RP, de Visser M, van Weerden WM, et al. Androgen-regulated gastrin-releasing peptide receptor expression in androgen-dependent human prostate tumor xenografts. *Int J Cancer.* 2010;126:2826-2834.
23. Mather SJ, Nock BA, Maina T, et al. GRP receptor imaging of prostate cancer using [(99m)Tc] Demobesin 4: a first-in-man study. *Mol Imaging Biol.* 2014;16:888-895.
24. Reubi JC, Wenger S, Schmuckli-Maurer J, Schaer JC, Gugger M. Bombesin receptor subtypes in human cancers: detection with the universal radioligand (125)I-[D-TYR(6), beta-ALA(11), PHE(13), NLE(14)] bombesin(6-14). *Clin Cancer Res.* 2002;8:1139-1146.
25. Reubi C, Gugger M, Waser B. Co-expressed peptide receptors in breast cancer as a molecular basis for in vivo multireceptor tumour targeting. *Eur J Nucl Med Mol Imaging.* 2002;29:855-862.
26. Gugger M, Reubi JC. Gastrin-releasing peptide receptors in non-neoplastic and neoplastic human breast. *Am J Pathol.* 1999;155:2067-2076.
27. Maina T, Nock B, Mather S. Targeting prostate cancer with radiolabelled bombesins. *Cancer Imaging.* 2006;6:153-157.
28. Yu Z, Ananias HJ, Carlucci G, et al. An update of radiolabeled bombesin analogs for gastrin-releasing peptide receptor targeting. *Curr Pharm Des.* 2013;19:3329-3341.
29. Cascato R, Maina T, Nock B, et al. Bombesin receptor antagonists may be preferable to agonists for tumor targeting. *J Nucl Med.* 2008;49:318-326.
30. Mansi R, Wang X, Forrer F, et al. Evaluation of a 1,4,7,10-tetraazacyclododecane-1,4,7,10-tetraacetic acid-conjugated bombesin-based radioantagonist for the labeling with single-photon emission computed tomography, positron emission tomography, and therapeutic radionuclides. *Clin Cancer Res.* 2009;15:5240-5249.
31. Bodei L, Ferrari M, Nunn A, et al. Lu-177-AMBA Bombesin analogue in hormone refractory prostate cancer patients: A phase I escalation study with single-cycle administrations. *European Journal of Nuclear Medicine and Molecular Imaging.* 2007;34:S221-S221.

3.2

PRECLINICAL AND FIRST CLINICAL EXPERIENCE WITH THE GASTRIN-RELEASING PEPTIDE RECEPTOR- ANTAGONIST [⁶⁸GA]SB3 AND PET/CT

Hendrik Bergsma¹ & Theodosia Maina², Harshad R. Kulkarni³, Dirk Mueller³, David Charalambidis², Eric P. Krenning¹, Berthold A. Nock², Marion de Jong¹, Richard P. Baum³

¹ Department of Radiology & Nuclear Medicine, Erasmus MC, University Medical Center, Rotterdam, The Netherlands

² Molecular Radiopharmacy, INRASTES, NCSR BDemokritos Athens, Greece

³ Molecular Radiotherapy and Molecular Imaging, Zentralklinik, Bad Berka, Germany

ABSTRACT

Gastrin-releasing peptide receptors (GRPR) represent attractive targets for tumor diagnosis and therapy because of their overexpression in major human cancers. Internalizing GRPR agonists were initially proposed for prolonged lesion retention, but a shift of paradigm to GRPR antagonists has recently been made. Surprisingly, radioantagonists, such as [^{99m}Tc]DB1 (^{99m}Tc -N₄'-DPhe⁶,Leu-NHET¹³]BBN(6–13)), displayed better pharmacokinetics than radioagonists, in addition to their higher inherent biosafety. We introduce here [^{68}Ga]SB3, a [^{99m}Tc]DB1 mimic-carrying, instead of the ^{99m}Tc -binding tetraamine, the chelator DOTA for labeling with the PET radiometal ^{68}Ga .

Methods:

Competition binding assays of SB3 and [$^{\text{nat}}\text{Ga}$]SB3 were conducted against [^{125}I -Tyr⁴]BBN in PC-3 cell membranes. Blood samples collected 5 min postinjection (pi) of the [^{67}Ga]SB3 surrogate in mice were analyzed using high-performance liquid chromatography (HPLC) for degradation products. Likewise, biodistribution was performed after injection of [^{67}Ga]SB3 (37 kBq, 100 μL , 10 pmol peptide) in severe combined immunodeficiency (SCID) mice bearing PC-3 xenografts. Eventually, [^{68}Ga]SB3 (283 ± 91 MBq, 23 ± 7 nmol) was injected into 17 patients with breast (8) and prostate (9) cancer. All patients had disseminated disease and had received previous therapies. PET/CT fusion images were acquired 60–115 min pi.

Results:

SB3 and [$^{\text{nat}}\text{Ga}$]SB3 bound to the human GRPR with high affinity (IC_{50} : 4.6 ± 0.5 nM and 1.5 ± 0.3 nM, respectively). [^{67}Ga]SB3 displayed good in vivo stability (>85 % intact at 5 min pi). [^{67}Ga]SB3 showed high, GRPR-specific and prolonged retention in PC-3 xenografts ($33.1 \pm 3.9\%$ ID/g at 1 h pi – $27.0 \pm 0.9\%$ ID/g at 24 h pi), but much faster clearance from the GRPR-rich pancreas ($\approx 160\%$ ID/g at 1 h pi to $<17\%$ ID/g at 24 h pi) in mice. In patients, [^{68}Ga]SB3 elicited no adverse effects and clearly visualized cancer lesions. Thus, 4 out of 8 (50 %) breast cancer and 5 out of 9 (55 %) prostate cancer patients showed pathological uptake on PET/CT with [^{68}Ga]SB3.

Conclusion:

[^{67}Ga]SB3 showed excellent pharmacokinetics in PC-3 tumor-bearing mice, while [^{68}Ga]SB3 PET/CT visualized lesions in about 50 % of patients with advanced and metastasized prostate and breast cancer. We expect imaging with [^{68}Ga]SB3 to be superior in patients with primary breast or prostate cancer.

Keywords:

PET/CT tumor imaging, ^{68}Ga radiotracer, Gastrin-releasing peptide receptor antagonist, Prostate cancer, Breast cancer

INTRODUCTION

Prostate (PC) and breast cancer (BC) rank first in incidence among men and women diagnosed with cancer in Western countries and are linked to considerable morbidity and mortality in the metastatic stages of the disease [1, 2]. Accordingly, the non-invasive and reliable diagnosis and staging of these cancers remain compelling medical requirements. This is reflected in the high number of inconclusive biopsies, which are associated with much patient discomfort and anxiety, and with an increase in healthcare costs [3, 4]. On the other hand, conventional imaging techniques, such as MRI, CT, ultrasound, or even established nuclear medicine procedures (e.g., ¹⁸FDG/PET) remain of limited diagnostic value because of their low specificity [5–8].

In this respect, receptor-targeted tumor imaging may represent an attractive alternative for diagnosing primary and/or disseminated disease with high specificity and sensitivity. This approach holds great promise in cases of PC and BC, owing to the high density expression of the gastrin-releasing peptide receptor (GRPR) target in pathological lesions. In particular, high GRPR expression has been documented in primary and well-differentiated PC (85–100 %), which, however, drops (50 %) in androgen-refractory bone metastases [9–13]. GRPR is also expressed in primary BC (>60 %), whereas all metastases originating from GRPR-positive primaries retain high levels of receptor expression [14–16]. Originally, radiolabeled analogs of the frog tetradecapeptide bombesin (BBN) have been developed for the *in vivo* targeting of GRPR-positive tumor sites, mainly owing to their ability to internalize rapidly and massively into cancer cells [17, 18]. At that time, internalization was considered essential for prolonged lesion retention, which would eventually translate into greater diagnostic sensitivity and therapeutic efficacy. However, this rationale has been challenged by accumulating evidence on the unexpectedly superior performance of radiolabeled GRPR antagonists in visualizing GRPR-positive tumors *in vivo* versus their agonist-based counterparts [19, 20]. Thus, the radioantagonist [^{99m}Tc]DB1 has displayed higher uptake and retention in GRPR-expressing tumors in combination with a much faster background clearance (including the GRPR-rich pancreas) than the radioagonist [^{99m}Tc]DB4 [19]. A further significant advantage of radioantagonists is their greater inherent biosafety. In contrast to agonists, GRPR antagonists do not elicit pharmacological effects after receptor binding and are consequently better tolerated after intravenous (iv) injection to patients [21].

In the current work, we introduce the [^{99m}Tc]DB1 mimic [⁶⁸Ga]SB3 (Figure 1), whereby the ^{99m}Tc-binding acyclic tetraamine unit has been replaced by the chelator DOTA to allow labeling with the PET radiometal ⁶⁸Ga. The new PET tracer has been characterized in GRPR-positive cells and animal models using the [⁶⁷Ga]SB3 surrogate. Furthermore, a first-in-man clinical evaluation of [⁶⁸Ga]SB3 has been performed in a small number of patients with recurrent PC or BC employing PET/CT.

values were calculated using nonlinear regression for a one-site model and represent mean \pm SD values from three independent experiments performed in triplicate.

The cell association of [⁶⁷Ga]SB3 in PC-3 cells was tested during a 1-h incubation period at 37 °C. Briefly, confluent PC-3 cells were seeded in six-well plates ($\sim 1.0 \times 10^6$ cells per well) 24 h before the experiment. Approximately 300,000 cpm of [⁶⁷Ga]SB3 (corresponding to 2 pmol total peptide in 150 μ L of 0.5 % BSA/PBS supplemented with Haemacel[®]) was added alone (total) or in the presence of 1 μ M [Tyr⁴]BBN (non-specific) and the experiment was performed as before [24]. Results were calculated as percentage internalized plus membrane bound activity versus total added activity per million cells.

Stability and biodistribution of [⁶⁷Ga]SB3 in mice

Blood collected 5 min pi of [⁶⁷Ga]SB3 in healthy mice was analyzed using high-performance liquid chromatography (HPLC) (Supplementary material).

For biodistribution studies, a ≈ 150 - μ L bolus containing a suspension of $\approx 1.5 \times 10^7$ freshly harvested human PC-3 cells in saline was subcutaneously injected into the flanks of female severe combined immunodeficiency (SCID) mice (15 ± 3 g, 6 weeks of age on the day of arrival; NCSR "Demokritos" Animal House Facility). The animals were kept under aseptic conditions and 2–3 weeks later developed well-palpable tumors at the inoculation sites (80–150 mg). A 100- μ L bolus (37 kBq, 10 pmol total peptide; in saline/EtOH 9/1 v/v) of [⁶⁷Ga]SB3 was injected into the tail vein and biodistribution was conducted for the 1-, 4-, and 24-h pi time intervals; for in vivo GRPR-blockade a separate 4-h animal group received excess [Tyr⁴]BBN (40 nmol [Tyr⁴]BBN in 50- μ L vehicle coinjected with the radioligand). Biodistribution data were calculated as percentage injected dose per gram of tissue (%ID/g) with the aid of suitable standards for the injected dose [24].

Statistical analysis using the unpaired two-tailed Student's t test was performed to compare values between the control and the in vivo GRPR-blockade animal groups at 4 h pi; values of $P < 0.05$ were considered statistically significant.

All animal experiments were carried out in compliance with European and national regulations and after approval of protocols by national authorities.

Patient selection and administration of [⁶⁸Ga]SB3

Seventeen patients (9 men and 8 women; age range, 40–74 years) with advanced PC or BC were iv injected with [⁶⁸Ga]SB3 (Supplemental table 1). The iv injection of [⁶⁸Ga]SB3 (mean administered activity of 283 ± 91 MBq associated with a peptide mass of 23 ± 0.7 nmol) was followed by the iv administration of furosemide (20 mg). Initial diagnosis

using the classification of malignant tumors (TMN) was made using histopathology and tomography. All patients had had confirmed metastases to distant organs at last imaging and had demonstrated evident progression of tumor disease, e.g., a rise in tumor markers (PSA, CEA, Ca15-3 or CA-125) and/or progression on recent imaging (CT, MRI, and/or PET). Hematological (Hb, WBC, and platelets), liver (ALAT, AP, and γ -GT), and renal functions (s-creatinine and eGFR) were measured before [^{68}Ga]SB3 injection. Heart rate, blood pressure, and oxygenation were monitored throughout administration. Patients were asked to report side effects (dizziness, vomiting, abdominal discomfort) during injection and imaging. At the follow-up visits they were asked to report side effects. In three patients (numbers 4, 7, and 17) with recurrent PC an [^{18}F]fluoromethylcholine PET/CT scan was conducted. Written informed consent was obtained from all patients in accordance with German regulations for the administration of radiolabeled substances to humans. Data recording in a database was approved by all patients and by the local ethics committee.

Imaging protocol

All patients were scanned on a dual-modality PET/CT tomography scanner (Biograph duo; Siemens Medical Solutions). The CT component consists of a two-row spiral CT system and the PET component is based on a full-ring lutetium orthosilicate (LSO) PET system. Acquisition started 60–115 min pi. PC patients were requested to empty their bladder immediately before the PET/CT examination. They were positioned head first supine on the common patient handling system with the arms raised.

First, a topogram was acquired over 1,024 mm axially. Coaxial whole-body imaging ranges were defined on the topogram, covering an area from the skull to the upper thighs. CT was performed in spiral mode using a continuous acquisition at 130 kVp, 115 mAs, 4-mm collimation, 5-mm slice width, a table feed of 8 mm per rotation at 0.8-s rotation time, and 2.4-mm slice spacing. During the CT acquisition patients were asked to hold their breath in normal expiration. Three-dimensional PET emission scanning started in the caudocranial direction. An emission scan time of 2–3 min per bed position was used for all patients, with a total emission scan time of 24 min.

Data acquisition and interpretation

[^{68}Ga]SB3 scans were acquired from July 2009 until March 2010. After scatter and attenuation correction, PET emission data were reconstructed using an attenuation-weighted ordered subsets maximization expectation (OSEM) approach with two iterations, 8 subsets on 128×128 matrices and a 5-mm Gaussian postreconstruction filtering.

The CT images were evaluated on a Syngo viewing station by a skilled radiologist. Two experienced nuclear medicine physicians assessed the PET/CT images using E.soft (Syngo-based nuclear medicine software from Siemens Medical Solutions). Scintigraphic findings were compared with previous diagnostic examinations. [⁶⁸Ga]SB3 scans were defined as positive when focal, not physiological, accumulation of the radiotracer was found.

The maximum intensity projection (MIP) images were visually inspected and each single transversal slice was viewed from head to mid-thigh in combination with the CT image. Slice number and anatomical localization were recorded when focal and abnormal tracer uptake was found. PET/CT fusion images were used for measurements of SUV_{max} in different organs/structures. Manually selected regions of interest (ROIs) were drawn on a single slice using the software provided by E.soft. SUV_{max} was calculated for the following organs: pancreas, kidney parenchyma, esophagogastric junction (EGJ), blood activity (blood pool), liver, lung, kidneys, and gluteus muscle.

RESULTS

In vitro studies

Both SB3 and [^{nat}Ga]SB3 were able to displace [¹²⁵I-Tyr⁴]BBN from GRPR sites on PC-3 membranes in a monophasic and dose-dependent manner (Figure 2). Incorporation of Ga³⁺ favored receptor binding, as evident from the pertinent IC₅₀ values of 4.6 ± 0.4 nM (SB3) and 1.5 ± 0.3 nM ([^{nat}Ga]SB3). During 1-h incubation of [⁶⁷Ga]SB3 with PC-3 cells at 37 °C, 22.2 ± 1.2 % of added radioactivity remained on the cell membrane, with only 5.5 ± 0.4 % detected within the cells, as consistent with an antagonist profile [19, 24]. In the presence of excess [Tyr⁴]BBN, these values dropped to 1.5 ± 0.1 % and 0.4 ± 0.1 % respectively, suggesting GRPR specificity.

Stability and biodistribution of [⁶⁷Ga]SB3 in mice

After entering the bloodstream of mice [⁶⁷Ga]SB3 remained >85 % stable, as revealed by HPLC analysis of blood samples collected 5 min pi (Figure S3). This stability was found to be superior to previously reported values of GRPR-targeting radioligands [24–26].

The biodistribution of [⁶⁷Ga]SB3 in SCID mice bearing human PC-3 xenografts is shown in Figure 3 for the 1-h, 4-h, and 24-h pi time points, with a separate 4-h animal group representing in vivo GRPR-blockade. The tracer rapidly cleared from blood, showing no retention in the kidneys. Likewise, background radioactivity declined with time, including GRPR-rich tissues, such as the mouse pancreas. In particular, the initially high pancreatic uptake of [⁶⁷Ga]SB3 at 1 h pi (≈160% ID/g) gradually dropped at the later time points (≥100% ID/g at 4 h and ≈ 17% ID/g at 24 h pi), as consistent with a

GRPR radioantagonist profile. Conversely, the uptake of $[^{67}\text{Ga}]\text{SB3}$ in the GRPR-positive xenografts remained remarkably high over time ($33.1 \pm 3.9\% \text{ID/g}$ at 1 h pi, $34 \pm 6.9\% \text{ID/g}$ at 4 h pi, and $27.1 \pm 0.9\% \text{ID/g}$ at 24 h pi). Uptake in tumor and mouse pancreas was significantly reduced in the animals treated with excess $[\text{Tyr}^4]\text{BBN}$, confirming GRPR specificity.

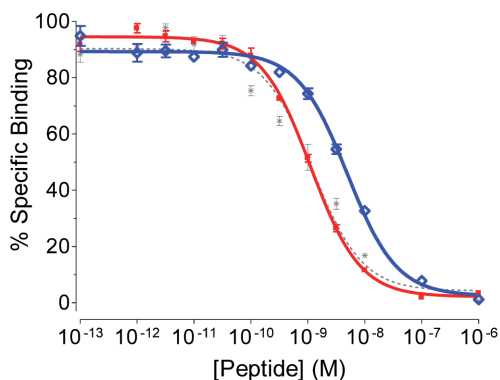


Figure 2 - Displacement of $[\text{Tyr}^4]\text{BBN}$ from gastrin-releasing peptide receptor (GRPR) sites in PC-3 cell membranes by increasing concentrations of: \diamond SB3 ($\text{IC}_{50} = 4.6 \pm 0.4 \text{ nM}$); \blacksquare $[\text{natGa}]\text{SB3}$ ($\text{IC}_{50} = 1.5 \pm 0.3 \text{ nM}$); reference: $*$ $[\text{Tyr}^4]\text{BBN}$ ($\text{IC}_{50} = 1.7 \pm 0.3 \text{ nM}$). Results represent the average IC_{50} values \pm SD of three independent experiments performed in triplicate.

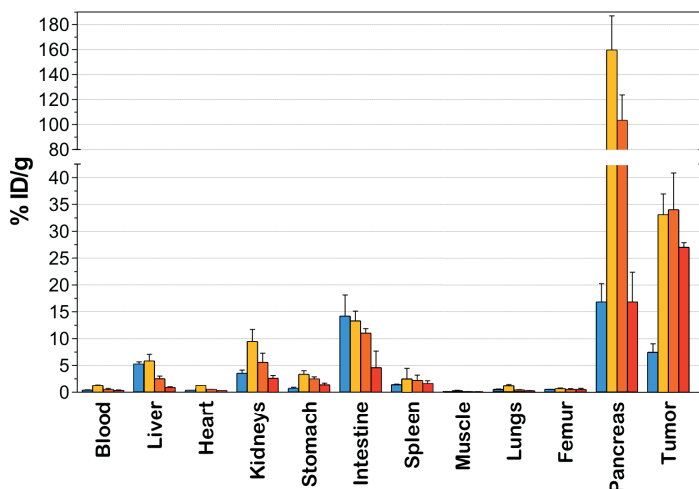


Figure 3 – Biodistribution of $[^{67}\text{Ga}]\text{SB3}$ in severe combined immunodeficiency (SCID) mice bearing human GRPR-positive 140 PC-3 xenografts. Data are expressed as $\% \text{ID/g}$ and represent mean \pm SD, $n=4$, for \blacksquare 1 h, \blacksquare 4 h and \blacksquare 24 h pi; a separate \blacksquare 4-h animal group represents in 40 vivo GRPR-blockade.

Safety, tolerability, and physiological distribution of [⁶⁸Ga]SB3 in patients

No local or systemic adverse effects were found. During injection, one patient had high blood pressure (RR 180/130), most likely due to anxiety. In this patient, diastolic and systolic pressure returned to normal levels within 1 h. The highest physiological uptake of [⁶⁸Ga]SB3 was found in the pancreas head (mean SUV 47.7). Mean SUV_{max} in the kidneys and at the EGJ was 5.4 and 3.3 respectively. High activity at the EGJ was previously described in preliminary clinical data with the GRPR agonist [⁶⁸Ga]AMBA [27]. An overview of the biodistribution is found in Figure 4 (Supplemental table 2).

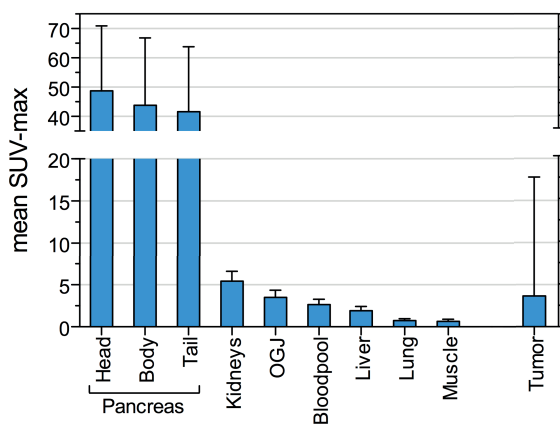


Figure 4 - SUV_{max} ± SD in regions of interest (ROI) of [⁶⁸Ga]SB3 scans, including values for normal organs (n=17 patients) and for [⁶⁸Ga]SB3-positive lesions in 9 patients.

PET/CT results

A total of 71 lesions in 9 patients with positive [⁶⁸Ga]SB3 scans were recorded (Supplemental table 2). Mean SUV_{max} of these lesions in 9 patients was 4.2 (range 0.7–17.8). Thirty-eight lesions in group 1 (BC) were positive, with a median SUV_{max} of 2.0 (range 0.6–7.8). Thirty-three positive lesions in group 2 (PC) were positive, with a median SUV_{max} of 4.4 (range 1.7–17.8; Figure 4; Supplemental tables 1-3).

The characteristics of 8 BC and 9 PC patients injected with [⁶⁸Ga]SB3 are presented in Tables 1 and 2 respectively. Four BC patients (50 %) and 5 of the 9 PC patients (55 %) had positive lesions visualized by [⁶⁸Ga]SB3. Abnormal focal uptake on the [⁶⁸Ga]SB3 scan was seen in 2 patients. The first patient showed uptake on the left side in the supraspinatus muscle (SUV_{max} 2.2) and proximal adductor muscles (SUV_{max} 2.4), which was attributed to local shoulder inflammation. The second patient showed local uptake in the prostate (SUV_{max} 4.7), which was negative on other imaging modalities and

attributed to calcifications in this tissue. One patient showed exceptionally high uptake on the ^{68}Ga]SB3 scan in several metastatic lymph nodes compared with the follow-up scan performed with ^{18}F]fluoromethylcholine (Figure 5).

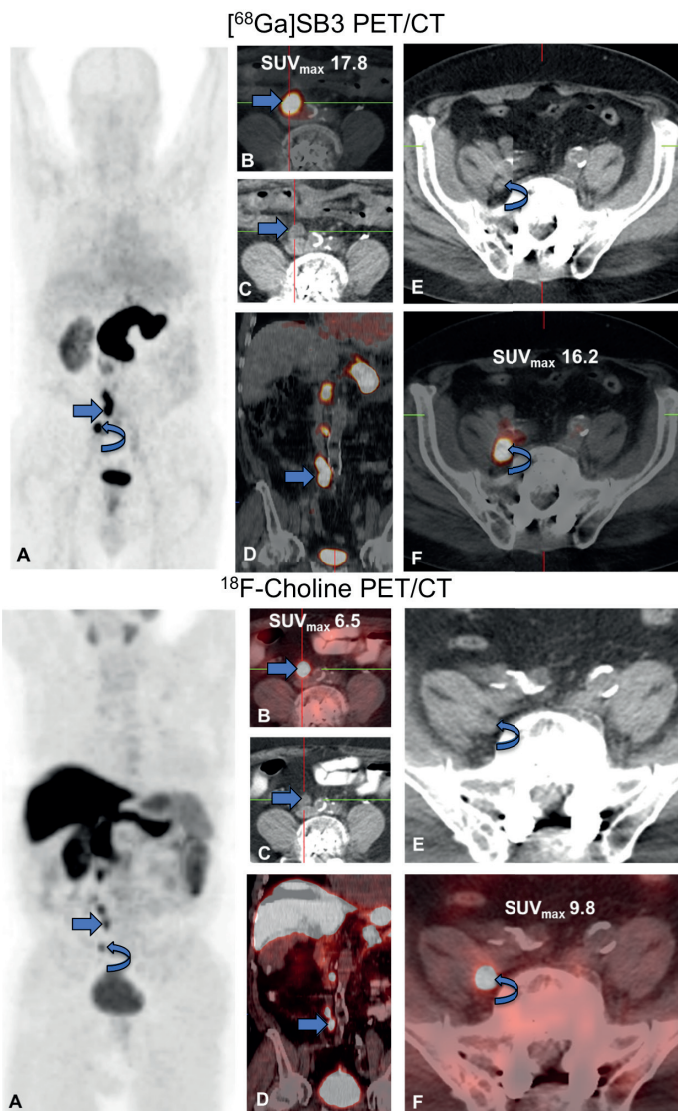


Figure 5 - Top ^{68}Ga]SB3 PET/CT and bottom ^{18}F -choline PET/CT scan in a prostate cancer (PC) patient (number 4), demonstrating GRPR-positive and choline-avid lymph node metastases respectively: right to the aortic bifurcation (**B–D**, straight arrow) and right iliac lymph node metastasis at the level of the S1 vertebra (**E, F**, curved arrow). **A** MIP; **B, F** fused axial PET/CT images; **C, E** axial CT images; **D** fused coronal PET/CT image.

The mean PSA level of PC patients was 64 ± 81 ng/mL (range 1.5–215 ng/mL). Four out of 5 patients with a positive [⁶⁸Ga]SB3 scan had elevated PSA levels (≥ 10 ng/mL). One out of 4 patients with a negative [⁶⁸Ga]SB3 scan had normal PSA levels (Table 2). Interestingly, osseous metastases could be well visualized in BC patients, as shown in Figure 6 for patient number 6.

Table 2 - Characteristics and scan results in the subgroup of 9 prostate cancer (PC) patients

Patient (number)	Age (years)	Final diagnosis	Initial stage	Year of diagnosis	Previous therapy	PSA (ng/ml)	[⁶⁸ Ga]SB3 scan
1	59	PC	TxNxM1	2006	Rad, chem	89	+
4	74	PC	T1N0M0	2003	Horm, nephr, rad	40	+
7	70	PC	T4N1M0	2005	Prost, rad, horm, phos	182	+
10	70	PC	T3N1Mx	2002	Prost, rad, chem	215	+
12	53	PC	TxNxM1	2004	Lymph, horm	4	-
13	71	PC	T4N0M0	2001	Prost, horm	2	-
15	61	PC	T4NxM1	2006	Horm, rad, chem	32	-
16	54	PC	TxNxM1	2009	Horm, phos	7	-
17	69	PC	T3N0Mx	2004	Prost, rad	5	+

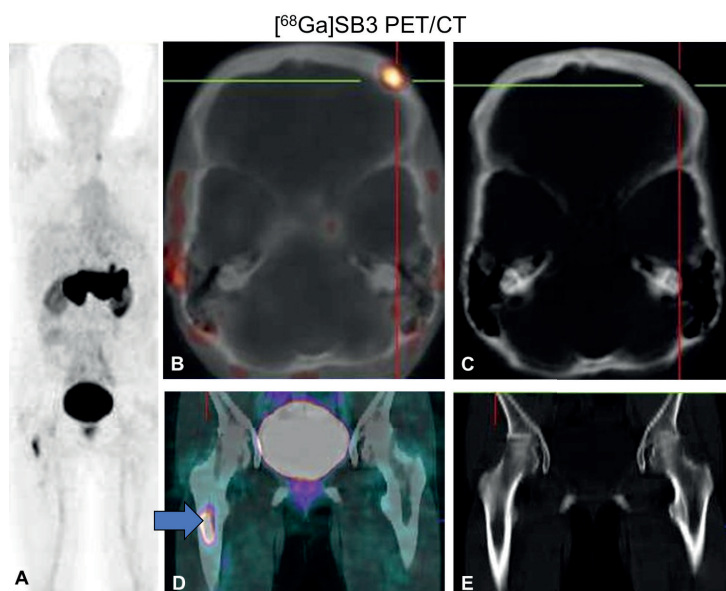


Figure 6 - [⁶⁸Ga]SB3 scan in a breast cancer (BC) patient (number 6), demonstrating GRPR-positive bone metastasis in the skull: frontal bone on the left side (B, SUV_{max} 2.4) and bone marrow metastasis in the right proximal femur (D, arrow, SUV_{max} 7.8), both negative on CT (C, E). A MIP; B fused axial PET/CT image; C, E axial CT images; D fused coronal PET/CT image.

DISCUSSION

The overexpression of GRPR in PC and BC offers promising opportunities for staging, monitoring, and potentially also for radionuclide therapy of these tumors with the application of GRPR-specific radiopeptide probes [9, 10, 14, 17, 18]. A great number of GRPR-directed radioligands studied in the past two decades are analogs of BBN, displaying agonistic activity at the GRPR. While internalization of radiolabeled GRPR agonists was originally considered advantageous for in vivo tumor targeting, injection into patients was soon linked to undesirable pharmacological effects, raising biosafety concerns [21]. Recent studies on GRPR radioantagonists with better inherent biosafety have inadvertently brought to light their superior tumor targeting efficacy and faster background clearance compared with agonists. Based on the well-characterized GRPR antagonist, [^{99m}Tc]DB1 [19], we introduce here its DOTA-modified mimic, SB3, which can be labeled with ^{68}Ga (Figure 1). We have thus designed a new ^{68}Ga -radiotracer suitable for PET and complementary to the existing SPECT radiotracer [^{99m}Tc]DB1. In addition, we have evaluated the novel PET radiotracer first in in vitro and animal GRPR-positive models and then in BC and PC patients, following an integrated “bench-to-patient” approach.

At the preclinical level, both SB3 and [$^{\text{nat}}\text{Ga}$]SB3 exhibited high affinity for the human GRPR expressed on PC-3 cells (Figure 2). Moreover, [^{67}Ga]SB3 strongly and specifically bound onto the membrane of PC-3 cells, internalizing poorly, as expected for a GRPR-radioantagonist [19, 24]. Of great advantage is the stability of [^{67}Ga]SB3 in the mouse blood-stream (Supplemental figure 3), favoring sufficient delivery to tumor sites, in contrast to the rapid in vivo catabolism previously reported for GRPR radioligands by neutral endopeptidase and possibly other enzymes [24, 26, 28]. High uptake of [^{67}Ga]SB3 was observed in PC xenografts in mice at 1 h pi (Figure 3), which remained at high levels up to 24 h pi. At the same time, values in the GRPR-rich mouse pancreas, although very high at the initial time points, declined rapidly over time. Likewise, background radioactivity cleared rapidly over time, leading to an attractive overall profile. On the other hand, the tumor uptake of [^{67}Ga]SB3 surpassed the values previously reported for [^{99m}Tc]DB1 in the same animal model at all time points [19]. Tumor retention in particular was clearly superior for [^{67}Ga]SB3 ($27.1 \pm 0.9\% \text{ID/g}$) compared with [^{99m}Tc]DB1 ($5.4 \pm 0.7\% \text{ID/g}$ at 24 h pi).

This attractive preclinical profile prompted us to further evaluate [^{68}Ga]SB3 in a first-in-man study including a small number of PC and BC patients. Several pilot clinical studies with GRPR radioligands have been reported, including both PC and BC patients [13, 17, 21, 27]. However, most of these radioligands were BBN-based receptor agonists. A ^{64}Cu -labeled GRPR radioantagonist, ^{64}Cu -CB-TE2A-AR06 [(^{64}Cu -4,11-bis(carboxymethyl)-1,4,8,11-tetraazabicyclo(6.6.2)hexadecane)-PEG₄-D-Phe-Gln-Trp-Ala-Val-Gly-His-Sta-

LeuNH₂], was recently studied in four patients with newly diagnosed PC using PET/CT. The radiotracer showed favorable tumor-to-normal organ ratios over time [29]. The most promising clinical results in 11 primary PC patients scheduled for radical prostatectomy were presented for the GRPR radioantagonist, [⁶⁸Ga]BAY86-7548 (⁶⁸Ga-DOTA-4-amino-1-carboxymethyl-piperidine-DPhe-Gln-Trp-Ala-Val-Gly-His-Sta-Leu-NH₂). Sensitivity and specificity of 88 % and 81 % were reported [30]. In the case of BC, no data have hitherto been provided on the diagnostic efficacy of a GRPR antagonist-based radioligand in patients. Good diagnostic sensitivity was demonstrated in early-stage BC patients during clinical evaluation of a series of ^{99m}Tc- radiotracers based on BBN, which were performed during the last decade [31–33]. In most of these studies, however, osseous involvement was not visualized, although the primary tumor and lymph node metastases were well visualized.

In the clinical part of our study, we have included patients with progressive disseminated disease for the evaluation of uptake in tumor metastases. For example, bone metastases were well visualized in patient number 6 with BC (Figure 6), highlighting the promising imaging qualities of [⁶⁸Ga]SB3. As our patients have a long history of recurrent disease, other (nuclear) imaging modalities were available and were additionally used for lesion detection. In one patient, [⁶⁸Ga]SB3 clearly demonstrated better performance in comparison with [¹⁸F]fluoromethylcholine PET/CT (Figure 5). However, the total number of positive [⁶⁸Ga]SB3 scans was lower compared with other studies, presumably as a result of recurrent, extensive disease history and previous therapies in our patients. It should be noted that GRPR is strongly upregulated in most of the primary prostate cancers that are still confined to the prostate, particularly in well-differentiated prostate tumors. On the other hand, a significant decline in GRPR expression is observed in the advanced androgen-independent stages of PC [9, 10, 12]. Recently, an inverse correlation was reported between GRPR expression vs high PSA values and high Gleason score [11]. Results were obtained from screening multiple prostate samples for GRPR expression in 530 patients, with most of the primary carcinoma specimens (77 %) acquired after radical prostatectomy. For BC, GRPR expression has been correlated with estrogen receptor levels [16, 34].

Despite the fact that all patients in our study had disseminated recurrent disease and many had a history of previous therapies, including anti-hormonal therapy, potentially leading to a state of androgen/estrogen independence and consequently to a higher number of negative scans with [⁶⁸Ga]SB3, we still found positive scans in about 50 % of cases, both in BC and in PC. This indicates the potential value of GRPR as a biomarker for monitoring after therapy. A preclinical study in nude mice with xenografted BC did indeed demonstrate better visualization and monitoring of hormone treatment with the bombesin agonist ⁶⁸Ga-AMBA vs ¹⁸F-FDG [35]. It is reasonable to assume that a

higher number of [^{68}Ga]SB3 scans would have been positive in early BC and PC cases. This hypothesis is currently under investigation in a clinical study in patients with primary PC initiated at Erasmus MC.

The benefit of choline PET/CT was recently shown in the preoperative staging of PC patients with an intermediate or high risk of extracapsular disease, leading to a different therapeutic treatment in 19 out of 130 patients (15 %) [36]. [^{68}Ga]SB3 could be used in addition to conventional imaging for upstaging nearby lymph nodes and/or distant metastases. In patients with local recurrent PC, choline PET/CT can be used to delineate local sites of recurrence. However, irradiation planning for the treatment of single lymph node metastases on the basis of choline PET/CT remains controversial owing to its limited lesion-based sensitivity in primary nodal staging [37]. Furthermore, the detection rate of choline-PET/CT is poor in patients with low PSA levels (<3.0 ng/ml) [37]. PET/CT with [^{68}Ga]SB3 may be valuable in this group of PC patients and could improve radiation treatment planning by enhancing the target volume to, for example, lymphatic drainage sites.

Prostate-specific membrane antigen (PSMA) is another interesting target for imaging. PSMA is expressed in normal and malignant prostatic epithelium with high expression in poorly differentiated metastatic carcinomas [38, 39]. Small molecule PSMA inhibitors demonstrated good imaging characteristics in patients with androgen-independent PC with bone metastasis, but have a lower sensitivity in patients with primary PC [40]. GRPR expression, on the other hand, is higher in the early stages of PC, in contrast to PSMA (Figure 7). A comparative study of [^{68}Ga]SB3 and a PSMA-targeted PET radiotracer in patients with primary or recurrent PC would therefore be of utmost interest for further evaluation and clinical use.

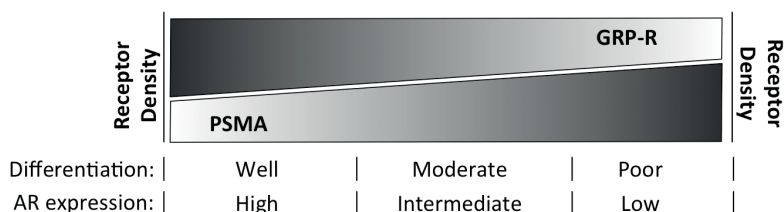


Figure 7 - Graphical representation of imaging characteristics for gastrin- releasing peptide receptor (GRPR) and prostate-specific membrane antigen (PSMA) in PC as a function of histological differentiation grade and androgen receptor (AR) expression.

CONCLUSION

We introduce here a new GRPR antagonist suitable for labeling with ⁶⁸Ga. Preclinical experience with the [⁶⁷Ga]SB3 surrogate revealed the most attractive radiotracer qualities, such as high GRPR-affinity, good in vivo stability, and excellent targeting efficacy in human GRPR-positive xenografts in mice. First clinical data with [⁶⁸Ga]SB3 PET/CT in patients with disseminated PC and BC showed encouraging results, as lesions were visualized in about 50 % of the patients, despite their advanced disease. The number of positive [⁶⁸Ga]SB3 scans is expected to be higher in patients with primary PC and BC. This prospect favors the application of [⁶⁸Ga]SB3 as an attractive tool for PC and BC staging, monitoring, and eventually patient stratification for radionuclide therapy with [¹⁷⁷Lu/⁹⁰Y/²¹³Bi]SB3.

SUPPLEMENTAL DATA

Preparation of [natGa]SB3

SB3 (600 µg) was incubated with a threefold molar excess of ^{nat}Ga(NO₃)₃·9H₂O (Alfa-Ventron) in acetate buffer (pH 4) at 90 °C 30 min. The excess ^{nat}Ga was then scavenged by addition of EDTA. Complete ^{nat}Ga-metalation of SB3 was verified by analytical HPLC, performed on a Waters Chromatograph coupled to a 996 photodiode array UV detector (Waters) and a Gabi gamma detector (Raytest RSM Analytische Instrumente GmbH). For analysis, an XBridge Shield RP18 (5 µm, 4.6 mm × 150 mm, Waters) cartridge column coupled to the respective 2-cm guard column was used. The column was eluted at 1 mL/min flow rate with a linear gradient of 0.1% aqueous trifluoroacetic acid (TFA) solution and acetonitrile (MeCN), starting from 20% MeCN with 1% increase of MeCN/min; *t_R*(SB3) = 15.4 min and *t_R*([^{nat}Ga]SB3) = 16.2 min.

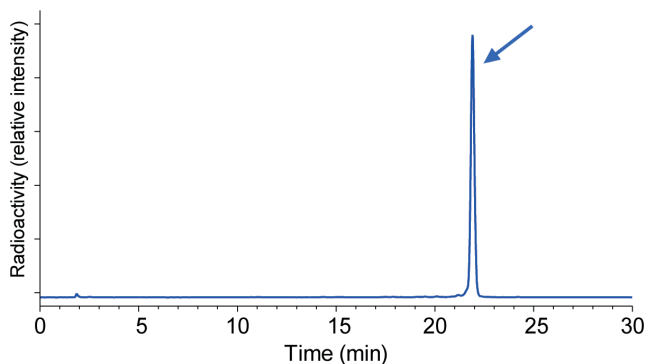
Preparation of [125I-Tyr4]BBN

[Tyr⁴]BBN (PSL GmbH) and ¹²⁵I (MDS Nordion) were used for the preparation of [¹²⁵I-Tyr⁴]BBN. Radioiodination was performed by the chloramine-T methodology, as previously described [41,42]. The forming sulfoxide (Met¹⁴=O) was reduced by dithiothreitol and [¹²⁵I-Tyr⁴]BBN was isolated in non-carrier added form by HPLC. Methionine was added to the purified radioligand solution to prevent re-oxidation of Met¹⁴ to the corresponding sulfoxide and the resulting stock solution in 0.1% BSA-PBS was kept at -20 °C; aliquots thereof were used for competition binding assays (specific activity of 2.2 Ci/µmol). Samples were measured for radioactivity in an automatic well-type gamma counter (NaI(Tl)) crystal, Canberra Packard Auto-Gamma 5000 series instrument).

Preparation and Quality Control of [^{67/68}Ga]SB3

Lyophilized SB3 was dissolved in HPLC-grade H₂O (2 mg/mL) and 50 µL aliquots thereof were stored in Eppendorf Protein LoBind tubes at -20 °C. For labeling, ⁶⁷GaCl₃ in dilute HCl at an activity concentration of 18.4–27.5 GBq/mL was provided by (MDS Nordion). [⁶⁷Ga]SB3 was obtained at specific activities of 3.7–7.4 MBq ⁶⁷Ga/nmol SB3. Briefly, 3–15 nmol of SB3 were mixed with 50–150 µL of 1 M pH 4.0 sodium acetate buffer and 5–15 µL of ⁶⁷GaCl₃ (11–111 MBq). The mixture was incubated at 90 °C for 30 min and Na₂-EDTA (0.1 M, pH 4.0) was added to a final concentration of 1 mM. For HPLC analysis, elution with a linear gradient was applied with 0.1% TFA/MeCN, starting from 20% MeCN and a 0.5% increase per min at 1 mL/min flow rate.

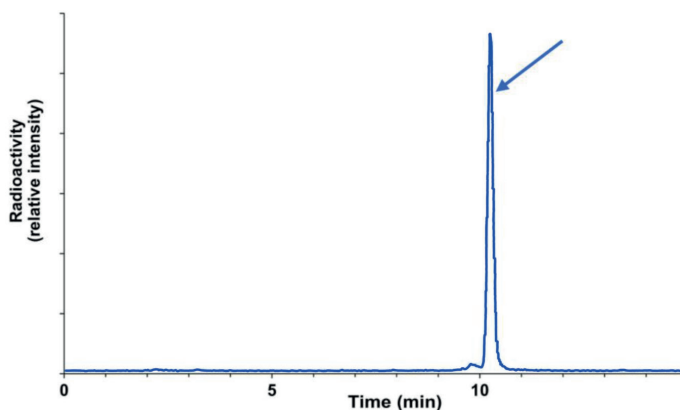
The radiochemical labeling yield (RCY) exceeded 98% and the radiochemical purity (RCP) of [⁶⁷Ga]SB3 was >99% (Supplemental figure 1).



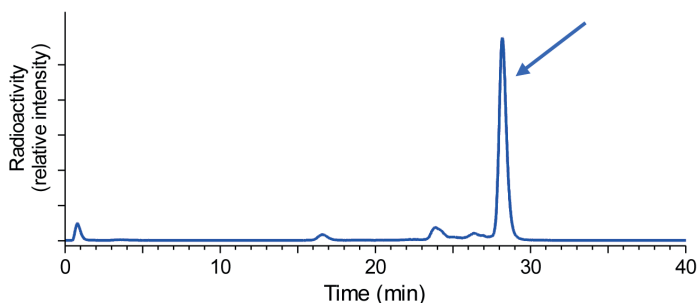
Supplemental figure 1 - Radioanalytical trace of [⁶⁷Ga]SB3 labeling reaction mixture by HPLC (the radiopeptide t_r is indicated by the arrow).

All reagents used for the preparation of [⁶⁸Ga]SB3 were purchased from commercial sources. Cartridges used for separation chemistry were bought from Varian and solutions were prepared with ultrapure water (Merck). All experiments were performed with a ⁶⁸Ge/⁶⁸Ga generator from Obninsk (Eckert & Ziegler Europe) or an IGG100 ⁶⁸Ge/⁶⁸Ga generator (Eckert & Ziegler Europe) eluate. [⁶⁸Ga]SB3 was prepared using either the cation-exchange method in hydrochloric acid/acetone [43] or the NaCl based method [S4]. In the first method [44], the SCX cartridge (Varian, Bond Elut-SCX, 100 mg, 1 mL) was preconditioned with 1 mL 5.5 M HCl and 10 mL water prior to the elution step. In the NaCl based method [44], the ⁶⁸Ge/⁶⁸Ga generator was eluted with 0.1 M HCl (10 mL in total) and ⁶⁸Ga was collected almost quantitatively on a SCX cartridge. The activity was eluted, with minimal loss (1-2%), using a mixture of 12.5 µL of 5.5 M HCl and 500 µL of 5 M NaCl (Ultrapur, Merck) into a solution of 400 µL 1 M ammonium acetate buffer

(pH 4.5), 40 µg of SB3, and 3.0 mL water. The end pH was 3.7 ± 2 . The reaction was completed after heating the solution for 7 min at 90 °C. A final purification step using a C-18 solid phase extraction cartridge was not needed. The RCY after sterile-filtration, expressed as percentage of the activity originally present and not decay-corrected, was approximately 65%. The final product was neutralized with 2 mL of sterile sodium phosphate buffer (Braun) and then diluted for dose administration.



Supplemental figure 2 - Radioanalytical HPLC of [⁶⁸Ga]SB3 labeling reaction mixture (the radiopeptide tR is indicated by the arrow).



Supplemental figure 3 - Radiochromatogram of HPLC analysis of mouse blood collected 5 min pi of [⁶⁷Ga]SB3 (>85% detected intact); the tR of the parent radiopeptide is indicated by the arrow.

The quality control combined TLC and HPLC methods. For TLC, ITLC-SG strips (Varian) were run using MeCN/H₂O 1:1 as mobile phase. For HPLC analyses the system applied included a Jasco PU-1580 pump of a quaternary gradient unit (Jasco LG-1580-04), a gamma detector (Biostep IsoScan LC) and a multi-wavelength detector (Jasco MD 1510). A RP-18 column (LiChroCART 250-4, LiChrospher 100, RP-18e; 5 µm, 250 mm × 4 mm) was eluted at 1.2 mL/min with the following gradient system: from 0-2 min 100%

A, 2-15 min to 100% B, whereby A: 0.1% TFA in 5/95 MeCN/H₂O and B: 0.1% TFA in 95/5 MeCN/H₂O. The RCP, as determined by HPLC and expressed as the percentage of activity in the [⁶⁸Ga]SB3 peak versus total activity, was >99%. As shown in Supplemental figure 2, the main peak for [⁶⁸Ga]SB3 eluted at t_r 10.0 min, whereas no free ⁶⁸Ga (t_r 2.3 min) was detected.

HPLC Analysis of Mouse Blood Samples

[⁶⁷Ga]SB3 was injected as a 100 µL bolus (11-22 MBq, 3 nmol total peptide) in the tail vein of male Swiss albino mice (30 ± 5 g, NCSR "Demokritos" Animal House Facility). Mice were anesthetized and blood (0.5-1 mL) was collected from the heart at 5 min post injection (pi). Blood samples were prepared for HPLC analysis, as previously described [45]. The Symmetry Shield RP18 (5 µm, 3.9 mm × 20 mm) column was eluted at a flow rate of 1.0 mL/min with the following gradient: 100% A to 90% A in 10 min and from 90% A to 60% for the next 60 min; (A= 0.1% aqueous TFA (v/v) and B = MeCN). The position of the intact radiopeptide was determined by coinjection with the [⁶⁷Ga]SB3 reference in the HPLC. The amount of [⁶⁷Ga]SB3 detected intact at 5 min pi in mouse circulation exceeded 85% (Supplemental figure 3).

Patient Data and Scan Results

Patient selection and characteristics are summarized in Supplemental table 1. An overview of the SUV_{max} biodistribution of [⁶⁸Ga]SB3 in 17 patients is found in Supplemental Table 2, whereas the localization of [⁶⁸Ga]SB3 positive lesions in 9 patients is listed in Supplemental Table 3.

Supplemental table 1 - Summary of disease characteristics of 17 patients. Breast Cancer (BC), Lung Cancer (LC), Mastectomy (mast1), Mastectomy plus Lymphadenectomy (mast2), Chemotherapy (chem), External Radiotherapy (rad), Anti-estrogen Therapy (horm), Biphosphonates Therapy (phos), [¹⁵³Sm]EDTMP (sam), immunotherapy (imm).

Patient no.	Age (yr)	Diagnosis	Date of Diagnosis	Initial Diagnosis	Histology	Previous therapy	PSA (ng/ml)	Demobesin scan
1	59	PC	November 2006	TxNxM1	Prostate Adenocarcinoma	Rad, chem	89	+
2	55	BC	November 1999	T2N1M0		Mast2, chem		+
3*	70	BC and LC	March 1998	T1N2M1	Lung (adenocarcinoma)	Mast2, rad, chem		+
			July 2008	Stadium IV				
4**	74	PC	July 2003	T1N0M0	Moderately differentiated small acinar cell Adenocarcinoma prostate	Horm, nefr, rad	40	+
5	49	BC	March 2001	T1N1M0	Invasive ductal Carcinoma. ER,PR+, HER2 - Ki67 < 5%	Mast2, chem, rad, horm, sam, phos, imm		+
6	48	Left BC	July 1998	T1N0M0	Left - Multifocal Ca, HER2 +	Mast2, chem, rad, horm, sam, phos, imm		+
		Right BC	July 2007	T3N0M1	Right - Inv. Lob. Ca, ER90%, PR -, HER2 3+, Ki67 - 60%	Mast2, chem, horm, rad, phos, sam		+
7	70	PC	June 2005	T4N1M0	Poorly differentiated Adenocarcinoma	Prost, rad, horm, phos	182	+
8	60	Lef BC	April 1993	TxNxMx	Left - Invasive ductal carcinoma	Left: Mast1		-
		Right BC	December 1999	T1N0M0	Right - Invasive ductal Carcinoma, ER, PR +, HER2 -	Right: Mast1		-
9	51	BC	March 1994	TxNxMx	Intraductal Carcinoma, HER2 3+	Mast, chem, rad, imm		-
10	70	PC	December 2002	T3N1Mx	Poorly diff. AdenoCarcinoma; lymphangitis carcinomatosis	Prost, rad, chem	215	+
11	69	BC	November 2004	T2N1M0	Multifocal inv. ductal Carcinoma, HER-2 neu: 3+, ER+, PR-	Mast, chem, rad, imm		-
12	53	PC	September 2004	TxNxM1	Poorly differentiated Carcinoma	Lymph, horm	4	-
13	71	PC	December 2001	T4N0M0	Prostate-Adenocarcinoma	Prost, horm	2	-
14	40	BC	November 1999	T2N1M0	Poorly differentiated Carcinoma left breast	Mast, chem		-
15	61	PC	November 2006	T4NxM1	Acinar Adenocarcinoma	Horm, rad, chem	32	-
16	54	PC	March 2009	TxNxM1	Acinar Carcinoma	Horm, phos	7	-
17	69	PC	October 2004	T3N0Mx	Acinar Adenocarcinoma	Prost, rad,	5	+

* Patient was also diagnosed with LC, ** Patient had nephrectomy of the left kidney

Supplemental table 2 - SUV_{max} biodistribution in 17 patients injected with [⁶⁸Ga]SB3.

Organ	Mean SUV _{max}	Standard deviation	Range
Pancreas			
- Head	48.7	22.2	14.7 – 90.9
- Corpus	43.8	23.0	6.4 – 84.5
- Tail	41.6	22.2	5.5 – 78.7
Kidneys (Parenchyma)	5.4	1.2	3.5 – 5.1
Oesophagogastric junction (OGJ)	3.5	0.8	2.1 – 5.1
Blood activity (Blood pool)	2.6	0.6	1.7 – 4.1
Liver	1.9	0.5	1.0 – 2.9
Lung	0.7	0.2	0.3 – 1.1
Background (M. Gluteus)	0.6	0.3	0.2 – 1.2
[⁶⁸Ga]SB3 positive lesions (n=71 in 9 patients)	3.7	3.2	0.6-17.8

Supplemental table 3 - Localisation of 71 [⁶⁸Ga]SB3 positive lesions in 4 patient with breast cancer (BC) and 5 patients with prostate cancer (PC).

Organ	Number of positive lesions in	
	Group 1 BC	Group 2 PC
Skull	2	0
Thorax	3	0
Liver	4	0
Abdomen	2	0
Lymph nodes	3	16
Skeletal lesions	24	17
Total lesions	71	

REFERENCES

1. Siegel R, Naishadham D, Jemal A. Cancer statistics, 2012. *CA Cancer J Clin.* 2012;62:10–29. doi:10.3322/caac.20138.
2. DeSantis C, Siegel R, Bandi P, Jemal A. Breast cancer statistics, 2011. *CA Cancer J Clin.* 2011;61:409–18. doi:10.3322/caac.20134.
3. Roehl KA, Antenor JA, Catalona WJ. Serial biopsy results in prostate cancer screening study. *J Urol.* 2002;167:2435–9.
4. Elter M, Schulz-Wendtland R, Wittenberg T. The prediction of breast cancer biopsy outcomes using two CAD approaches that both emphasize an intelligible decision process. *Med Phys.* 2007;34:4164–72.
5. Hricak H, Choyke PL, Eberhardt SC, Leibel SA, Scardino PT. Imaging prostate cancer: a multidisciplinary perspective. *Radiology.* 2007;243:28–53. doi:10.1148/radiol.2431030580.
6. Berg WA, Gutierrez L, NessAiver MS, Carter WB, Bhargavan M, Lewis RS, et al. Diagnostic accuracy of mammography, clinical examination, US, and MR imaging in preoperative assessment of breast cancer. *Radiology.* 2004;233:830–49. doi:10.1148/radiol.2333031484. 7.
7. Jadvar H. Imaging evaluation of prostate cancer with 18F-fluorodeoxyglucose PET/CT: utility and limitations. *Eur J Nucl Med Mol Imaging.* 2013;40 (Suppl 1):S5–10. doi:10.1007/s00259-013-2361-7.
8. Escalona S, Blasco JA, Reza MM, Andradas E, Gomez N. A systematic review of FDG-PET in breast cancer. *Med Oncol.* 2010;27: 114–29. doi:10.1007/s12032-009-9182-3.
9. Markwalder R, Reubi JC. Gastrin-releasing peptide receptors in the human prostate: relation to neoplastic transformation. *Cancer Res.* 1999;59:1152–9.
10. Körner M, Waser B, Rehmann R, Reubi JC. Early over-expression of GRP receptors in prostatic carcinogenesis. *Prostate.* 2014;74: 217–24. doi:10.1002/pros.22743.
11. Beer M, Montani M, Gerhardt J, Wild PJ, Hany TF, Hermanns T, et al. Profiling gastrin-releasing peptide receptor in prostate tissues: clinical implications and molecular correlates. *Prostate.* 2012;72: 318–25. doi:10.1002/pros.21434.
12. Schroeder RP, de Visser M, van Weerden WM, de Ridder CM, Reneman S, Melis M, et al. Androgen-regulated gastrin-releasing peptide receptor expression in androgen-dependent human prostate tumor xenografts. *Int J Cancer.* 2010;126:2826–34. doi:10.1002/ijc.25000.
13. Mather SJ, Nock BA, Maina T, Gibson V, Ellison D, Murray I, et al. GRP receptor imaging of prostate cancer using [99mTc]Demobesin 4: a first-in-man study. *Mol Imaging Biol.* 2014;16:888–95. doi:10.1007/s11307-014-0754-z.
14. Gugger M, Reubi JC. Gastrin-releasing peptide receptors in non- neoplastic and neoplastic human breast. *Am J Pathol.* 1999;155: 2067–76. doi:10.1016/S0002-9440(10)65525-3.
15. Reubi C, Gugger M, Waser B. Co-expressed peptide receptors in breast cancer as a molecular basis for in vivo multireceptor tumour targeting. *Eur J Nucl Med Mol Imaging.* 2002;29:855–62. doi:10.1007/s00259-002-0794-5.
16. Halmos G, Wittliff JL, Schally AV. Characterization of bombesin/ gastrin-releasing peptide receptors in human breast cancer and their relationship to steroid receptor expression. *Cancer Res.* 1995;55: 280–7.
17. Maina T, Nock B, Mather S. Targeting prostate cancer with radiolabelled bombesins. *Cancer Imaging.* 2006;6:153–7. doi:10.1102/1470-7330.2006.0025.
18. Yu Z, Ananias HJ, Carlucci G, Hoving HD, Helfrich W, Dierckx RA, et al. An update of radiolabeled bombesin analogs for gastrin- releasing peptide receptor targeting. *Curr Pharm Des.* 2013;19: 3329–41.

19. Cescato R, Maina T, Nock B, Nikolopoulou A, Charalambidis D, Piccand V, et al. Bombesin receptor antagonists may be preferable to agonists for tumor targeting. *J Nucl Med.* 2008;49:318–26. doi: 10.2967/jnumed.107.045054.
20. Mansi R, Wang X, Forrer F, Kneifel S, Tamma ML, Waser B, et al. Evaluation of a 1,4,7,10-tetraazacyclododecane-1,4,7,10-tetraacetic acid-conjugated bombesin-based radioantagonist for the labeling with single-photon emission computed tomography, positron emission tomography, and therapeutic radionuclides. *Clin Cancer Res.* 2009;15:5240–9. doi:10.1158/1078-0432.CCR-08-3145.
21. Bodei L, Ferrari M, Nunn A, Lllull J, Cremonesi M, Martano L, et al. ¹⁷⁷Lu-AMBA bombesin analogue in hormone refractory prostate cancer patients: a phase I escalation study with single-cycle administrations. *Eur J Nucl Med Mol Imaging.* 2007;34:S221.
22. Reile H, Armatis PE, Schally AV. Characterization of high-affinity receptors for bombesin/gastrin releasing peptide on the human prostate cancer cell lines PC-3 and DU-145: internalization of receptor bound ¹²⁵I-(Tyr⁴)bombesin by tumor cells. *Prostate.* 1994;25:29–38.
23. Nock BA, Nikolopoulou A, Galanis A, Cordopatis P, Waser B, Reubi JC, et al. Potent bombesin-like peptides for GRP-receptor targeting of tumors with ^{99m}Tc: a preclinical study. *J Med Chem.* 2005;48:100–10. doi:10.1021/jm049437y.
24. Marsouvanidis PJ, Nock BA, Hajjaj B, Fehrentz JA, Brunel L, M'Kadmi C, et al. Gastrin releasing peptide receptor-directed radioligands based on a bombesin antagonist: synthesis, ¹¹¹In-labeling, and preclinical profile. *J Med Chem.* 2013;56:2374–84. doi:10.1021/jm301692p.
25. Marsouvanidis PJ, Maina T, Sallegger W, Krenning EP, de Jong M, Nock BA. Tumor diagnosis with new ¹¹¹In-radioligands based on truncated human gastrin releasing peptide sequences: synthesis and preclinical comparison. *J Med Chem.* 2013;56:8579–87. doi:10.1021/jm4010237.
26. Nock BA, Maina T, Krenning EP, de Jong M. BTo serve and protect[^]: enzyme inhibitors as radiopeptide escorts promote tumor targeting. *J Nucl Med.* 2014;55:121–7. doi:10.2967/jnumed.113.129411.
27. Baum RP, Prasad V, Frischknecht M, Maecke H, Reubi J. Bombesin receptor imaging in various tumors: first results of Ga-68 AMBA PET/CT. *Eur J Nucl Med Mol Imaging.* 2007;34:S193–S.
28. Linder KE, Metcalfe E, Arunachalam T, Chen J, Eaton SM, Feng W, et al. In vitro and in vivo metabolism of Lu-AMBA, a GRP- receptor binding compound, and the synthesis and characterization of its metabolites. *Bioconj Chem.* 2009;20:1171–8. doi:10.1021/bc9000189.
29. Wieser G, Mansi R, Grosu AL, Schultze-Seemann W, Dumont- Walter RA, Meyer PT, et al. Positron emission tomography (PET) imaging of prostate cancer with a gastrin releasing peptide receptor antagonist—from mice to men. *Theranostics.* 2014;4:412–9. doi: 10.7150/thno.7324.
30. Kähkönen E, Jambor I, Kemppainen J, Lehtio K, Gronroos TJ, Kuisma A, et al. In vivo imaging of prostate cancer using [⁶⁸Ga]- labeled bombesin analog BAY86-7548. *Clin Cancer Res.* 2013;19:5434–43. doi:10.1158/1078-0432.CCR-12-3490.
31. Van de Wiele C, Phonteyne P, Pauwels P, Goethals I, Van den Broecke R, Cocquyt V, et al. Gastrin-releasing peptide receptor imaging in human breast carcinoma versus immunohistochemistry. *J Nucl Med.* 2008;49:260–4. doi:10.2967/jnumed.107.047167.
32. Shariati F, Aryana K, Fattahi A, Forghani MN, Azarian A, Zakavi SR, et al. Diagnostic value of ^{99m}Tc-bombesin scintigraphy for differentiation of malignant from benign breast lesions. *Nucl Med Commun.* 2014;35:620–5. doi:10.1097/MNM.000000000000112.33.
33. Scopinaro F, Di Santo GP, Tofani A, Massari R, Trotta C, Ragone M, et al. Fast cancer uptake of ^{99m}Tc-labelled bombesin (^{99m}Tc BN1). *In Vivo.* 2005;19:1071–6. 34.

34. Dalm SU, Martens JW, Sieuwerts AM, van Deurzen CH, Koelewijn SJ, de Blois E, et al. In-vitro and in-vivo application of radiolabeled gastrin releasing peptide receptor ligands in breast cancer. *J Nucl Med.* 2015;56:752–7. doi:10.2967/jnumed.114.153023.
35. Prignon A, Nataf V, Provost C, Cagnolini A, Montravers F, Gruaz- Guyon A, et al. ⁶⁸Ga-AMBA and ¹⁸F-FDG for preclinical PET imaging of breast cancer: effect of tamoxifen treatment on tracer uptake by tumor. *Nucl Med Biol.* 2015;42:92–8. doi:10.1016/j.nucmedbio.2014.10.003.
36. Beheshti M, Imamovic L, Broinger G, Vali R, Waldenberger P, Stoiber F, et al. ¹⁸F choline PET/CT in the preoperative staging of prostate cancer in patients with intermediate or high risk of extracapsular disease: a prospective study of 130 patients. *Radiology.* 2010;254:925–33. doi:10.1148/radiol.09090413.
37. Kitajima K, Murphy RC, Nathan MA. Choline PET/CT for imaging prostate cancer: an update. *Ann Nucl Med.* 2013;27:581–91. doi:10.1007/s12149-013-0731-7.
38. Silver DA, Pellicer I, Fair WR, Heston WD, Cordon-Cardo C. Prostate-specific membrane antigen expression in normal and malignant human tissues. *Clin Cancer Res.* 1997;3:81–5.
39. Wright Jr GL, Grob BM, Haley C, Grossman K, Newhall K, Petrylak D, et al. Upregulation of prostate-specific membrane antigen after androgen-deprivation therapy. *Urology.* 1996;48:326–34.
40. Ristau BT, O’Keefe DS, Bacich DJ. The prostate-specific membrane antigen: lessons and current clinical implications from 20 years of research. *Urol Oncol.* 2014;32:272–9. doi:10.1016/j.urolonc.2013.09.003.
41. Williams BY, Schonbrunn A. Bombesin receptors in a human duodenal tumor cell line: binding properties and function. *Cancer Res.* 1994;54:818-24.
42. Vigna SR, Giraud AS, Reeve JR, Jr., Walsh JH. Biological activity of oxidized and reduced iodinated bombesins. *Peptides.* 1988;9:923-6.
43. Zhernosekov KP, Filosofov DV, Baum RP, Aschoff P, Bihl H, Razbash AA, et al. Processing of generator-produced ⁶⁸Ga for medical application. *J Nucl Med.* 2007;48:1741-8. doi:10.2967/jnumed.107.040378.
44. Mueller D, Klette I, Baum RP, Gottschaldt M, Schultz MK, Breeman WA. Simplified NaCl based ⁶⁸Ga concentration and labeling procedure for rapid synthesis of ⁶⁸Ga radiopharmaceuticals in high radiochemical purity. *Bioconjug Chem.* 2012;23:1712-7. doi:10.1021/bc300103t.
45. Marsouvanidis PJ, Nock BA, Hajjaj B, Fehrentz JA, Brunel L, M’Kadmi C, et al. Gastrin releasing peptide receptor-directed radioligands based on a bombesin antagonist: synthesis, ¹¹¹In-labeling, and preclinical profile. *J Med Chem.* 2013;56:2374-84. doi:10.1021/jm301692p.



4

SUMMARY, DISCUSSION AND FUTURE

4.1

SUMMARY

ENGLISH AND DUTCH

SUMMARY

Neuroendocrine tumors (NET) are rare neoplasms with differences in clinical presentation, course and prognosis. The age-adjusted incidence varies between 3-6 new cases per 100.000 persons per year (1). Most of the NETs express the somatostatin receptor, which can be utilized for imaging and therapy. Radiolabelled somatostatin analogs (like ^{111}In -DTPA⁰octreotide, OctreoScan[®]) bind to the somatostatin receptor and the emitted gamma-rays can be detected by a positron (PET) or photon emission computed tomography (SPECT) scanner.

Radiolabeled somatostatin analogs can also be used for peptide receptor radionuclide therapy (PRRT) in NET patients. In the '90s, PRRT with high amounts of ^{111}In -octreotide was administered to NET patients, resulting in an improvement of quality of life. However, tumor response rates were low and serious side effects were reported in patients receiving PRRT with ^{111}In -octreotide. However, the new DOTA chelators enabled the use of other radionuclides, like ^{90}Y (yttrium (^{90}Y)) and ^{177}Lu (lutetium (^{177}Lu)). Since 2000, NET patients are treated with [^{177}Lu -DOTA⁰,Tyr³]octreotate (^{177}Lu -DOTATATE). Other medical centers started using ^{90}Y based somatostatin analogs, like [^{90}Y -DOTA⁰,Tyr³]octreotide (^{90}Y -octreotide).

Other tumors also have receptors that can be used for imaging and therapy. Prostate and breast cancer express the Gastrin-releasing Peptide Receptor (GRPR) on the cell surface. The radiolabelled Gastrin-Releasing Peptide (GRP) has a high affinity with the membrane receptor (GRPR) and can be used for imaging. In the future, radiolabeled GRP analogs might be used for PRRT in patients with extensive metastasized breast- and prostate cancer, in analogy to PRRT in NET patients.

In this thesis, the most important (long-term) side effect after PRRT with ^{177}Lu -DOTATATE will be discussed (**Chapter 2**). Furthermore, a first-in-man clinical evaluation of a new radiolabelled GRP compound with (^{68}Ga), [^{68}Ga]SB3, will be presented in patients with metastasized prostate- and breast-cancer (**Chapter 3**)

Chapter 1.1 is an introduction to NETs containing epidemiology, diagnostics and different treatment options. Also an overview is presented regarding dosimetry for PRRT and the clinical parameters for assessment of the side effects.

Chapter 1.2 is an overview of the current literature on PRRT. In the past 20 years, PRRT with radiolabeled somatostatin analogs has been administered to patients with somatostatin receptor positive tumors. In the department of nuclear medicine & radiology at the Erasmus MC, PRRT with ^{177}Lu -DOTATATE have been successfully administered in NET patients resulting in a complete and partial remission of 30%. In

general, PRRT is well tolerated, however the kidneys and bone marrow are the most important dose limiting organs.

^{177}Lu -DOTATATE is mainly excreted by and partially reabsorbed in the kidneys, which can cause radiation damage to the glomeruli (renal filters). Therefore amino acids are given during PRRT to reduce the absorption of ^{177}Lu -DOTATATE in the kidneys. Despite administration of amino acids during PRRT, an annual loss of renal function can be observed, particular in patients with diabetes mellitus, hypertension and alkylating chemotherapy in the past (2,3). In **Chapter 2.1**, the incidence of renal toxicity, associated risk factors (like hypertension, diabetes mellitus, administered dose and radiation dose to the kidneys) and renal function during follow-up was analyzed in 209 patients treated with ^{177}Lu -DOTATATE. Also the radiation dose to the kidneys was calculated and compared with the accepted dose limits adopted from radiotherapy. A non-linear effect regression model was used for assessment of the risk factors. Only 1% of the treated patients had a grade 2 renal toxicity, no grade 3-4 renal toxicity was observed. The annual decline in renal function was $3.4 \pm 0.4\%$. No risk factors could be identified which had a significant effect on the fitted non-linear model. The mean radiation dose to the kidneys was 20.1 ± 4.9 Gy. In the radiotherapy, the maximum accepted dose to the kidneys is 18 Gy.

In conclusion, the incidence of renal toxicity in patients treated with ^{177}Lu -DOTATATE is low and no grade 3-4 renal toxicity is observed. Moreover, no patients had a annual decline in renal function of more than $>20\%$. Our data supports the idea that the radiation dose threshold, adopted from external beam radiotherapy and PRRT with ^{90}Y -labelled somatostatin analogues, does not seem valid for PRRT with ^{177}Lu -DOTATATE.

Irradiation and damage to the bone marrow after PRRT with ^{177}Lu -DOTATATE lead to hematological toxicity (decrease in cell count). In Chapter 2.2 (sub)acute hematological toxicity after PRRT is outlined in 320 patients treated with ^{177}Lu -DOTATATE. First of all, the incidence and duration of hematological toxicity (according to CTCAE v3.0) is discussed and risk factors assessment is performed. Also the mean radiation dose to the bone marrow per administered ^{177}Lu -DOTATATE is calculated, based on 32 patients with individualized dosimetry. The median radiation dose to the bone marrow of 320 patients is compared to the accepted dose limit of 2 Gy, adopted from patients treated with radioiodine (^{131}I). Thirty-four (11%) patients developed grade 3-4 hematological toxicity, including 15 patients with hematological toxicity for more than 6 months or required blood transfusions. The risk factors associated with hematological toxicity are: low renal function, advanced age (> 70 years), decreased WBC count ($< 4.0 \cdot 10^9/\text{l}$), metastasized disease and high tumor uptake on OctreoScan®. Surprisingly,

previous treatment with chemotherapy was not associated with grade 3-4 (sub)acute hematological toxicity, while other studies identified previous chemotherapy as a risk factor (3-5). A possible explanation for this difference could be given by the fact that we have a limited number of patients in our study with previous chemotherapy in the past. The average radiation dose to the bone marrow was 67 ± 7 mGy/GBq, which is equal to a cumulative bone marrow dose of 2 Gy when four cycles of 7.4 GBq ^{177}Lu -DOTATATE are given. Hematological toxicity after PRRT with ^{177}Lu -DOTATATE is mild, however patients with associated risk factors are at risk. The BM dose upper limit of 2 Gy, adopted from ^{131}I therapy, seems not to be valid for PRRT with ^{177}Lu -DOTATATE.

Long-term side effects of the bone marrow after PRRT with ^{177}Lu -DOTATATE are identified by the rise in hematological neoplasms. Myelodysplastic syndrome (MDS) and acute myeloid leukemia (AML) are the most frequently found hematological neoplasms after irradiation. MDS and AML are acquired in only 2-3% of the patients treated with PRRT, however the exact mechanisms and correlations are ambiguous. Several factors that might contribute to the development of MDS after PRRT with ^{177}Lu -DOTATATE are; AML, cumulative administered activity, duration/number of PRRT treatments, CTCAE toxicity grade during PRRT in hemoglobin, platelets and white blood cells (3). **Chapter 2.3** deals with the incidence, course and predicting factors in patients with (suspicion of) hematological neoplasms after PRRT with ^{177}Lu -DOTATATE. Based on data from the Dutch cancer registration, the expected number of 'de novo' hematological neoplasms is 3 patients. Eight (2%) patients were diagnosed with hematological neoplasms, according to the World Health Organization (WHO) (6) and 5 (1.5%) patients with bonemarrow failure (not classified according to WHO). The relative risk for developing hematological neoplasms after PRRT in GEP-NET patients is 3.6 times higher than without treatment. The median latency time of hematological neoplasms is 41 (range 15 – 84) months after the last PRRT cycle in GEP-NET patients. Sub acute hematological toxicity grade 3 or 4 during PRRT is a marginally significant risk factor for the development of persistent hematological dysfunction after PRRT.

The spleen is the only lymphoid organ, since it is directly connected to the main blood circulation, which receives a high radiation dose during PRRT. The clinical consequences of this exposure to radiation are unknown. Therefore, **Chapter 2.4** discusses the change in spleen size and the blood cell counts after (re)treatment with ^{177}Lu -DOTATATE. In 35 patients, treated with a cumulative injected dose of 45 GBq ^{177}Lu -DOTATATE, spleen volumes were measured at baseline and during follow-up. The radiation dose to the spleen was calculated in 27 patients, according to Medical Internal Radiation Dose (MIRD) scheme. The spleen was significantly smaller (55%) after the first and the second

series of PRRT cycles compared to baseline volumes. The median absorbed dose to the spleen was 52 (range 23 – 110) Gy. No minimal dose threshold was observed for spleen reduction. In all patients, a reduction in white blood cell count was observed after PRRT with ^{177}Lu -DOTATATE. No correlation was found for: absorbed spleen dose, number of white blood cells, number of lymphocytes and/or spleen volume. None of the patients had an infection with a specific group of bacteria (*Streptococcus pneumoniae*, *Haemophilus influenzae* type B, *Neisseria meningitidis*).

In analogy with PRRT in NET patients, PRRT can also be used in other tumor types. Prostate carcinoma is the most common cancer in men, whereas for women breast cancer has the highest incidence rate. **Chapter 3.1** gives an introduction regarding targeted nuclear imaging and therapy in prostate- and breast cancer. The two tumors types express the Gastrin-Releasing Peptide Receptor (GRPR) on the cell membrane. Therefore, GRPR is an attractive molecular target for complementary radioligands. Preclinical studies demonstrated better imaging characteristics for GRPR antagonists, like [$^{99\text{m}}\text{Tc}$]DB1, in comparison to GRPR agonists (7,8). Moreover, GRPR antagonists have a higher inherent safety profile, since they do not elicit pharmacological effects after binding. In **chapter 3.2** we present a different version of [$^{99\text{m}}\text{Tc}$]DB1, namely [^{68}Ga]SB3, which is investigated in a (pre)clinical setting. Competitive- and bindings experiments on PC-3 cell membranes demonstrated a high affinity of SB3 with the humanlike GRP receptor. There was good *in vivo* stability and long tumor retention of the radioligand in mice. After the encouraging preclinical results, [^{68}Ga]SB3 was administered to 17 patients with extensive prostate- and breast cancer. Uptake of [^{68}Ga]SB3 was the highest in the GRPR-rich pancreas. [^{68}Ga]SB3 PET scans were positive in 4 out of 8 patients with breast cancer and 5 out of 9 patients with prostate cancer. In one patient with prostate cancer, uptake on [^{68}Ga]SB3 PET/CT was higher than ^{18}F -choline PET/CT. In conclusion, good visualization of the tumor lesions was possible with [^{68}Ga]SB3 in 50% of the patients with metastasized prostate- and breast-cancer. Therefore [^{68}Ga]SB3 can be a potential candidate for stage and monitoring of patients with prostate- or breast cancer.

Chapter 4.2 is the final chapter of this thesis in which new developments and future perspectives are discussed regarding PRRT in patients with NET, prostate cancer and breast cancer.

SAMENVATTING

Neuroendocriene tumoren (NETs) zijn zeldzame tumoren met grote verschillen in presentatie, beloop en prognose. De incidentie ligt tussen de 3-6 nieuwe gevallen per 100.000 inwoners per jaar (1). Het grootste gedeelte van de NETs hebben somatostatine receptoren op hun celoppervlak en deze kunnen gebruikt voor beeldvorming en therapie. Radioactief gelabelde somatostatine analogen (zoals ^{111}In -DTPA⁰ octreotide, OctreoScan[®];) binden aan de somatostatine receptor en de uitgezonden gammastralen kunnen worden gebruikt voor beeldvorming van NETs. Naast visualisatie van NETs is tevens therapie mogelijk met radioactief gelabelde somatostatine analogen, wat ook wel bekend staat onder de naam Peptide Receptor Radionuclide Therapie (PRRT). Tussen 1990-2000 werd PRRT met hoge dosis ^{111}In -octreotide gegeven bij patiënten met NETs en dit resulteerde in een verbetering van klachten. Echter, de bijwerkingen waren fors en de mate van tumorverkleining teleurstellend. Door het gebruik van een ander bindingsmolecuul (een DOTA chelator i.p.v. DTPA) werd het mogelijk om andere radionucliden te gebruiken, zoals ^{90}Y (^{90}Y) en ^{177}Lu (^{177}Lu). Vanaf 2000 wordt PRRT in Rotterdam verricht met [^{177}Lu -DOTA⁰,Tyr³]octreotaat (^{177}Lu -DOTATAAT). ^{90}Y gebaseerde somatostatine analoga, zoals [^{90}Y -DOTA⁰,Tyr³]octreotide, worden meer gebruikt in andere centra.

Ook andere soorten tumoren hebben receptoren die gebruikt kunnen worden voor beeldvorming en therapie. Prostaat- en borst tumoren brengen onder andere de Gastrin-Releasing Peptide Receptor (GRPR) tot expressie op het celoppervlak. Het radioactief gelabelde Gastrin-Releasing Peptide (GRP) bindt in hoge mate aan de membraan receptor GRPR en kan waardevol zijn voor het visualiseren van prostaat- en borstkanker. Wellicht zou het mogelijk zijn om radioactieve GRP analogen te gebruiken voor therapie bij uitgebreide gemetastaseerde borst- en prostaat kanker, in analogie met PRRT voor NET patiënten.

In dit proefschrift worden de belangrijkste korte en lange termijn bijwerkingen van PRRT met ^{177}Lu -DOTATAAT beschreven (**Hoofdstuk 2**). Daarnaast beschrijven we de eerste resultaten van een nieuw radioactief (^{68}Ga , ^{68}Ga) gelabeld GRP radioligand, genaamd [^{68}Ga]SB3, bij patiënten met gemetastaseerde prostaat- en borstkanker (**Hoofdstuk 3**).

Hoofdstuk 1.1 is een algemene inleiding over NETs, inclusief bespreking van de epidemiologie, diagnostiek en de verschillende behandelingen. Daarnaast wordt een overzicht gegeven van de stralingsmodellen voor PRRT en belangrijke klinische parameters voor bijwerkingen. **Hoofdstuk 1.2** geeft een overzicht van de literatuur over

PRRT. In de afgelopen 20 jaar is PRRT met gelabelde somatostatine analoga toegepast bij patiënten met somatostatine receptor-positieve tumoren. Op de afdeling Radiologie & Nucleaire Geneeskunde van het Erasmus MC wordt PRRT met ^{177}Lu -DOTATAAT succesvol toegepast bij patiënten met NETs met een kans op complete en partiële remissies van 30%. Over het algemeen wordt PRRT goed verdragen, echter de nieren en beenmerg zijn de belangrijkste dosis-limiterende organen.

De nieren zijn belangrijk voor het uitscheiden van de toegediende ^{177}Lu -DOTATAAT uit het lichaam, dit kan echter stralingsschade aan de glomeruli (nierfilters) veroorzaken, omdat de nieren het radiopeptide ook opnemen in bepaalde cellen. Er worden daarom aminozuren toegediend tijdens de PRRT om de absorptie van ^{177}Lu -DOTATAAT in de nieren te verminderen. Ondanks de toediening van de aminozuren tijdens PRRT kan er, met name bij patiënten met slecht gereguleerde diabetes mellitus (suikerziekte), hoge bloeddruk en alkylerende chemotherapieën in de voorgeschiedenis, een belangrijk jaarlijks verlies van nierfunctie ontstaan (2,3). **Hoofdstuk 2.1** beschrijft de incidentie van niertoxiciteit, geassocieerde risicofactoren (o.a. hypertensie, diabetes mellitus, toegediende dosis en stralingsdosis op de nieren) en de nierfunctie tijdens follow-up in 209 patiënten behandeld met ^{177}Lu -DOTATAAT. Tevens is de stralingsdosis op de nieren berekend en vergeleken met de geaccepteerde dosislimieten in de radiotherapie. Een “non-linear effect regression model” is gebruikt om de risicofactoren te onderzoeken. De eerste bevinding was dat in slechts 1% van de behandelde patiënten een graad 2 nier-toxiciteit voorkwam en er werd geen graad 3 of 4 nier-toxiciteit geobserveerd. De jaarlijkse percentuele vermindering in nierfunctie was $3.4 \pm 0.4\%$. Daarnaast konden er geen risicofactoren worden geïdentificeerd die een significant effect hadden op het gebruikte niet-lineaire model. De gemiddelde stralingsdosis op de nieren was 20.1 ± 4.9 Gy. In de radiotherapie is de geaccepteerde dosislimiet op de nieren 18 Gy.

We concludeerden dat de incidentie van nierschade bij patiënten behandeld met ^{177}Lu -DOTATAAT laag is en dat er geen graad 3 of 4 nier-toxiciteit is geobserveerd. Tevens waren er geen patiënten met een jaarlijkse nierfunctiedaling van $>20\%$. Ons onderzoek ondersteunt de hypothese dat de bekende en vastgestelde stralingsdosisgrenzen uit de radiotherapie niet van toepassing zijn voor PRRT met ^{177}Lu -DOTATAAT.

Hematologische (beenmerg en bloedcellen) toxiciteit na PRRT met ^{177}Lu -DOTATAAT is het gevolg van bestraling en schade aan het beenmerg. In **Hoofdstuk 2.2** wordt dieper ingegaan op de (sub)acute hematologische toxiciteit na PRRT met ^{177}Lu -DOTATAAT bij 320 patiënten. Ten eerste wordt de incidentie en duur beschreven van hematologische toxiciteit volgens CTCAE v3.0 en worden geassocieerde risicofactoren onderzocht. Tevens wordt er een gemiddelde stralingsdosis naar het beenmerg per toegediende

hoeveelheid ^{177}Lu -DOTATAAT berekend op basis van individueel berekende stralingswaarden bij 32 patiënten. De gemiddelde stralingsdosis van de gehele groep patiënten wordt vergeleken met de gangbare dosis norm op het beenmerg van 2 Gy bij patiënten behandeld met radioactief Jodium-131. Vierendertig (11%) patiënten ontwikkelden hematologische graad 3 en/of 4 toxiciteit, waarbij bij 15 van de 34 patiënten de toxiciteit langer dan 6 maanden duurde, of er noodzaak ontstond om bloedtransfusies te geven. De risicofactoren geassocieerd met hematologische toxiciteit zijn: slechte nierfunctie, leeftijd (> 70 jaar), verminderd aantal witte bloedcellen ($< 4.0 \cdot 10^9/\text{l}$), uitgebreid gemetastaseerde ziekte en hoge tumoropname op OctreoScan[®]. Verwonderlijk is dat voorgaande behandelingen met chemotherapie niet geassocieerd zijn met graad 3-4 (sub)acute hematologische toxiciteit, terwijl dit door andere onderzoeksgroepen wel is beschreven (3-5). Een verklaring hiervoor kan zijn dat een beperkt aantal patiënten in onze studie chemotherapie in de voorgeschiedenis heeft ontvangen. In onze studie is de gemiddelde stralingsdosis op het beenmerg 67 ± 7 mGy/GBq, dit komt neer op een beenmerg dosis van 2 Gy wanneer vier cycli van 7.4 GBq ^{177}Lu -DOTATAAT worden toegediend. Bovenstaande onderzoeksresultaten ondersteunen dat de (sub)acute hematologische toxiciteit na PRRT met ^{177}Lu -DOTATAAT aanvaardbaar is, echter patiënten met risicofactoren hebben een verhoogde kans op hematologische toxiciteit. De gebruikelijke beenmerg dosislimiet van 2 Gy lijkt hierdoor niet van toepassing op PRRT met ^{177}Lu -DOTATAAT.

Lange termijn effecten op het beenmerg door PRRT uiten zich door het ontstaan van hematologische neoplasmata. De twee meest voorkomende zijn myelodysplastisch syndroom (MDS) en Acute myeloïde leukemie (AML). Zij worden slechts gezien bij 2-3% van de behandelde patiënten. De precieze mechanismen en risicofactoren in relatie tot PRRT blijven echter onbegrepen. Enkele mogelijke factoren voor het ontstaan van MDS na PRRT met ^{177}Lu -DOTATAAT zijn: acute leukemie, cumulatieve geïnjecteerde activiteit en duur/aantal behandelingen PRRT, toxiciteit graad in hemoglobine, bloedplaatjes en witte bloedcellen (3). **Hoofdstuk 2.3** behandelt de incidentie, het beloop en de voorspellende factoren van patiënten met (verdenking op) hematologische neoplasmata na PRRT met ^{177}Lu -DOTATAAT. Op basis van cijfers uit de Nederlandse kankerregistratie (NKR) verwachten we 4.3 patiënten met een 'de novo' hematologische maligniteit. Er waren 8 (2%) patiënten gediagnosticeerd met hematologische maligniteit volgens de World Health Organization (WHO) (6) en 5 (1.5%) patiënten met langdurig beenmerg falen zonder WHO classificatie. Het relatieve risico op het krijgen van hematologische neoplasmata na PRRT is 3.6 keer hoger dan zonder behandeling. De mediane latente periode van hematologische neoplasmata ligt op 36 (bereik 5 - 84) maanden na laatste PRRT behandeling. Subacute hematologische toxiciteit graad 3 of 4 tijdens PRRT met

^{177}Lu -DOTATAAT is de enige marginale risicofactor geassocieerd met het ontstaan van hematologische neoplasmata na PRRT.

De milt is het enige lymfoïde orgaan dat, gezien het direct op de bloedcirculatie is aangesloten, een hoge stralingsdosis ontvangt tijdens PRRT behandeling. De klinische consequenties voor deze hoge blootstelling aan straling zijn onbekend. Daarom is **Hoofdstuk 2.4** gewijd aan de verandering in miltgrootte en bloedwaarden na (her) behandeling met PRRT. Bij 35 patiënten behandeld met een cumulatief geïnjecteerde dosis van 45 GBq ^{177}Lu -DOTATAAT werd het miltvolume opgemeten en op verschillende tijdstippen vervolgd. De stralingsdosis op de milt werd berekend in 27 patiënten volgens het Medical Internal Radiation Dose (MIRD) schema. De milt was evident (55%) kleiner geworden na de eerste serie behandelingen PRRT en na een tweede serie herbehandelingen ten opzichte van het volume vooraf aan PRRT. De mediaan geabsorbeerde dosis naar de milt was 52 (bereik 23 – 110) Gy en er leek geen minimale drempelwaarde voor de ^{177}Lu -DOTATAAT dosis te zijn voor miltreductie. Bij alle patiënten trad er een verlaging op van het aantal witte bloedcellen na behandeling. Er werd geen onderlinge relatie aangetoond tussen: geabsorbeerde milt-dosis, verlaging van aantal witte bloedcellen, aantal lymfocyten en/of miltgrootte. Geen van de onderzochte patiënten had een infectie met een bepaalde groep bacteriën (*Streptococcus pneumoniae*, *Haemophilus influenzae* type B, *Neisseria meningitidis*).

Naar analogie van PRRT bij NET-patiënten kan de therapie tevens worden gebruikt bij andere tumoren. Prostaat kanker is bij mannen de meest voorkomende ziekte en bij vrouwen is dit borstkanker. **Hoofdstuk 3.1** geeft een introductie over doelgerichte nucleaire beeldvorming en therapie bij prostaat- en borstkanker. Beide type tumoren brengen de Gastrin-Releasing Peptide Receptor (GRPR) tot expressie op het celoppervlak. Hierdoor is de GRPR een aantrekkelijk doelwit waar radioliganden voor gemaakt kunnen worden. Onderzoek heeft aangetoond dat beeldvorming met GRPR antagonisten, zoals [^{99m}Tc]DB1, beter is dan met GRPR agonisten (7,8). Daarnaast zijn GRPR antagonisten veiliger, omdat ze geen farmacologische effecten veroorzaken na binding. In **Hoofdstuk 3.2** wordt een variant van [^{99m}Tc]DB1, genaamd [^{68}Ga]SB3, beschreven, die in preklinische en klinische onderzoeken onderzocht is. Competitie en bindingsexperimenten op PC-3 celmembranen toonden een hoge affiniteit van SB3 met de menselijke GRPR. Er was een goede *in vivo* stabiliteit en langdurige tumorretentie van het radioligand bij muizen. Na de gunstige preklinische resultaten werd [^{68}Ga]SB3 toegediend aan 17 patiënten met uitgebreide prostaat- of borstkanker. De stapeling van [^{68}Ga]SB3 was het hoogste in de GRPR-rijke pancreas. [^{68}Ga]SB3 PET scans waren positief bij 4/8 patiënten met borstkanker en 5/9 patiënten met prostaat-kanker. Bij één

patiënt met prostaatkanker was de stapeling van [⁶⁸Ga]SB3 PET/CT zelfs hoger dan die van ¹⁸F-choline gemeten door middel van PET/CT. Wij konden concluderen dat [⁶⁸Ga]SB3 de tumorlaesies goed visualiseert bij ongeveer 50% van de patiënten met uitgebreide prostaat- en borstkanker. Dit maakt dat [⁶⁸Ga]SB3 een potentieel geschikt radioligand is voor het stageren en monitoren van prostaat- en borstkanker bij patiënten.

Tot slot worden in **Hoofdstuk 4.2** de resultaten van de artikelen in dit proefschrift besproken in het kader van de nieuwe ontwikkelingen en toekomstige therapeutische opties van PRRT bij patiënten met NET en prostaat- en borstkanker.

REFERENTIES

1. Hallet J, Law CH, Cukier M, Saskin R, Liu N, Singh S. Exploring the rising incidence of neuroendocrine tumors: a population-based analysis of epidemiology, metastatic presentation, and outcomes. *Cancer*. 2015;121:589-597.
2. Bodei L, Cremonesi M, Ferrari M, et al. Long-term evaluation of renal toxicity after peptide receptor radionuclide therapy with ⁹⁰Y-DOTATOC and ¹⁷⁷Lu-DOTATATE: the role of associated risk factors. *Eur J Nucl Med Mol Imaging*. 2008;35:1847-1856.
3. Bodei L, Kidd M, Paganelli G, et al. Long-term tolerability of PRRT in 807 patients with neuroendocrine tumours: the value and limitations of clinical factors. *Eur J Nucl Med Mol Imaging*. 2015;42:5-19.
4. Delpassand ES, Samarghandi A, Zamanian S, et al. Peptide receptor radionuclide therapy with ¹⁷⁷Lu-DOTATATE for patients with somatostatin receptor-expressing neuroendocrine tumors: the first US phase 2 experience. *Pancreas*. 2014;43:518-525.
5. Sabet A, Ezziddin K, Pape UF, et al. Long-term hematotoxicity after peptide receptor radionuclide therapy with ¹⁷⁷Lu-octreotate. *J Nucl Med*. 2013;54:1857-1861.
6. Arber DA, Orazi A, Hasserjian R, et al. The 2016 revision to the World Health Organization classification of myeloid neoplasms and acute leukemia. *Blood*. 2016;127:2391-2405.
7. Cescato R, Maina T, Nock B, et al. Bombesin receptor antagonists may be preferable to agonists for tumor targeting. *J Nucl Med*. 2008;49:318-326.
8. Mansi R, Wang X, Forrer F, et al. Evaluation of a 1,4,7,10-tetraazacyclododecane-1,4,7,10-tetraacetic acid-conjugated bombesin-based radioantagonist for the labeling with single-photon emission computed tomography, positron emission tomography, and therapeutic radionuclides. *Clin Cancer Res*. 2009;15:5240-5249.

4.2

DISCUSSION AND FUTURE PERSPECTIVES

PRRT in NET patients

In **Chapter 1**, the past and current status of peptide receptor radionuclide therapy (PRRT) for patients with neuroendocrine tumors (NETs) has been discussed (see Figure 1). **Chapter 2** outlined the (long-term) side effects of PRRT in patients. In 2017, an important phase III study (NETTER-1) was published, reporting the safety and efficacy of ^{177}Lu -DOTATATE in patients with neuroendocrine tumors (NETs). This randomized control trial validated the experience that was gained over the past two decades and demonstrated that PRRT with ^{177}Lu -DOTATATE has matured into a full treatment modality. However, new challenges and future improvements remain in the field of PRRT.

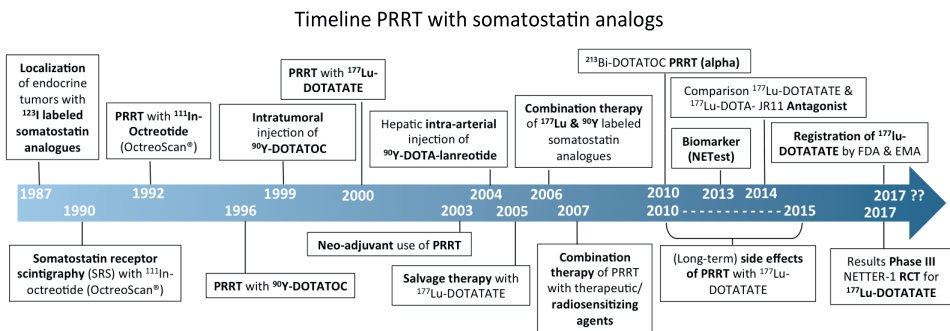


Figure 1 – Timeline of PRRT in the past 25 years. Peptide Receptor Radionuclide Therapy (PRRT), NETest® is a circulating tumor molecular marker test for neuroendocrine tumor, Food and Drug Administration (FDA), European Medicines Agency (EMA). References (1-14).

Recently, a blood gene transcript analysis in NET patients has demonstrated an advantage in the early detection of residual disease (15). Also the measurement of circulating transcripts can predict the therapeutic efficacy of PRRT in NET patients (16). New biomarkers, like CTCs (circulating tumor cells), or circulating tumor DNA, as well as genetic profiling of tumors might play a more prominent role in the future in the management of NET patients, in analogy with genomic tests in breast cancer patients (17).

The increasing number of treatment options for patients with GEP-NETs raised questions regarding timing, sequencing, and selection of therapies. Since there is limited data available, clinical judgment continues to play a critical role in the management of patients with GEP-NETs. Well-differentiated tumors may dedifferentiate to high-grade neoplasms, requiring more aggressive treatments (18). Treatment-related characteristics such as drug tolerability and therapy goals (tumor shrinkage versus delay of progression) are also important in defining treatment strategy. An interesting example of sequential

therapy is the ongoing HEPAR Plus trial, which evaluates radiological anti-tumor response after ^{166}Ho -radioembolization (^{166}Ho -RE) (19) and previous PRRT with ^{177}Lu -DOTATATE.

Targeted alpha therapy is another and interesting form of PRRT, where the radionuclide ^{177}Lu is replaced with an alpha emitter, like in ^{213}Bi -DOTATOC (20). However, limited data on alpha therapy in NET patients are still available. Also patients with recurrent metastasized prostate cancer could benefit from alpha therapy (21,22). However, since the physical characteristics of α -particles are different from dose of β -particles, (long-term) toxicity profiles might also be different compared to PRRT with ^{177}Lu -DOTATATE.

All somatostatin analogs that are currently used in the clinic (i.e., DOTA-TATE, DOTA-TOC, DOTA-NOC) are receptor agonists, inducing internalization of the receptor-ligand complex upon their binding to the receptor. PRRT with the somatostatin receptor antagonist ^{177}Lu -DOTA-JR11 has demonstrated a higher tumor dose, compared to ^{177}Lu -DOTATATE (11). Interestingly, the two radiocompounds, ^{68}Ga -DOTA-JR11 and ^{177}Lu -DOTA-JR11 are currently evaluated in an ongoing study in NET patients (ClinicalTrials.gov NCT02609737). Little information is still available on the (long-term) toxicity of these new compounds.

Dosimetry

In this thesis, dosimetry was based on planar (2-dimensional) scans as well as radioactivity measured in urine and blood. Large errors have been reported when using this method of internal dose calculations and these uncertainties will obscure dose-effect relations. Therefore, MIRD pamphlet no. 23 reported that patient-specific dosimetry should be performed using quantitative SPECT (23). However, accurate dosimetry for PRRT is time-consuming and not patient-friendly, since multiple scans need to be performed after each therapy cycle. Ideal dosimetry practice would entail simple, accurate dosimetry with minimal burden for the patient. Therefore we performed the first steps in a feasibility study for surrogate bonemarrow dosimetry, resulting in a lutetium dosimetry brace (LDB) placed on the upper thigh, see Figure 2 (24). This LDB can provide the kinetics, which leads to complete dose information when combined with SPECT/CT for the spatial distribution of the radionuclide. Currently, it is technical feasible to make a LDB with off the shelf electrical components. However, further development of the brace is needed. A future pilot study can explore ease of use and first clinical dosimetric results in comparison to full patient specific dosimetry. Not only dosimetry of the bone marrow but also of tumor lesions is feasible with this device.



Figure 2 – Feasibility analysis of lutetium dosimetry brace (LDB) (24).

Current dosimetry in PRRT faces a fundamental problem since both the dose calculation models and the toxicity dose thresholds are often based on idealized situations. The influences of low dose rates and inhomogeneous radiation exposure on dose response effects like secondary cancer induction are not well known. Large multi-cohort studies are needed to show incidence of second primary malignancies and with only retrospective cohort-based dosimetry available no clear indication of a dependency with absorbed dose can be found, let aside a clear safe threshold dose.

Radiobiological parameter values in tumors are affected by tumor type and by a number of tumor biology-specific factors that include the hypoxic and metabolic or proliferative fraction of the tumor. The radiation sensitivity of neuroendocrine tumors has not been established. Therapies with ^{90}Y -DOTATOC and ^{177}Lu -DOTATATE did show significant reduction in volume after absorbed doses of more than 200 Gy (25,26). However, the large gap between this 200 Gy dose and the typical 70-80 Gy curative dose with external beam radiotherapy can be explained by the difference in dose rate and homogeneity. The study of Konijnenberg *et al.* (27) demonstrated a great impact on heterogeneity in renal dose distribution. In pancreatic NETs, extensive degenerative changes are seen microscopically after PRRT with ^{177}Lu -DOTATATE (28). These changes of sclerosis and hyalinization modify the degree of homogeneity, influencing the absorbed dose to the tumor after consecutive cycles of PRRT.

Factors that play a role in the tumor dose after PRRT are more complex than in the external beam exposure field; Receptor-expressing tumor tissue is getting a high absorbed dose and it is intermingled with stromal tissue getting a lower cross-dose. At low tumor doses (< 200 Gy) the cross-dose to the interstitial stromal cells will be too low to create damage and subsequent reduction in volume, but might induce an immunological response, resulting in volume reduction. This concept was demonstrated in a case report, where immunotherapy was combined with radiation therapy and elicited a significant response, both within and outside the field of radiation.

Depending upon the scale of the dosimetry calculation, the radiobiological parameters will vary across the normal tissue or tumor volume. To address this problem, new fundamental radiobiological research has to be done.

With PRRT using ^{177}Lu -DOTATATE, most published data are based on a fixed treatment schedule using 4 consecutive cycles of 7.4 GBq. This approach strongly relies on a cohort-based average dose treatment planning and is acceptable when the absorbed doses in organs at risk do not show much variation or when no toxicity is observed. Since the absorbed dose to the kidneys and bone marrow does show a variation between patients, this fixed dose regime reduces side effects but also potentially undertreats certain patients, resulting in a loss of effectiveness. In Sweden, implementation of patient-specific dosimetry has been applied in a large group of patients treated with ^{177}Lu -DOTATATE (29). However, this study used the conservative dose thresholds for the bone marrow and kidneys adopted from external beam radiotherapy (EBRT) resulting also in an under treatment in certain patients, despite these conventional dose thresholds, 50% of the patients received more than 4 therapy cycles. The effectiveness of PRRT might improve if a minimum target dose to the tumor is specified. In a recent study from Uppsala University Hospital (30), this approach resulted in confirmation of old results with ^{90}Y -DOTATOC (25).

Dosimetry might also be used as a tool for further exploration of different treatment schedules in Peptide Receptor Radionuclide Therapy (PRRT). In the study of Sarnelli *et al.* (31), clinical data was used to derive representative absorbed doses for several treatment schemes for PRRT with different radionuclides (like ^{177}Lu , ^{90}Y). Both uniform and non-uniform activity distributions were considered for the kidneys and potential uptake reduction and inter-patient radiosensitivity variability were investigated for tumors. Normal-Tissue-Complication-Probability (NTCP) and Tumor-Control-Probability (TCP) were evaluated. For all ^{177}Lu -schemes the renal toxicity risk is negligible while for some ^{90}Y -schemes the NTCP is not zero. In case of tumor uptake reduction with cycles the treatment efficacy is reduced with a BED loss up to 46%.

The publication by Sarnelli *et al.* (31) has some limitations, since fundamental radiobiological data is currently not known e.g. for calculating the inter-patient radiosensitivity for tumors. Also no data about cumulative dose to the kidneys after PRRT with different radionuclides (like ^{90}Y , ^{177}Lu) is at hand. Therefore the article by Sarnelli *et al.* (31) is more a theoretical exercise and presents a set of tools for future dosimetric modeling.

Gastrin-releasing peptide receptor radioligands

In **Chapter 3** the gastrin releasing peptide receptor (GRPR) radioligand successor of ^{99m}Tc -Demobesin-1, ^{68}Ga -SB3 was introduced. This radiolabelled GRP receptor antagonist successfully localized early-stage lesions. However, in breast and prostate cancer patients with more advanced disease stages (including those who underwent multiple previous anticancer treatments), ^{68}Ga -SB3 did not visualize all known lesions. Our results are in line with previous reports on the GRPR-expression levels during prostate cancer propagation and its relation to androgens (32-34). Therefore, in a subsequent ongoing study only patients with primary and therapy-naïve prostate cancer were included (35). Moreover, the intensity of tumor uptake was related to GRPR expression, determined in (surgically) excised biopsy material from patients. Preliminary results indicate that the effective targeting of ^{68}Ga -SB3 seems higher in patients with primary prostate cancer than in patients with more advanced disease. The radiocompound labeled with ^{111}In and ^{177}Lu has also been investigated in mice, demonstrating a lower *in vivo* stability and an inferior uptake in prostate cancer xenografts as compared to ^{68}Ga -SB3 (36). SB3 seems therefore restricted to PET imaging of GRPR tumors. However in mice, $^{111}\text{In}/^{177}\text{Lu}$ -SB3 coinjected with the protease inhibitor phosphoramidon achieved tumor uptake comparable to ^{68}Ga -SB3. Other research groups have demonstrated that coadministration of key enzyme inhibitors can effectively prolong the survival of these radiolabeled peptides *in vivo* in the circulation, resulting in an effective transport to their target (37).

In the quest of radioligands with higher stability, a novel GRPR antagonist, NeoBOMB1 was developed (38), based on a well-characterized GRPR antagonist (39). NeoBOMB1 was labeled with ^{68}Ga (for PET), ^{111}In (for SPECT), and ^{177}Lu (for radionuclide therapy). GRPR affinity and *in vivo* stability of the radiocompounds showed comparable behavior in prostate cancer models. Moreover, prostate cancer lesions were successfully visualized with ^{68}Ga -NeoBOMB1 PET/CT in men.

Another interesting target in prostate cancer is the prostate-specific membrane antigen (PSMA), which is expressed at the cell membrane of normal prostate cells, but is significantly up-regulated in primary and metastatic prostate cancer. ^{18}F and ^{68}Ga -labeled small molecule PSMA inhibitors, demonstrated fast blood clearance and rapid and high tumor uptake in metastatic prostate cancer (43,44). The German retrospective multicenter study using ^{177}Lu -PSMA-617 demonstrated favorable safety and high efficacy exceeding those of other third-line systemic therapies in prostate cancer patients. Future phase II/III studies are planned to further elucidate the survival benefit of this new therapy in patients with metastatic castration-resistant prostate cancer patients.

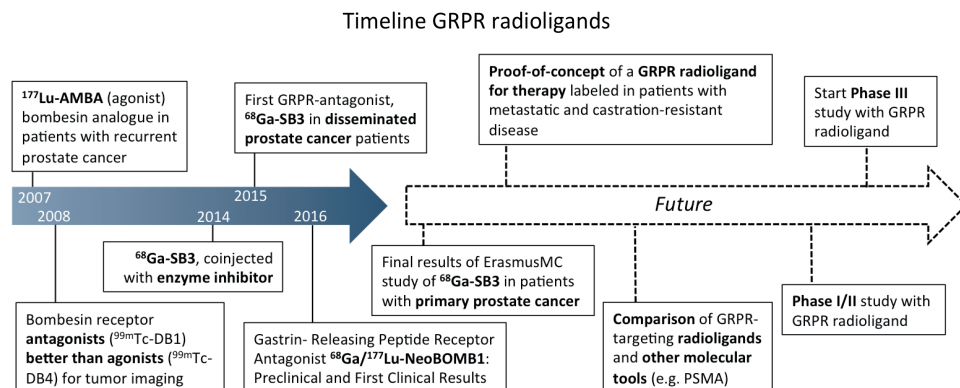


Figure 3 – Timeline of Gastrin Releasing Peptide Receptor (GRPR) radioligands recent past and future. Prostate-specific membrane antigen (PSMA). References; (40),(36,41),(42),(38).

The most widely used ^{68}Ga -labeled bombesin analog in a clinical setting is ^{68}Ga -RM2/ ^{68}Ga -BAY 86-7548

(45). Recently a comparative study was performed between ^{68}Ga -RM2 PET/MR imaging with ^{68}Ga -PSMA-11 PET/CT in a small group of patients with recurrent prostate cancer (46). The study highlighted the differences in biodistribution between the 2 PET radiopharmaceuticals; PSMA-11 is excreted both renal and hepatobiliary, whereas RM2 is excreted mainly renal, which might have implications in the detection of pelvic and abdominal lesions. The two radiopharmaceuticals demonstrated similar, but not identical uptake patterns of distribution in the suspected lesions, demonstrating the difference between PSMA and GRPR in the course of the disease.

Future studies have to be performed to compare the ability of GRPR agents to visualize primary and metastatic prostate cancer. Because of the heterogeneity of prostate cancer, it is likely that several imaging probes will prove clinically useful for imaging various types and stages of prostate cancer.

REFERENCES

1. Krenning EP, Bakker WH, Breeman WA, et al. Localisation of endocrine-related tumours with radiiodinated analogue of somatostatin. *Lancet*. 1989;1:242-244.
2. Krenning EP, Kwekkeboom DJ, Bakker WH, et al. Somatostatin receptor scintigraphy with [111In-DTPA-D-Phe1]- and [123I-Tyr3]-octreotide: the Rotterdam experience with more than 1000 patients. *Eur J Nucl Med*. 1993;20:716-731.
3. Krenning EP, Kooij PP, Bakker WH, et al. Radiotherapy with a radiolabeled somatostatin analogue, [111In-DTPA-D-Phe1]-octreotide. A case history. *Ann N Y Acad Sci*. 1994;733:496-506.
4. Otte A, Herrmann R, Heppeler A, et al. Yttrium-90 DOTATOC: first clinical results. *Eur J Nucl Med*. 1999;26:1439-1447.
5. Merlo A, Hausmann O, Wasner M, et al. Locoregional regulatory peptide receptor targeting with the diffusible somatostatin analogue 90Y-labeled DOTA0-D-Phe1-Tyr3-octreotide (DOTATOC): a pilot study in human gliomas. *Clin Cancer Res*. 1999;5:1025-1033.
6. Kwekkeboom DJ, Bakker WH, Kam BL, et al. Treatment of patients with gastro-entero-pancreatic (GEP) tumours with the novel radiolabelled somatostatin analogue [177Lu-DOTA(0),Tyr3]octreotate. *Eur J Nucl Med Mol Imaging*. 2003;30:417-422.
7. van Essen M, Krenning EP, Kam BL, de Herder WW, Feelders RA, Kwekkeboom DJ. Salvage therapy with (177)Lu-octreotate in patients with bronchial and gastroenteropancreatic neuroendocrine tumors. *J Nucl Med*. 2010;51:383-390.
8. Kwekkeboom DJ, de Herder WW, Kam BL, et al. Treatment with the radiolabeled somatostatin analog [177 Lu-DOTA 0,Tyr3]octreotate: toxicity, efficacy, and survival. *J Clin Oncol*. 2008;26:2124-2130.
9. Frilling A, Weber F, Saner F, et al. Treatment with (90)Y- and (177)Lu-DOTATOC in patients with metastatic neuroendocrine tumors. *Surgery*. 2006;140:968-976; discussion 976-967.
10. van Essen M, Krenning EP, Kam BL, de Herder WW, van Aken MO, Kwekkeboom DJ. Report on short-term side effects of treatments with 177Lu-octreotate in combination with capecitabine in seven patients with gastroenteropancreatic neuroendocrine tumours. *Eur J Nucl Med Mol Imaging*. 2008;35:743-748.
11. Wild D, Fani M, Fischer R, et al. Comparison of somatostatin receptor agonist and antagonist for peptide receptor radionuclide therapy: a pilot study. *J Nucl Med*. 2014;55:1248-1252.
12. Modlin IM, Drozdov I, Alaimo D, et al. A multianalyte PCR blood test outperforms single analyte ELISAs (chromogranin A, pancreastatin, neurokinin A) for neuroendocrine tumor detection. *Endocr Relat Cancer*. 2014;21:615-628.
13. Bodei L, Kidd M, Paganelli G, et al. Long-term tolerability of PRRT in 807 patients with neuroendocrine tumours: the value and limitations of clinical factors. *Eur J Nucl Med Mol Imaging*. 2015;42:5-19.
14. Strosberg J, El-Haddad G, Wolin E, et al. Phase 3 Trial of 177Lu-Dotatate for Midgut Neuroendocrine Tumors. *N Engl J Med*. 2017;376:125-135.
15. Modlin IM, Frilling A, Salem RR, et al. Blood measurement of neuroendocrine gene transcripts defines the effectiveness of operative resection and ablation strategies. *Surgery*. 2016;159:336-347.
16. Bodei L, Kidd M, Modlin IM, et al. Measurement of circulating transcripts and gene cluster analysis predicts and defines therapeutic efficacy of peptide receptor radionuclide therapy (PRRT) in neuroendocrine tumors. *Eur J Nucl Med Mol Imaging*. 2016;43:839-851.
17. Duffy MJ, Harbeck N, Nap M, et al. Clinical use of biomarkers in breast cancer: Updated guidelines from the European Group on Tumor Markers (EGTM). *Eur J Cancer*. 2017;75:284-298.

18. Paul D, Ostwal V, Bose S, Basu S, Gupta S. Personalized treatment approach to gastroenteropancreatic neuroendocrine tumors: a medical oncologist's perspective. *Eur J Gastroenterol Hepatol*. 2016;28:985-990.
19. Smits ML, Nijsen JF, van den Bosch MA, et al. Holmium-166 radioembolization for the treatment of patients with liver metastases: design of the phase I HEPAR trial. *J Exp Clin Cancer Res*. 2010;29:70.
20. Kratochwil C, Giesel FL, Bruchertseifer F, et al. (2)(1)(3)Bi-DOTATOC receptor-targeted alpha-radionuclide therapy induces remission in neuroendocrine tumours refractory to beta radiation: a first-in-human experience. *Eur J Nucl Med Mol Imaging*. 2014;41:2106-2119.
21. Sathekge M, Knoesen O, Meckel M, Modiselle M, Vorster M, Marx S. 213Bi-PSMA-617 targeted alpha-radionuclide therapy in metastatic castration-resistant prostate cancer. *Eur J Nucl Med Mol Imaging*. 2017;44:1099-1100.
22. Kratochwil C, Bruchertseifer F, Giesel FL, et al. 225Ac-PSMA-617 for PSMA-Targeted alpha-Radiation Therapy of Metastatic Castration-Resistant Prostate Cancer. *J Nucl Med*. 2016;57:1941-1944.
23. Dewaraja YK, Frey EC, Sgouros G, et al. MIRD pamphlet No. 23: quantitative SPECT for patient-specific 3-dimensional dosimetry in internal radionuclide therapy. *J Nucl Med*. 2012;53:1310-1325.
24. Rozemuller M, Grosscurt E, Bloemendaal M, Bergsma H, Konijnenberg M. Feasibility study lutetium dosimetry brace (LDB). 2012.
25. Pauwels S, Barone R, Walrand S, et al. Practical dosimetry of peptide receptor radionuclide therapy with (90)Y-labeled somatostatin analogs. *J Nucl Med*. 2005;46 Suppl 1:925-985.
26. Delker A, Ilhan H, Zach C, et al. The Influence of Early Measurements Onto the Estimated Kidney Dose in [(177)Lu][DOTA(0),Tyr(3)] Octreotate Peptide Receptor Radiotherapy of Neuroendocrine Tumors. *Mol Imaging Biol*. 2015;17:726-734.
27. Konijnenberg M, Melis M, Valkema R, Krenning E, de Jong M. Radiation dose distribution in human kidneys by octreotides in peptide receptor radionuclide therapy. *J Nucl Med*. 2007;48:134-142.
28. van Vliet EI, van Eijck CH, de Krijger RR, et al. Neoadjuvant Treatment of Nonfunctioning Pancreatic Neuroendocrine Tumors with [177Lu-DOTA0,Tyr3]Octreotate. *J Nucl Med*. 2015;56:1647-1653.
29. Sandstrom M, Garske-Roman U, Granberg D, et al. Individualized dosimetry of kidney and bone marrow in patients undergoing 177Lu-DOTA-octreotate treatment. *J Nucl Med*. 2013;54:33-41.
30. Ilan E, Sandstrom M, Wassberg C, et al. Dose response of pancreatic neuroendocrine tumors treated with peptide receptor radionuclide therapy using 177Lu-DOTATATE. *J Nucl Med*. 2015;56:177-182.
31. Sarnelli A, Guerriero F, Botta F, et al. Therapeutic schemes in 177Lu and 90Y-PRRT: radiobiological considerations. *Q J Nucl Med Mol Imaging*. 2017;61:216-231.
32. Markwalder R, Reubi JC. Gastrin-releasing peptide receptors in the human prostate: relation to neoplastic transformation. *Cancer Res*. 1999;59:1152-1159.
33. Beer M, Montani M, Gerhardt J, et al. Profiling gastrin-releasing peptide receptor in prostate tissues: clinical implications and molecular correlates. *Prostate*. 2012;72:318-325.
34. Schroeder RP, de Visser M, van Weerden WM, et al. Androgen-regulated gastrin-releasing peptide receptor expression in androgen-dependent human prostate tumor xenografts. *Int J Cancer*. 2010;126:2826-2834.
35. Bakker I, Fröberg A, Busstra M, et al. PET imaging of therapy-naïve primary prostate cancer patients using the GRPr-targeting ligand Sarabesin 3. *European Urology Supplements*. 2016;3:e567.

36. Lymperis E, Maina-Nock T, Kaloudi A, Krenning E, de Jong M, Nock B. Transient in vivo NEP inhibition enhances the theranostic potential of the new GRPR-antagonist [¹¹¹In/177Lu] SB3. Paper presented at: EUROPEAN JOURNAL OF NUCLEAR MEDICINE AND MOLECULAR IMAGING, 2014.
37. Nock BA, Maina T, Krenning EP, de Jong M. "To serve and protect": enzyme inhibitors as radiopeptide escorts promote tumor targeting. *J Nucl Med.* 2014;55:121-127.
38. Nock BA, Kaloudi A, Lymperis E, et al. Theranostic Perspectives in Prostate Cancer with the Gastrin-Releasing Peptide Receptor Antagonist NeoBOMB1: Preclinical and First Clinical Results. *J Nucl Med.* 2017;58:75-80.
39. Heimbrook DC, Saari WS, Balishin NL, et al. Gastrin releasing peptide antagonists with improved potency and stability. *J Med Chem.* 1991;34:2102-2107.
40. Bodei L, Ferrari M. ¹⁷⁷Lu-AMBA Bombesin analogue in hormone refractory prostate cancer patients: a phase I escalation study with single-cycle administrations. *Eur J Med Mol Imaging.* 2007;34:S221.
41. Cescato R, Maina T, Nock B, et al. Bombesin receptor antagonists may be preferable to agonists for tumor targeting. *J Nucl Med.* 2008;49:318-326.
42. Maina T, Bergsma H, Kulkarni HR, et al. Preclinical and first clinical experience with the gastrin-releasing peptide receptor-antagonist [(6)(8)Ga]SB3 and PET/CT. *Eur J Nucl Med Mol Imaging.* 2016;43:964-973.
43. Cho SY, Gage KL, Mease RC, et al. Biodistribution, tumor detection, and radiation dosimetry of ¹⁸F-DCFBC, a low-molecular-weight inhibitor of prostate-specific membrane antigen, in patients with metastatic prostate cancer. *J Nucl Med.* 2012;53:1883-1891.
44. Afshar-Oromieh A, Malcher A, Eder M, et al. PET imaging with a [⁶⁸Ga]gallium-labelled PSMA ligand for the diagnosis of prostate cancer: biodistribution in humans and first evaluation of tumour lesions. *Eur J Nucl Med Mol Imaging.* 2013;40:486-495.
45. Kahkonen E, Jambor I, Kemppainen J, et al. In vivo imaging of prostate cancer using [⁶⁸Ga]-labeled bombesin analog BAY86-7548. *Clin Cancer Res.* 2013;19:5434-5443.
46. Minamimoto R, Hancock S, Schneider B, et al. Pilot Comparison of (6)(8)Ga-RM2 PET and (6)(8)Ga-PSMA-11 PET in Patients with Biochemically Recurrent Prostate Cancer. *J Nucl Med.* 2016;57:557-562.

APPENDICES

LIST OF ABBREVIATIONS

[^{99m}Tc]DB1	^{99m} Tc-(N ¹)-DPhe-Gln-Trp-Ala-Val-Gly-His-Leu- NH ₂ Et)
[^{99m}Tc]DB4	^{99m} Tc-N ₄ -Pro-Gln-Arg-Tyr-Gly-Asn-Gln-Trp-Ala-Val- Gly-His-Leu-Nle-NH ₂
5-FU	5-Fluorouacil
5-HIAA	5-Hydroxy Indole Acetic Acid
⁶⁸Ga-DOTATATE	Gallium-68 labelled Octreotate
¹¹¹In	Indium-111
¹³¹I	Iodine-131
¹⁷⁷Lu	Lutetium-177
¹⁷⁷Lu-DOTA(-)TATE	¹⁷⁷ Lu-Octreotate
¹⁷⁷Lu-Octreotate	¹⁷⁷ Lu-[DOTA ⁰ , Naphthyl ³ , Thr ⁸]octreotate
⁹⁰Y	Yttrium-90
μmol	Micromolar
AA	Amino Acid(s)
AL	Acute Leukemia
AF	Alkaline Phosphatase
ALAT (ALT)	Alanine Amino-Transferase
AML	Acute Myeloid Leukemia
ANOVA	Analysis of Variance
Arg	Arginine
ASAT (AST)	Asparatate Transaminase
BED	Biologically Effective Dose
Bq	Becquerel. Conversion to Ci is obtained as follows: 1 mCi=37 MBq.
BSA	Body Surface Area
C-G	Cockcroft-Gault
CgA	Chromogranin A
Ci	Curie. Has been replaced by the SI-unit Becquerel (Bq).
CI	Confidence Interval
CLR	Creatinine Clearance
CT	Computed Tomography
CTCAE	Common Terminology Criteria for Adverse Events
DOTA	1,4,7,10-tetraazacyclododecane-1,4,7,10-tetraacetic acid
DOTA(-)NOC	[DOTA ⁰ , Naphthyl ³]octreotate
DOTA(-)TATE	[DOTA ⁰ , Naphthyl ³ , Thr ⁸]octreotate
DOTA(-)TOC	[DOTA ⁰ , Tyr ³]octreotide

DLT	Dose Limiting Toxicity
EBRT	External Beam Radiation Therapy
ECF	Extracellular Fraction
ENETS	European Neuroendocrine Tumor Society
Erasmus MC	Erasmus Medical Center
EUS	Endoscopic Ultrasound
exMDRD	Extended Modification of Diet in Renal Disease
FDA	Food and Drug Administration (USA)
FDG	[¹⁸ F]-Fluorodeoxyglucose
G1	Grade 1
G2	Grade 2
G3	Grade 3
Gamma-GT	Gamma Glutamyl Transpeptidase
GBq	Gigabecquerel (10 ⁹ Bq)
GEP	Gastro-Entero-Pancreatic
GEP-NET(s)	Gastro-Entero-Pancreatic Neuroendocrine Tumor(s)
GFR	Glomerular Filtration Rate
GI	Gastrointestinal
Gy	Gray (J/kg)
h	Hour
Hb	Hemoglobin
HbA1c	Glycosylated Hemoglobin
HPF	High Power Field
HPLC	High Performance Liquid Chromatography
HR	Hazard Ratio
IA	Infused Activity (Radioactivity)
IC₅₀	inhibiting concentration 50%
ICRP	International Commission on Radiological Protection
IFN-α	Interferon-alfa
IFN-β	Interferon-beta
iv	intravenous
keV	Kilo Electron Volt
Ki-67	Ki-67 labeling index (using MIB-1 antibody)
L	Litre(s)
LAR	Long-Acting Release/Repeatable
LDH	Lactate Dehydrogenase

LDST	Low-Dose Short Synacthen
LH	Luteinizing Hormone
LTB	Low Tumor Burden
LQ	Linear Quadratic (model)
Lys	Lysine
Luthatera	^{177}Lu -octreotate, [^{177}Lu -DOTA ⁰ ,Tyr ³]octreotate
MBq	Megabecquerel (10 ⁶ Bq)
mCi	milliCurie
MCNP	Monte Carlo Neutral Particle Transport
MDRD	Modification of Diet in Renal Disease
MDS	Myelodysplastic Syndrome
MDS/MPN	Myelodysplastic/Myeloproliferative neoplasms
MIBG	Metaiodobenzylguanidine
MIRD	Medical Internal Radiation Dose Committee (part of the SNM)
mmol	Millimolar
mo	Months
MPN	Myeloproliferative Neoplasms
MRI	Magnetic Resonance Imaging
mSv	milliSievert
MTC	Medullary Thyroid Carcinoma
mTOR	mammalian Target of Rapamycin
n	Number (of Patients)
NA	Not Available
NaCl	Sodium Chloride
NaI	Sodium Iodide
NEC	Neuroendocrine Carcinoma
NET	Neuroendocrine Tumor
NR	Not Reported
NSE	Neuron-specific Enolase
NQ	Not quantifiable
Octreoscan[®]	^{111}In -[DTPA ⁰]octreotide
OS	Overall Survival
PD	Progressive Disease
PET	Positron Emission Tomography
PET/CT	Positron Emission Tomography/Computed Tomography
PFS	Progression-Free Survival

PHD	Persistent Hematological Dysfunction
PK	Pharmacokinetics
PR	Partial Response
PSA	Prostate Specific Antigen
PRRT	Peptide Receptor Radio(nuclide)therapy
RADAR	Radiation Dose Assessment Resource
RECIST	Response Evaluation Criteria in Solid Tumors
RFA	Radiofrequency Ablation
ROI	Region of Interest
RP-HPLC	Reverse Phase High Performance Liquid Chromatography
RR	Relative Risk
SCLC	Small Cell Lung Carcinoma
SD	Standard Deviation
SD	Stable Disease
SI-unit	International System of Units
SPECT	Single Positron Emission Computed Tomography
SPSS	Statistical Package for Social Sciences
SRS	Somatostatin Receptor Scintigraphy
SSA	Somatostatin Analog
sst	Somatostatin receptor
sst₁₋₅	Somatostatin receptor subtype 1-5
TACE	Transcatheter Arterial Chemoembolization
TNM	Tumor, Lymph Node, Metastases
ULN	Upper Limit of Normal
WB	Whole Body
WBC	White Blood Cells
WHO	World Health Organization

LIST OF SYMBOLS

Table 1 – Symbols used in dosimetric equations.

Symbol	Meaning
sf	Surviving fraction of cells
D	Absorbed dose
α, β	Tissue specific constants
T	Time
$g(T)$	Dimensionless function, which describes the probability of lethal combinations of reparable events over time (T)
$D(T)$	Absorbed dose over time (T)
BED	Biological Effective Dose
RE	Relative effectiveness and
N	Number of given fractions
$P(D)$	Probability of a clinical effect as a function of absorbed dose (D)
D_{50}	Absorbed radiation dose which leads to 50% cure/complication probability
D_{rm}	Absorbed dose to the bone marrow
k	Slope of the dose-response curve
h_r, r_s, r_t	Irradiation source
h_k, k, r_T, r_t	Irradiated target
$D(r_T, T_D), D(r_t)$	Mean absorbed dose to target tissue (r_T) over a dose integration period (T_D)
$DF(r_t \leftarrow r_s)$	dose factors for red marrow to red marrow
T_D	Dose integration period
$\tilde{A}_n, \tilde{A}_s, \tilde{A}_h, \tilde{A}_{rb}$	Time-integrated activity = number of nuclear transformations
$\tilde{A}(r_s, T_D)$	Time-integrated activity (number of nuclear transformations) in an irradiation source (r_s) over a dose integration period (T_D)
\tilde{A}_{rm}	Time-integrated activity in the bone marrow
S	Absorbed dose rate
$S(r_T \leftarrow r_s)$	Absorbed dose rate in the irradiated target (r_T, r_t) per nuclear transformation in the irradiation source (r_s, r_s)
C^{1-9}	Compartments (or organs) 1 to 9
$k(i,j)$	Kinetic transfer components between the indicated compartments i and j (organs)
$D_{kidneys}$	Absorbed dose to the kidneys
$A_{kidneys}$	Number of nuclear transformations in kidneys
$S(kidneys \leftarrow kidneys)$	Absorbed dose rate for the kidneys
rm	Red marrow = bone marrow
h	large organs and tumors with high radioactivity uptake
D_{rm}^{Self}	Absorbed self-dose to the bonemarrow
D_{rm}^{Cross}	Absorbed cross-dose to the bonemarrow

Table 2 – Symbols used in renal function equations & statistics.

Renal	
CLR	Creatinine clearance in ml/min
$\widehat{\text{CLR}}$	Estimated average Creatinine clearance in ml/min
age	Age of patient in years
weight, body-weight	Weight of patient in kg
s-creat	Serum creatinine in $\mu\text{mol/l}$
b_0	Estimated average CLR at time 0 when all other covariates are zero
b_1	Estimated average change in CLR in percent/time
factor ₁ , factor ₂	Constants
time	Time in weeks
GFR, C_x	Glomerular Filtration Rate in ml/min, based on 24-h urine collection
$U_{\text{creatinine}}$	Concentration creatinine in urine in $\mu\text{mol/l}$
V	Urine production in ml/min
c-CLR	Estimated creatinine clearance (CLR) in ml/min/ 1.73 m ² according to Cockcroft-Gault
BSA	Body surface area according to Du Bois and Du Bois
height	Height of patient in cm
BUN	Patient's Blood Urea Nitrogen in mmol/l
Alb	Patient's Albumin g/l
Statistics	
95%CI	95% Confidence Interval
a	Number of exposed patients with a positive (bad) outcome
b	Number of exposed patients with a negative (good) outcome
c	Number of non-exposed patients with a positive (bad) outcome
d	Number of non-exposed patients with a negative (good) outcome
p	Probability value for a given statistical model
R^2	Correlation Coefficient (Pearson-R Squared)
R_{spearman}, r_s	Spearman's rank correlation coefficient
r_p	Pearson correlation coefficient
RR	Relative Risk
SE	Standard error
χ^2	Chi-squared test

CURRICULUM VITAE

Hendrik Bergsma was born on the 13th of July 1982 in Meppel, The Netherlands. He attended his high school at the Lauwers College in Grijpskerk and Buitenpost where he graduated in 2001. From 2001 to 2005, he studied applied physics at the University of Groningen and graduated with his research project, entitled 'Coronary artery imaging using ECG-gated multidetector CT'.

After passing the decentralized selection procedure in ErasmusMC, he was offered a position for studying medicine and started his medical training in 2005. During medical school he worked three years in the nursing staff at the Geriatric-Oncological ward of the ErasmusMC. In 2008 he worked on dual-isotope quantitative imaging at the preclinical department of nuclear medicine. After his medical internship, he did a research project on a eye-tracking device for detection of early glaucoma in patients, at the department of Neuroscience in ErasmusMC.

In June 2011, he started his PhD research project at the Department of Nuclear Medicine at the Erasmus MC, Rotterdam, under supervision of Prof. dr. D.J. Kwekkeboom, Prof. dr. M. de Jong and dr. M. Konijnenberg. The research performed during this period is described in this thesis. In December 2015, he started his clinical residency to become a radiologist in Erasmus MC, but has decided to stop his training. In the future he would like to continue working in a hospital in the field of biomedical engineering.

He is married to Anne-Hendrike Schuurman and in July 2017 their first child, Jonathan, was born.

PHD PORTFOLIO

Summary of PhD training and teaching

Name PhD student:	Hendrik Bergsma	PhD period:	1-6-2011 to 26-9-2017
Erasmus MC Department:	Nuclear Medicine	Promotors:	Prof. Dr. Ir. M. de Jong
Research School:	Moleculair Imaging		Prof. Dr. D.J. Kwkkeboom† Prof. Dr. W.W. de Herder
		Supervisor:	Dr. M.W. Konijnenberg

1. PhD training

	Year	Workload (Hours/ECTS)
General courses		
- Basic course for clinical investigators (BROK) (19-3 to 23-3)	2012	1 ECTS
- Biomedical Writing Course – Molmed (27-11 to 8-1)	2012/2013	2 ECTS
- Course integrity (12, 19 & 26 november)	2013	2 ECTS
- Recertification basic course for clinical investigators (BROK) (25-11)	2016	0.3 ECTS
Specific courses (e.g. Research school, Medical Training)		
- Radiological Health Physics, Delft, The Netherlands (14-1 to 16-5)	2011	6 ECTS
- Visit Zentral Klinik Bad Berka, Germany (14-8 to 27-8)	2011	6 ECTS
- Basic Clinical Radiobiology, Paris, France (16-9 to 20-9)	2017	2 ECTS
Seminars and workshops		
- NET-WORK Europe 2013, Munich, Germany (30-01 to 1-02)	2013	1 ECTS
Presentations & Posters		
- From radiobiology to radiotherapy, Toulouse, France (3-4 to 6-4)	2013	2 ECTS
- Nephrotoxicity after PRRNT with ¹⁷⁷ Lu-DOTA-Octreotate (Poster)	2016	1 ECTS
- ENETS		
- Prediction and Modeling of response to Molecular and External Beam Radiotherapies, Le Bono, France (20-9 to 23-9)	2017	2 ECTS
(Inter)national conferences		
- 1 st congress on Ga-68 and PRRNT, Bad Berka, Germany (23-6 to 26-6)	2011	1 ECTS
- ENETS 2012, Copenhagen, Denmark (7-3 to 9-3)	2012	1 ECTS
- ENETS 2013, Barcelona, Spain (6-3 to 8-3)	2013	1 ECTS
- Five-yearly anniversary congress NVNG 'Imaging the future' (8-11)	2013	0.3 ECTS
- ENETS 2014, Barcelona, Spain (5-3 to 7-3)	2014	1 ECTS
- PSMA Radioligand Therapy in patients with Prostate Cancer	2017	0.3 ECTS

2. Teaching

Lecturing

- | | | |
|--|------|--------|
| - Bone marrow dosimetry of Radionuclide Therapy with ^{177}Lu -octreotate | 2013 | 1 ECTS |
| - Nurse symposium – NET and radiation safety, 5M/5N | 2014 | 1 ECTS |

Supervising practicals and excursions, Tutoring

- | | | |
|--|-----------|--------|
| - TU-Delft students (Minor) – Medical Delta (9-1 to 20-1) | 2012 | 3 ECTS |
| - For MD's from other hospitals at several occasions:
Principles and effects of peptide receptor radionuclide therapy | 2011-2015 | 2 ECTS |

ACKNOWLEDGEMENT (DANKWOORD)

Tijdens mijn promotie ben ik vele mensen tegengekomen die hebben bijgedragen aan mijn wetenschappelijke vorming en dit promotieboekje. Graag wil ik hen hiervoor bedanken.

Allereerst wil ik de patiënten en hun families hartelijk danken voor deelname aan onze studie. Van heinde en verre kwamen patiënten om in het Erasmus MC behandeld te worden. Zonder hen was er geen onderzoek mogelijk geweest. Tevens, wil ik de patiënten bedanken die in de Zentral Klinik in Bad Berka (Duitsland) een Sarabesin 3 scan hebben gekregen. Tevens wil ik alle verwijzers bedanken voor het prettige contact.

Mijn promotor, Prof. Dr. Ir. M. de Jong. Beste Marion, hartelijk dank dat je me op weg hebt geholpen in het begin van mijn promotietraject waarmee een basis voor de rest van de promotie is gelegd. Je hebt me middels het Sarabesin 3 project geïntroduceerd in de (internationale) wetenschappelijke wereld van de radiopeptides, waar soms ook politieke correctheid van belang is. Tijdens mijn eerste congres in Bad Berka heb ik van je mogen leren hoe goed je privé en werk weet te combineren. Ik wens je nog vele jaren als hoogleraar van de prekliniek toe.

Mijn promotor, Prof. Dr. D.J. Kwekkeboom. Beste Dik, ondanks dat je mijn promotie niet kan meemaken ben je aanwezig in de geschreven artikelen. Dank voor je steun/adviezen op zowel werk als persoonlijk vlak. Ook dank voor je kritische klinische blik naar de artikelen en sepsis ten aanzien van de dosimetrie, hoewel ik deze niet altijd met je deelde! Je (droge) humor zal me bijblijven en zo zie je maar met dit proefschrift: Ook al zeggen noordelingen soms weinig en knauwen ze, promoveren kunnen ze!

Mijn copromotor, Dr. Mark Konijnenberg. Beste Mark, dank voor je begeleiding en discussies over de dosimetrie en de klinische relevantie ervan. Door jouw ervaring en kennis van de (deeltjes)-fysica heb ik de natuurkunde en wiskunde weer op kunnen pakken. Dank voor de workshops en cursussen die je voorstelde zodat ik me de dosimetrie goed eigen heb kunnen maken.

Prof. emeritus Dr. E.P. Krenning. Beste Eric, jij stond aan de wieg van de ontwikkeling van de somatostatine receptor scintigrafie en de peptide receptor radionuclide therapie. Hartelijk dank voor je enthousiaste discussies o.a. over de rol van dosimetrie in de kliniek. Tevens wil ik je bedanken voor de vervangende begeleiding in de laatste periode van mijn promotie. Succes met het uitbouwen en ontwikkelen van de Cyclotron faciliteit.

Mijn vervangende promotor, Prof. dr. W.W. de Herder. Beste Wouter, hartelijk dank voor je begeleiding van het laatste gedeelte van m'n promotie. Ik waardeer je zorg en aandacht voor patiënten en beschikbaarheid voor overleg in de kliniek, ook al is het twee uur 's nachts in de tijdszone waar je verblijft. Bedankt voor je betrokkenheid en snelle input bij verscheidene van mijn artikelen.

De overige leden van de grote commissie, Prof.dr. L.J. Hofland, Prof.dr. A.G. Vulto en Prof. dr. M.L. Lam, hartelijk dank voor het plaatsnemen in de commissie.

I also want to thank the international collaborators I worked with. Thea Maina and Berthold Nock thank you for all the fruitful discussions and critical feedback that led to the improvement of our manuscripts. Prof. dr. Richard Baum, thanks for inviting me to Zentral Klinik in Bad Barka where I gathered patient data for the Sarabesin 3 article. Thanks to Dr. Harshad Kulkarni, Prof. Dirk Mueller and Sabine Seifert for an unforgettable time in Bad Berka.

K.A.L. Mauff. Dear Katya, thank you for working on the statistical part of the nephrotoxicity article and your profound knowledge of R® (The R Foundation). Thank you for the collaboration.

Mijn supervisors bij de PRRT, Boen en Jaap. Boen, hartelijk dank voor je expertise, discussies en gezelligheid. Je inzet voor de therapie en de organisatie ervan is bewonderenswaardig. Ook dank voor de gezelligheid bij o.a. de ENETS congressen. Helaas is mijn liefde voor voetbal niet aangewakkerd hoewel je er veel met Esther (en Wouter) over praatte. Jaap, hartelijk dank voor je precieze blik zowel in de kliniek als tijdens het becommentariëren van mijn artikelen. Ik heb veel van je geleerd.

Mijn collega-onderzoekers. Allereerst Esther, jij hebt me de fijne kneepjes van het (PRRT) vak geleerd en er voor gezorgd dat de kliniek en onderzoek (tijd technisch) beter werd ingedeeld. Ik vond het een eer om paranimf bij jou te mogen zijn. Veel geluk toegewenst met je mannen, Bas, Karel en Jan. Je zult een goede huisarts worden! Beste Wouter, bedankt voor de prettige samenwerking en praktische aanpak, met jou hebben we o.a. de overstap gemaakt naar het digitale patiëntendossier. Fijn dat je mijn paranimf wilt zijn. Veel succes verder met jouw promotie onderzoek. Beste Daan, ik heb maar kort met je samengewerkt, maar het was altijd gezellig. Ik wens je veel succes toe bij jouw promotietraject,

De 'Lu-dames', de verpleegkundigen van het PRRRRRRRRRT-team. Beste Agnes, Bep, Carla, Daniëlle, Els, Lucinda, Marleen, Theresia, en natuurlijk Anja en Fania, hartelijk dank voor de prettige samenwerking. Samen hebben we geprobeerd om goede zorg te geven aan de patiënten, met veel/weinig personeel, op de Daniel of in de centrum locatie, in drukke- en rustige tijden, dank hiervoor. Het was altijd gezellig en we hebben veel gelachen. Ik hoop dat jullie een mooie plek krijgen naast de huidige nucleaire geneeskunde afdeling in de centrum locatie.

Al het personeel van de afdeling Nucleaire Geneeskunde, de MNW'ers, de MNAA'ers (Carlijn, Emar, Arthur, Heleen, Linda, Erica, Jopie), klinisch fysici (Marcel en Peter Kooij) en de mensen van de administratie, dank voor jullie ondersteuning, zonder jullie allen is er geen Lutetium therapie mogelijk. De mensen van de automatisering, Amroos, Tuki, Paul en in het bijzonder Ronald. Dank voor je bereikbaarheid en inzet voor als ik weer beelden nodig had uit Clinical Index. Wout, Erik en Ho Sze fijn dat jullie deur altijd open stond voor het uitgeven van 'activiteit' en discussies over labelingen.

De AIOS Nucleaire Geneeskunde, Martijn, Stoffel, Kathleen, Stefan, Hanneke, Tessa, Laura en Asahi, hartelijk dank voor de gezellige tijd. De overige stafleden van de afdeling Nucleaire Geneeskunde. Prof. dr. J.F. Verzijlbergen, bedankt voor het aansturen van de afdeling in roerige tijden. Roelf Valkema, beste Roelf, hartelijk dank voor al je vragen en discussies tijdens de overleggen en daarbuiten. Lideke Froberg, beste Lideke, bedankt voor de prettige samenwerking. Jasper Emmering, beste Jasper, bedankt voor de gezellige tijd.

De artsen en verpleegkundigen van de afdeling Endocrinologie, hartelijk dank voor jullie inzet en zorg voor de PRRT patiënten. Dr. R.A. Feelders, beste Richard, Dr. R.P. Peeters, beste Robin, dank voor het altijd laagdrempelige overleg over de PRRT patiënten. Beste Wanda, dank voor de prettige samenwerking.

Daarnaast wil ik graag alle medeauteurs van de diverse artikelen bedanken voor hun input en expertise.

Ton, bedankt voor het meedenken over de voorkant/layout en het maken van de foto's tijdens de promotie.

Van de afdeling Pathologie wil ik Prof. dr. Leendert Looijenga en Hans Stoop bedanken voor de samenwerking in het testes-project. Het snijden van weefsel en immunokleuringen werd snel gedaan zodat we de resultaten met elkaar konden bespreken.

Mijn kamergenoten en mede promovendi Simone, Ingrid, Costanza, Sandra en Kristell, bedankt voor jullie gezelligheid. Af en toe moest ik streng tegen jullie zijn om de orde te bewaren, maar vaak leefden we met elkaar mee tijdens bijzondere gebeurtenissen, zoals bruiloften. Succes in jullie werk en privé leven, welke richting jullie ook kiezen. Marleen Melis en Ingrid, bedankt voor jullie uitleg en het uitvoeren van de autoradiografieën, door met jullie samen te werken heb ik veel geleerd over de verschillende preklinische onderzoeksmethoden.

Prof. dr. Gabriel Krestin bedankt voor de mogelijkheid om mijn PhD project op de afdeling Radiologie & Nucleaire Geneeskunde te mogen uitvoeren. Dr. W. van Lankeren, beste Winnifred, bedankt voor alle steun tijdens de ziekteperiode van mijn vader. Je relativeringsvermogen en nuchterheid is prettig, waardoor ik overwogen keuzes heb kunnen maken voor de toekomst. Jolanda Meijer, beste Jolanda, bedankt voor de ruimte die geboden is om tijdens mijn herstelperiode aan m'n promotie te werken.

Danny Hommel, beste Danny, super dat je m'n paranimf wilt zijn, straks ga jij je proefschrift verdedigen, hierbij alvast een voorproefje van wat je te wachten staat! De (filosofische) gesprekken in de pauzes tijdens onze studie geneeskunde zullen me altijd bijblijven!

Lieve Anne-Hendrike, je betekent alles voor mij. Bedankt voor je onvoorwaardelijke liefde en vertrouwen. Je hebt me geholpen met je relativeringsvermogen als ik weer eens zat te tobben over iets. Ik bewonder je enthousiasme, zorgzaamheid en oog voor detail. Ik kijk er naar uit om samen met jou een gezin te stichten. Ik hou van je!

LIST OF PUBLICATIONS

- **Hendrik Bergsma**, Esther I. van Vliet, Jaap J.M. Teunissen, Boen L.R. Kam, Wouter W. de Herder, Robin P. Peeters, Eric P. Krenning, Dik J. Kwekkeboom - Peptide receptor radionuclide therapy (PRRT) for GEP-NETs - Best Practice & Research Clinical Gastroenterology. 2012 Dec; 26(6): 867-81N
- Esther I. van Vliet, Eric P. Krenning, Jaap J.M. Teunissen, **Hendrik Bergsma**, Boen L.R. Kam, Dik J. Kwekkeboom - Comparison of response evaluation in patients with gastroenteropancreatic and thoracic neuroendocrine tumors after treatment with [¹⁷⁷Lu-DOTA⁰,Tyr³]octreotate – Journal of Nuclear Medicine. 2013 Oct; 54(10): 1689-96
- **Hendrik Bergsma**, Mark W. Konijnenberg, Boen L.R. Kam, Teunissen JJM, Kooij PP, de Herder WW, Franssen GJH, van Eijck CHJ, Krenning EP, Kwekkeboom DJ - Subacute haematotoxicity after PRRT with ¹⁷⁷Lu-DOTA-octreotate: prognostic factors, incidence and course - European Journal of Nuclear Medicine and Molecular Imaging. 2016 Mar; 43(3): 453-63
- **Hendrik Bergsma** & Theodosia Maina, Harshad R. Kulkarni, Dirk Mueller, David Charalambidis, Eric P. Krenning, Berthold A. Nock, Marion de Jong, Richard P. Baum - Preclinical and first clinical experience with the gastrin-releasing peptide receptor-antagonist [⁶⁸Ga]SB3 and PET/CT - European Journal of Nuclear Medicine and Molecular Imaging. 2016 May;43(5): 964-73
- **Hendrik Bergsma** & Mark W. Konijnenberg, Wouter A. van der Zwan, Boen L.R. Kam, Jaap J.M. Teunissen, Peter P. Kooij, Katya A.L. Mauff, Eric P. Krenning, Dik J. Kwekkeboom - Nephrotoxicity in PRRT with ¹⁷⁷Lu-DOTA-Octreotate - European Journal of Nuclear Medicine and Molecular Imaging. 2016 Sep; 43(10): 1802-11
- **Hendrik Bergsma**, Kirsten van Lom, Mark H.G.P. Raaijmakers, Mark W. Konijnenberg, Boen L.R. Kam, Jaap J.M. Teunissen, Wouter W. de Herder, Eric P. Krenning, Dik J. Kwekkeboom – Therapy-related hematological malignancies after PRRT with ¹⁷⁷Lu-DOTA-Octreotate: Incidence, course & predicting factors – Journal of Nuclear Medicine. 2017
- Wouter A. van der Zwan, Mark W. Konijnenberg, Jifke F. Veenland, Eric P. Krenning, Saima Khan, **Hendrik Bergsma**, Dik J. Kwekkeboom - Spleen volume decrease after PRRT: Clinical and dosimetrical correlation - Submitted

